

Methods to investigate glycogen structure in Glycogen Storage Diseases (GSDs)

Gaia Fancellu

A thesis presented for the degree of
Master of Philosophy by Research



School of Chemistry
University of East Anglia

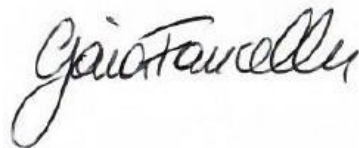
October 2022

This copy of the thesis has been supplied on condition that anyone who consults it is understood to recognise that its copyright rests with the author and that use of any information derived therefrom must be in accordance with current UK Copyright Law. In addition, any quotation or extract must include full attribution.

Declaration

I declare that the work contained in this thesis submitted for the Degree of Master of Philosophy by Research is my work, except where due reference is made to other studies, and has not previously submitted by me for a degree at this or any other university.

Gaia Fancellu

A handwritten signature in black ink, reading "Gaia Fancellu". The signature is written in a cursive style with a large initial 'G' and a long, sweeping underline.

Acknowledgments

My deepest gratitude goes to PoLiMeR and to my Supervisory team,

In 2019, I decided to explore science from a researcher perspective, and the PoLiMeR consortium gave me this opportunity. I joined an international team made of incredible young scientists who became my friends and supported me throughout my journey. I could never forget the hours we spent together to discuss about science, to plan activities, to enjoy our nights out, and to help each other during difficult periods as the one we faced during the pandemic. I am also thankful to Prof. Barbara Bakker and Dr Karen Van Eunen, the founders of PoLiMeR and of this unforgettable experience.

This endeavour would not have been possible without Prof Rob Field, Dr Simone Dedola, and Dr María J. Marín, who supported me in the past three years. I am extremely grateful for having you as my mentors during this challenging period. Thanks for being patient and supportive in every situation, and for never stopped encouraging me to pursue my goals.

A special thanks goes to Iceni Glycoscience, my second *home* for the past three years. Thanks to the team of Iceni for helping me with my daily challenges, and I would like to especially thanks Simona, Irina, and Giulia for being on my side in the times of need.

Thanks to my family,

Being abroad and far from my family was not easy, and a pandemic did not make things easier than they were. Words cannot express how lucky I was to have my family always by my side, no matter what my decision was. Thanks to Papà, Mamma, Gabriele, and to my little flurry sister Athena.

Thanks to my friends,

The experience I had was incredible, but the company made everything even more special.

Thanks to Pedro and Carla who were my pillars since the beginning of the project, and without whom I could not face all the challenges that I encountered in my journey. You are both amazing scientists and I wish you only the best for your future.

Thanks to my Italian friends Felicia, Chiara, Giulia, Caterina, and Morgana who supported my rollercoaster of feelings despite the distance.

Thanks to my Mancunian friends and Field's research group who turned the last part of my journey into a more entertaining experience.

Abstract

Glycogen is the primary source of energy in mammals. It acts as a metabolic buffer, storing or releasing glucose from liver and skeletal muscles in response to an excess or demand of energy. Inherited metabolic disorders that affect glycogen metabolism, such as Glycogen Storage Diseases (GSDs), are related to the appearance of aberrant glycogen structures, which impact on the rate and extent of glucose availability. To date, details on the structure and metabolism of glycogen are still not sufficient to provide an accurate insight into GSDs. The aim of this project is to develop easy-to-use methodologies to analyse and better define the structure of glycogen from healthy and GSDs sources.

To achieve the goal of this project, two methodologies were developed. The first one consisted in the enzymatic debranching of glycogen to determine the chain length distribution and the degree of branching. The method was established on commercially available glycogen (from oyster) and validated on glycogen extracted from HepG2 cells and HepG2 cells bearing GSD type Ia (glucose 6-phosphatase deficiency). The second method aimed at elucidating the position of the branching points by a stepwise enzymatic digestion of the branches and the external chains of the standard glycogen. The results obtained from this second method were then integrated with a theoretical model (called DP15) to have a better understanding on the branches arrangement. The development of both methodologies was supported by analytical techniques, such as thin-layer chromatography (TLC), high-performance anion exchange chromatography coupled with pulsed amperometric detector (HPAEC-PAD), and bicinchoninic acid (BCA) assay to assess the hydrolysed products qualitatively and quantitatively.

The application of the first methodology showed that the structure of the glycogen standard contained 10% of branching points, and the chains were predominantly longer than DP6 in agreement with literature. The same structural analysis was applied on glycogen from mammalian HepG2 cells and mouse liver after the development of a novel extraction protocol. Preliminary studies showed that HepG2 glycogen had 20% of branching points, equivalent to twice the amount observed in oyster glycogen, and was mainly made of chains longer than DP7. The comparison of the chain length distribution between HepG2 cells and GSDIa HepG2 cells showed that this genetic mutation does not impact the length of the branches and the activity of the glycogen branching enzyme. The same methodology was also applied to glycogen from mouse liver, and the results showed a group of predominant chains between DP4 and DP8. The lack of a peak in the chain length distribution of mouse liver glycogen was attributed to the activity of glucosidases present in liver tissues.

The results obtained from the second methodology showed that the glycogen β - and phosphorylase-limit dextrans have chain length distributions (CLDs) shifted towards a low DP, namely DP2, DP3 and DP4, when compared to oyster glycogen. The combination of the CLDs collected experimentally into the DP15 model led to select branched structures bearing branching points at the 3rd or 4th glucose residues from the reducing end of the main chain, suggesting that glycogen branching enzyme potentially branches every three or four glucose units.

To conclude, the methodologies presented in this thesis were demonstrated to be feasible and applicable on commercially available standards or samples isolated from mammalian cells for the investigation of the structure of glycogen. Further applications on samples from GSDs sources could elucidate the impact of these genetic mutations on glycogen structure.

Access Condition and Agreement

Each deposit in UEA Digital Repository is protected by copyright and other intellectual property rights, and duplication or sale of all or part of any of the Data Collections is not permitted, except that material may be duplicated by you for your research use or for educational purposes in electronic or print form. You must obtain permission from the copyright holder, usually the author, for any other use. Exceptions only apply where a deposit may be explicitly provided under a stated licence, such as a Creative Commons licence or Open Government licence.

Electronic or print copies may not be offered, whether for sale or otherwise to anyone, unless explicitly stated under a Creative Commons or Open Government license. Unauthorised reproduction, editing or reformatting for resale purposes is explicitly prohibited (except where approved by the copyright holder themselves) and UEA reserves the right to take immediate 'take down' action on behalf of the copyright and/or rights holder if this Access condition of the UEA Digital Repository is breached. Any material in this database has been supplied on the understanding that it is copyright material and that no quotation from the material may be published without proper acknowledgement.

Table of Contents

List of abbreviations.....	9
Chapter 1 - Introduction	12
1.1. Structural features of glycogen.....	13
1.1.1. Degree of branching.....	15
1.1.2. Chain length distribution	16
1.1.3. The organization of glycogen molecules into granules.....	17
1.2. Glycogen metabolism	18
1.2.1. Glycogen Synthesis	19
1.2.2. Glycogen degradation.....	27
1.2.3. Lysosomal degradation of <i>mis-branched</i> glycogen.....	31
1.3. Glycogen Storage Diseases (GSDs).....	33
1.3.1. Glycogenin deficiency – GSD type XV	34
1.3.2. Glycogen synthase deficiency – GSD type 0	35
1.3.3. Glycogen branching enzyme deficiency – GSD type IV.....	36
1.3.4. Glycogen phosphorylase deficiency – GSD type V/VI.....	37
1.3.5. Glycogen debranching enzyme deficiency – GSD type III	38
1.3.6. Glucose 6-phosphatase deficiency - GSD type I.....	38
1.4. About PoLiMeR project.....	40
1.5. Aim of the Project	41
Chapter 2 – Enzymatic assays and analytical techniques employed in the present studies	42
2.1. Chemical treatments vs. Enzymatic assays.....	42
2.1.1. Debranching enzymes.....	44
2.1.2. Amylolytic Enzymes.....	49
2.1.3. Phosphorolytic Enzyme.....	52
2.2. Analytical techniques commonly employed to determine the chain length distribution	55
2.2.1. Fluorophore-Assisted Capillary Electrophoresis (FACE).....	55
2.2.2. High-Performance Anion Exchange Chromatography coupled with Pulsed Amperometric Detection (HPAEC-PAD).....	56
2.2.3. Size-Exclusion Chromatography (SEC)	57
2.3. Quantification of glucan chains reducing ends to determine the degree of branching.....	58
2.3.1. Bicinchoninic Acid (BCA) assay.....	58
2.3.2. Dinitrosalicylic acid (DNS) and Nelson-Somogyi (NS) assay.....	61
Chapter 3 – DP15 model	62
3.1. Branching mechanism used to build up the DP15 models	63

3.1.1.	Selection of the branched models based on the substrate specificity of glycogen branching enzyme.....	64
3.2.	Theoretical chain length distribution using the branched DP15 models.....	65
3.3.	Digestion of the DP15 models with β -amylase and glycogen phosphorylase	70
Chapter 4 – Stepwise enzymatic digestion of glycogen and combination of the results with theoretical models		74
4.1.	Enzymatic debranching of glycogen by isoamylase and pullulanase.....	74
4.1.1.	Digestion of glycogen with isoamylase	74
4.1.2.	Digestion of glycogen with pullulanase	82
4.2.	Digestion of the external chains with β -amylase.....	87
4.2.1.	Exhaustive digestion of glycogen with β -amylase	87
4.2.2.	Quantification of maltose and β -limit dextrins.....	88
4.2.3.	Investigation of the chain length distribution of the β -limit dextrin	89
4.2.4.	Quantification of the branches released from β -limit dextrin.....	91
4.3.	Digestion of glycogen with glycogen phosphorylase	92
4.3.1.	Exhaustive digestion of glycogen with glycogen phosphorylase	92
4.3.2.	Quantification of glucose 1-phosphate and phosphorylase-limit dextrin	92
4.3.3.	Investigation of the chain-length distribution in phosphorylase-limit dextrin.....	94
4.4.	Discussion.....	96
4.4.1.	The digestion of glycogen with pullulanase and isoamylase provides insights into the distribution of short and long chains	96
4.4.2.	Potential branching arrangements in the outer layers of glycogen	97
4.4.3.	The substrate specificity of GBE can be speculated by investigating the CLD of glycogen	102
Chapter 5 - Investigation of the structure of glycogen from mammalian sources.....		108
5.1.	Review of the current methodologies to extract glycogen from mammalian sources	108
5.1.1.	Development of the protocol to extract glycogen from tissues and cells	110
5.2.	Chain length distribution of glycogen from HepG2 cells and mouse liver	112
5.2.1.	Preliminary measurements of the degree of branching in glycogen from HepG2 cells	113
5.3.	Discussion.....	115
5.3.1.	The peak in the CLD of HepG2 glycogen is a possible anchoring point for the branching activity of GBE	115
5.3.2.	Possible degradation of mouse liver glycogen by degradative enzymes	116
5.4.	Preliminary studies on the structure of glycogen from GSDIa HepG2 cells.....	117
5.4.1.	Results and Discussions.....	118
Chapter 6 - Conclusions		120

Chapter 7 - Materials and Methods.....	122
7.1. Purification of commercially available oyster glycogen.....	123
7.2. Enzymatic treatments	123
7.2.1. Debranching of oyster glycogen with ISA and Pull	123
7.2.2. Digestion of oyster glycogen with BMY or GP	124
7.2.3. Dephosphorylation of G1P.....	125
7.2.4. Digestion of glycogen, BLD and PLD by enzymatic cocktail	125
7.2.5. Digestion of the samples with OGL.....	125
7.3. Quantitative and qualitative analysis of the samples	125
7.3.1. Quantification of the samples by BCA assay.....	125
7.3.2. HPAEC analysis of the chain length distribution of glycogen, PLD, and BLD	126
7.3.3. GPC analysis of the samples digested by ISA and Pull	126
7.4. Growth of HepG2 cells for the extraction of glycogen	127
7.4.1. Thawing cells.....	127
7.4.2. Passaging cells.....	127
7.4.3. Extraction of glycogen.....	127
Chapter 8 – References.....	129
Appendix 1	142
Appendix 2	144
Appendix 3	149

List of abbreviations

AAG	Acid α -glucosidase
ALP	Alkaline Phosphatase
AMG	Amyloglucosidase
AMP	Adenine Mono Phosphate
AMY	α -Amylase
ANTS	8-Aminonaphthalene-1,3,6-Trisulfonic acid
APBD	Adult Polyglucosan Bodies Disease
APTS	8-Aminopyrene-1,3,6-Trisulfonic acid
BCA	Bicinchoninic Acid
BLD	β -Limit Dextrins
BMV	β -Amylase
CBM	Carbohydrate Binding Module
CH ₃ CN	Acetonitrile
CuSO ₄ x 5 H ₂ O	Copper sulphate pentahydrate
DMEM	Dulbecco's Modified Eagle Medium
DNS	Dinitrosalicylic acid
DPBS	Dulbecco's Phosphate-Buffered Saline
DRI	Differential Refractive Index
EPM2a	Laforin glycogen phosphatase gene
ESR	Early Stage Researchers
EtOAc	Ethyl acetate
EtOH	Ethanol
FACE	Fluorophore-Assisted Capillary Electrophoresis
FBS	Foetal Bovine Serum
G1	Glucose
G1-G3	6 ³ - α -glucosyl-maltotriose
G2	Maltose
G3	Maltotriose
G3-G3	6 ³ - α -maltotriosyl-maltotriose
G4	Maltotetraose

G5	Maltopentaose
G6	Maltohexaose
G6Pase	Glucose 6-phosphatase
G6PC	Glucose 6-phosphatase Catalytic subunit
G6PT	Glucose 6-phosphatase Transfer subunit
G7	Maltoheptaose
GH	Glycosyl Hydrolase
GPC	Gel-Permeation Chromatography
GYG1	Gene encoding glycogenin in skeletal muscles
GYG2	Gene encoding glycogenin in liver
GYS1	Gene encoding glycogen synthase in skeletal muscles
GYS2	Gene encoding glycogen synthase in liver
H ₂ O	Water
H ₂ SO ₄	Sulfuric acid
HepG2	Mammalian cell line from liver
hGBE	Human GBE
HPAEC-PAD	High-Performance Anion Exchange Chromatography coupled with Pulsed Amperometric Detector
HPLC	High Performance Liquid Chromatography
iPrOH	Isopropanol
ISA	<i>Pseudomonas</i> isoamylase
LB	Lafora bodies
LIF	Laser-Induced Fluorescence
mFAO	mitochondrial Fatty-Acids Oxidation
MtGBE	<i>Mycobacterium tuberculosis</i> GBE
Na ₂ CO ₃	Sodium carbonate
NADP/NADPH	Nicotinamide Adenine Dinucleotide Diphosphate
NaHCO ₃	Sodium bicarbonate
NaOAc	Sodium acetate
NaOH	Sodium hydroxide
NS	Nelson-Somogyi

OG	Oyster glycogen
OGL	Oligo $\alpha(1,6)$ -glucosidase
OsBE	<i>Oryza sativa</i> branching enzyme
PAS	Periodic Acid Schiff
PB	Phosphate Buffer
P _i	Inorganic phosphate
PKA	Protein Kinase A
PLD	Phosphorylase-limit dextrans
PP1	Protein Phosphatase 1
PPP1R3A-PP1	Glycogen-targeting subunit for PP1
PSA	Phenol-Sulfuric Acid
PTFE	Polytetrafluoroethylene
Pull	Pullulanase
PYGL	Gene encoding glycogen phosphorylase in liver
SEC	Size-Exclusion Chromatography
Std	Standard
TCA	Trichloroacetic Acid
TLC	Thin-Layer Chromatography
WPs	Work Packages

Chapter 1 - Introduction

Glycogen was discovered in 1857 by the French scientist Claude Bernard during his studies on the metabolism of sugars in animals.¹ Since then, efforts have been focused to unravel the structure of glycogen and its role in the organism. The analysis of glycogen structural features revealed the capacity of this molecule to store large quantities of glucose units, maintaining a soluble and organised structure.^{2,3} In addition, the investigation of glycogen in a biological context elucidated the influence that insulin and glucagon have on glycogen synthesis and degradation in response to the uptake of glucose from diet; or its mobilisation from liver and muscles due to exercise and stress. Consequently, glycogen was defined the storage form of energy and the substance used by the whole body to maintain glucose homeostasis.⁴

Glycogen was initially considered as an “*inert*” molecule with the simple function of storing and releasing glucose in times of plenty or need.⁴⁻⁶ However, the role of glycogen as simple storage unit was challenged when severe clinical manifestations were diagnosed in relation to impairments in its metabolism.⁷ Hepatomegaly, hypoglycaemia, accumulation of glycogen, and muscle weakness were the common hallmarks in patients affected by these disorders called Glycogen Storage Diseases (GSDs).³ While the cause of GSDs was related to genetic mutations affecting the activity of enzymes involved in glycogen metabolic pathways, it was not clear how an apparently “*inert*” molecule had deleterious consequences for the whole body. These posed several questions such as: *How does the deficiency of an enzyme involved in glycogen synthesis or degradation has an impact on overall metabolism? Why can glycogen not be used as a source of energy in GSDs? Is glycogen only responsible of storing energy or does it play other roles?* Despite the many efforts made by the scientific community since the discovery of glycogen, these questions still need to be addressed.

The scope of this chapter is to review the information available on glycogen structure and metabolism, and how this could be exploited to propose new research lines to address unanswered questions. Firstly, structural features of glycogen and their impact in the physiochemical properties of the polysaccharide are presented. Secondly, an overview on glycogen metabolism with a focus on enzyme structures and the impact that mutations associated with glycogen storage diseases have on their activity is provided. The discovery of the role of glycogen as a sensor molecule for signalling network is also briefly introduced.

1.1. Structural features of glycogen

Glycogen is mainly stored in the cytosol of the cells found in skeletal muscles, brain, and liver.⁴ Being the energy reservoir of the organism, the structure of glycogen requires a well-designed organization to ensure the maximum storage capacity without interfering with the surrounding environment. To avoid an impact on the cell osmolarity, glucose units are linked by $\alpha(1,4)$ - and $\alpha(1,6)$ -glycosidic bonds to form linear chains and branching points, respectively.⁸ The combination of both type of linkages creates a complex branched network, and it has been estimated that this arrangement facilitates the storage of approximately 55,000 glucose units.² If this same number of monomers was stored as free glucose in the cytoplasm, it would cause a dramatic increase in the cell osmolarity. The storage of such a high number of glucose units in the form of glycogen reduces the concentration of soluble sugars from *ca.* 400 mM to only 0.01 μ M.^{9,10}

The chemical structure of glycogen shares similarities with that of starch, the storage polysaccharide in plants.¹¹ For this reason, most of the terminology used to describe glycogen structural organisation is the same reported for starch, starting from the nomenclature used for the branches. The type of chains distributed within the glycogen structure are classified as follows (**Fig. 1**): A-chains with no branching point; B-chains containing one or more branching points; and C-chains containing two or more branching points and bound to the protein core of glycogen (glycogenin) *via* reducing end.^{12,13} Furthermore, the glucose residues between two branching points forms the *internal chains*, whereas those between a branching point and a non-reducing end constitute the *external chains*.

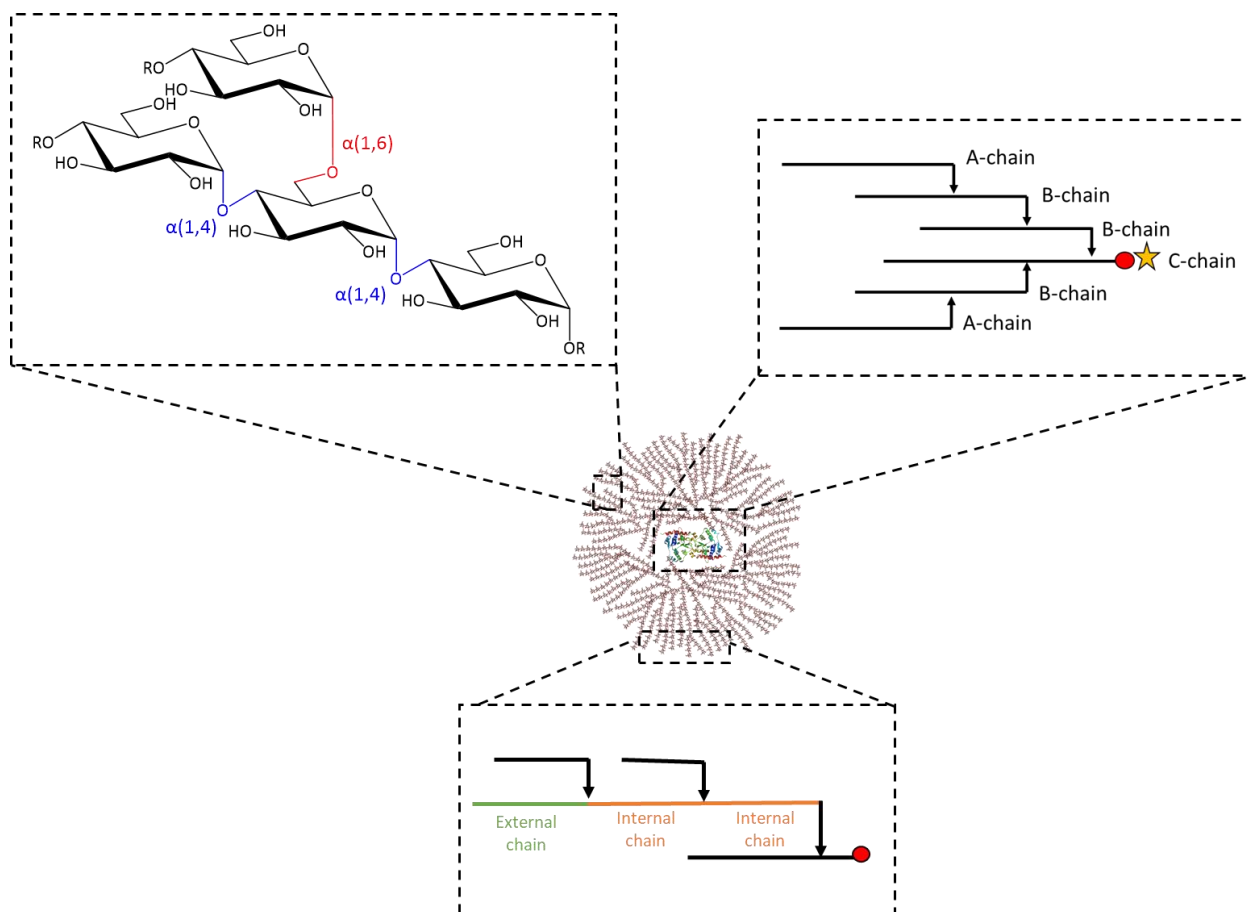


Figure 1 Schematic illustration of glycogen (in the centre) with a focus on the chemical structure (top left) and on the type of chains (top right and bottom). A-chains = no branching points; B-chains = one or more branching point; C-chains = more than one branching point and bearing the reducing end (red circle) linked to the protein glycogenin (yellow star). External chains are between a non-reducing end and the branching point; internal chains are between two branching points. The black arrows indicate the branching point. Glycogen image adapted from McArdle et al.¹⁴

The arrangement of the glucose units as showed in **Fig. 1** was proposed to follow a tier model (**Fig. 2**).^{2,8} In this model, elaborated using mathematical models, glycogen is organised in several concentric layers in which the number of glucose units and branching points increase from the inner to the outer layers. The first tier contains glycogenin and the first branching point, while the others contain only glucan chains with multiple $\alpha(1,6)$ -glycosidic bonds. In addition, this arrangement also included the bulky enzymes required for the synthesis and degradation of glycogen. According to the model, 12 is the maximum number of tiers contained in glycogen as beyond that the structure hinders the activity of glycogen-active enzymes.^{2,8} Later, this model was supported by Deng *et al.*¹⁵ by correlating the reduction in space from the inner to the outer layers to the substrate specificity of the glycogen branching enzyme (GBE), one of the enzymes involved in glycogen synthesis. This latest model will be discussed in Chapter 2.

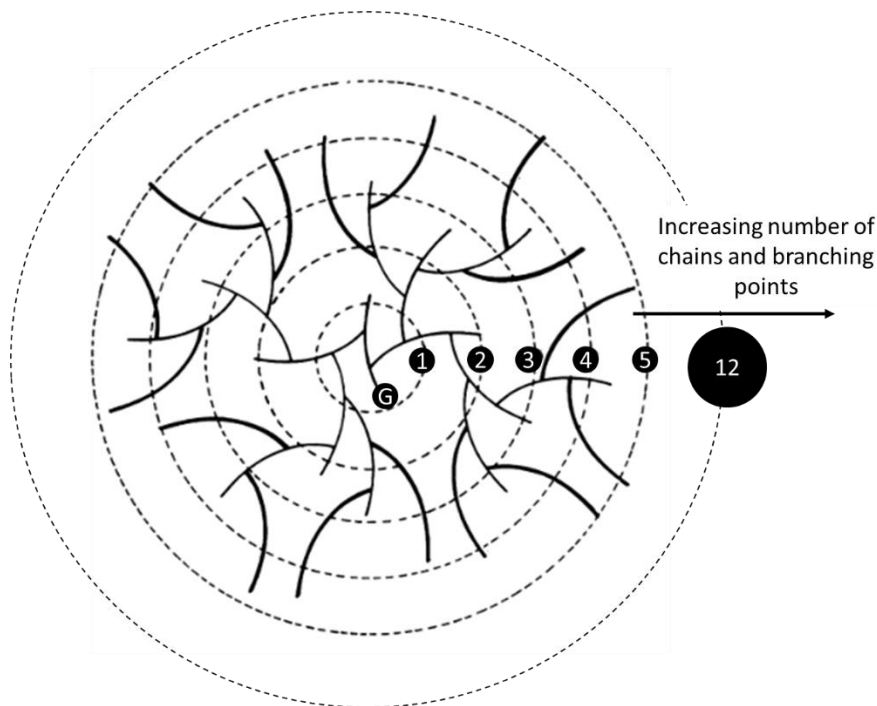


Figure 2 Scheme showing the glycogen structure following the tier model; only 5 tiers are represented with the glycogenin core indicated with G. Image adapted from Melendez et al. ⁹

However, up to date, the 12-tier model has not been demonstrated experimentally. The sequential digestion of glycogen tiers is a challenging task due to the lack of enzymes or chemical treatments that target a single layer without disrupting the following one. Therefore, mathematical and computer modelling are the only resources currently used to evaluate this model.^{2,9,10,15}

1.1.1. Degree of branching

The degree of branching (DB) is the percentage of branching points in a glycogen sample and indicates the ratio between $\alpha(1,4)$ - and $\alpha(1,6)$ -glycosidic bonds. The information currently available on DB suggests that glycogen from a healthy source should have between 8% and 12% of branches.^{16,17} Due to variations in glycogen structure depending on the species, DB is reported as a range. Furthermore, there is insufficient information to establish the exact distance between branching points. Based on mathematical models, glycogen can have a branching point every three glucose residues, on average, meaning that there is an $\alpha(1,6)$ -linkage every 0 to 6 glucose residues.¹⁷⁻¹⁹ However, these are theoretical data that have not been demonstrated experimentally yet.

The DB depends on the branching process catalysed by GBE, the mechanism of which will be discussed in-depth in the section 1.2.1.3. The branching frequency, namely the number of

branching points, and the distance between them, is crucial to maintain the solubility of glycogen in the cytosol. In fact, an increase in the number of glucose residues between two successive $\alpha(1,6)$ -linkages creates long chains resembling starch-derived amylopectin. As a consequence, the interaction between long unbranched chains results in insoluble aggregates that precipitate in the cytoplasm.^{20,21} It is interesting to notice that these *amylopectin-like* structures interfere with glycogen metabolic pathways,^{22,23} but they do not have the same effects on starch metabolism.

The DB is not only important for the physiochemical properties of glycogen, but it has been demonstrated to play an important role in the signalling network. Recent studies from McBride *et al.*²⁴ showed that AMPK, the main regulator of energy in the body, binds to the branching points of glycogen. By binding glycogen, AMPK is inactivated, and thus it cannot promote glycogen synthesis through the activation of glycogen synthase. When the degradation of glycogen commences, the number of branching points decreases. As a result, AMPK loses affinity towards glycogen and activates glycogen synthesis. These studies represented one of the first reports of glycogen as a regulatory molecule, and more investigations are needed to identify the potential branching arrangements responsible for the inhibition of AMPK.

1.1.2. Chain length distribution

The number of chains of a given degree of polymerization (DP) distributed across the structure of glycogen is known as chain length distribution (CLD), and it represents one of the structural features of glycogen. In initial studies of Illingworth *et al.*¹² and in those that followed,^{25,26} the structural analysis of glycogen was limited to the investigation of the average chain length (ACL) found in the overall polysaccharide. The ACL was calculated theoretically using the reciprocal of the percentage of the branching points, *e. g.* the ACL of rabbit liver glycogen with a DB of 6.6% is equal to 15.¹² Following the development of more sophisticated techniques, such as high-performance chromatography or capillary electrophoresis, the ACL is being measured experimentally by integration of the peaks per DP divided per total area of the chromatogram.²⁷ This new application enabled scientists to collect more accurate data on the ACL, and also to investigate the CLD.

The analysis of the CLD on glycogen samples revealed that this feature correlates with several factors. One of them is the species object of the studies, *e. g.* healthy mouse liver glycogen

has chains predominantly between DP16 and DP20, whereas oyster glycogen shows a large abundance of DP6 in the distribution.^{28,29} The other variable is the presence of pathological conditions in the selected source. Sullivan *et al.*³⁰ analysed the CLD of diabetes type II and observed a small variation in the distribution of the chains compared to the one from glycogen extracted from healthy mice liver. Yet, in other studies from Sullivan *et al.*³¹ it was demonstrated the dramatic change in the CLD of mice bearing metabolic diseases, such as GSD type IV or Lafora disease (LD) (**Fig. 3**). Thus, the investigation of the CLD of glycogen represents an important tool, more informative than the ACL.

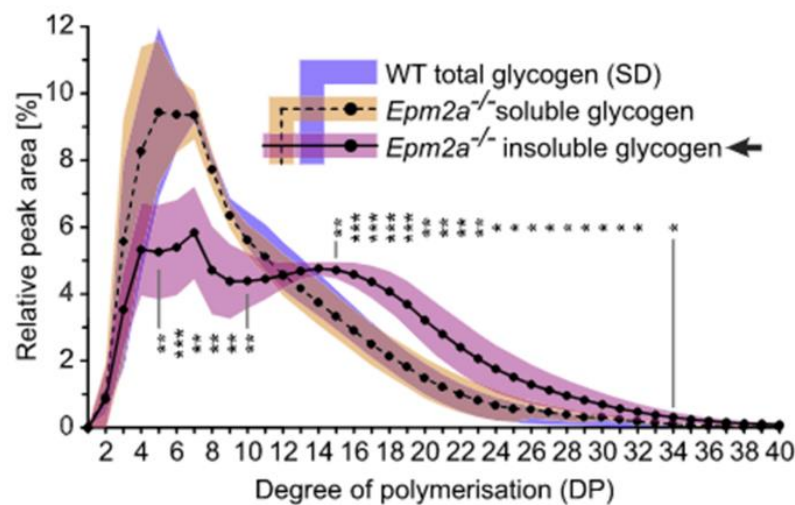


Figure 3 Chain length distribution of glycogen from skeletal muscles of healthy mice (in purple) and from mice with Lafora Disease (*Epm2a*^{-/-}, in pink or yellow). Image taken from Sullivan *et al.*³¹

1.1.3. The organization of glycogen molecules into granules

Each glycogen molecule is associated with proteins, such as laforin and malin, involved in its metabolism resulting in an organelle-like structure called *glycosome* or *glycogen granules*.⁸ Studies performed by electron microscopy² and light scattering^{8,32} showed that there are two types of granules. The first type are β -granules with a size of 20-40 nm and are located in liver and skeletal muscles, while the second ones are the α -granules, they can reach a size of almost 300 nm and are observed only in liver.

The aggregation of glycogen molecules into granules is still poorly understood. One of the most debated hypotheses is the presence of proteins that promote the aggregation between small granules,^{8,33} but experimental evidence on a protein component with this role has not been reported so far. The presence of one type of granules instead of the other, however, seems to play a role in the maintenance of glucose homeostasis, as observed in mice with

diabetes type II.^{34,35} In these animal models, it was demonstrated that the aggregation of β -granules into α -granules was impaired. Since the β -granules facilitate the rapid release of glucose in skeletal muscles, it was proposed that the uncontrolled release of glucose in the blood circulation was also caused by the presence of small rather than large glycogen granules.³⁶ However, it was not clear whether the presence of β -granules was a consequence of or a cause of diabetes, and further investigations are required to address this point.

1.2. Glycogen metabolism

Glycogen metabolism is controlled by hormones (**Fig. 4**).³⁷ In the feeding state, insulin promotes the uptake of glucose in the cells *via* glucose transporters (GLUT). The transported glucose is then converted into UDP-glucose prior its use. Glycogen synthase (GS) is also activated by insulin, and it catalyses the synthesis of glucan chains using UDP-glucose as building block. The activity of GS is balanced with Glycogen branching enzyme (GBE) whose role is to form branching points. Another enzyme called glycogenin (GN) is involved in glycogen synthesis and its function is to form a primer chain for GS activity. The activation of GN seems to involve a protein called *glycogenin-targeting protein* (GNIP) but its role in glycogen synthesis is still unclear.³⁸

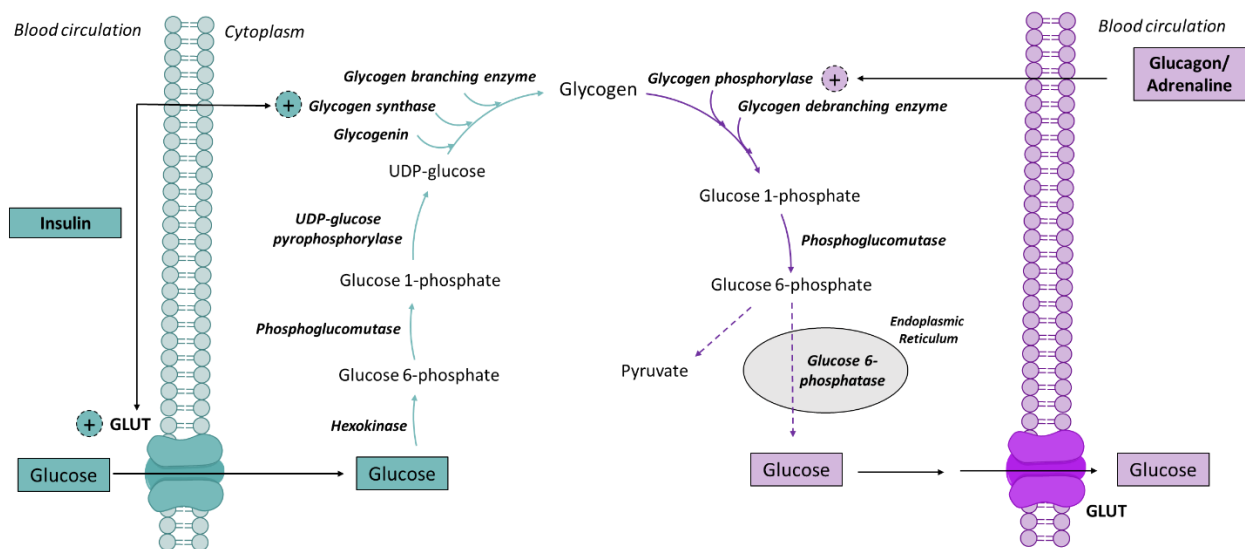


Figure 4 Schematic illustration of glycogen synthesis (in green) and degradation (in purple).

During the fasting state or exercise, glucagon (in liver) and adrenaline (in skeletal muscles) activate an enzymatic cascade that terminates with the phosphorylation of glycogen phosphorylase (GP). The phosphorylated GP (active form) catalyses the removal of glucose residues from glycogen as glucose 1-phosphate (G1P), while the branching points are digested

by glycogen debranching enzyme (GDE). Successively, the G1P is converted into glucose 6-phosphate (G6P) by phosphoglucomutase *via* a reversible reaction. At this point, G6P can enter the glycolysis pathway (in skeletal muscles) to form pyruvate or can be dephosphorylated by glucose 6-phosphatase in the endoplasmic reticulum (ER) to release glucose into blood circulation.⁶

Fig. 4 shows a simplified version of glycogen metabolism, and the number of signalling molecules involved in the regulation of glycogenesis and glycogenolysis are more than those illustrated.³⁹ However, from **Fig. 4**, it is possible to understand that each reaction is highly dependent on the product of the previous reaction. In fact, the deficiency of a single enzyme involved in one of the metabolic pathways generates a cascade of events that interferes with the overall metabolism, as observed in GSDs. Thus, the scope of this section is to review the structural properties of the enzymes directly involved in the synthesis and degradation of glycogen, and how their activity is impaired by GSDs.

1.2.1. Glycogen Synthesis

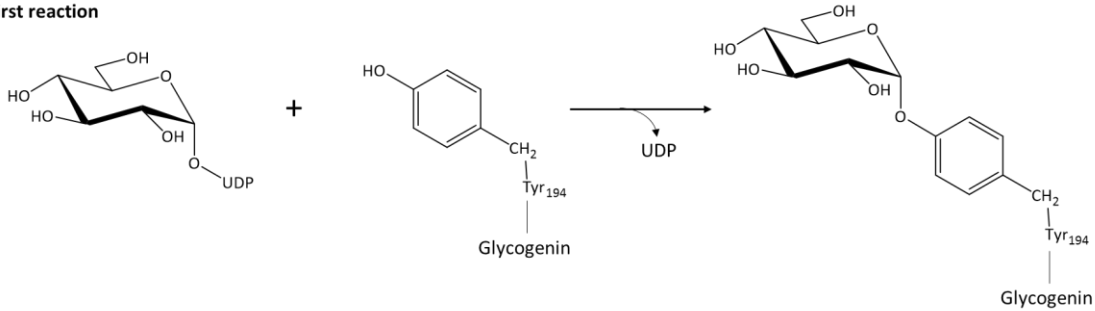
1.2.1.1. *The role of glycogenin as initiator of glycogen synthesis*

When GS and GP were discovered,⁴⁰ scientists believed these two enzymes to be responsible for the synthesis of glycogen. *In vitro* experiments, however, demonstrated that these enzymes were not sufficient to initiate the synthesis of a glucan chain, starting solely from UDP-glucose or G1P. In 1975, Krisman and Barengo⁴¹ extracted, from rat liver, a protein with the molecular weight of 38 kDa covalently bound to glycogen. Later, this protein was named glycogen-initiator synthase or glycogenin (GN),⁴² as its function was correlated with the *de novo* synthesis of glycogen.

GN belongs to glycosyltransferase (GT8) family, and it carries out a peculiar, if not unique, activity. This protein accounts two chemically distinct reactions and serves as the acceptor substrate for glucan chain initiation (**Fig. 5**).^{43,44} In the first reaction, GN catalyses the self-glycosylation of its Tyr194 residue through the formation of glucose 1-*O*-tyrosyl linkage using UDP-glucose as donor. In the second reaction the glucose covalently bound to the protein is elongated to form a linear glucan chain with an average of 11 units.⁴⁵ The importance of Tyr194 was confirmed by Lin *et al.*⁴³ by showing that the substitution of Tyr194 with Phe inhibited the self-glycosylating activity. To date, GN is known to be expressed in muscles

(*glycogenin-1*) and liver (*glycogenin-2*).⁴ The two isoforms differ in the position of the amino acid involved in the linkage of the first glucose residue: in *glycogenin-1*, the tyrosine-O-glucose bond is at position Tyr195, whereas in *glycogenin-2* the glucose is attached to Tyr228.⁴⁶

First reaction



Second reaction

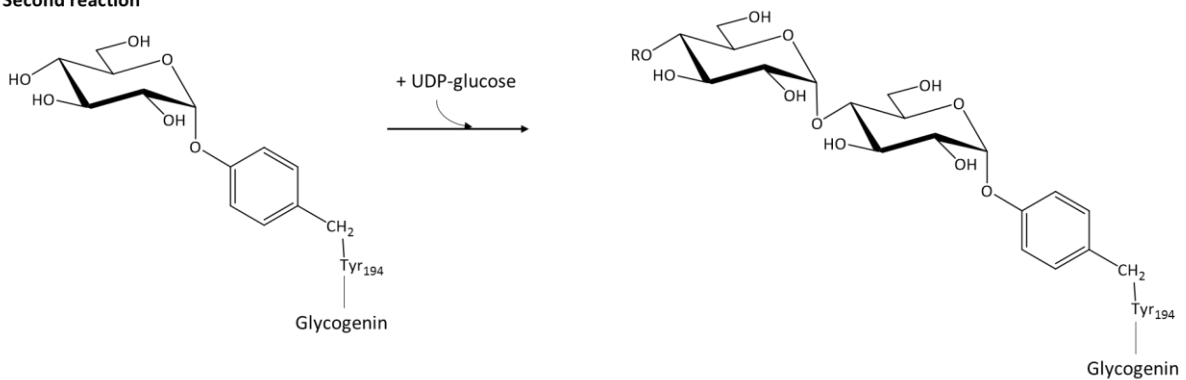


Figure 5 Mechanism of self-glucosylation of glycogenin; R = glucose units.

In 2002, Gibbons *et al.*⁴⁴ solved the crystal structure of GN (**Fig. 6**), showing that the N-terminal residue has the function of binding to UDP-glucose, whereas a loop of 35 residues at its C-terminus forms a complex with GS. The crystal structure also revealed that the Tyr194 was located approximately 15 Å from the active site for UDP-glucose, an unfavourable distance for GN to carry out its self-glucosylation.⁴⁴

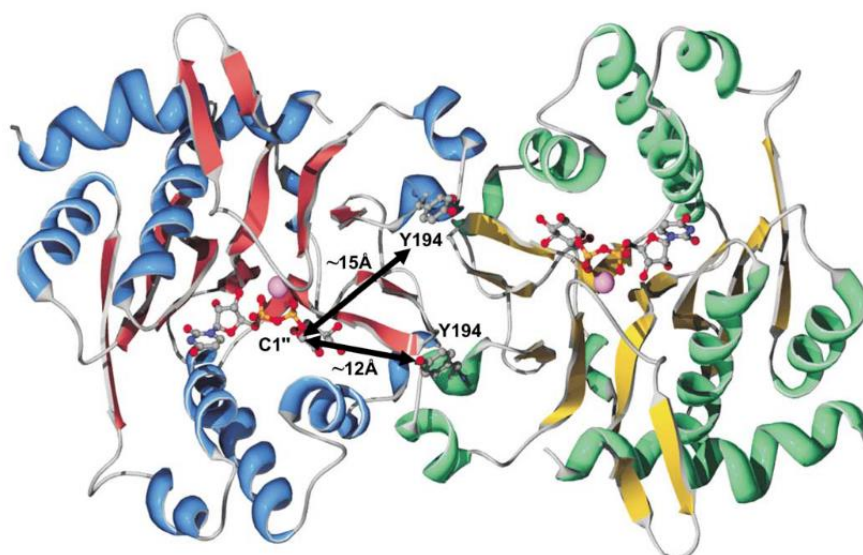


Figure 6 Crystal structure of glycogenin taken from Gibbons *et al.*⁴⁴ The dimer of glycogenin is represented with ribbons: α -helices coloured in blue and green; β -sheets coloured in red and yellow; and coils coloured in grey. UDP – glucose molecules and Tyr194 sidechains are shown as ball-and-stick models. The distances between the UDP glucose and the Tyr194 hydroxyls are indicated with the arrows.

Lin *et al.*⁴⁷ proposed a mechanism performed by GN to initiate glycogen synthesis, which was later confirmed by several investigations (**Fig. 7**).^{44,48,49} GN is found *in vivo* as a dimer and the Tyr194 (Tyr195 in human GN) is placed in the contact surface of the two subunits. To initiate the auto-glycosylation, one monomer transfers glucose units to the Tyr194 of the opposite monomer *via* an inter-subunit mechanism. After Tyr194 has acquired four to seven glucose units,⁴⁷ the short oligosaccharides can be elongated by *intra*-subunit glycosylation within the same monomer.

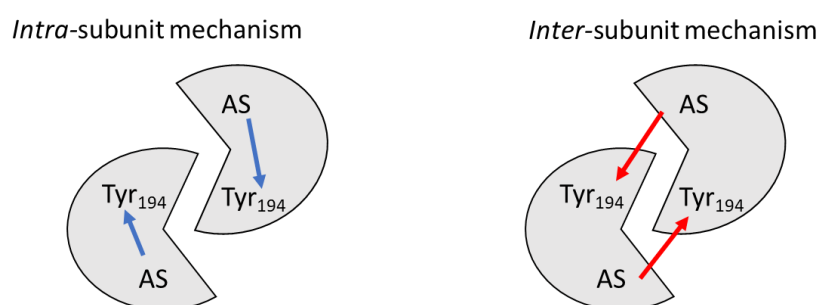


Figure 7 Mechanism of glucosylation of the Tyr194. The intra-subunit mechanism consists in the transfer of the glucan chain from the active site to the amino acid residue. The inter-subunit mechanism involves both monomers, and the glucan chain is transferred from the active site of one monomer to the Tyr194 of the opposite monomer. AS = active site.

Further investigations on GN self-glycosylation were published in 2011.⁵⁰ The co-crystallization of GN with UDP-glucose showed that a native glucan chain induces a

conformational change of the protein. This causes the movement of a “loop” from the active site enabling the entrance of UDP-glucose. Nevertheless, it is not clear how this mechanism promotes the self-glycosylation of GN.

With the elongation of the primer chain by GN, the catalytic efficiency of this enzyme decreases dramatically with the increase of the chain length, as demonstrated by Romero *et al.*⁵¹ The authors found that after reaching a chain length of 13 glucose residues, GN was no longer able to transfer glucose units to the native chain due to the helical structure adopted by the protein-bound oligosaccharide. As a consequence, GS takes over the synthesis while GN remains linked to the oligosaccharide to form the core of the newly synthesised glycogen molecule.

1.2.1.2. *The elongation of the primer chain by glycogen synthase*

GS belongs to glycosyltransferases (GT3) family and is expressed in two isoforms found in skeletal muscles (GS-1) and liver (GS-2). The activity of GS consists in the addition of glucose units to the non-reducing end of the existing chain by formation of new $\alpha(1,4)$ -glycosidic bonds.⁵²

Despite the fact that GS was discovered almost a century ago,⁵³ the crystal structure was initially investigated by Buschiazzo *et al.*⁵⁴ in 2004 and further studied in 2010 by Baskaran *et al.*⁵⁵ GS presents multiple phosphorylation sites at its N- and C-terminal residues that are phosphorylated in a hierarchical fashion, meaning that the recognition of one phosphorylated site promotes the addition of phosphate groups to the following one.^{56,57}

GS catalyses the rate-limiting reaction in the glycogenesis, and as such, its regulation is strictly controlled by phosphorylation or promoted allosterically by G6P. The implications of the phosphorylation and allosteric activation on GS structure were elucidated only in 2022 when Marr *et al.*⁵⁸ provided an in-depth study on the full-length crystal structure of GS and its complex with GN. The authors demonstrated that four GS molecules interact with four units of GN resulting in an octameric complex with GN is linked to GS through its C-terminal residue (**Fig. 8**). This conformation exposes the C-terminal residues of one tetramer to the N-terminal of the other tetramer creating a contact surface containing the main phosphoregulatory unit ($\alpha 22$) and phosphorylation site (S641). When GS is in the inactive and phosphorylated state, the interaction of two amino acid residues (R588 and R591) with S641 within the $\alpha 22$ region

locks the structure of GS in a “tense” conformation. The dephosphorylation by phosphatases or the allosteric binding of G6P “relax” the structure promoting the activation of the enzyme.

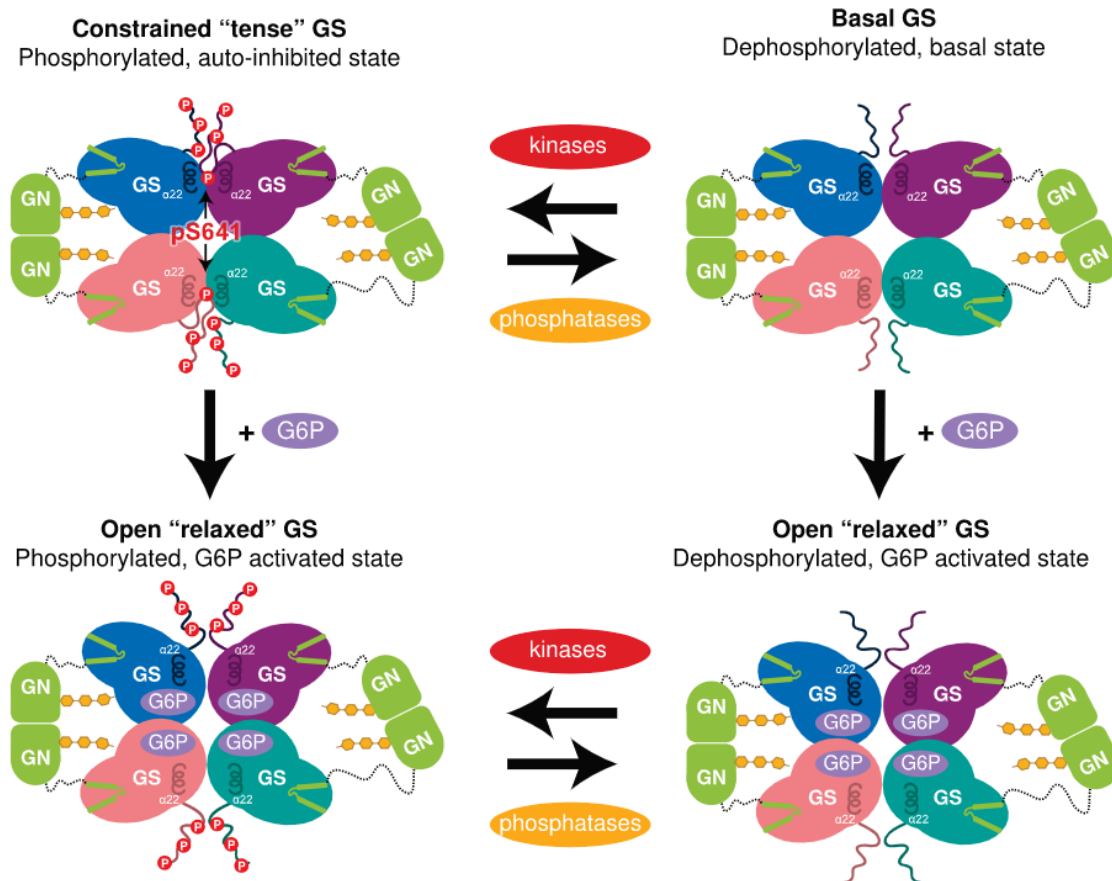


Figure 8 Mechanism of activation of GS in complex with GN. GN interacts with GS to direct the primer chain into the GS active site for elongation. GS is regulated by allosteric activation and inhibitory phosphorylation. Phospho-S641 (pS641) interacts with the regulatory helices $\alpha 22$ to cause enzyme inhibition. This can be relieved by glucose-6-phosphate (G6P), with or without phosphatases, to reach a high activity state. Kinases can phosphorylate GS to inhibit the enzyme. Image taken from Marr *et al.*⁵⁸

When the crystal structure of GS was elucidated, Baskaran *et al.*⁵⁹ noticed the lack of a carbohydrate-binding module (CBM) commonly present in enzymes involved in the metabolism of polysaccharides.^{60,61} In GS, four maltodextrin-binding sites, distinct from the active site, play the same role of the CBM by binding glycogen chains or the primer oligosaccharide generated by GN.⁵⁹

1.2.1.3. The formation of new branching points by glycogen branching enzyme

The branching process is important to maintain the physicochemical properties of glycogen, and dysfunctions of this mechanism result in insoluble aggregates as seen in GSD type IV.⁶²

For this reason, GBE plays a crucial role in glycogen synthesis, and in determining the degree of branching of a glycogen molecule.⁶³

The crystal structure of human GBE (**Fig. 9**) was solved by Froese *et al.*⁶² in 2015 following its expression in insect cell. GBE has an elongated structure containing four regions: the N-terminal segment, the carbohydrate-binding module 48 (CBM48), the catalytic core in the central area, and the α -amylase C-terminal domain. The CBM48 found in a distinct pocket from the catalytic cleft represents one of the binding sites on the enzyme surface responsible to anchor glycogen. In addition, this non-catalytic pocket was proposed as a 'molecular ruler' to select the substrates used for the branching activity.^{62,64}

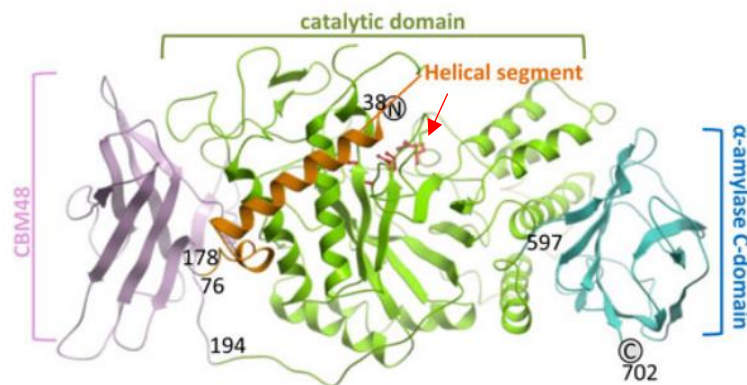
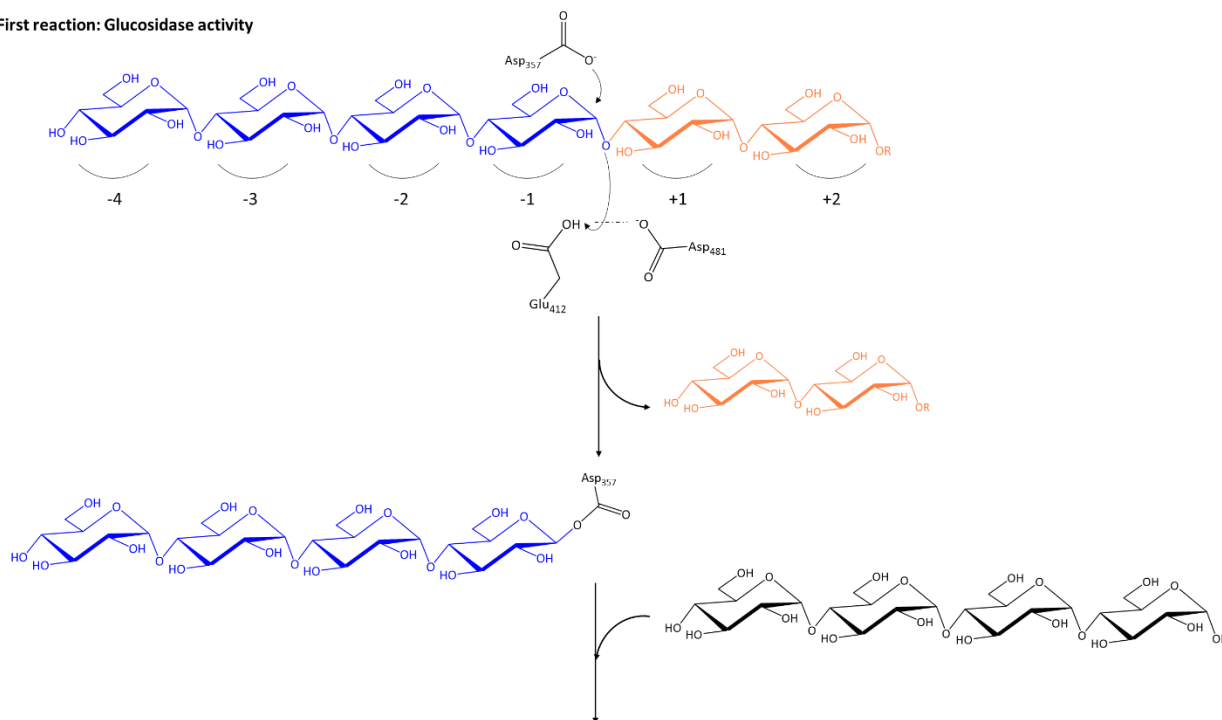


Figure 9 Crystal structure of hGBE via orthogonal views. The N-terminal helical segment is in orange, the CBM48 is in pink, the central catalytic domain in green and the C-terminal domain in blue. The catalytic triad Asp357-Glu412-Asp481 is shown as red sticks and indicated with the red arrow. Image taken from Froese *et al.*⁶²

The active site of hGBE is placed in the central region of the enzyme, and a catalytic triad formed by Asp357, Glu412 and Asp481 is responsible for the two activities of GBE (**Fig. 10**): hydrolysis and glycosyltransferase activity. The first reaction consists of the cleavage of the $\alpha(1,4)$ -glycosidic bond from a glucan chain. The chain is approached from the non-reducing ends, and the cleavage site (between -1 and +1) is oriented towards the Asp357. The covalent linkage of the glucose residue with Asp357 forms an intermediate that promotes the release of the remaining glucan chain bearing the reducing end. In the second reaction, the Asp357 is displaced by the hydroxyl group in C6 of a glucose residue part of the same (*intra-molecular transfer*) or another (*inter-molecular transfer*) glucan chain. The amino acids Glu412 and Asp481 facilitate the formation of the new $\alpha(1,6)$ -glycosidic bond. By following this mechanism, GBE doubles the number of accessible residues (number of non-reducing ends) to GS for the elongation and it promotes the synthesis of one branching point at the time.

First reaction: Glucosidase activity



Second reaction: Transglucosylation activity

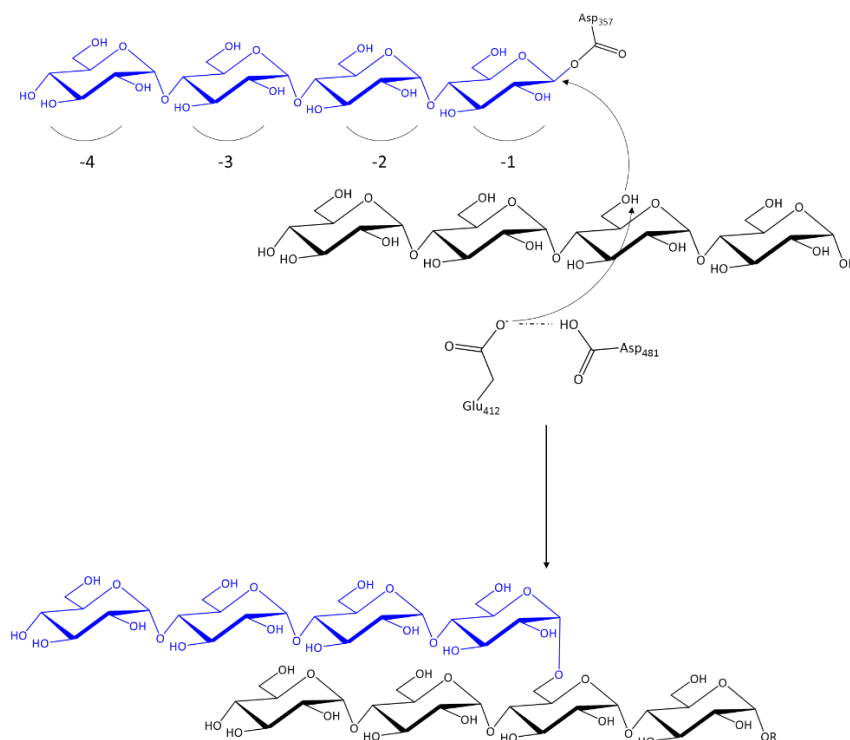


Figure 10 Mechanism of branching of GBE using the catalytic triad Asp357, Glu412, and Asp481. Image adapted from Froese et al.⁶²

The crystal structure of GBE did not provide insights into its substrate specificity towards chains of variable lengths due to the unsuccessful co-crystallization of GBE with maltoheptaose.⁶² For this reason, the length of the branched chain, the distance between

branching points, and the selectivity towards inter vs. intra molecular transfer is still poorly understood.

Despite the challenges related to the investigation of the substrate specificity of GBE *via* crystallization, there are other potential approaches that can be investigated for this purpose. Human GBE shares 54% sequence homology of the central catalytic core (aa 184-600) with *Oryza sativa* branching enzyme I (*OsBEI*), and 28% with GBE from *Mycobacterium tuberculosis* (*MtGBE*).⁶² The homologies that hGBE shares with these branching enzymes are mainly within the active site and the CBM48 domain, and they can be exploited to speculate on the substrate specificity of hGBE. Among the mentioned species, extensive studies have been performed on the activity of starch-branching enzymes such as *OsBEI*.⁶⁴ It was demonstrated that this *OsBEI* prefers to use unbranched substrates, such as amylose, with a minimum length of 15 glucose residues, and it transfers short glucan chains between 6 and 14 glucose residues.^{65,66} If the same substrate specificity is applied to hGBE, the structure of glycogen would be expected to be populated by chains between DP6 and DP14. This hypothesis is based on the assumption that the outer layers of glycogen are branched by GBE using its minimum substrate length as proposed by Deng *et al.*¹⁵ To date, information on the chain length distribution of human glycogen is not available, and thus this hypothesis cannot be yet supported by scientific evidence. However, the analysis of the chain length distribution of glycogen represents an alternative means to investigate the substrate specificity of GBE of a certain species as will be presented in Chapter 4 using experimental data.

1.2.2. Glycogen degradation

1.2.2.1. *The initiation of glycogen degradation by phosphorolysis*

GP was discovered in 1939 by the Nobel laureates Cori and Cori,⁵³ and it was crystallized in 1943 by Green and Cori.⁶⁷ This enzyme controls the glucose homeostasis by mobilization of glycogen deposits (rate-limiting enzyme),⁴ and as such it is involved in many studies aimed at reducing the amount of circulating glucose in type II diabetes patients.⁶⁷⁻⁷⁰

The role of GP is to release G1P from glycogen branches starting from their non-reducing ends until three or four glucose residues before the branching point. The remaining stubs are then transferred onto other chains by GDE.^{54,71} Although phosphorylases have reversible activity, as observed for starch phosphorylases,^{72,73} the *in vivo* phosphorolysis of glycogen by GP is considered to be regulated irreversible due to the high ratio of P_i /G1P within the cells.

GP exists in two interconvertible forms, *a* and *b*, by allosteric ligands or inhibitors, e. g. AMP and caffeine, that bind to different binding sites within the protein (**Fig. 11**).⁶⁸ GP*b* is the inactive form of the enzyme that can be found in the inactive “tense” (T) state, or “relaxed” (R) state. The passage from T to R state is caused by AMP that induces a conformational change in the protein. When GP must be activated to promote glycogenolysis, the GP*b* in the R state is phosphorylated at its Ser14 residues by phosphorylase kinase (PKA) and converted into the GP*a* active and R state. The inactivation of GP*a* can occur by allosteric inhibition by ATP, glucose, caffeine, indole, and carboxamides, leading to the T inactive but still phosphorylated state. Finally, the conversion from GP*a* to dephosphorylated GP*b* is carried out by the phosphatase PPP1R3-PP1.^{67,68,74} This last protein is crucial in the regulation of glycogen synthesis and degradation. The C-terminal residue of the GP*a* interacts with PPP1R3-PP1, a glycogen-targeting subunit of protein phosphatase 1 (PP1), which is also responsible for activating GS. However, the dephosphorylation of GS by PPP1R3-PP1 cannot occur until this protein is linked to GP*a*. Only when GP*a* is dephosphorylated and in its inactive form, PPP1R3-PP1 can activate GS by dephosphorylation. For this reason, glycogen synthesis cannot occur at the same time of glycogen degradation.⁷⁴

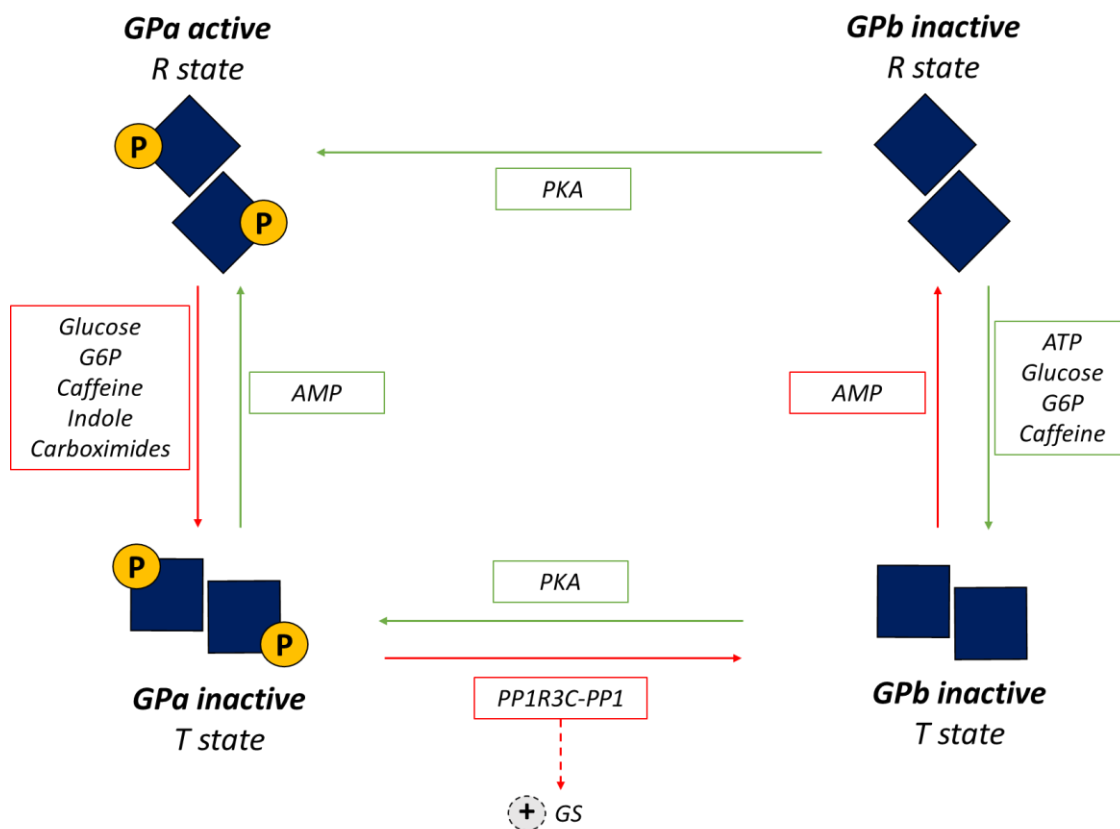


Figure 11 Mechanism of activation of glycogen phosphorylase.

1.2.2.2. Removal of branching points by glycogen debranching enzyme

Following the shortening of the chains by GP, the resulting structure of glycogen bearing maltotetraose or maltopentaose stubs undergoes debranching by GDE (**Fig. 12**). While debranching enzymes acting on starch, such as isoamylase and pullulanase, directly cleave the $\alpha(1,6)$ -glycosidic bonds, GDE debranches the structure of glycogen with a unique *indirect* two-step mechanism.⁷⁵ At first, a maltotriose residue resulting from the phosphorolysis is cleaved and transferred onto the same (*intra*-molecular mechanism) or another (*inter*-molecular mechanism) glucan chain. Then, the remaining glucose residue linked by a $\alpha(1,6)$ -glycosidic bond is removed and released as free-glucose. This mechanism is possible for GDE dual activity as glucosidase and transferase that are carried out by two distinct active sites.

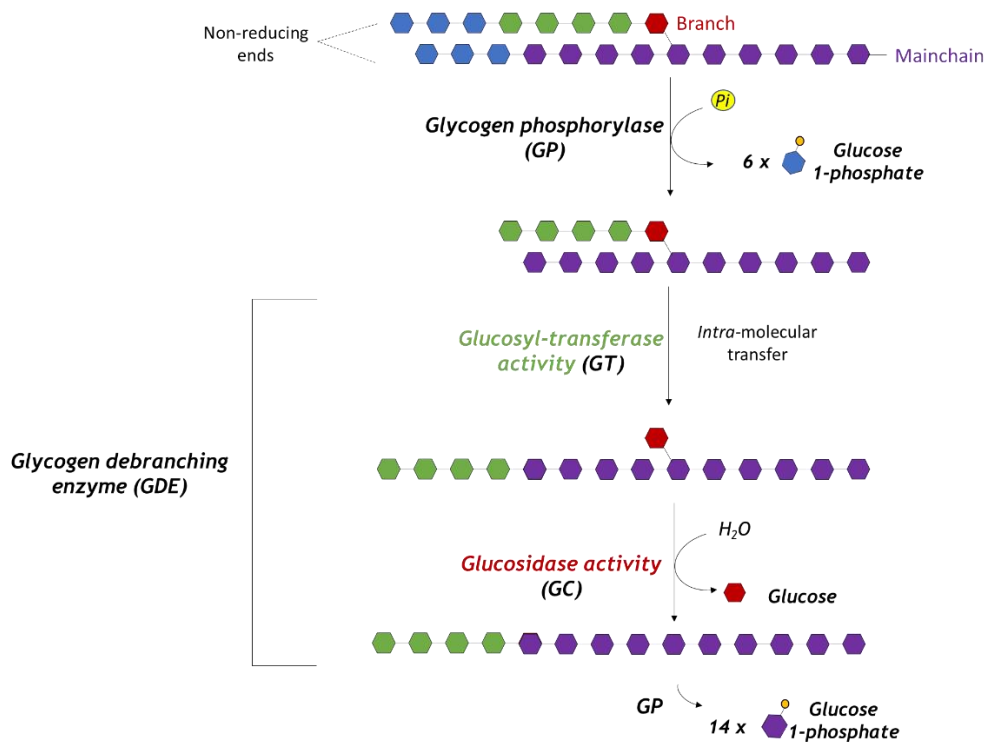


Figure 12 Schematic representation of GDE activity. The hexagons of different colours indicate glucose units linked by $\alpha(1,4)$ - or $\alpha(1,6)$ - glycosidic bonds.

The crystal structure of GDE (**Fig. 13**) was solved by Zai *et al.*⁷⁵ by expressing GDE from *Candida glabrata* (38% sequence identity to the human GDE) in *E. coli*, and the interactions with glycogen were investigated by co-crystallization of the protein with maltopentaose. GDE has an elongated structure with four domains. The N-terminal region hosts the active site for the glucosidase (GC) activity which is located at the opposite site of the C-terminal region where the glycosyltransferase (GT) activity occurs. In addition, two domains (M1 and M2) create an intermediate region that widely interacts with both N- and C-termini, and that possesses multiple non-catalytic binding sites.

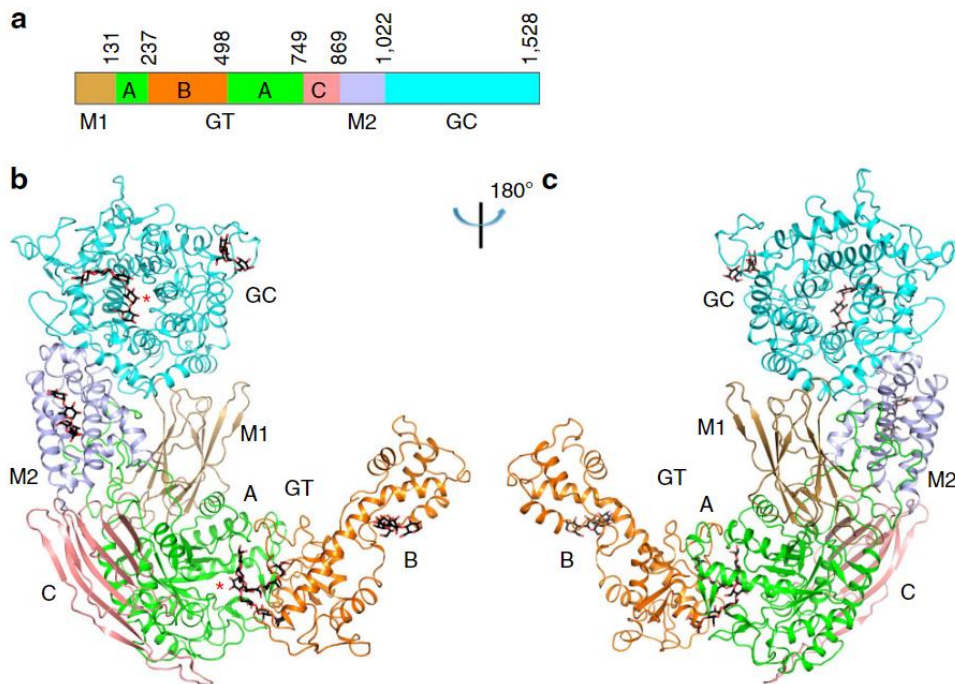


Figure 13 Crystal structure of GDE and the arrangement of the domains. Domains M1, M2 and GC, and the GT subdomains A, B and C are colour coded. The views are related by a 180° rotation around the vertical axis. The red stars indicate the active sites. Bound oligosaccharides are shown in stick representation with their carbon atoms in black. Image taken from Zhai *et al.*⁷⁵

The co-crystallization of GDE with maltopentaose in the GT active site showed that two oligosaccharides corresponding to the branch (four glucose residues) and main chain (five glucose residues) can be fitted into the pocket, whereas chains longer than five glucose residues caused steric clashes. These studies suggested that the donor chain cannot be longer than five residues whereas the acceptor chain can be of any size. The substrate specificity suggested by the described crystal structure was later supported by the studies of Watanabe *et al.*⁷⁶ and Ikeda *et al.*⁷⁷ Both research groups demonstrated that GDE uses the stubs resulting from the phosphorolysis as donor substrates to be transferred onto an unbranched chain longer than 5 units. For this reason, GP becomes the rate-limiting enzyme, because without the shortening of the chains by this enzyme, GDE cannot act upon long chains.

Interestingly, the authors showed by TLC analysis that the glycosyltransferase activity of GDE with maltopentaose resulted in a series of oligosaccharides from 3 to 7 and more glucose residues.⁷⁵ Based on the activity of GDE, a maltopentaose should be cleaved between the first and second glucose residues from the reducing end, thus releasing a maltotetraose that is transferred onto another maltopentaose, and a glucose residue. However, no glucose residue was observed. Furthermore, a chain with three glucose residues was also found as one of the

products. This means that GDE may have transferred free-glucose residues onto another chain or to other glucose residues to form a new chain as a DP3. This hypothetical mechanism suggests that the single glucose units released from the cleavage of each branching points may be “recycled” by GDE to elongate existing chains. This is a role of GDE that would be of interest for further investigations.

1.2.3. Lysosomal degradation of *mis-branched* glycogen

An alternative pathway to the cytosolic degradation of glycogen is the lysosomal digestion that solely involve the enzyme acid α -glucosidase (AAG) to generate glucose.⁶ Lysosomes degrade material taken up from the inside or outside of the cells *via* autophagy, which is the same way used to take glycogen. Interestingly, glycogen granules were found in these organelles in the form of large particles, and it naturally arises the question about its role and its location in such unexpected part of the cells. In addition, the importance of this metabolic pathway is highlighted by the onset of a congenital disorder known as Pompe’s disease or GSD type II when AAG is defected.^{6,78}

Considering the role of lysosomes in the break-down of malfunctioning proteins or other molecules, it was proposed that the glycogen in these organelles is *mis-branched*.⁷⁹ This means that aberrant glycogen structures are recognised and destroyed by the lysosomes before they are accumulated in the cytosol, suggesting a “quality control mechanism”. This interesting aspect of the lysosomes role was postulated successively to the findings that HOIL-1 mutants mouse models accumulate insoluble glycogen structures, known as polyglucosan bodies (PB). HOIL-1 is a ubiquitin ligase that ubiquitylates the hydroxyl groups of serine and threonine residues of proteins that must be degraded. This protein is a small component of a larger complex known as Linear Ubiquitin Chain Assembly Complex (LUBAC) which was found to be associated with glycogen. The mechanism proposed and demonstrated by Kellsall *et al.*⁸⁰ consists in the ubiquitylation of poorly branched chains by HOIL-1 at the C6-hydroxyl group leading to their recognition by the glycophyagy machinery and uptake into lysosomes for their hydrolysis (**Fig. 14**).

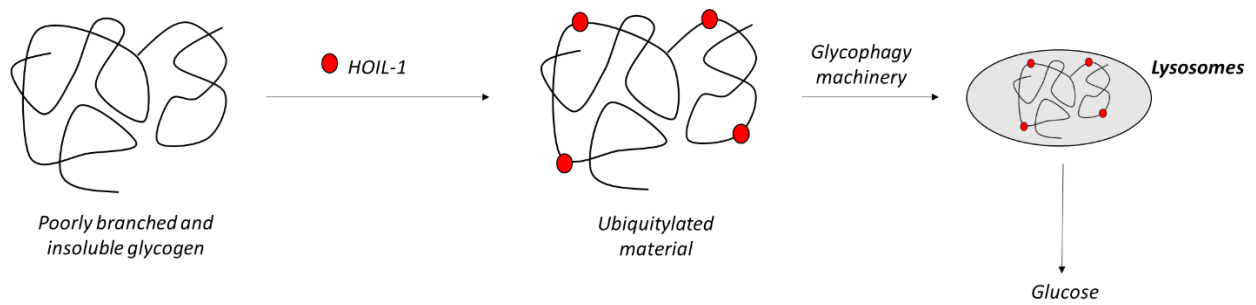


Figure 14 Hypothetical mechanism of ubiquitylation of mis-branched glycogen by HOIL-1, followed by lysosomal degradation.

Other studies focused on the investigation of Lafora bodies (LB) in Lafora disease (LD) also highlighted the role of lysosomes in the digestion of *mis*-assembled material.^{81,82} Laforin and malin are a protein phosphatase and a ubiquitin-ligase, respectively. They form a complex that is associated with glycogen in the first stages of its synthesis, but their role in this process is still unclear. Among the two of them, Laforin binds to several glycogen-associated proteins and one of them is the starch binding protein 1 (Stbd1), which in turn interacts with an autophagy protein (GABARAPL1).⁸³ When there is a mutation in the genes encoding for laforin or malin, two consequences are observed: the accumulation of hyperphosphorylated and insoluble glycogen in the cytosol, and dysfunctions in the processes of autophagy.⁷⁹ Being laforin a phosphatase, it was proposed that this enzyme dephosphorylates glycogen during its synthesis, and that deficiencies in this process lead to the hyperphosphorylation of glycogen that precipitate in the cell. These structures cannot be removed from the cytosol because laforin activates the mTOR (mammalian Target Of Rapamycin), the master inhibitor of autophagy, that might somehow inhibit the recruitment of *mis-branched* glycogen by Stbd1 for glycophagy. However, this is a hypothesis that requires further experimental evidence to substantiate it.

1.3. Glycogen Storage Diseases (GSDs)

Glycogen metabolism plays a key role in the regulation of blood glucose, and its importance is further highlighted by the fact that deficiencies of enzymes involved in glycogen synthesis and degradation have consequences in the overall organism. Glycogen Storage Diseases (GSDs) are the class of metabolic disorders that impair glycogen metabolic pathways.³ The clinical manifestations of GSDs depend on the relative expression and type of defected enzyme since glycogen deposits can be found in several organs, such as liver, skeletal muscles, heart, and brain. However, fasting and ketotic hypoglycaemia, hepatomegaly, and muscle weakness, are the common hallmarks for GSDs. To date, several GSDs are known and classified based on the enzyme affected by the genetic mutation as showed in **Fig. 15**. It is important to mention that only a part of the GSDs *directly* affect the metabolism of glycogen, whereas the others affect enzymes that are involved in its regulation or in the glycolysis pathways. Nevertheless, the use of glycogen or glucose as energy storage and fuel is hindered regardless of the enzyme affected by GSDs.

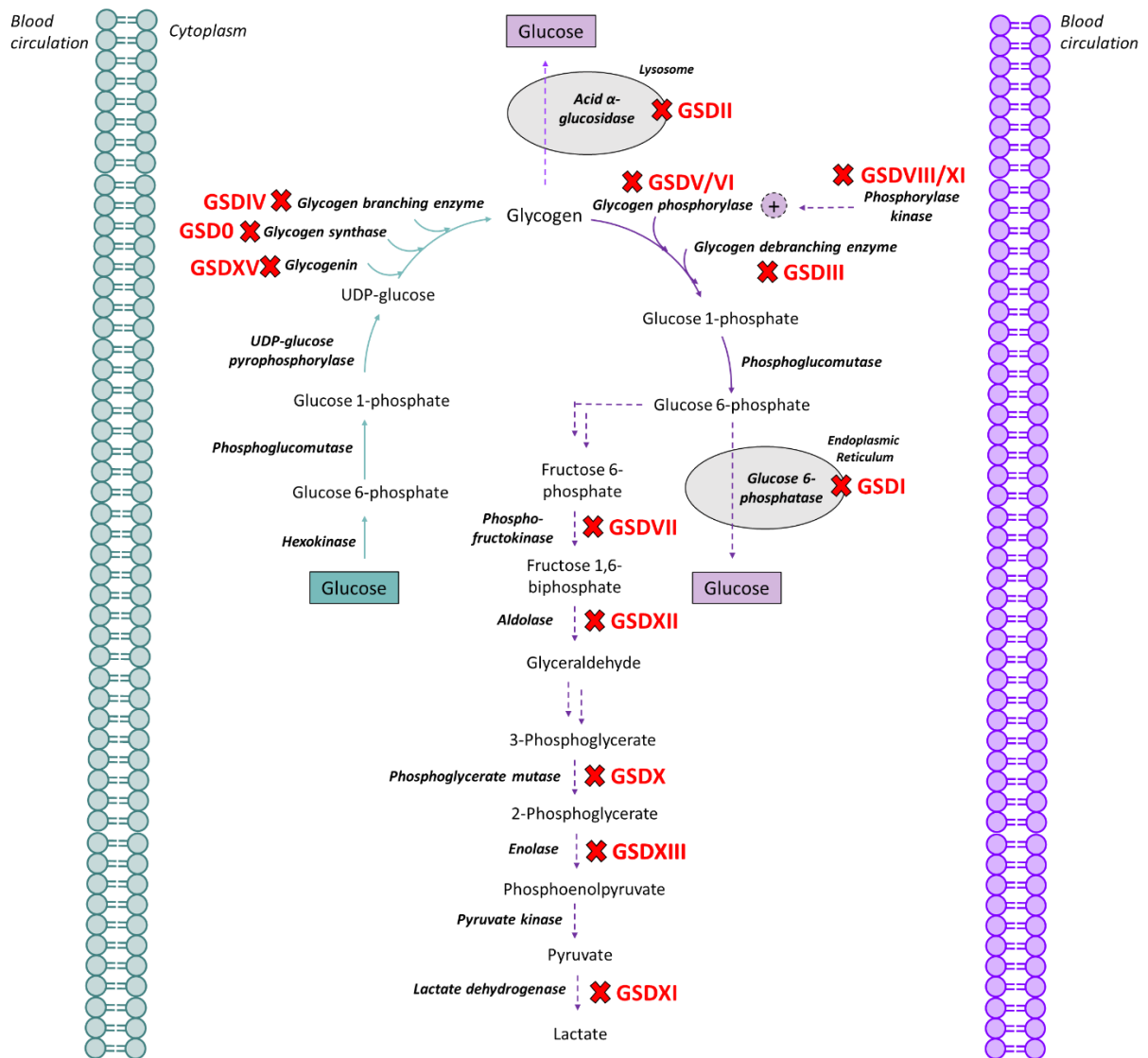


Figure 15 Map of GSDs defected enzymes involved in glycogen synthesis (in green) and degradation (in purple), and other related pathways.

The focus of the following section is on liver GSDs that have a direct impact on glycogen metabolism. The information available in literature is reviewed to gain an in-depth knowledge on the amino acids affected by the genetic mutations and their consequences on the activity of the enzymes and glycogen structure. Among them, GSDI is *indirectly* related to glycogen degradation, and it is the only one selected to study how an *indirect* mutation in glycogen metabolism may affect the structure of glycogen.

1.3.1. Glycogenin deficiency – GSD type XV

GSD type XV, known as *polyglucosan body myopathy 2* is caused by mutations in the *GYG1* gene that encodes for the isoform *glycogenin-1* expressed both in liver and muscles. The first case of a patient affected by GSDXV was reported in 2010 by Moslemi *et al.*,⁸⁴ and since then

30 patients have been identified with this disorder. The amino acids affected by the mutations were mainly involved in the stabilization of the non-reducing end of the growing chain (Asp102 and Asp163) and in the chain “loop” responsible to accommodate UDP-glucose into the active site (Thr83). In both situations, the glycosylating property of GN was inhibited.⁵⁰

Considering the crucial role of GN in the *de novo* synthesis of glycogen, glycogen deposits were not expected to be identified in the patients. Surprisingly, the absence of *glycogenin-1* was associated to the storage of glycogen and polyglucosan bodies in the affected patients.⁸⁴ The presence of glycogen was assessed by Periodic Acid-Schiff (PAS)-staining of the tissue and the results showed an accumulation of abnormal material identified as polyglucosan bodies.⁴⁶ However, no structural studies on glycogen were performed to confirm the abnormal chain lengths commonly associated with polyglucosan bodies. These findings challenged previous studies that indicated the role of GN as the initiator of glycogen synthesis. One of the hypotheses is that the second isoform of GN is relocated in the affected tissues,⁸⁴ but evidence in support of that has not been reported. Another hypothesis speculates on the role of GS as primer of the glycogen synthesis. In bacteria and starch, there is no evidence of a GN-like protein and synthases are responsible for the synthesis of the polysaccharide by elongation of a short oligosaccharide.^{85,86} Thus, it is possible that GS in animal species may possess the same auto-glycosylating or primer function of GN. Nevertheless, these are only speculations that will require further investigations.

1.3.2. Glycogen synthase deficiency – GSD type 0

GSD type 0 is caused by deficiency of the hepatic isoform of glycogen synthase (*GYS2*).⁷ The clinical manifestation of GSD0 is unusual if compared with the other GSDs. It does not show hepatomegaly or accumulation of glycogen in liver, and it is rather characterised by ketosis with atypical symptoms such as lethargy and nausea, and no storage of the polysaccharide.⁸⁷ The lack of glycogen reservoir is consistent with the role that this enzyme plays in glycogen synthesis, but the clinical features are not as deleterious as expected to be in absence of such an important component. In fact, GSD0 is often incorrectly diagnosed as diabetes type II.⁸⁸ GSD0 has a frequency of less than 1% of all GSD cases,⁸⁹ and there is insufficient information to understand the biochemical aspect of this disorders. Several mutations⁸⁸ have been identified in patients bearing GSD0, and the relative consequences on the activity and structure of the enzyme are still poorly understood. Based on the crystal structure and on the

amino acids substituted by genetic mutations, it is possible to speculate on the consequences that GSD0 has on the activity of GS. For instance, the substitution of Arg582 with Lys may impair the binding of G6P to GS.⁸⁸ Other mutations, however, are more challenging to understand because they occur in part of the protein not involved in any of the known functions described in literature, e. g. the substitution of Thr445 with Arg is found in an intermediate region between two subunits and far from the phosphoregulatory unit and active site.

1.3.3. Glycogen branching enzyme deficiency – GSD type IV

GSD type IV is the genetic mutation that affects the activity of GBE. The first cases were reported by Illingworth *et al.*⁹⁰ by analysis of liver samples from patients presenting hepatomegaly and hyperglycaemia, the common symptoms of GSDs. The hallmark of GSDIV was an accumulation of glycogen with an amylopectin-like structure. For this reason, GSDIV is also known as *amylopectinosis*, or *adult polyglucosan body disease (APBD)* when the onset occurs at adult age.⁶² Considering that abnormal glycogen contains 5-6% of branches as amylopectin, it is important to understand at what extent and how the activity of GBE is impaired by mapping the mutations in the structure.

To date, 25 mutations of GBE have been identified and reported in the Human Gene Mutation Database¹, and most of them is located within or in the surrounding environment of the catalytic core. They are classified as “destabilising substitutions” that disrupt the GBE structure, thus preventing the interaction with the substrate, or “catalytic substitutions” that are more likely to interfere with the binding of the substrate and its catalysis.⁶² The former group includes the most common mutation found in GSDIV patients that is the substitution of Tyr329 with a Ser329 which was demonstrated by Froese *et al.*⁶² to destabilise the protein structure. The structural analysis of glycogen from APBD mouse models bearing Tyr329Ser showed two types of soluble and insoluble polysaccharide. The soluble glycogen showed a chain length distribution with a peak at DP6, whereas the insoluble glycogen was predominantly made of chains between DP16 and DP22 indicating that the branching frequency was severely altered.³¹ These findings suggest that patients with APBD may still be able to use glycogen as a source of energy in their first years of life until the large

¹ <http://www.hgmd.cf.ac.uk/ac/index.php>

accumulation of abnormal glycogen creates a steric hindrance that prevents access to the metabolic enzyme. This may be the explanation of why the APBD is the adult form of GSDIV.

The percentage of GBE residual activity remaining in GSDIV was seen to correlate with the phenotype; and the activity of GBE is commonly assessed using the enzyme extracted from leukocytes.^{78,91} In absence of GBE activity (0%), the clinical manifestations occur at an early stage of life and are lethal for the patient⁷⁸ With low but detectable activity (0-20%),⁷⁸ there is an onset of a juvenile form, characterised by cardiomyopathy. When GBE shows a partial activity (20-50%),^{78,91} GSDIV is more likely to manifest at adult stage. As a consequence, the reduced activity of GBE compared to GS leads to an elevated level of chain elongation compared to the branching process.

The presented findings highlight the importance of GBE in maintaining the branching architecture of glycogen to prevent the onset of polyglucosan bodies. Nevertheless, Lafora disease (LD) is a neuronal disorder affecting the activity of laforin that also causes the accumulation of polyglucosan bodies in the affected organs.⁹² Laforin is a protein involved in the early stage of glycogen synthesis and its role in this process is still unclear. These results suggest that the regulation of the branching process may be more complex and involved more enzymes than the single GBE.

1.3.4. Glycogen phosphorylase deficiency – GSD type V/VI

GP catalyses the rate limiting step in glycogen degradation; mutations affecting its activity cause GSD type V (skeletal muscles) or VI (liver), which is characterised by hepatomegaly and hypoglycaemia.⁷⁸ Studies on the effects of GSDVI on glycogen structure and metabolism are limited besides clinical case reports, and only in 2019 the first mouse model with the mutation of the liver form of GP was developed to gain knowledge on GSDVI.⁹³ The results showed an increased amount of glycogen in the *Pygl* knockout mouse (*ca.* 4 mg of glycogen per mg of protein) compared to the wild type (<100 µg of glycogen per mg of protein), and this accumulation of glycogen correlated with the onset of fibrosis in adult animals. The structural analysis of glycogen was not performed, and thus it is not clear whether the glycogen stored is normal or resembles the one observed in GSDIV.

Earlier in this section the importance of GP in the activation of GS through PPP1R3C was mentioned. If GP is defected, it is possible that PPP1R3C activates GS and, without the

presence of GP, this activation is constant, therefore promoting the accumulation of glycogen which cannot be degraded. More investigations are needed to evaluate this hypothesis.

1.3.5. Glycogen debranching enzyme deficiency – GSD type III

Glycogen storage disease type III (GSDIII), or Cori Disease, is caused by deficiency of the gene encoding for GDE; to date 70 mutations of the enzyme have been identified.⁷⁸ Most of the mutations are in the catalytic site and affect the binding of the substrates drastically decreasing the activity of the enzyme. Other mutations might disrupt the correct folding and/or stability of GDE, indirectly affecting its activity.⁷⁵

The first case of GSDIII was discovered by Illingworth and Cori¹⁶ in a liver sample isolated from a patient presenting the common GSDs symptoms. The analysis of the structure of glycogen by periodate oxidation and methylation analysis revealed short chains with a high degree of branching when compared to glycogen isolated from healthy patients. This is the only information available on the structure of glycogen from GSDIII, and no engineered mouse models have been developed so far to further investigate this disorder at the glycogen structural level.

1.3.6. Glucose 6-phosphatase deficiency - GSD type I

When glucose 6-phosphate is generated from glycogen, it is converted into glucose by glucose 6-phosphatase (G6Pase) found as a transmembrane protein in the endoplasmic reticulum (ER). G6Pase comprises a catalytic subunit (G6PC) and the transporter subunit for G6P (G6PT) that translocate G6P from the cytoplasm to the lumen of the ER for its conversion into glucose.⁹⁴ There are two types of GSDI: GSDIa that affects the G6PC unit of G6Pase causing the accumulation of G6P in the ER, and GSDIb that affects the G6PT unit leading to high G6P levels in the cytoplasm. In both cases, the inability to produce glucose from either glycogenolysis or gluconeogenesis leads to the accumulation of glycogen in the liver. In addition, the resulting hypoglycaemia causes an excess of free fatty acids to be released in the form of ketones, thus leading to ketosis.^{78,94}

GSDIa is the most common metabolic disorder among those listed so far. Although GSDIa does not directly impair glycogen metabolism, it is not clear whether there is an impact on the synthesis and degradation, or structural properties of glycogen. G6P is an allosteric inhibitor of GP, and the accumulation of this molecule in the cytosol might inactivate the degradation

of glycogen. With GP inactivated, GS and GBE promote the synthesis of glycogen leading to its potential accumulation. Nevertheless, there are several metabolic pathways involved and more insight into glycogen metabolism and structure are needed. For this reason, GSDIa was selected in the present studies as model to investigate the impact of a genetic mutation not directly related to glycogen metabolism on glycogen structure (**Fig. 16**).

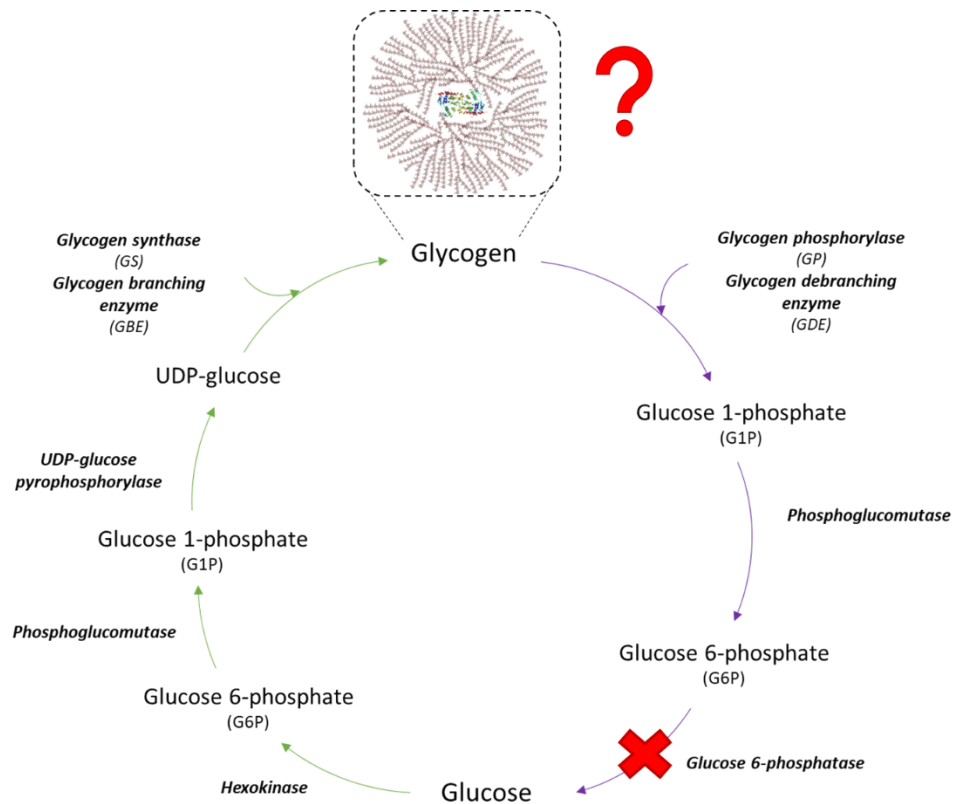


Figure 16 Schematic representation of glycogen metabolism. Glycogen synthesis is illustrated with green arrows, and glycogen degradation with purple arrows. The red cross at the top of glucose 6-phosphatase indicates the enzyme affected by GSDIa.

1.4.About PoLiMeR project

The PoLiMeR consortium (Polymers in the Liver – Metabolism and Regulation) supports a multidisciplinary research project funded by the European Union (EU). The aim of PoLiMeR is to shed light on the rare liver-related metabolic disorders that impair the metabolism of glycogen and fatty acids. These inherited disorders are known as hepatic Glycogen Storage Diseases (GSDs) and mitochondrial Fatty-Acids Oxidation disorders (mFAO). Glycogen and fatty acids are large metabolites that are in some metabolic diseases, and there are many challenges associated with investigating such complex molecules with a single approach. Furthermore, the way that metabolic pathways are activated varies among patients. For this reason, PoLiMeR aims at approaching GSDs and mFAO from a *systems medicine* perspective and at training 15 early stage researchers (ESRs) in this field. A system medicine approach is based on computational models fed with experimental data and information from patients to provide the basis for personalised treatments. With a focus on this methodology, the 15 research projects are divided into 5 work packages (WPs) to investigate the different aspects of the metabolic disorders. The project discussed in this thesis is part of the WP2, which consists in the collaboration of 3 ESRs focused on the elucidation of the structure of glycogen in GSDs using a combination of experimental and computational data as illustrated in **Fig. 17**.

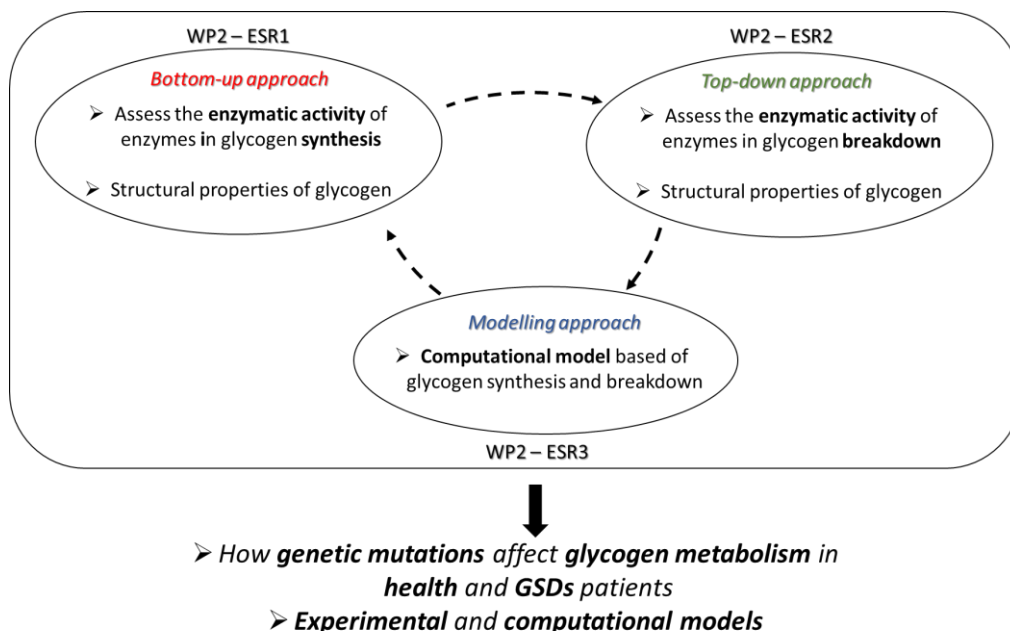


Figure 17 Goal of the individual research projects and of the WP2.

1.5. Aim of the Project

The complex branched architecture of glycogen is the result of a balanced synthesis and degradation and the alteration of any step of the two pathways results in the onset of GSDs and in the accumulation of abnormal glycogen in the affected organs. Despite efforts made by the scientific community and the progresses achieved in the past years in our understanding of glycogen metabolism, the substrate specificity of the enzymes acting on glycogen and the impact that GSDs have on their activity or on the structure of glycogen are poorly understood. Furthermore, a common methodology to extract glycogen and determine its structural features is missing, making the studies more challenging.

The goal of this project is to investigate the chain length distribution and degree of branching of glycogen from mammalian sources, and to correlate these structural features of glycogen with the activity of the branching enzyme. To this end, a simple methodology based on a stepwise enzymatic degradation was developed and optimised on commercially available glycogen. In addition, a new theoretical model called DP15 was designed and combined with the experimental approach to have a better understanding on the branches arrangements generated by the branching enzyme.

Firstly, the products expected from the enzymatic treatments were speculated using the DP15 model. Secondly, the experimental part consisted of the use of commercial standard glycogen (from oyster) to develop the methodology. The chain length distribution and degree of branching were investigated by direct debranching of glycogen with *Pseudomonas* isoamylase and pullulanase. The external chains were shortened with two enzymes, glycogen phosphorylase and β -amylase, and the resulting chain length distribution assessed with analytical techniques. The data collected experimentally were incorporated into the theoretical model to study the possible branching pattern of glycogen and activity of GBE. Finally, the debranching protocol was applied on glycogen bearing GSDs source to investigate the impact of GSDIa on glycogen structure.

Chapter 2 – Enzymatic assays and analytical techniques employed in the present studies

The CLD and DB are key structural features of glycogen. The aim of this chapter is to discuss the most common analytical techniques employed for the assessment of CLD and DB with a focus on those selected in the present studies.

2.1. Chemical treatments vs. Enzymatic assays

When glycogen was discovered and studied between the 19th and 20th century,^{1,95} chemical treatments, such as periodate oxidation and methylation of the hydroxyl groups, were the first techniques to be employed in the structural analysis of this polysaccharide. These approaches predate the development of enzymatic assays.^{12,26}

The vicinal hydroxyl groups of glucose units within the chain or at the non-reducing end of each chain were the target of the chemical reactions. The periodate oxidation converts polysaccharides with free vicinal hydroxyl groups into formic acid and polyaldehydes. The amount of formic acid titrated is equal to the number of non-reducing ends (**Fig. 18**) and cleavable vicinal diols;^{96,97} this chemical modification has been implemented over the past years and it is now known as Periodic Acid Schiff (PAS) reaction.⁹⁸ In contrast, the methylation method derivatises free hydroxyl groups of glucose units to form methylated compounds, such as the 2,3,4,6-tetramethylglucoside (Hakomori reaction), that are hydrolysed with acids and acetylated to form volatile compounds for gas-liquid chromatography.⁹⁹ Despite the selectivity of both chemical reactions towards the functional groups of monosaccharides, their application requires relatively large amounts of material, tedious and time-consuming optimisation steps. In addition, depolymerisation of complex molecules can be a side reaction that depends on various factors questioning the reliability of the results.⁹⁸

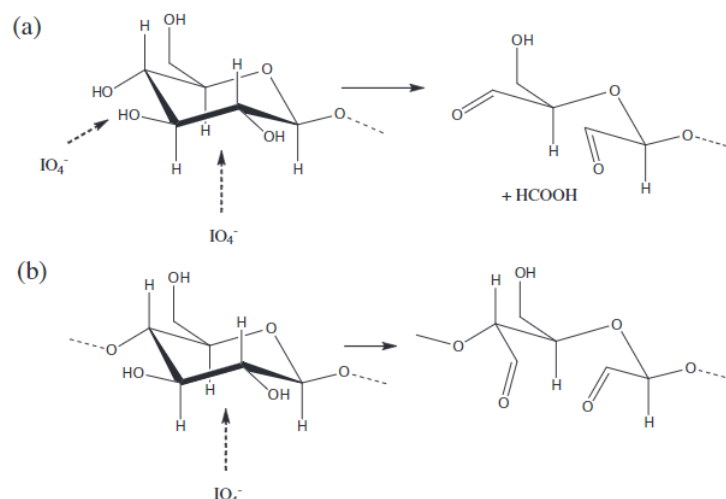


Figure 18 General principles of periodate oxidation of polysaccharides. **(a)** double oxidation occurs at the non-reducing end between C2 and C3, and between C3 and C4 with the release of C3 as formaldehyde (HCOOH); **(b)** in (1,4)-linked residues, the cleavage occurs between C2 and C3. Image taken from Kristiansen et al.⁹⁷

Enzymatic methods can overcome the limitations presented by chemical treatments, enhancing selectivity and yield of the reaction. As a matter of fact, enzymes can digest selected glycosidic linkages¹⁰⁰ limiting side-products, thus resulting in a much simpler and more precise structural analysis of complex polysaccharides. With starch and glycogen, the reducing end of each branch is the target of the enzymatic digestion for the determination of the average chain length and the degree of branching.^{26,101} The quantification of the reducing ends can be performed by colorimetric assays, such as bicinchoninic acid (BCA) assay,¹⁰² dinitrosalicylic acid (DNS) assay,^{103,104} and Nelson-Somogyi (NS) assay¹⁰⁵ (see section 2.3 for more details). Quantitative assays are commonly coupled with analytical techniques such as thin-layer chromatography (TLC), high-performance anion exchange chromatography coupled with pulsed amperometric detector (HPAEC-PAD), fluorophore-assisted carbohydrates electrophoresis (FACE), and size-exclusion chromatography (SEC), to get insights into the chain length distribution and size of the particles.

Herein, we decided to investigate the structure of glycogen by enzymatic digestion employing debranching enzymes (e. g. isoamylase, pullulanase, oligo $\alpha(1,6)$ -glucosidase and amyloglucosidase), amylolytic enzymes (e. g. α - and β -amylase), or phosphorylases (i. e. glycogen phosphorylase). The enzymatic digestion was combined with quantitative (BCA assay, and HPAEC-PAD) and qualitative techniques (TLC) to measure the degree of branching and the degree of polymerisation of glycogen, as schematically represented in **Fig. 19**.

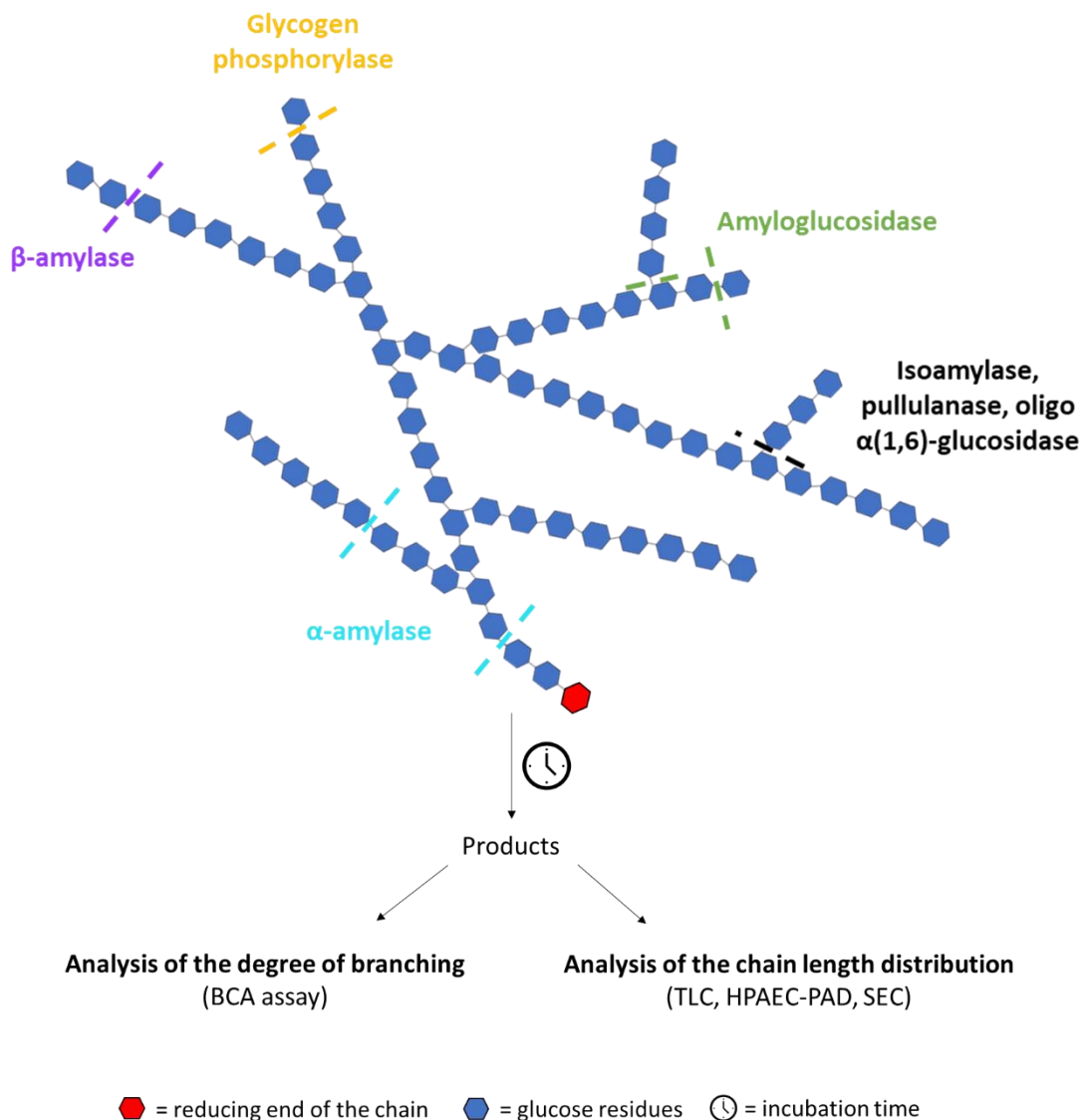


Figure 19 Schematic illustration of the enzymatic digestion of a branched substrate followed by the investigation of its degree of branching using the BCA assay, and its chain length distribution and size of the glycogen particles by analytical techniques (TLC, HPAEC-PAD and SEC).

2.1.1. Debranching enzymes

2.1.1.1. Isoamylase and pullulanase

Isoamylase (ISA) was isolated for the first time in 1968 by Harada *et al.*¹⁰⁶ using the strain *Pseudomonas amyloclavata* (SB15), while the three-dimensional structure was determined in 1998 from Katsuya *et al.*¹⁰⁷ by X-ray diffraction. Based on the CAZy database, isoamylase is part of the glycoside hydrolase (GH) family 13 presenting the active site and the catalytic residues Asp375, Glu435 and Asp510 in the N-terminal region of the protein. Pullulanase (Pull)

is also part of the GH13 family, and this enzyme was isolated by Bender and Wallenfels in 1961 in the organism *Klebsiella pneumonia*.^{108,109}

Both ISA and Pull are direct debranching enzymes, meaning that they digest *endo*- α -1,6 glycosidic bonds of B-chains (chains bearing more than one branch) and A-chains (chains with no branches) generating linear oligosaccharides.^{108,109} Whilst isoamylase only cleaves branching points, there are two types of pullulanase known as type I and type II. The former is only capable of cleaving α (1,6)- linkages and the latter digests both α (1,4)- and α (1,6)- glycosidic bonds; the experiments reported in this thesis were performed with pullulanase type I from *Klebsiella pneumonia*.¹⁸

2.1.1.1.1. Substrate specificity of isoamylase and pullulanase

Kainuma *et al.*¹¹⁰ and Abdullah and French¹¹¹ examined the action pattern of ISA and Pull on large polysaccharides and short-branched oligosaccharides. Briefly, the substrates were incubated for 10 minutes with either ISA or Pull, and the products released within this time frame were quantified by the Nelson-Somogyi method. **Fig. 20** reports the rate of hydrolysis calculated by the authors based on the enzymes preferential substrates; for isoamylase, 100% was taken as the initial rate of hydrolysis of amylopectin and, for pullulanase, 100% was the initial rate of hydrolysis of pullulan. For complex polysaccharides, such as glycogen and amylopectin, the debranching with ISA resulted in a higher initial rate of hydrolysis than the digestion with Pull.

Substrates	Ps. isoamylase	Pullulanase
Amylopectin	100	15
β -limit dextrin of amylopectin	80.3	56.9
Oyster glycogen	124	1
β -limit dextrin of oyster glycogen	214	10.2
Pullulan	<1	100

Figure 20 Relative rate of hydrolysis of isoamylase and pullulanase towards complex branched polysaccharides reported in the table. Figure adapted from Kainuma *et al.*¹¹⁰

The digestion of short-branched fragments by ISA and Pull was dictated by the length of the main chain and branch, and the distance of the branching point from the reducing end of the main chain (**Fig. 21**). For example, ISA cleaved maltotriosyl branches faster than maltosyl branches, and accepted branches placed three units from the reducing end of the chain.

Conversely, pullulanase digested branches of two glucose residues located on the third glucose residue from the reducing end, e. g. pullulan-like structures. Lastly, glucosyl stubs were not released by both enzymes from branched structures containing $\alpha(1,6)$ -glycosidic bonds on their reducing ends, such as in isomaltose, isomaltotriose, and isomaltotetraose. Following these studies, other authors reported differences in the substrate specificity of isoamylase and pullulanase, concluding that the former is as efficient towards complex branched structures as the latter is with short-branched polysaccharides.^{109,112}

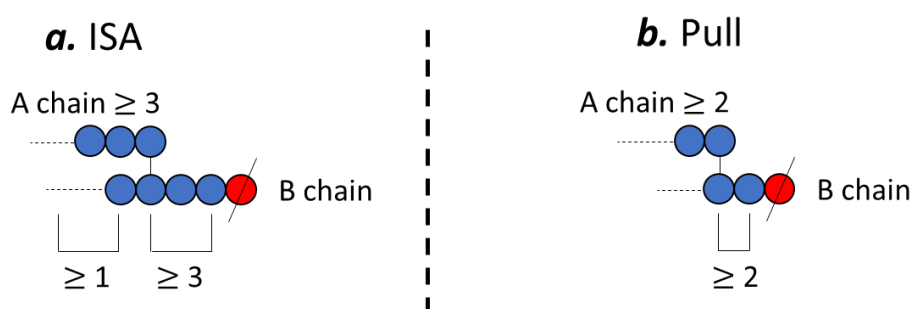


Figure 21 Schematic representation of the substrate specificity of (a) isoamylase and (b) pullulanase for short-branched structures investigated by Kainuma et al.¹¹⁰ Blue dots = glucose residues, red dots = glucose residues with free reducing-end.

To confirm the data reported in literature and for a better understanding of the results presented in the next chapters, the activity of commercial ISA and Pull was assessed on commercially available short-branched oligosaccharides, such as isomaltose, isomaltotriose, 6³- α -glucosyl-maltotriose (G1-G3), and 6³- α -maltotriosyl-maltotriose (G3-G3). The products were assessed by TLC. **Fig. 22** shows that neither ISA or Pull debranched isomaltose, isomaltotriose, or G1-G3, namely structures bearing branches of single glucosyl unit. In contrast, G3-G3, a pullulan-like structure, was partially digested by ISA and completely converted into maltotriose by Pull in the same time frame.

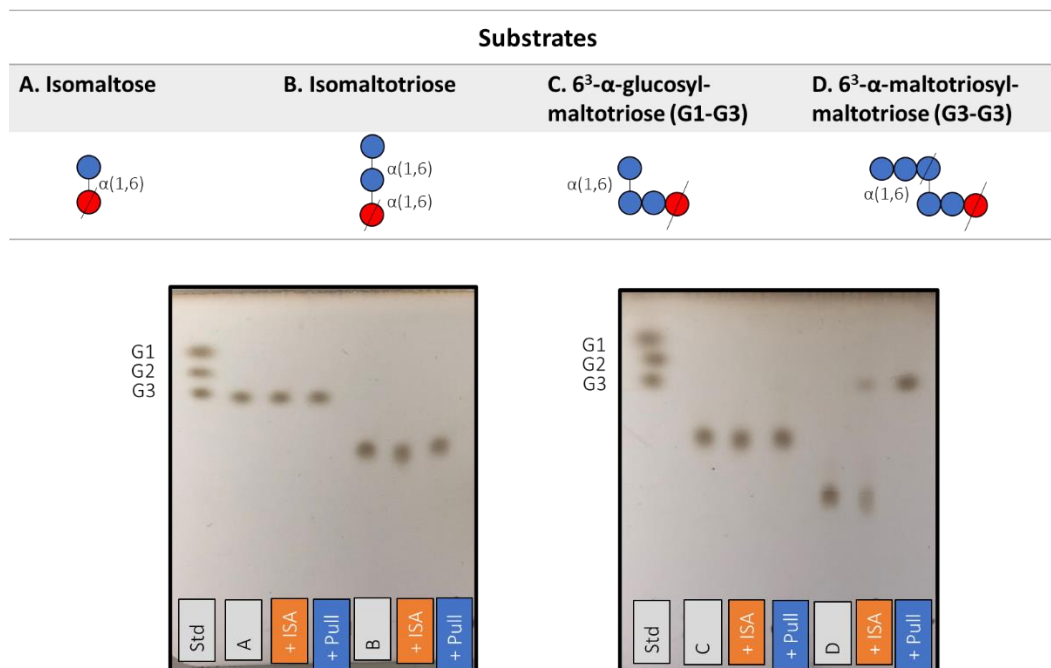


Figure 22 Activity of ISA and Pull with short-branched oligosaccharides. At the top, schematic representation of the structures of each oligosaccharide: a. isomaltose, b. isomaltotriose, c. 6³- α -glucosyl-maltotriose (G1-G3), and 6³- α -maltosyl-maltotriose (G3-G3); blue dots = glucose residues, red dots = glucose residues with free reducing-end. The standards (2 mg/mL) were incubated with Pull (0.15 U) or ISA (0.15 U) for 24 h at 40 °C. At the bottom, TLC analysis of the results; std = standards glucose (G1), maltose (G2), and maltotriose (G3); mobile phase CH₃CN: EtOAc: iPrOH: H₂O (85:20:50:50). The TLC plate was eluted three times before its development with a solution of 5% H₂SO₄ in EtOH and heating with a heat gun.

The action pattern of ISA and Pull examined with the four commercially available showed that Pull digests short-branched structures more efficiently than what ISA does in the same units and incubation time, and glucose stubs at the non-reducing end of the main chain are not substrates for both enzymes. These results were supported by the findings of Kainuma *et al.*¹¹⁰

2.1.1.2. Oligo $\alpha(1,6)$ -glucosidase and amyloglucosidase

Oligo $\alpha(1,6)$ -glucosidase (OGL) or isomaltase can be found in the animal kingdom, some bacteria species, and fungi,¹¹³ and it belongs to the GH13 family. It hydrolyses *exo*- $\alpha(1,6)$ -glucosyl stubs from the non-reducing ends of α -limit dextrin and isomaltooligosaccharides to generate α -glucose units. Amyloglucosidase (AMG) is also part of the GH13 family, and it is an *exo*-enzyme that breaks down both $\alpha(1,4)$ - and $\alpha(1,6)$ - glycosidic linkages to release α -glucose from the non-reducing of a chain (**Fig. 23**).¹¹⁴ In humans, OGL and AMG takes part in the

digestion of starch in the small intestine generating glucose molecules that are transferred in the blood system *via* glucose transporters.¹¹⁴

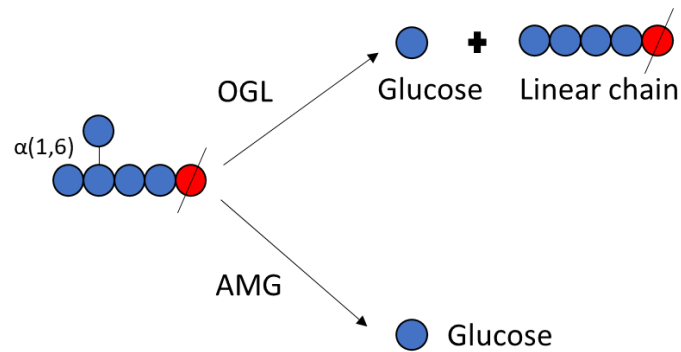


Figure 23 Schematic representation of the activity of oligo $\alpha(1,6)$ -glucosidase (OGL) and amyloglucosidase (AMG). OGL only digests the glucosyl stub, whereas AMG cleaves both $\alpha(1,4)$ - and $\alpha(1,6)$ - glucosidase. Blue dots = glucose residues, red dots = glucose residues with free reducing-end.

In the presented studies, OGL was employed to determine the presence of eventual glucosyl stubs generated by stepwise enzymatic digestion of glycogen. In addition, AMG was included in an enzymatic cocktail to readily digest glycogen into glucose which will be discussed later in this section. To study the activity of OGL, we incubated the enzyme with short-branched oligosaccharides in sodium acetate buffer (0.1 M, pH 4.5) for 24 h at 40 °C and the products were assessed by TLC. **Fig. 24** shows that isomaltooligosaccharides, such as isomaltose and isomaltotriose, were converted into glucose, while G1-G3 was split into glucose and maltotriose. As expected from the specificity of this enzyme towards glucosyl stubs, the incubation of G3-G3 with OGL did not generate any products confirming that OGL operates at the non-reducing terminus of $\alpha(1,6)$ -glycosidic linkages.

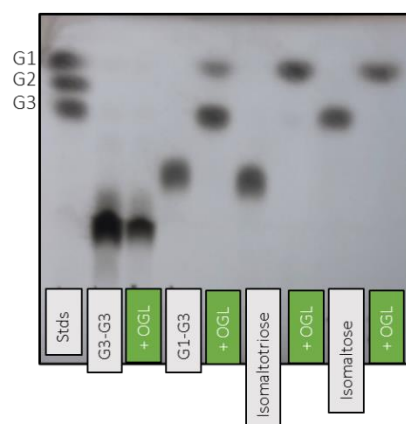


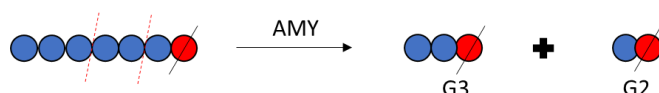
Figure 24 TLC analysis of the activity of oligo $\alpha(1,6)$ -glucosidase (OGL) with short-branched oligosaccharides. Each substrate (2 mg/mL) was incubated with 0.025 U of enzyme in sodium acetate buffer (pH 4.5, 0.1 M) for 24 h at 40 °C; stds = standards glucose (G1), maltose (G2), and maltotriose (G3). The schematic structures of the substrates are illustrated in **Fig. 22**.

2.1.2. Amylolytic Enzymes

2.1.2.1. α -Amylase

α -Amylase (AMY) was isolated in 1833,¹¹³ and it is part of the GH13 family. As an *endo*-acting enzyme, it catalyses the hydrolysis of $\alpha(1,4)$ -glycosidic bonds in starch and glycogen by releasing short-branched structures (α -limit dextrin), maltose (G2), and maltotriose (G3) (**Fig. 25**). In these studies, AMY was included in an enzyme cocktail to digest glycogen into glucose.

Odd- and even- linear chain



Branched fragments

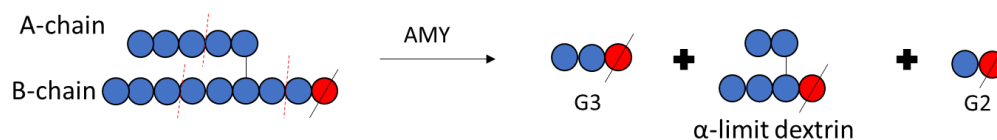


Figure 25 Schematic representation of the activity of α -amylase (AMY) on linear chains and branched fragments. *Blue dots* = glucose residues, *red dots* = glucose residues with free reducing-end, *A-chain* = branch with no branching points, *B-chain* = chain bearing one or more branching point; the red dotted line (---) indicates the cleavage point; G2 = maltose, G3 = maltotriose.

2.1.2.2. β -Amylase

β -amylase (BMY) was discovered in 1924 by Kuhn and crystallised in 1948 by Balls *et al.*¹¹⁵ BMY is an *exo*-acting enzyme that cleaves maltosyl residues from the non-reducing ends of starch, glycogen, or related polysaccharides. The term “beta” does not refer to the configuration of the linkage substrate of BMY, and it rather indicates the inversion of the anomeric configuration of the maltose residues when they are cleaved;^{109,116} for its mechanism, BMY is part of the GH14 family. Literature reports that when BMY acts on linear chains with an odd number of glucose residues (DP7, DP9, etc.), maltose (G2) and maltotriose (G3) are released and the ratio G2:G3 depends on the chain length. With branched polysaccharides such as glycogen, BMY halts 2 or 3 glucose residues before a branching point, since $\alpha(1,6)$ -glycosidic bonds cannot be bypassed by this enzyme. The activity of BMY on branched structures generates products with external chains of 3-4 glucose residues that are called β -limit dextrin (**Fig. 26**).^{109,116}

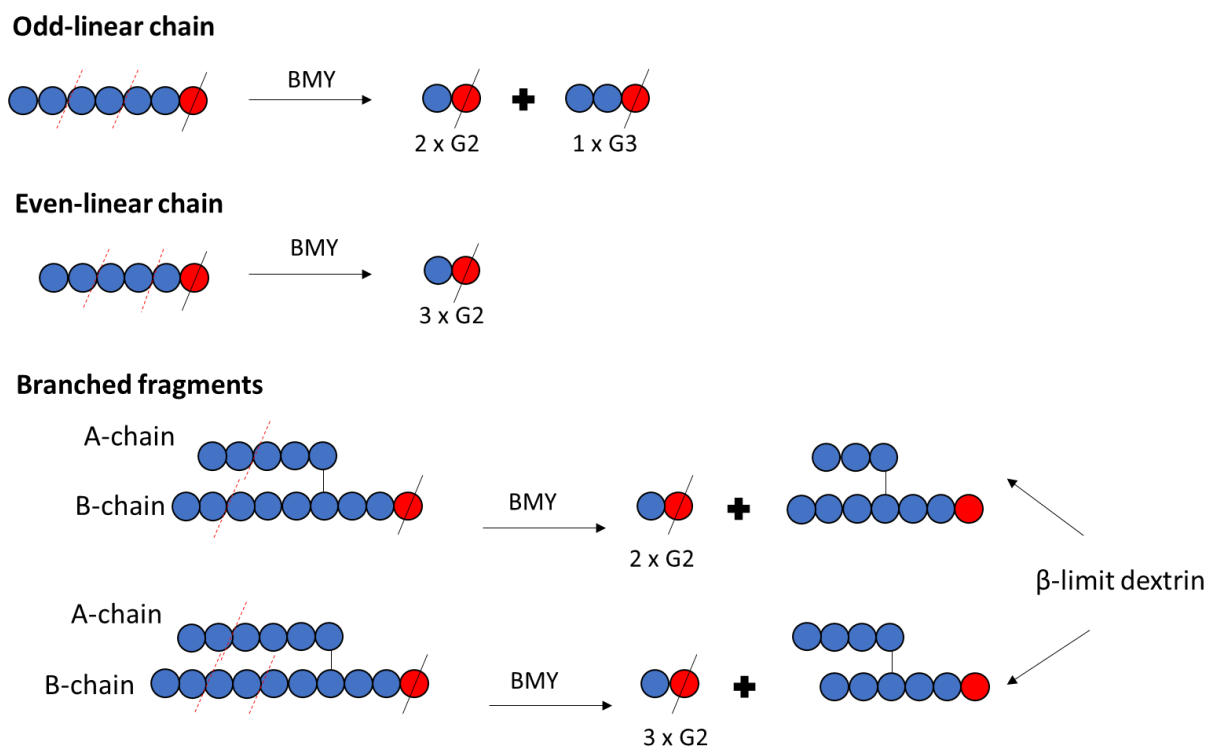


Figure 26 Schematic representation of the activity of β -amylase (BMY) on linear chains and branched fragments. Blue dots = glucose residues, red dots = glucose residues with free reducing-end, A-chain = branch with no branching points, B-chain = chain bearing one or more branching point; G2 = maltose, G3 = maltotriose; the red dotted line (---) indicates the cleavage point.

To evaluate the activity of BMY, linear and short-branched oligosaccharides were digested with the enzyme for 24 h, the same incubation time used for the reactions with glycogen reported in Chapter 4. The conditions for the enzymatic treatment were those suggested by the supplier (Megazyme), namely sodium phosphate buffer (pH 6.0, 0.2 M) at 37 °C. In contrast, the units of enzyme were established based on the amount of glycogen employed for the reactions presented in the next chapter, and the products were assessed by TLC. **Fig. 27** shows that the linear oligosaccharides with an even number of glucose residues (maltotetraose-G4 and maltohexaose-G6) were converted into maltose, while those with an odd number of glucose units (maltotriose-G3, maltopentaose-G5, and maltoheptaose-G7) were mainly converted into G2, and in a smaller amount into G1 and G3. Considering the activity of BMY reported in literature, we believed that this enzyme initially digested odd-length linear chains into G2 and G3, and due to the prolonged incubation (24 h), the reaction proceeded with the split of G3 into G1 and G2. Based on this assumption, the ratio of G1:G2:G3 expected and estimated by TLC depends on the chain length of the initial substrate, e. g. maltohexaose is initially split into G2 and G3 with a ratio of 2:1, and after 24 h, the

products are G1 and G2 in the ratio of 1:3. Looking at the results reported in **Fig. 27**, the ratio G1:G2 for both G5 and G7 is very small as expected by the number of maltose residues in these oligosaccharides. Differently, for G3, an equal ratio of G1:G2 was expected, but **Fig. 27** shows that G2 is more abundant than G1. In 1966, Lee and Whelan¹¹⁷ published about the complete digestion of maltotriose into maltose and glucose by BMY and the authors did not detect any starting material in the products, as instead reported in **Fig. 27**. In 1984, Kainuma *et al.*¹¹⁸ reported an unusual activity of BMY. The authors found that BMY extracted from the plant *Stachyurus praecox* converted G3 into G2 following a glucose transfer mechanism illustrated in **Fig. 27**: a) G3 is split into G2 and G1, b) G1 is used to convert G3 into G4, c) G4 is then digested into two moles of G2. However, the suggested mechanism has not been reported for BMY from barley, the source used for the present experiments. Thus, it is not possible to confirm that this is the mechanism that led to the unexpected ratio of G1:G2 generated by G3.

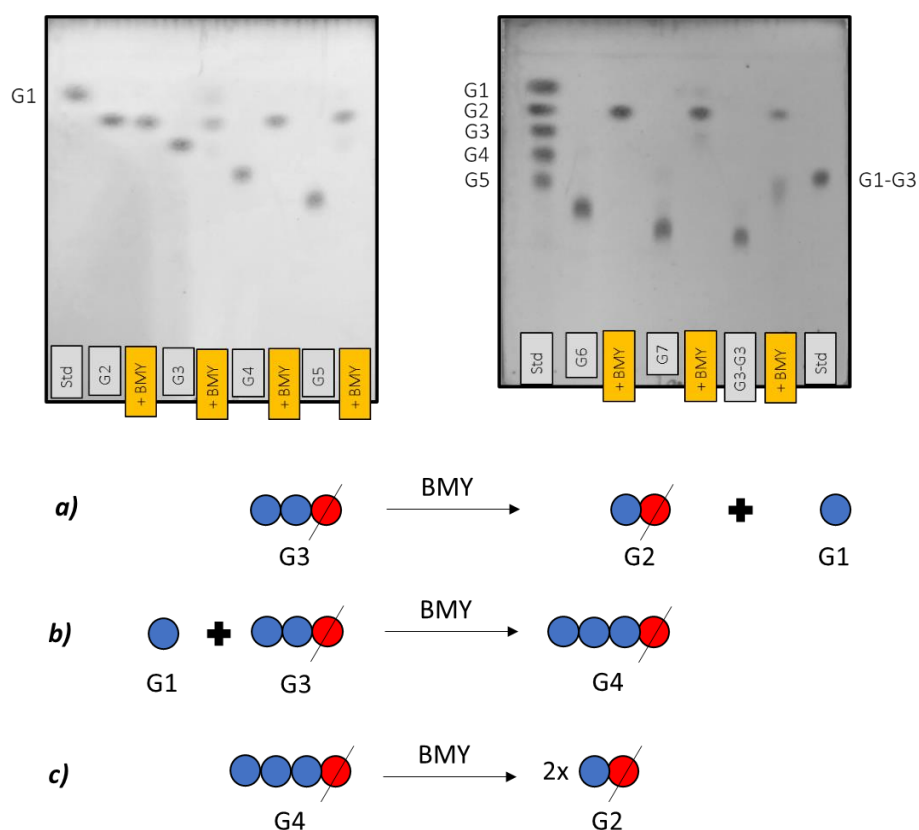


Figure 27 On top, enzymatic digestion of oligosaccharides (2 mg/mL) by β -amylase (BMY, 60 U) in potassium phosphate buffer (pH 6.0, 0.2 M) at 37 °C for 24 h; mobile phase $\text{CH}_3\text{CN}:\text{EtOAc}:\text{iPrOH}:\text{H}_2\text{O}$ (85:20:50:50); the TLC plate was eluted three times before its development with a solution of 5% H_2SO_4 in EtOH and heating with a heat gun. On the bottom, mechanism of BMY with maltotriose, described from Kainuma K.¹¹⁸ Blue dots = glucose residues, red dots = glucose residues with free reducing-end.

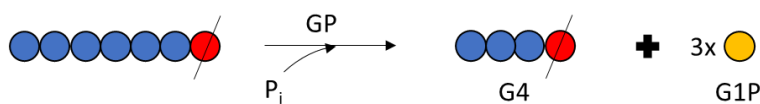
Finally, the hydrolysis of G3-G3 by BMY resulted in the product G1-G3 suggesting that with prolonged treatments odd linear chains can be converted into glucosyl stubs, rather than G3 as reported in the literature for BMY from sweet potato.¹¹⁹

2.1.3. Phosphorolytic Enzyme

2.1.3.1. Glycogen phosphorylase

Glycogen phosphorylase (GP) is a key enzyme in glycogen degradation that catalyses the conversion of unbranched or branched chains into maltotetraose stubs by releasing single G1P units from the non-reducing end (**Fig. 28**).^{120,121} However, depending on the ratio of G1P and inorganic phosphate (P_i), GP can elongate existing chains by addition of G1P to the non-reducing end.¹²² In the cytosol of the cells, the addition of glucose from G1P to glycogen by GP does not occur due to the ratio of $P_i/G1P$ which was estimated by Brown *et al.*¹²² in 1961 to be greater than 3.37 at physiological conditions (pH 6.8, 37 °C) (**Fig. 29**).

Odd- and even- linear chain

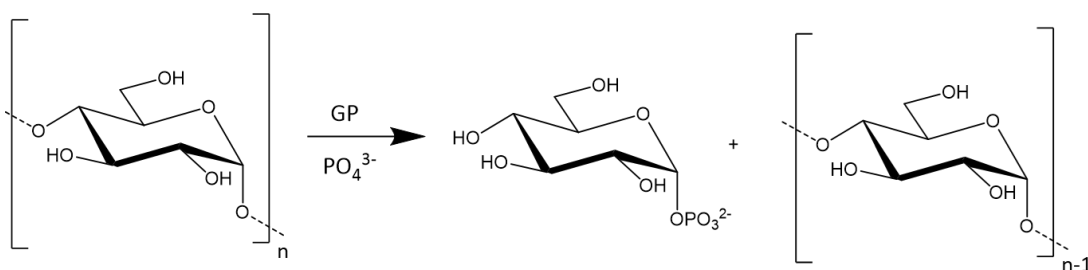


Branched fragments



Figure 28 Schematic representation of the activity of glycogen phosphorylase (GP). Blue dots = glucose residues, red dots = reducing ends, yellow dots = glucose 1-phosphate, G4 = maltotetraose, P_i = inorganic phosphate.

a. $P_i/G1P \gg 3.37$



b. $P_i/G1P \ll 3.37$

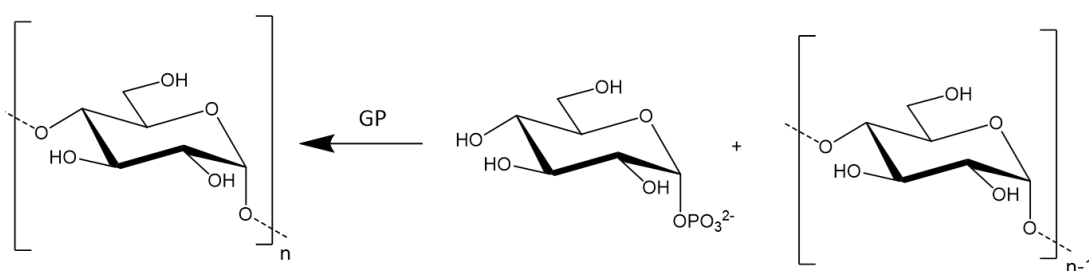


Figure 29 Activity of glycogen phosphorylase (GP) based on the ratio of inorganic phosphate (P_i) and glucose 1-phosphate (G1P) equal to 3.37.¹²²

In the present studies, we adapted the working conditions reported from Zhai *et al.*⁷⁵ to promote the phosphorolysis of glycogen, and the products (phosphorylase-limit dextrin) were studied to estimate their chain length distribution and arrangement of the branching points which will be discussed in the next chapters.

To favour the top reaction of **Fig. 29**, the ratio of P_i in solution and G1P released from glycogen by GP must be higher than 3.37. Considering that the percentage of G1P expected from literature is equal to 40%,¹⁶ it was estimated that *ca.* 2 mg (11 μ mol) is the quantity of G1P released from 5 mg of glycogen (**Table 1**), and the total amount of PO_4^{3-} in solution is 100 μ mol. Thus, the ratio of $PO_4^{3-}/G1P$ substantially exceeds 3.37.

Table 1 Calculations of the amount of glucose 1-phosphate expected and inorganic phosphate required for the digestion of glycogen by glycogen phosphorylase (GP).

Amount of glycogen (mg)	Glucose 1-phosphate expected	Inorganic phosphate (P_i) required	Inorganic phosphate (P_i) used in the reaction	Ratio $P_i/G1P$ expected in the reaction
5 mg	2 mg, 11.1 μ mol (0.011 mmol)	11.1 μ mol (0.011 mmol)	100 μ mol (0.1 mmol)	$\gg 3.37$

To evaluate the activity of GP with the conditions selected, standard linear and branched oligosaccharides were digested for 1h and 24 h, and the products assessed by TLC. The TLC in **Fig. 30** shows that linear chains longer than five glucose residues were mostly converted into maltotetraose (G4) and G1P, and in a smaller proportion into maltopentaose (G5) in an hour, whereas no activity was observed on G3 and G3-G3 (**Fig. 30a** and **30b**). To further assess the digestion of G4 and G5 into short chains during prolonged treatments, these oligosaccharides were incubated with GP for 24 h. The TLC in **Fig. 30c** shows that no chains shorter than G4 were generated. These results agree with data from literature,¹²³ and they confirmed that the conditions selected promote the phosphorolysis of the substrate by GP.

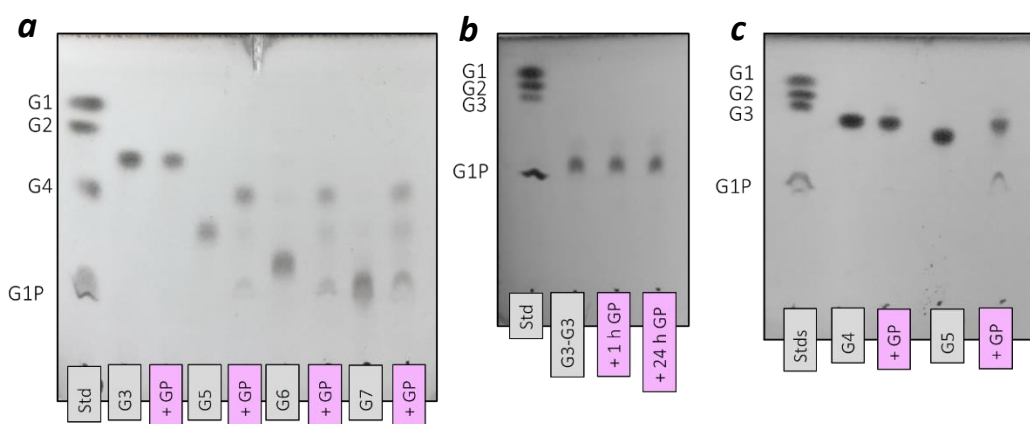


Figure 30 Activity of 10 U of glycogen phosphorylase (GP) with linear and branched oligosaccharides (2 mg/mL) in potassium phosphate buffer (pH 6.8, 0.2 M) at 37 °C. **a**) G3, G5, G6, and G7 were incubated for 1 h; **b**) the branched oligosaccharide G3-G3 was incubated for 1 h and 24 h; **c**) G4 and G5 were incubated for 24 h. Samples were desalted with an anion exchange resin before their application onto the TLC. Mobile phase CH₃CN: EtOAc: iPrOH: H₂O (85:20:50:50). The TLC plate was eluted three times before its development with a solution of 5% H₂SO₄ in EtOH and heating with a heat gun.

2.2. Analytical techniques commonly employed to determine the chain length distribution

Glycogen chain length distribution (CLD) is important for understanding the activity of the enzymes active in glycogen metabolism. As a matter of fact, it is the target of many investigations for determining the impact of metabolic disorders, such as diabetes,^{30,124} GSDs,¹⁶ and Lafora disease (LD)⁹² on glycogen structure. Nevertheless, the analysis of the CLD of polysaccharides can be very challenging due to their uncharged nature and lack of functional groups that facilitate their detection by spectrophotometric techniques. To overcome these problems, three analytical techniques have been developed and optimised over the past years for studies on starch and glycogen. These methods are known as fluorophore-assisted carbohydrate electrophoresis (FACE), high performance anion exchange chromatography (HPAEC), and size-exclusion chromatography (SEC, or also termed GPC, gel-permeation chromatography).

2.2.1. Fluorophore-Assisted Capillary Electrophoresis (FACE)

Fluorophore-Assisted Capillary Electrophoresis (FACE) technique consists of the derivatization of glycan chains with a charged fluorophore by reductive amination at the reducing end.¹²⁵ The fluorescent tag provides a negative net charge to the chain, which can migrate in an electric field by capillary electrophoresis. The most common fluorophores are 8-amino-1,3,6-pyrenetrisulfonic acid (APTS) or 8-amino-1,3,6-naphthalene trisulfonic acid (ANTS) that are suitable for laser-induced fluorescence (LIF) detection, as used in FACE.¹²⁶ Each labelled glycan is detected as a single peak, the area of which is directly proportional to the concentration of chains per degree of polymerisation. Peak assignment is obtained merely by counting the peak after calibration of the instrument with one oligosaccharide with known degree of polymerisation, e. g. maltopentaose (DP5) as reference peak and the successive peaks are $DP5+1$, $DP5+2$, ..., $DP5+n$.¹²⁷ **Fig. 31** shows the workflow for the analysis of glycogen chain length distribution by FACE.

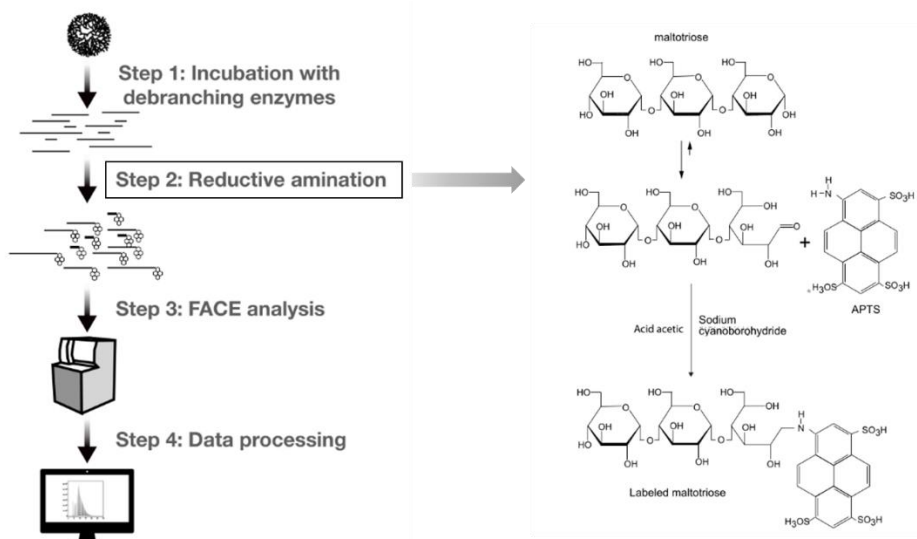


Figure 31 Workflow to determine the chain length distribution of glycogen employing FACE analysis. On the right, the mechanism of the reductive amination reaction of the hemiacetal group by primary amine function of 8-amino-1,3,6-pyrenetrisulfonic acid (APTS). Image taken from Fermont et al.¹²⁵

Despite the relatively simple procedure of FACE, a successful FACE analysis relies on the efficiency and specificity of the derivatisation step.¹²⁸ Therefore, the type and concentration of the fluorophore, the screening of the working conditions suitable for the substrate represent crucial steps that may sometimes be time-consuming. In addition, instruments for capillary electrophoresis are not widely available in every lab limiting the analysis of the samples with FACE.¹²⁸

2.2.2. High-Performance Anion Exchange Chromatography coupled with Pulsed Amperometric Detection (HPAEC-PAD)

High-performance anion exchange chromatography coupled with pulsed amperometric detection (HPAEC-PAD), developed in the 1980s, overcame the problems related to the derivatisation step required for sugars analysis. HPAEC is a sensitive technique that can separate picomole of sugars without the additional derivatisation step.¹²⁹ The principle of the HPAEC is to convert glucan chains, that are weak acids (pKa 12-14), into oxyanions under alkaline conditions using NaOH (pH>12).¹³⁰ The oxyanions pass through an anion-exchange column made of quaternary ammonium resin resistant to high pH, and their elution occurs *via* displacement method using NaOAc buffer. In this way, the retention time of the glucan chains depends on the affinity that they have towards the column compared to the acetates; the chain length, the linkage position, and the accessibility of the oxyanions to the functional groups of the resin are some of the factors that can influence this affinity.¹³⁰ An example of chromatogram expected¹³⁰ from the HPAEC is showed in **Fig. 32**. The linear oligosaccharides of glucose are separated based on the chain length and on the presence of

branching points, i. e. a maltotetraose (G4) is more retained on the column than a branched oligosaccharide of the same DP (G1-G3).

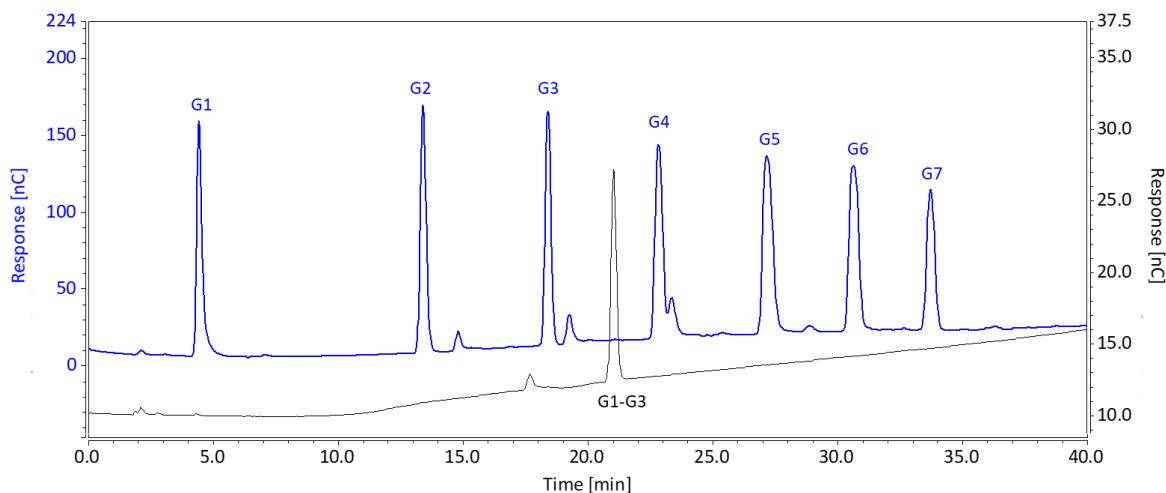


Figure 32 Separation of *linear oligosaccharides* with a chain length between one (glucose, G1) and seven glucose residues (maltoheptaose, G7). The chromatogram is overlaid with the one collected for the branched oligosaccharide **6³- α -glucosyl-maltotriose** (indicated with G1-G3; structure illustrated in **Fig. 6**). Both chromatograms were obtained with a CarboPac PA1 column (2x250 mm) using a flow rate of 0.250 mL/min and the following gradient: 0-2' of 150 mM NaOH (100%), 2'-55' of 600 mM NaOAc buffer (0-100%), and 55'-60' of 150 mM NaOH (100%).

The detect^on of each glucan chain occurs by pulsed amperometric detector (PAD) based on three potentials and on a gold electrode;¹²⁹ the word “pulsed” refers to the waveform generated by the three different potentials used for the detection. The initial increase of the potential is required to oxidise the sugar at its reducing end and convert it into gluconic acid. When the material has been detected, the drop in the potential promotes the inactivation and the cleaning of the electrode from any material left. To reactivate the electrode, the potential returns to the initial value. The signal obtained by the oxidation of the sugar is proportional to the concentration of the glucan chain. However, some papers^{127,131,132} claimed that HPAEC is a semiquantitative technique because the detector (PAD) gives a different response for chains of different length, resulting in peak area not proportional to the CLD.

2.2.3. Size-Exclusion Chromatography (SEC)

Size-Exclusion Chromatography (SEC) is a chromatographic technique that separates the glucan chains based on their molecular weight and the hydrodynamic volume occupied inside the column.¹³³ SEC uses differential refractive index (DRI) instead of a fluorescence or pulsed amperometric detector as in FACE and HPAEC, respectively. When the samples are eluted from the largest to the smallest, the DRI measures their refractive index and compare it to a reference cell containing only solvent. With this type of detection, the signal is not directly proportional to the

concentration of each glucan chain ($N_{de}(X)$), but it is rather a representation of the weight (W) distribution defined as $W_{de}(X)$. In addition, SEC separation suffers of band broadening resulting in a lack of baseline resolution as instead obtained with FACE and HPAEC.

Considering the benefits and drawbacks of each technique mentioned above, we decided to combine the TLC analysis of the samples with the HPAEC and SEC (GPC) separation for a better investigation of glycogen structures.

2.3. Quantification of glucan chains reducing ends to determine the degree of branching

When a branched polysaccharide is digested with an isoamylase-type debranching enzyme, the products are linear chains with a free reducing end that can participate in redox reactions. The DB is then calculated by the ratio between the number of $\alpha(1,6)$ -, namely branching points, and $\alpha(1,4)$ -glycosidic linkages that characterise glycogen of a certain species. Most of the reducing end methods are based on colorimetric assays, such as the bicinchoninic acid (BCA) assay,¹⁰² dinitrosalicylic acid (DNS) assay,^{103,104} and Nelson-Somogyi (NS) assay.¹⁰⁵

2.3.1. Bicinchoninic Acid (BCA) assay

The BCA assay is a colorimetric method for the quantification of carbohydrates having reducing end moieties. In alkaline solution, the reducing sugar reduces cupric (Cu^{2+}) to cuprous ion (Cu^+), which forms a purple complex with the bicinchoninic acid. The total concentration of reducing ends is extrapolated from a standard calibration curve against the absorbance intensity of the Cu^+ -BCA complex at 560 nm (**Fig. 33**).^{102,134,135} The preparation of the sample involves the mixture of an alkaline solution with a copper reagent which solution is added to the sample in 1:1 proportion. This assay shows accurate data when applied to mixture of oligosaccharides with different degree of polymerisation. However, the BCA assay can also be used for the quantification of proteins.¹³⁶ Therefore, the application of this assay to samples containing a mixture of sugars and proteins does not provide an accurate response.

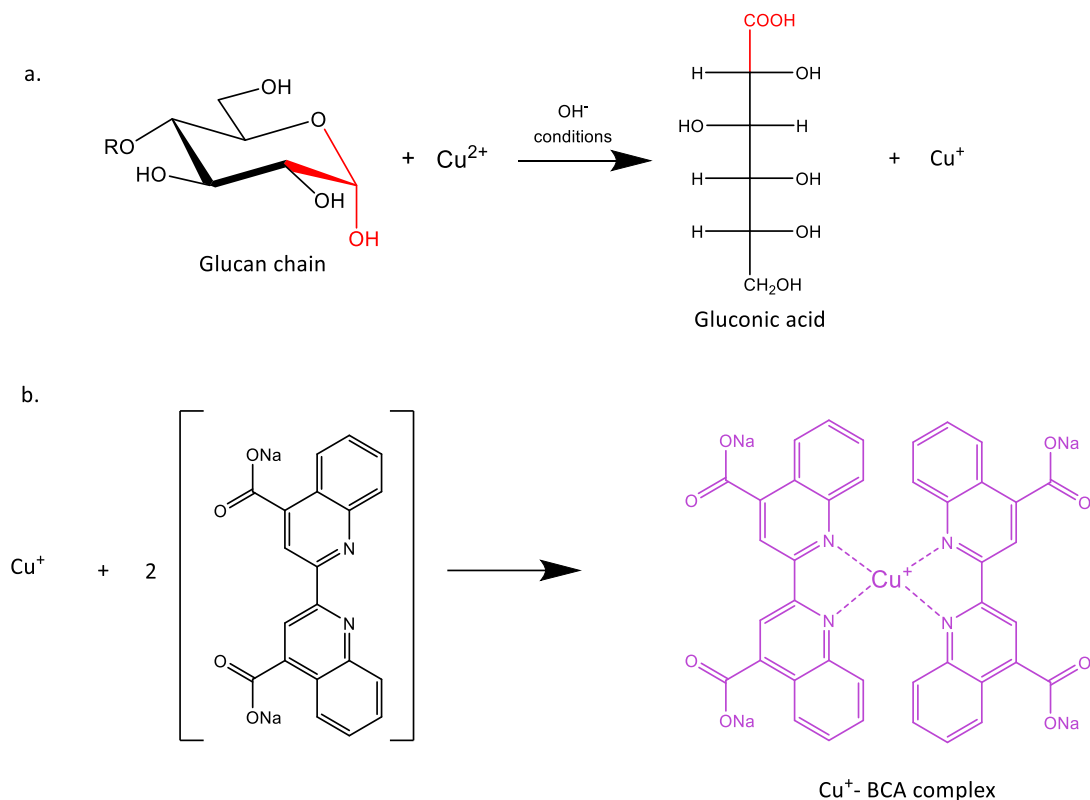


Figure 33 Principle of BCA assay. Reaction **a**: in alkaline conditions, the reducing end of glucose (in red) is exposed to the oxidation into gluconic acid while Cu^{2+} is reduced to Cu^+ ; reaction **b**: Cu^+ reacts with two molecules of bicinchoninic acid disodium salt to form a purple complex that absorbs at 540 nm.

In our studies, we selected the BCA assay to quantify the branching points in glycogen samples. Before its application, we evaluated the limits of detection for the lowest and highest concentrations of sugars that the BCA assay can detect (**Fig. 34**). We found that the linear range is within 0.5 and 10 $\mu\text{g}/\text{mL}$.

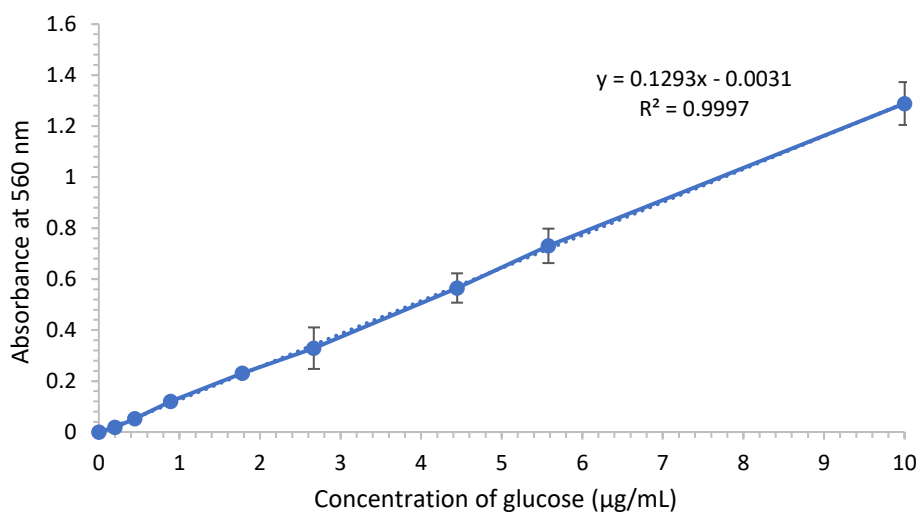


Figure 34 Calibration curve of the BCA assay performed with glucose in triplicates.

2.3.1.1. Quantification of glycogen in a sample based on reducing-end assay

The quantification of glycogen in a sample can be performed with the phenol-sulfuric acid (PSA) assay or a commercially available kit. The PSA assay is specific towards sugars and is based on the chemical cleavage of the glycosidic bonds in strong acid conditions followed by reaction of the aldehyde groups with phenol (**Fig. 35**).^{137,138} As result, an orange complex absorbing at 450 nm is formed. The PSA assay has a simple protocol, and it consists of the addition of 95% H₂SO₄ and 5% phenol to the sample followed by 5 mins at 95 °C.^{139,140} However, the use of harmful and toxic reagents combined with the difficulties to pipette viscous solutions such as concentrated sulfuric acid challenge the reproducibility of this assay. In the commercially available kit, glycogen samples are converted into glucose by enzymatic digestion with amyloglucosidase. Then, glucose takes part in a redox reaction to generate a product that reacts with a coloured probe. In both cases, the digestion of glycogen cannot be followed to confirm the completion of the reaction, and the methods are either harmful (PSA assay) or expensive (glycogen kit assays). Therefore, we developed a method to quantify the amount of glycogen in a sample using an enzymatic cocktail of three enzymes followed by quantification of glucose with the BCA assay.

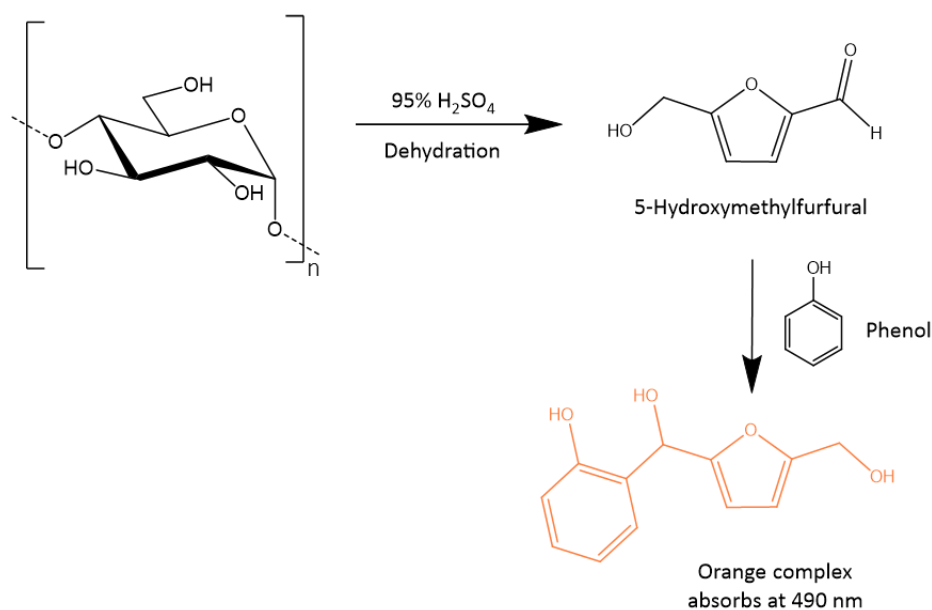


Figure 35 Reaction of the phenol-sulfuric acid (PSA) assay as reported by Zhang *et al.*¹³⁸

The enzyme cocktail consists of two *endo*-acting enzymes, ISA and AMY, and an *exo*-acting enzyme AMG. While ISA and AMY cleave *endo*- α (1,6)- and *endo*- α (1,4)- glycosidic bonds to release linear chains and small-branched structures, AMG breaks the products into glucose. In the literature, it is reported that the combination of AMG and AMY can digest starch at a much faster rate than single enzymes. Thus, we decided to use both enzymes for the digestion of glycogen.¹¹⁴ We used 500 μ g

of glycogen and assessed the completion of the reaction by TLC. We estimated *ca.* 500 μg of glucose from the conversion of glycogen considering a negligible amount of protein complexed with the polysaccharide. The quantification of glucose was performed with the BCA assay and the results compared with those obtained by PSA method. **Fig. 36** shows that the application of the BCA for the measurement of glucose is subjected to less variability within replicates compared to the PSA assay. Based on these results, we decided to use the enzymatic cocktail for the quantification of glucose when needed.

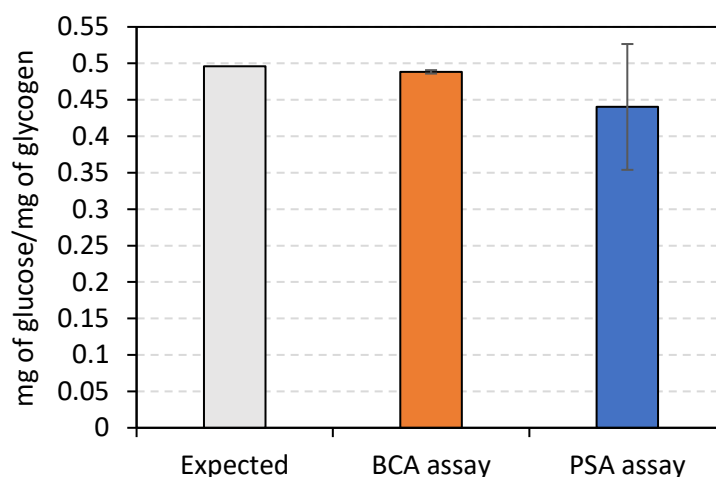


Figure 36 Quantification of the amount of glucose in a glycogen sample using bichoninic acid (BCA) assay and phenol-sulfuric acid (PSA) assay. The **grey** column indicates the expected amount of glucose (*ca.* 500 μg) from a glycogen sample, the **orange** and **blue** column represents the results obtained by BCA assay and PSA assay, respectively. The error bars are from three different experiments.

2.3.2. Dinitrosalicylic acid (DNS) and Nelson-Somogyi (NS) assay

The DNS assay was developed by Sumner in 1921 and modified by Miller in 1951.¹⁴¹ It is a rapid test that consists in the addition of the DNS reagent to the sample in a 1:1 proportion followed by a boiling step for 5 mins before analysis by spectrophotometry. The chemistry of the DNS method is relatively simple because it utilizes the reducing power of the free reducing end of each glucan chain to reduce the 3,5-dinitrosalicylic acid to 3-amino-5-nitrosalicylic acid, which absorbs at 540 nm. Similarly, the NS method, developed in 1954, uses the reducing end of the chain to reduce Cu^{2+} into Cu^{+} which further reduces the arseno-molybdate complex resulting in a blue dye that absorbs at 500 nm.¹⁰⁵ Despite the simple and rapid protocols of both methods, they suffer from several limitations. In the presence of glucose concentrations lower than 0.1 or 1 mM, the assays lack accuracy. In addition, the response per reducing group is dependent on the length of the oligosaccharide,¹⁰³ hence, they are not ideal assays for quantitative determination of the reducing ends in a mixture of different oligosaccharides as in the present studies.

Chapter 3 – DP15 model

In this chapter, a theoretical model called DP15 is presented. The purpose of the DP15 was to create hypothetical branched structures to help understanding about the position of the branching points in glycogen, based on its experimental chain length distribution (**Fig. 37**).

Initially, the rationale used to build up the model is discussed, along with the combinations of the branches created. Then, the resulting structures are subjected to the theoretical digestion using the enzymes mentioned in the previous section. Although the substrate specificity of the enzymes was assayed experimentally, the digestion of the DP15 models was based solely on the information reported in literature. Finally, the theoretical products were exploited to predict the chain length distribution expected from each enzymatic digestion, and the results will be compared with data obtained experimentally from commercial or mammalian glycogen sources, as presented in Chapter 4.

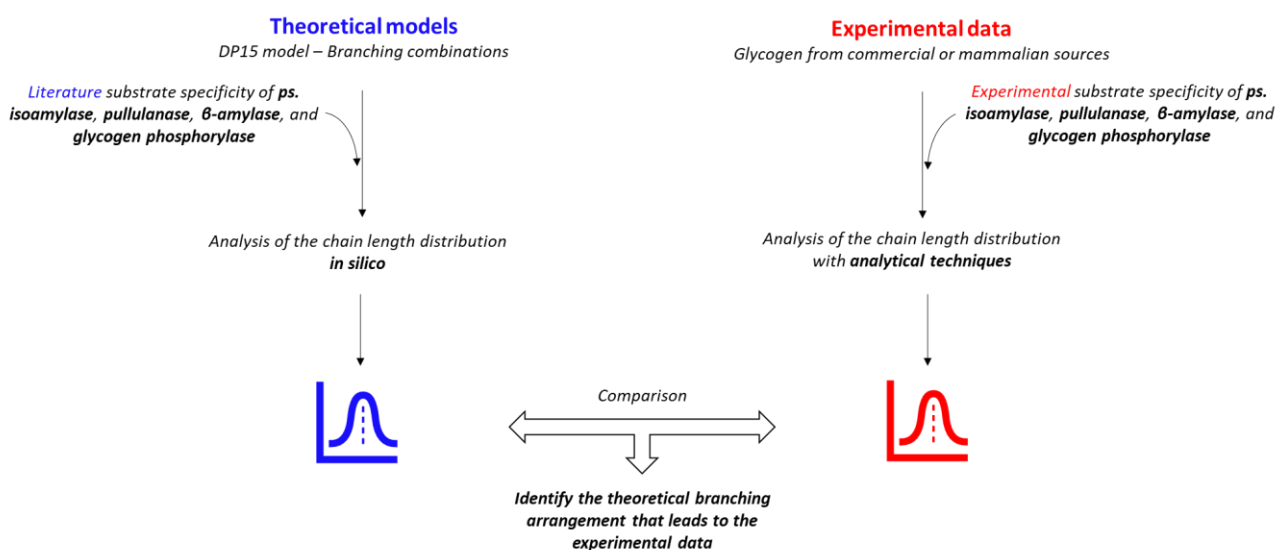


Figure 37 Schematic representation of the rationale used to create the *theoretical models* (DP15) and chain length distribution (on the left), and comparison of the results with the *experimental data* (on the right) to understand the position of the branching points in the structure of glycogen.

3.1. Branching mechanism used to build up the DP15 models

The library of theoretical branched structures was created by branching a substrate of 15 glucose residues (DP15) using the intramolecular transfer described in Chapter 1. **Fig. 38** shows that the linear chain of DP15 bears the reducing end on the right and the non-reducing end on the left (**Fig. 38a**). The chain is split into two fragments called X_1 and X_2 (**Fig. 38b**), and X_1 is transferred onto every glucose residue of the remaining chain X_2 to form each branched combination (**Fig. 38c**). As result, the transfer of X_1 onto X_2 generated over 100 branched structures (**Fig. 38d**) that are illustrated in **Appendix 1**. The number of combinations for each X_1 and X_2 in **Appendix 1** depends on the number of glucose residues in X_2 . An example of a branched structure formed following this method is reported in **Fig. 39** using DP6 as X_1 and DP9 as X_2 . As result, 9 positions and combinations are generated.

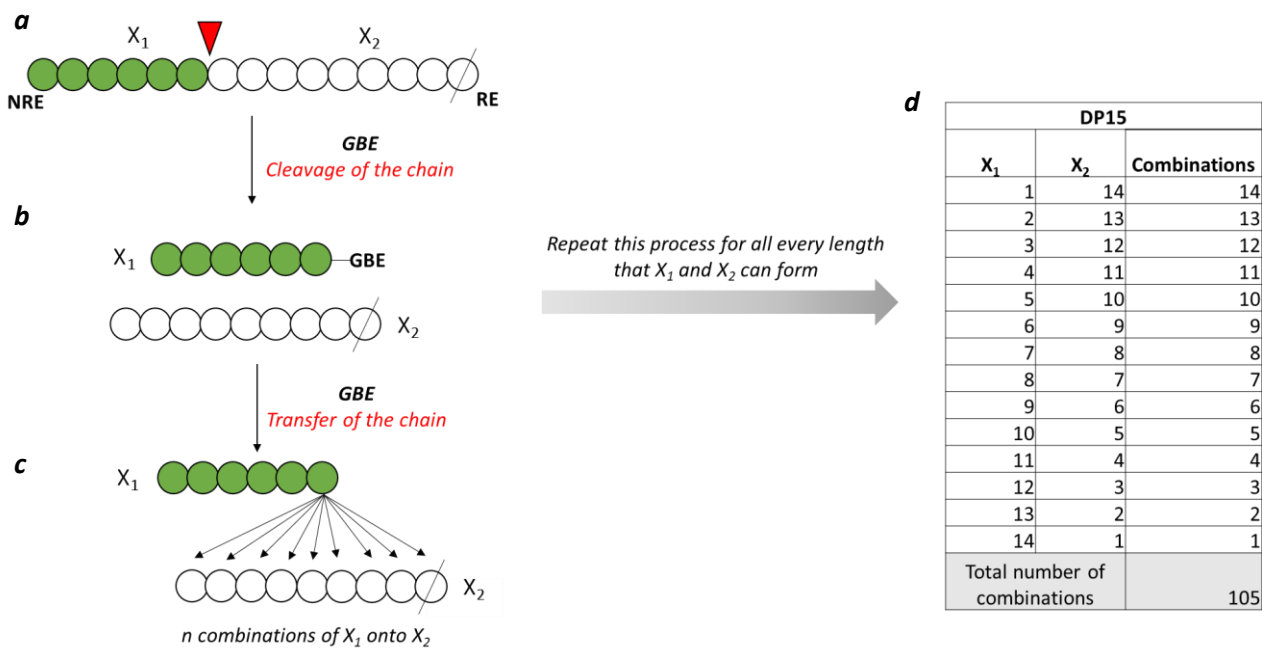


Figure 38 Theoretical branching process used to build up the DP15 model. A linear chain of 15 glucose residues is split into two chains X_1 (green circles) and X_2 (white circles). To create the possible branching arrangements, X_1 is transferred onto X_2 occupying every glucose residue of this chain. The red cursor represents the theoretical cleavage site to form the two chains. NRE = non reducing end; RE = reducing end indicated with a crossed circle.

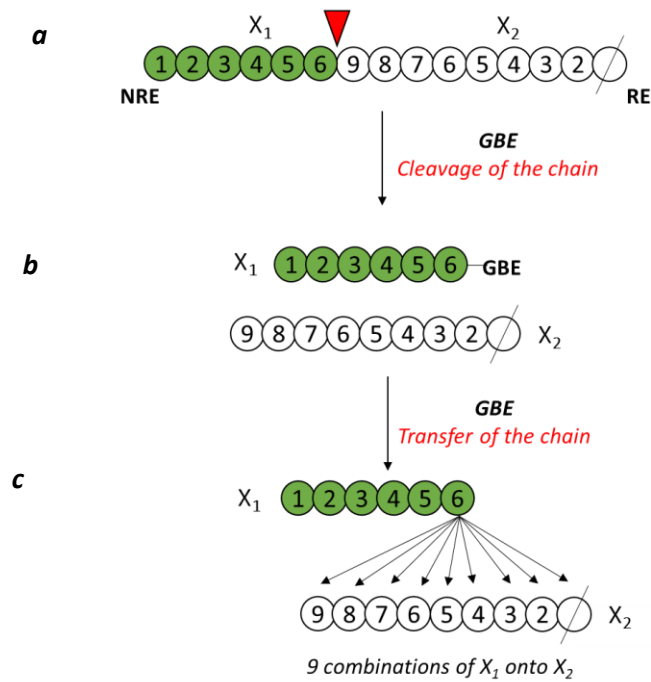


Figure 39 Example of the branching arrangements created with a chain of DP6 (X_1) and DP9 (X_2) starting from DP15. **(a)** The first step is the cleavage of the chain (red arrow) between the ninth and the tenth glucose residue from the reducing end. **(b)** The second step is the split of the chain into DP6 and DP9, and **(c)** the final step is the transferred of the DP6 onto DP9 to form 9 combinations. The red cursor represents the theoretical cleavage site to form the two chains. NRE = non reducing end; RE = reducing end indicated with the crossed circle.

3.1.1. Selection of the branched models based on the substrate specificity of glycogen branching enzyme

Froese *et al.*⁶² stated that “GBE cleaves every 8–14 glucose residues of a glucan chain, an α -1,4-linked segment of more than six glucose units from the non-reducing end”. Although no reference to literature was mentioned by the authors, the substrate specificity of GBE reported by Froese *et al.*⁶² was used to rule out some of the branched models in **Appendix 1**.

According to the specificity of GBE, X_1 must be equal or longer than DP6 while X_2 is equal to the length of the initial chain minus X_1 . Therefore, the compounds that must be discarded are those bearing X_1 shorter than 6 glucose units (**Fig. 40**). As result, the combinations are reduced to 45, and the branched compounds are those generated by X_1 between DP6 and DP14, and X_2 between DP9 and DP1.

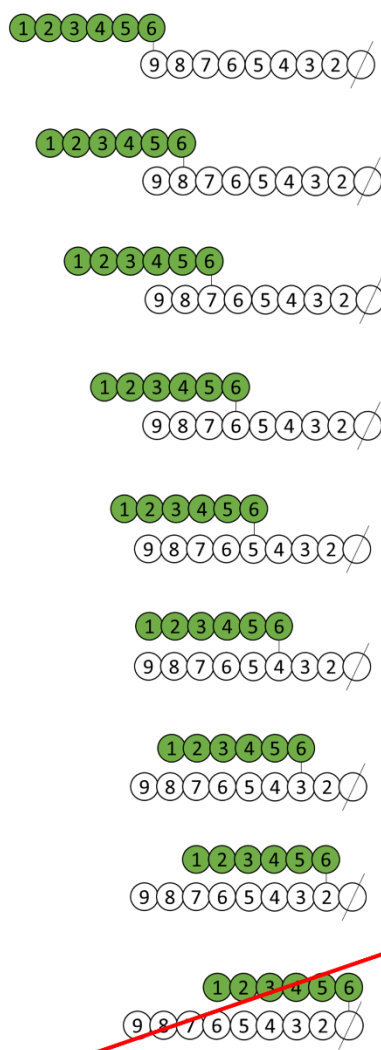
DP15		
X_1	X_2	Combinations
1	14	14
2	13	13
3	12	12
4	11	11
5	10	10
6	9	9
7	8	8
8	7	7
9	6	6
10	5	5
11	4	4
12	3	3
13	2	2
14	1	1
Total number of remaining combinations		45

Figure 40 The combinations of X_1 with X_2 selected according to the substrate specificity of GBE reported by Froese *et al.*⁶² The combinations discarded are those in the red rows, while those selected are in the blank rows.

3.2. Theoretical chain length distribution using the branched DP15 models

The selected combinations illustrated in **Fig. 40** were used to investigate the theoretical CLD that could potentially be generated by a glycogen bearing the proposed combinations. To this end, each branched structure was digested *in silico* into linear chains following the substrate specificities of the debranching enzymes ISA and Pull. The most extensive work on the characteristics of ISA and Pull was carried out by Kainuma *et al.*¹¹⁰ (1978) as already discussed in Chapter 2. According to the enzymes' specificities, structures bearing glucose stubs or branches placed on the reducing end must be discarded because they are not substrates of ISA and Pull. Among other substrates evaluated by Kainuma *et al.*,¹¹⁰ the short-branched structures with the branch on the second glucose residue from the reducing end were digested by Pull but not by ISA. However, these structures were not discarded as both enzymes were included in the model. **Fig. 41** illustrates an example of the branched structures discarded from the models generated by the combination of DP6 with DP9, and DP7 with DP8.

DP6 + DP9



DP7 + DP8

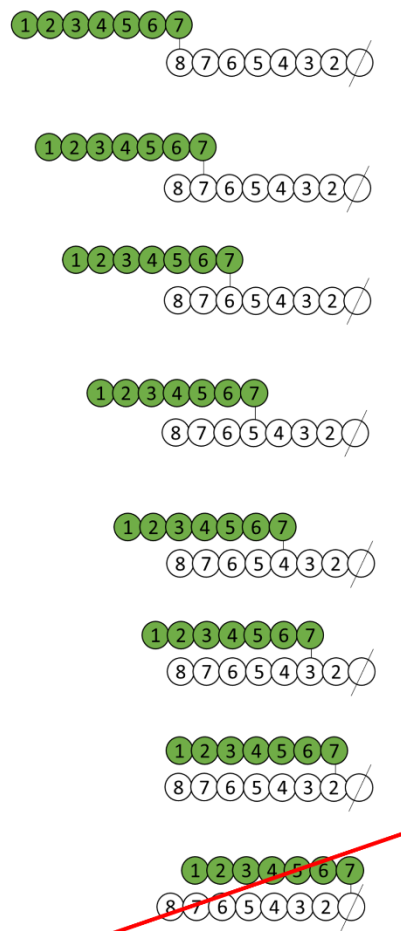


Figure 41 Branched structures selected to investigate the chain length distribution generated by their debranching; the structures crossed in red are those discarded according to the substrate specificity of ISA and Pull. The reducing end is illustrated with crossed circle.

Following the method depicted in **Fig. 42**, the chain length distribution was modelled according to the specificity of ISA and Pull. Each glycan reported in **Appendix 1** was counted only once, and an absolute value of one was assigned to every chain released from every model. For example, **Fig. 42** shows two combinations of DP6 and DP9: in model A, DP6 is placed on the fifth glucose residue of DP9, while in model B, DP9 is branched on the fourth glucose residue. From both models A and B, two chains of DP6 and two chains of DP9 are released after debranching treatment. Then, the absolute numbers of chains per degree of polymerisation were placed in an Excel file and plotted in a chart.

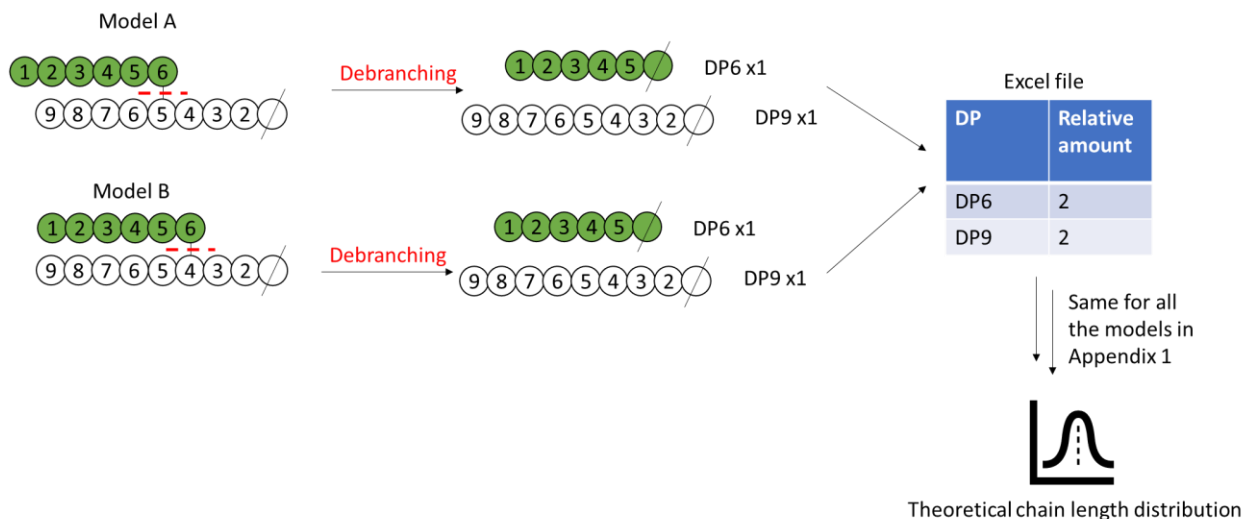


Figure 42 Method developed to create a theoretical chain length distribution of glycogen from the DP15 models reported in Appendix 1. The reducing end is illustrated with a crossed circle.

By application of the method in **Fig. 42**, it is possible to predict the chain length distribution as showed in **Fig. 43**. In the calculated data, the chains between DP6 and DP9 are more abundant than shorter or longer DPs; any DP1 or DP14 is obtained because the only possible combination of these two DPs is not a suitable substrate of ISA and Pull.

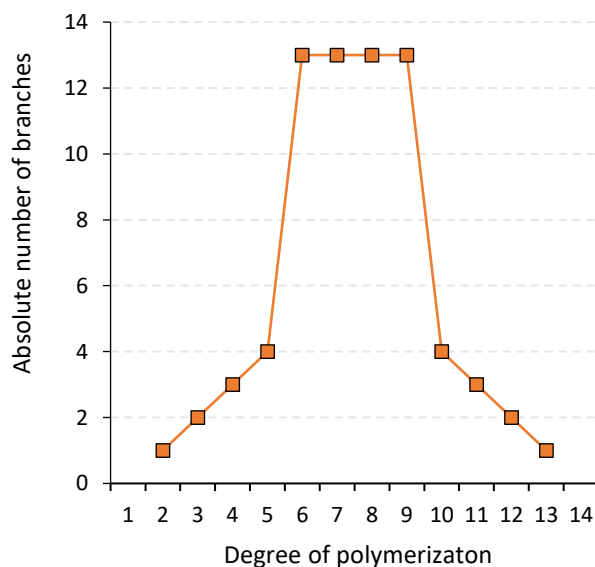


Figure 43 Hypothetical chain length distribution obtained with the models reported in **Appendix 1**.

In the literature, the structure of glycogen is characterised by a peak depending on the source, and short chains (< DP10) are always more abundant than long ones (>DP10).¹⁴² In **Fig. 44**, the glycogen chain length distribution from three different animals was investigated experimentally by Matsui *et al.*¹⁴² using HPAEC analysis. A group of short chains between DP2 and DP5 was detected, and the concentration of each DP within this range depended on the source. In our model, short chains

between DP2 and DP5 are only obtained when X_1 is equal or longer than DP10 suggesting that the short chains observed experimentally might represent the remaining stubs, namely X_2 , left after the cleavage of X_1 by GBE.

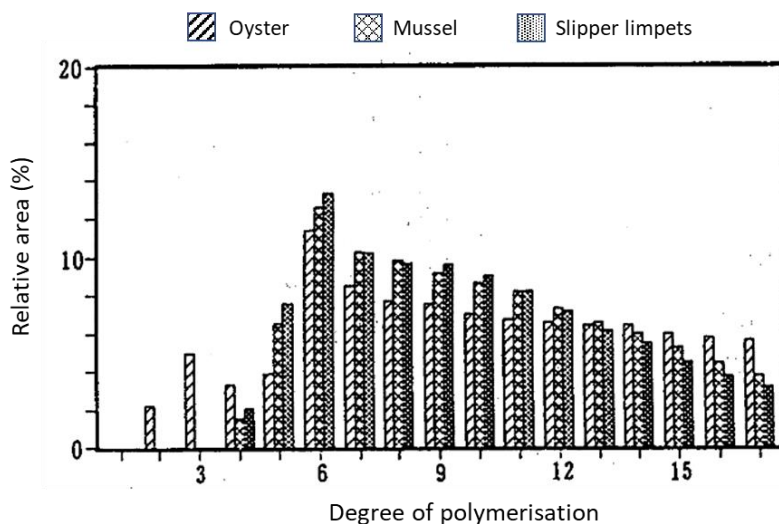


Figure 44 Chain length distribution of glycogen from oyster, mussel, and slipper limpets. Image adapted from Matsui *et al.*¹⁴²

The experimental data of Matsui *et al.*¹⁴² show a peak at DP6, and the abundance of branches longer than six glucose residues decreases by increasing the DP. Differently, no major peak is obtained in the theoretical model of **Fig. 43**. An explanation for the observed discrepancy between the *in vitro* and *in silico* data might be due to the preference of GBE to select one chain more frequently than others. As a result, the preferred DP becomes the most abundant and predominant peak in the chain length distribution of glycogen. In our model, the selection of DP6 as preferential chain (X_1) would lead to a chain length distribution with only two chains, DP6 and DP9, as illustrated in **Fig. 45**. In our opinion, it is possible that the large abundance of DP6 may be the result of the cleavage of this chain length from substrates shorter and longer than DP15. However, this mechanism would imply a more complex model than DP15, which scope goes beyond the aim of this chapter.

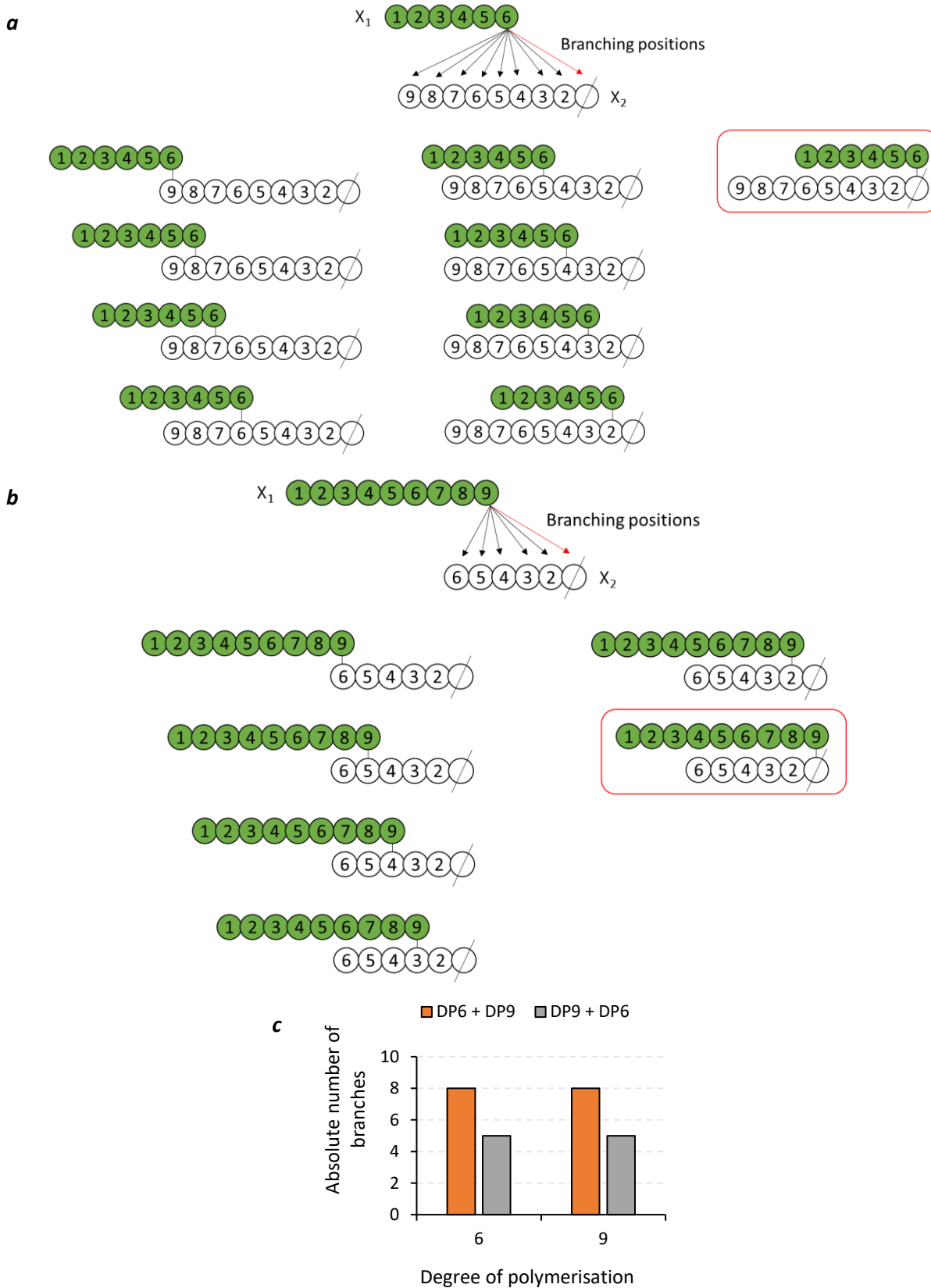


Figure 45 Theoretical models created by the combination of (a) DP6 onto DP9 and (b) DP9 onto DP6. A hypothetical debranching treatment was performed for each structure and the theoretical chain length distribution (c) was calculated following the method explained in Fig. 38.

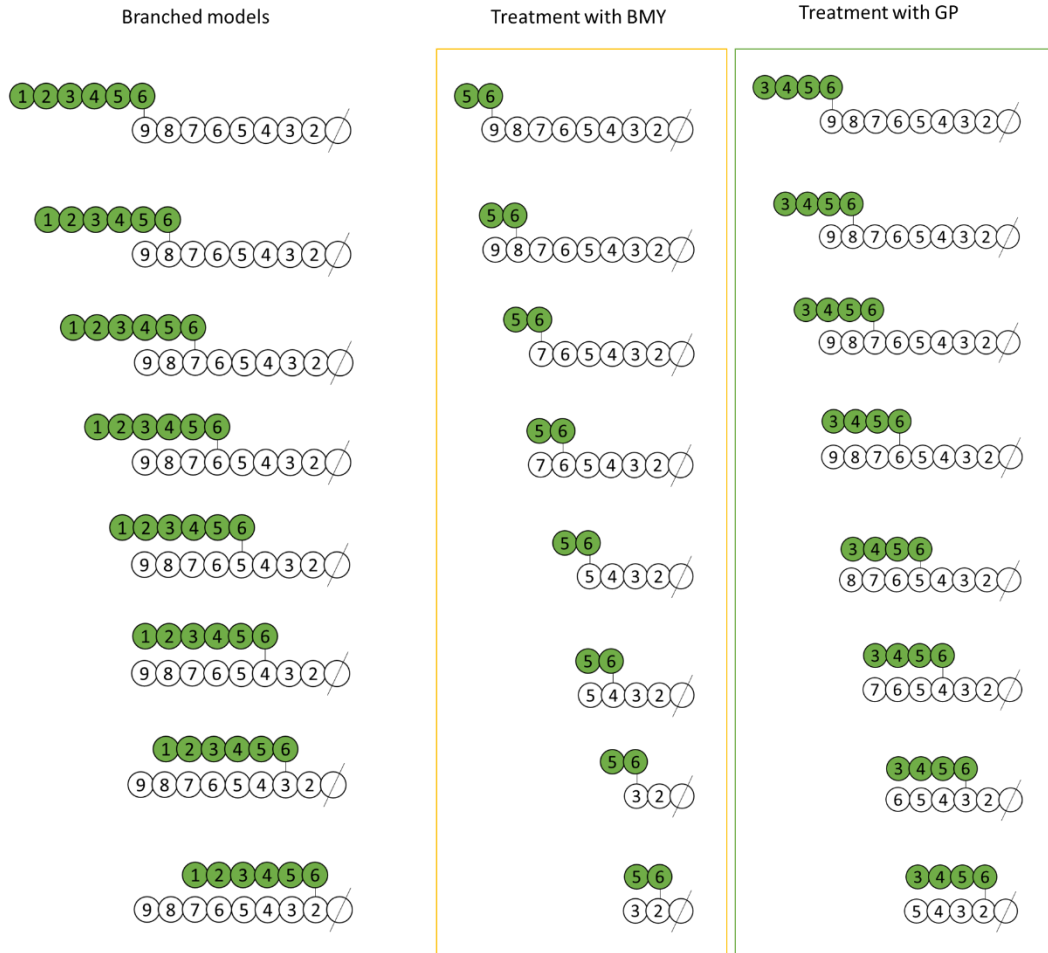
3.3. Digestion of the DP15 models with β -amylase and glycogen phosphorylase

The theoretical model presented in the previous section showed discrepancies with the experimental data reported in literature. However, the branched structures obtained with the DP15 model can help understanding the branching arrangement in glycogen by comparison of the chain length distribution of glycogen β - or phosphorylase- limit dextrin from *in vitro* and *in silico* models. To this purpose, the digestion of the glycans with BMY and GP leads to products that differ from each other based on the position of the branching point on X_2 . Therefore, the analysis of β - and phosphorylase- limit dextrin can provide a better understanding of the branching arrangements within glycogen structure. In the literature, BMY and GP are described as enzymes that act upon unbranched chains releasing maltose (DP2) and glucose 1-phosphate (G1P), respectively, and their activity is halted by branching points. While BMY produces maltose or maltotriose stubs depending on even or odd substrates, GP creates maltotriose residues regardless of the number of glucose residues in the chain. As result, β -limit dextrans are be populated by DP2 and DP3 whereas phosphorylase-limit dextrans by DP4. Bearing in mind that the structure of glycogen is branched, chains longer than DP2/DP3 or DP4 are indicative of chains that contained $\alpha(1,6)$ -glycosidic bonds that prevented their further digestion by BMY or GP.

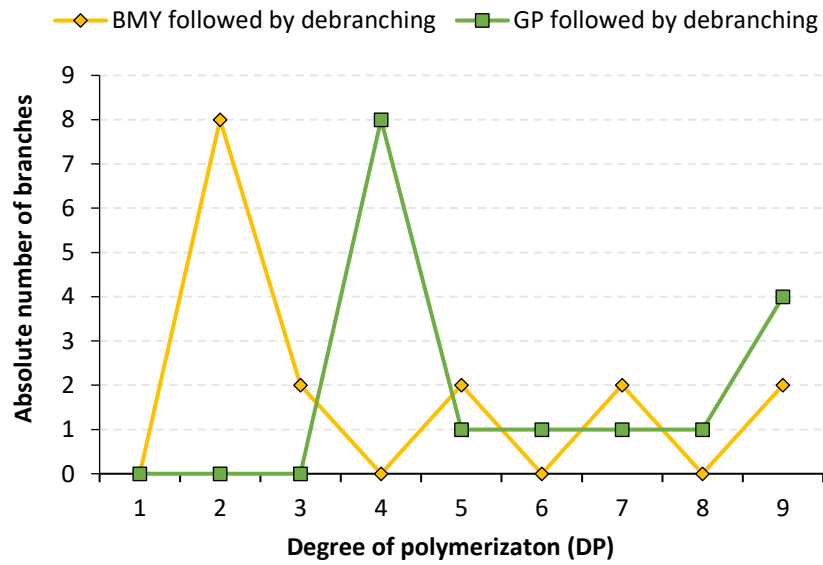
To investigate the theoretical CLD of *in silico* β - and phosphorylase- limit dextrans, the branched glycans illustrated in **Fig. 46** were treated with BMY and GP followed by treatment with the debranching enzymes. The combinations of DP6 and DP9 illustrated in **Fig. 46** were the only models selected for these enzymatic treatments to understand the CLD expected from a structure bearing a peak chain length of DP6 as occurs in oyster glycogen. The method applied to calculate the CLD was the same reported in **Fig. 38**.

When X_1 and X_2 are either DP6 or DP9, the major peaks in the β -limit dextrans are DP2 and DP3, whereas DP4 is the major one in phosphorylase-limit dextrans (**Fig. 46b** and **c**). For phosphorylase-limit dextrans, the amount of DP4 observed *in silico* in **Fig. 46b** is higher than that in **Fig. 46c** because the number of DP4 counted for each model is equivalent to the number of positions that X_1 occupies onto X_2 . As a matter of fact, the number of combinations of DP6 onto DP9 is bigger than the opposite arrangement. It is interesting to note that in both β - and phosphorylase-limit dextrans, the length of the chains longer than DP2 and DP3, and DP4 depends on the position of the branching point, and this information could be exploited to understand the branching arrangement in experimental data.

a



b



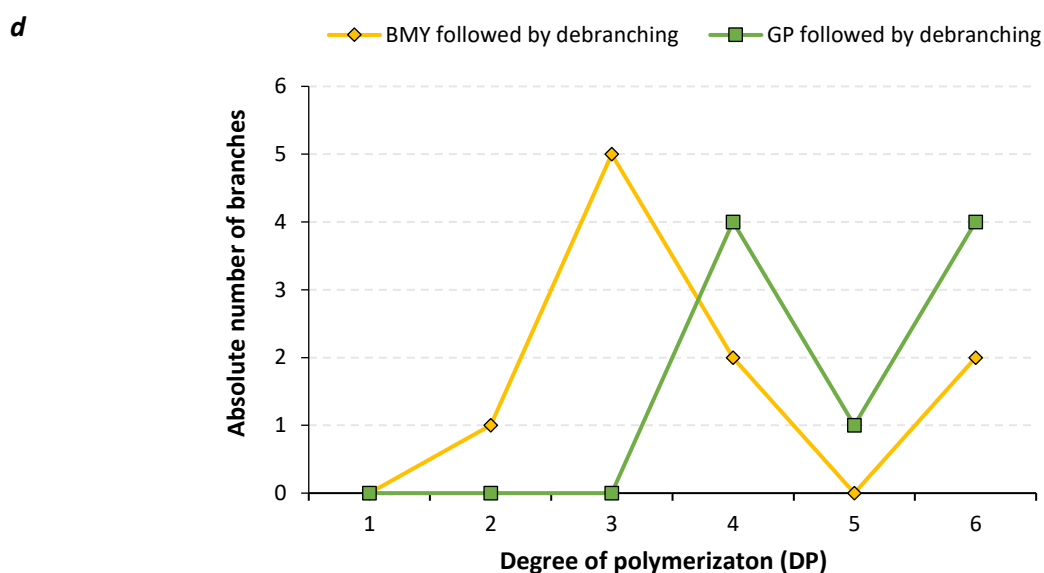
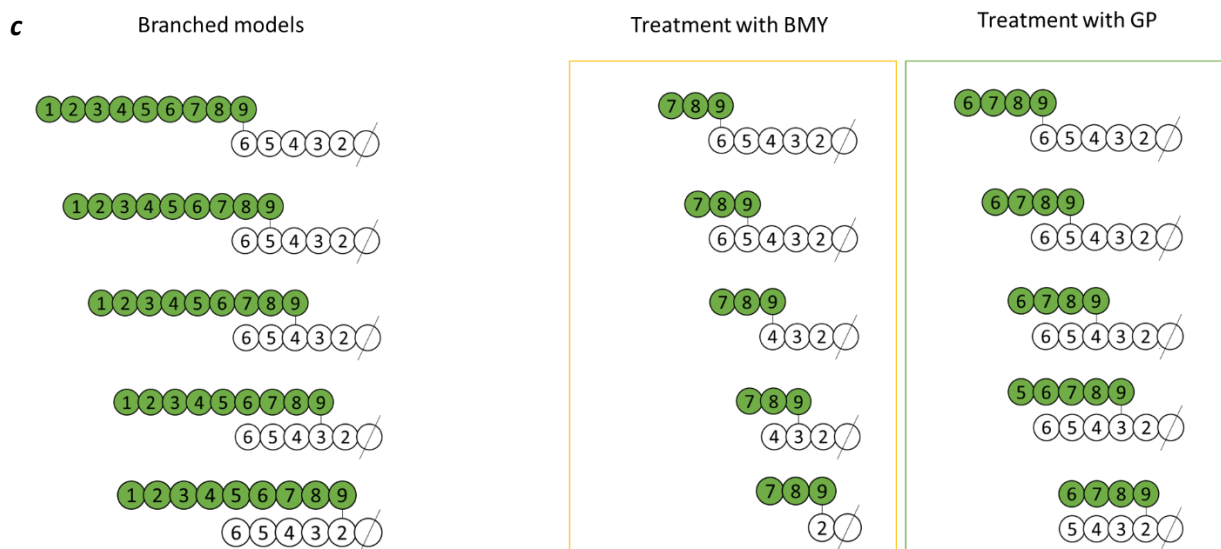


Figure 46 β -amylolysis and phosphorylase of the branched models created by the combination of (a) DP6 onto DP9 and (c) DP9 onto DP6. A hypothetical debranching treatment was performed on each limit dextrin resulted from the enzymatic digestion, and the theoretical chain length distribution (b-d) was calculated following the method explained in Fig. 38.

The analysis of the proposed theoretical models using mainly DP6 and DP9 as X_1 and X_2 provided insights into the CLD that can be generated from structures bearing a peak at DP6 as oyster glycogen. The few experimental data published about glycogen β - and phosphorylase-limit dextrans (Bertoft and Makela, 2007)⁵ shows the presence of chain lengths both observed in Fig. 46b and 46d. For instance, DP4, DP6 and DP8 are not found in the models of Fig. 46a but they are generated by structures in Fig. 46b suggesting that both combinations can be part of the glycogen structure. However, these are theoretical studies that require further validation with experimental data.

In Chapter 4, the theoretical models obtained according to the substrate specificity of GBE stated by Froese *et al.*⁶² were used to interpret the experimental chain length distribution determined in the present study. In the case that the models proposed will not be sufficient to provide support to the experimental data, further branched structures will be suggested and described in the discussion section. For instance, the theoretical chain length distribution reported for the limit dextrin is the result of the single combination generated by DP6 and DP9. If the selected combinations are not somehow relevant to interpret the results, more models will be included using chains shorter or longer than the DPs chosen.

Chapter 4 – Stepwise enzymatic digestion of glycogen and combination of the results with theoretical models

In this chapter, the methodology developed to investigate DB, the position of the branching points, and the CLD of glycogen is discussed. Initially, the conditions for the reactions with ISA and Pull (Section 4.1) are investigated to achieve a stepwise debranching of glycogen. Then, the enzymatic debranching procedure is applied to β - and phosphorylase- limit dextrins (Section 4.2 and 4.3) to study the impact of β -amylolysis and phosphorolysis on the chain length distribution of glycogen. Finally, the results obtained from the debranching of glycogen and limit dextrins are compared with the theoretical model to evaluate on the branching arrangement that populates the outer most layers of glycogen and to gain more insights into the activity of GBE (Section 4.4).

4.1. Enzymatic debranching of glycogen by isoamylase and pullulanase

4.1.1. Digestion of glycogen with isoamylase

4.1.1.1. Assessment of the debranching conditions

Commercially available oyster glycogen was the substrate of choice for the enzymatic debranching with *Pseudomonas* isoamylase (ISA). The working conditions employed by Harada *et al.*¹⁰⁸ were followed to achieve exhaustive release of chains from glycogen in 24 h, as illustrated in **Fig. 47** from their studies.

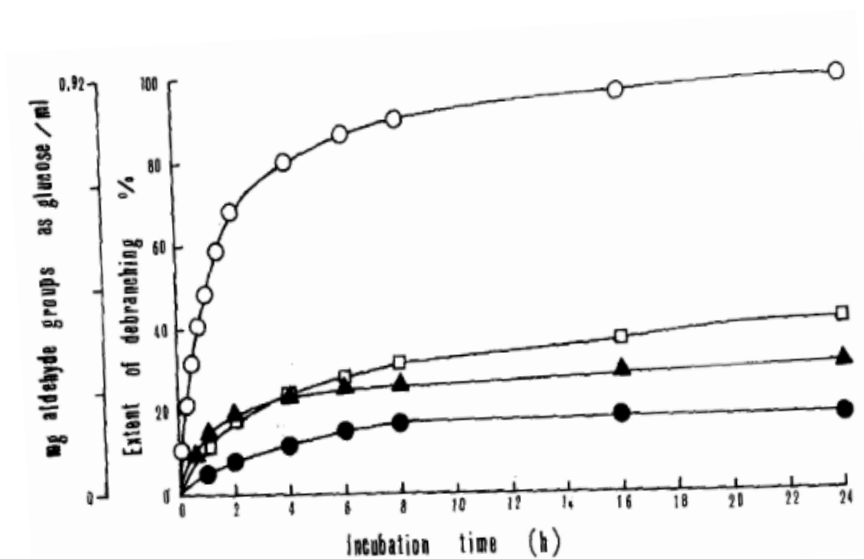


Figure 47 Image adapted from Harada *et al.*¹⁴³ Debranching of 10 mg/mL of oyster glycogen in 0.05 M acetate buffer at pH 3.5 with 0.0027 mg (\square) and 0.027 mg (\circ) of isoamylase, or with 2.9 mg (\bullet) and 29 mg (\blacktriangle) of pullulanase at pH 5.0.

Briefly, the authors expressed and purified ISA from *E. coli* and used 0.027 mg (*ca.* 1600 U)¹⁴³ of the purified enzyme to debranch the polysaccharide in 24 h. The degree of branching, measured by the Nelson-Somogyi assay, was *ca.* 10%, namely 0.092 g of reducing termini released for 1 g of substrate, and the completion of the reaction was assessed by SEC separation using a Sephadex G75 column. In the present studies, commercial ISA extracted from *Pseudomonas* was selected. Thus, the units of enzyme were calculated based on the specific activity of ISA reported by the supplier and the amount of substrate employed for this experiment.

Initially, oyster glycogen was incubated with three different units of ISA (0.15 U, 0.06 U, and 0.006 U) for 1 h to determine the most promising amount of enzyme for a stepwise debranching as the one reported in **Fig. 48**. It was estimated that *ca.* 12 mg of glycogen is made by *ca.* 12 mg (70 μ mol) of glucose molecules linked by α (1,4)-glycosidic bonds and *ca.* 10% (7 μ mol) by α (1,6)-glycosidic bonds. Based on the units of enzyme employed and the incubation time (**Table 2**), 0.006 U was expected to be the most promising amount of enzyme compared to the other two which were supposed to complete the debranching in one or two hours. Nevertheless, the analysis of the results by TLC showed that 0.006 U of ISA debranched glycogen so slowly that the products, mainly chains longer than 6 glucose residues (DP6), were barely detected by TLC (**Fig. 48a**). In contrast, 0.06 U and 0.15 U of ISA (**Fig. 48b** and **48c**) digested a greater quantity of products as observed by the gradual darkening of the TLC spots over an hour. Among those units of enzyme, 0.15 U of ISA were selected to assess the debranching of glycogen over 24 h.

Table 2 Estimated time required to debranch oyster glycogen by *Ps. isoamylase* (ISA) per units of enzyme employed; 1 U = 1 μ mole of D-glucose reducing sugar per min.

Enzyme	<i>Ps. isoamylase</i> (ISA)		
Units of enzyme used	0.15 U	0.06 U	0.006 U
Amount of time required to digest <i>ca.</i> 7 μ mol of reducing ends	< 1 h	<i>ca.</i> 2 h	<i>ca.</i> 20 h

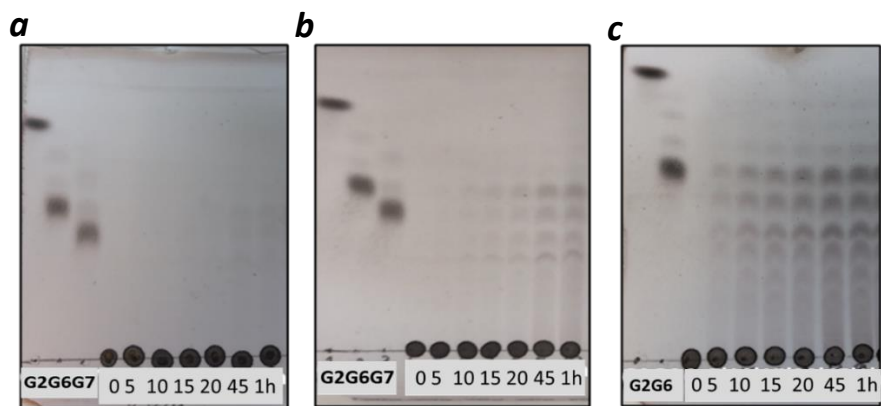


Figure 48 Qualitative analysis of the chains released from oyster glycogen (10 mg/mL) per time point (0', 5', 10', 15', 20', 45', 1 h) using (a) 0.006, (b) 0.06, and (c) 0.15 U of ISA; the standards are indicated with G2 (maltose), G6 (maltohexaose), and G7 (maltoheptaose), and the TLC plate was developed three times in the solvent mixture CH₃CN: EtOAc: H₂O: iPrOH (85:20:50:50) before staining with 5% H₂SO₄ in EtOH.

4.1.1.2. BCA assay and HPAEC analysis of the products released from glycogen using the selected debranching conditions

The TLC analysis of each time point up to 24 h (**Fig. 49a**) shows the presence of linear oligosaccharides mostly longer than DP6, as observed by the comparison with the standard maltohexaose (G6). However, it was noticed that the differences in the staining intensity were evident until 1 h, and that products larger than DP10 deposited at the bottom line of the TLC plate (dark dots). To have a better understanding of the debranching progress over 24 h, the material released per time point was quantified by BCA assay. Furthermore, the HPAEC was performed to analyse the chain length distribution of oyster glycogen at completion of the debranching.

The plot of the number of chains as reducing ends released per time point (**Fig. 49b**) resulted in a progress curve that follows the same trend reported by Harada *et al.*¹⁰⁸ (**Fig. 47**). In the first hour, *ca.* 3.5 μmol of chains were released by ISA, which value is equal to half of the total amount of branches calculated (*ca.* 7 μmol) per quantity of substrate employed. After an hour, ISA activity decreased and the enzyme slowly debranched the remaining glycogen in the following 23 h. To confirm that the debranching of oyster glycogen with ISA achieved completion in 24 h, the sample collected at 24 h was treated with an excess of enzyme (15 U) and incubated for one hour before quantification by BCA assay. The results in **Fig. 49c** confirmed that the debranching of glycogen was complete because the reducing power of the solution did not change.

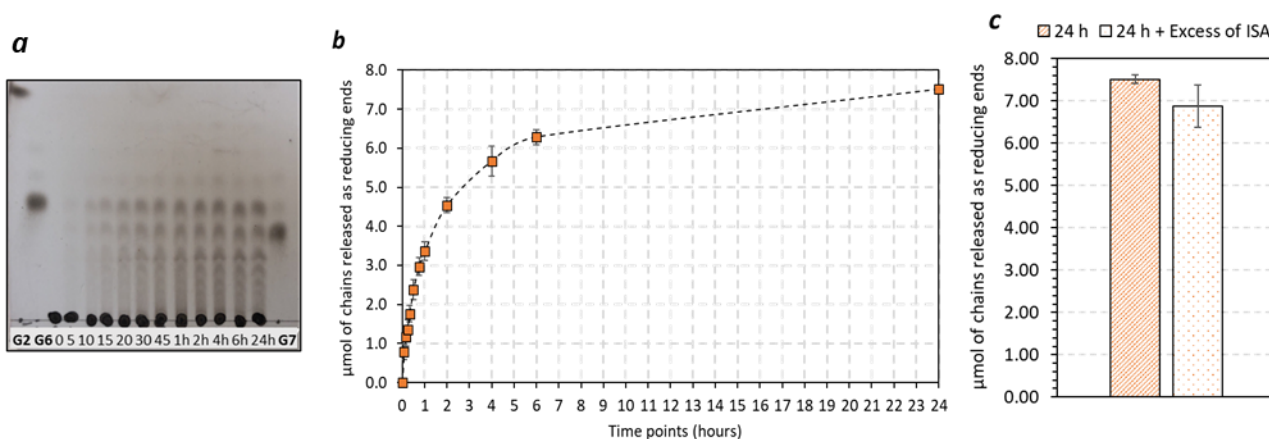


Figure 49 Debranching of oyster glycogen (10 mg/mL) by ISA (0.15 U) in sodium acetate buffer (pH 3.5, 0.05 M) at 40 °C. The progress of the reaction was followed by TLC (**a**) and the material released per time point was quantified by BCA assay (**b**); the standards are indicated with G2 (maltose), G6 (maltohexaose), and G7 (maltoheptaose), and the TLC plate was developed three times in the solvent mixture $\text{CH}_3\text{CN}:\text{EtOAc}:\text{H}_2\text{O}:\text{IPA}$ (85:20:50:50) before staining with 5% H_2SO_4 in EtOH. To confirm that the branching with ISA was completed in 24 h, 15 U of enzyme was added to the sample and any increase was recorded by BCA assay (**c**). Error bars are from triplicates of three different experiments.

Following the quantification of the products released by ISA, the sample collected at completion of the debranching (24 h) was analysed by HPAEC (**Fig. 50a** and **50b**). The chain length distribution of

glycogen is characterised by a small percentage of short chains (DP2-DP5) and a peak at DP6; a decreasing concentration per DP is observed for chains longer than DP7. These results support the TLC analysis reported in **Fig. 50a**, and the distribution of chains longer than DP6 is consistent with those reported in literature.^{5,17} In contrast, the proportion of short chains between DP2-DP5 differed from that available in literature. For instance, **Fig. 50b** shows that DP2 and DP4 are in lower concentration than DP3 and DP5, whereas Matsui *et al.*³ found that chains from DP2 to DP5 shared the same abundance. Small discrepancies among glycogen of the same species may be attributed to the metabolic turnover that this molecule is subjected to, e. g. feeding and fasting state, or seasonal variations.^{28,144,145}

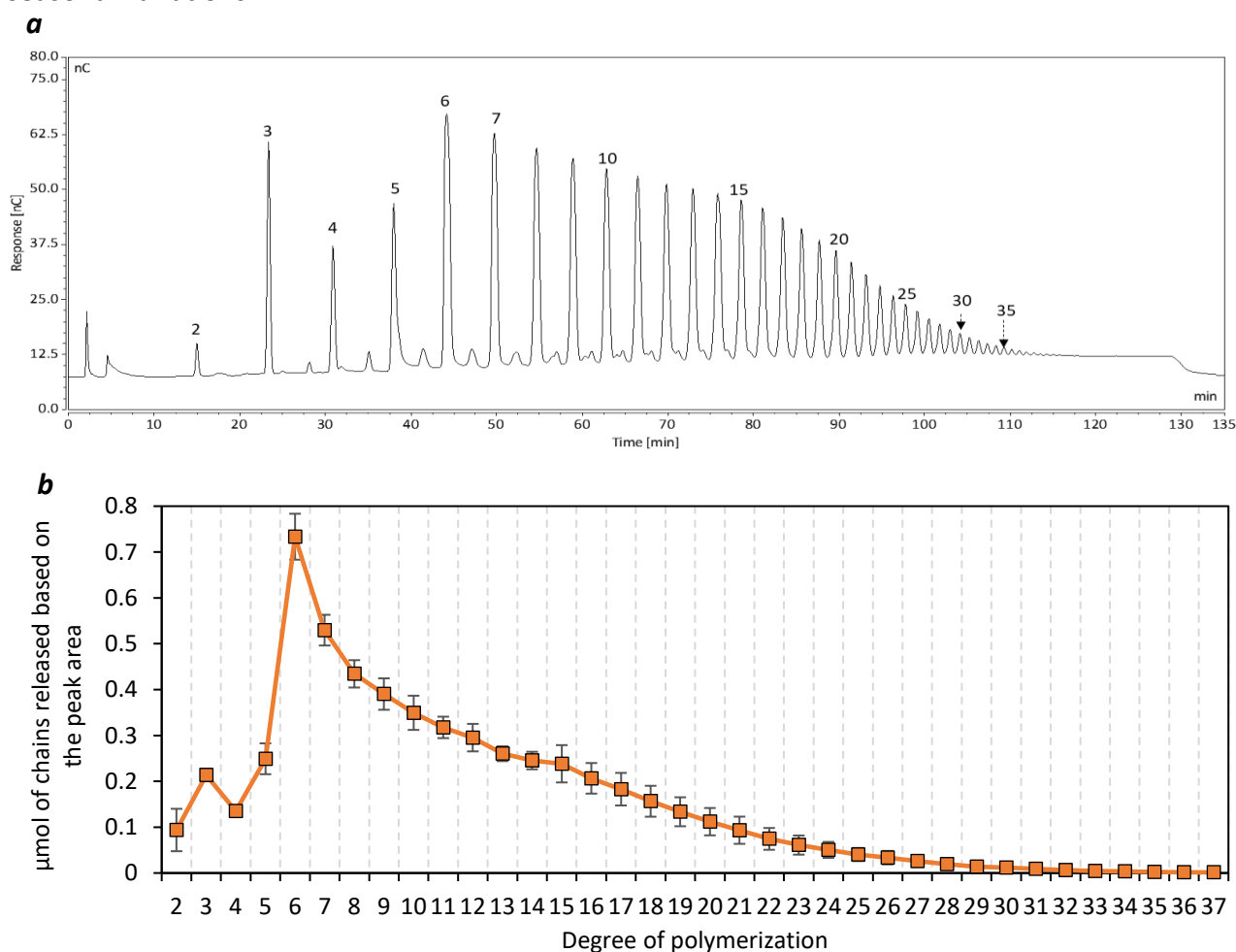


Figure 50 Chain length distribution of oyster glycogen digested with ISA (0.15 U) in sodium acetate buffer (0.1 M, pH 4.5) in 24 h at 40 °C. At the top (**a**), the chromatogram collected with raw data; the number at the top of the peaks indicate the degree of polymerisation. The chromatogram was obtained with a CarboPac PA1 (2x250 mm) column using a flow rate of 0.250 mL/min and the following gradient: 0-2 min of 150 mM NaOH (100%), 2-120 min of 600 mM NaOAc buffer (0-100%), 120-135 min of 150 mM NaOH (100%). At the bottom (**b**), the μmol of chains per each degree of polymerization was calculated using the area (nC x min) of 0.5 μmol glucose standard. Chains from 2 to 7 glucose residues were confirmed with the standards. Error bars are from triplicates of three different experiments.

Looking at the raw data reported in **Fig. 50a**, small humps were detected between two identified peaks. It was hypothesised that glycogen has short-branched structures, e. g. single glucose

residues, that ISA cannot debranch (see Chapter 2.1.1.1 for substrate specificity). These products remain in solution as components of the debranched mixture and have different retention time than the linear oligosaccharides of the same DP, e. g. maltotetraose is eluted later than 6³- α -glucosyl-maltotriose (**Fig. 32**). To prove that the intermediate peaks are chains with glucose branches, the mixture of ISA-debranched was digested products with oligo $\alpha(1,6)$ -glucosidase (OGL) that selectively debranches glucosyl chains. To perform this experiment, a one-pot reaction was prepared in sodium acetate buffer (pH 4.5, 0.1 M). The selected working conditions were slightly more basic than those used in the previous section (sodium acetate buffer pH 3.5, 0.05 M) for the treatment with ISA because OGL has its maximum activity at pH 4.5 as reported by the supplier (Megazyme). In addition, the use of a pH suitable for both enzymes eliminated additional steps required to adjust the pH. Considering the activity of OGL, it was expected to have an increase in the amount of glucose accompanied by a decrease in the intensity of some intermediate peaks. The separation of the products by TLC and HPAEC (**Fig. 51**) showed a different outcome with neither glucose detected or loss of peaks intensities.

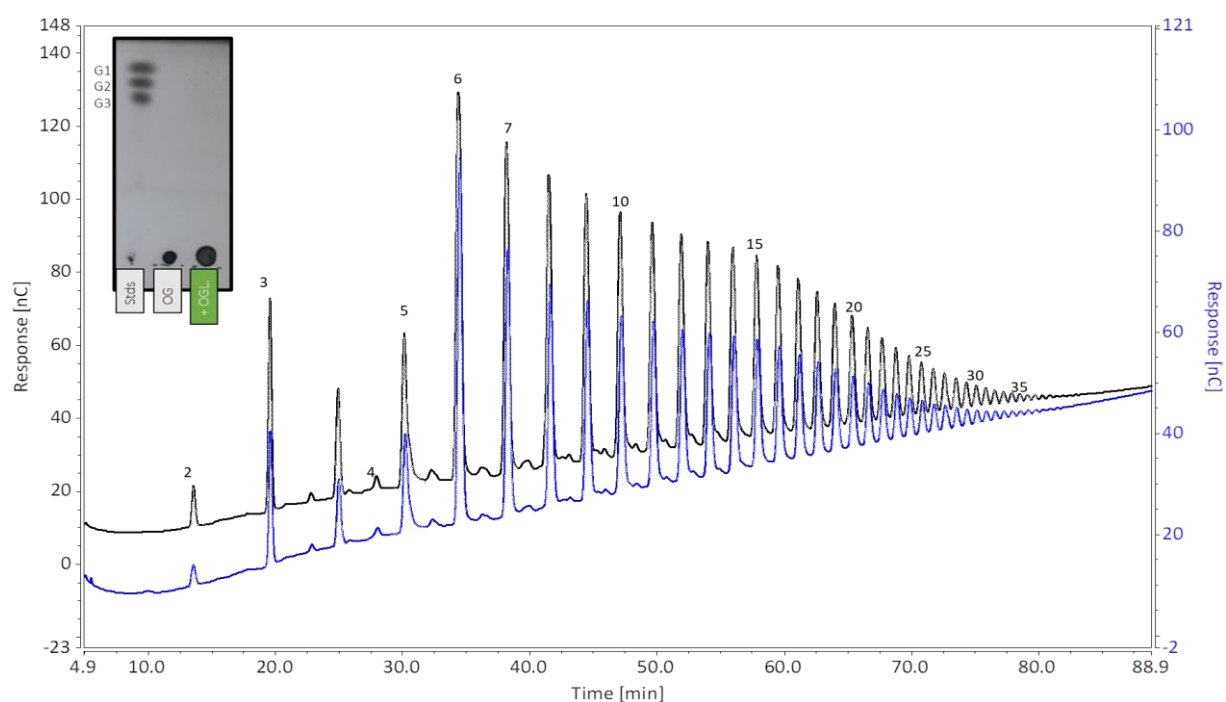


Figure 51 Digestion of glycogen with oligo $\alpha(1,6)$ -glucosidase (OGL) in sodium acetate buffer (0.1 M, pH 4.5) in 24 h at 40 °C. Comparison of the chain lengths distribution of oyster glycogen before (in **black**) and after (in **blue**) addition of the enzyme. The number at the top of the peaks indicate the degree of polymerisation. Both chromatograms were obtained with a CarboPac PA1 (2x250 mm) column using a flow rate of 0.250 mL/min and the following gradient: 0-2 min of 150 mM NaOH (100%), 2-120 min of 600 mM NaOAc buffer (0-100%), 120-135 min of 150 mM NaOH (100%). The insert represents the TLC analysis of the enzymatic digestion.

4.1.1.3. GPC analysis of the mixture of debranched oligosaccharides

To further investigate the intermediate peaks, we employed gel-permeation chromatography (GPC) to separate the components of the debranched mixture. Differences in the hydrodynamic volume in linear and branched oligosaccharides can be exploited to separate and characterise these products by SEC,¹⁴⁶ as also explained in Chapter 2.2.3. Therefore, the mixture of oligosaccharides collected after 24 h of debranching underwent GPC analysis (**Fig. 52**).

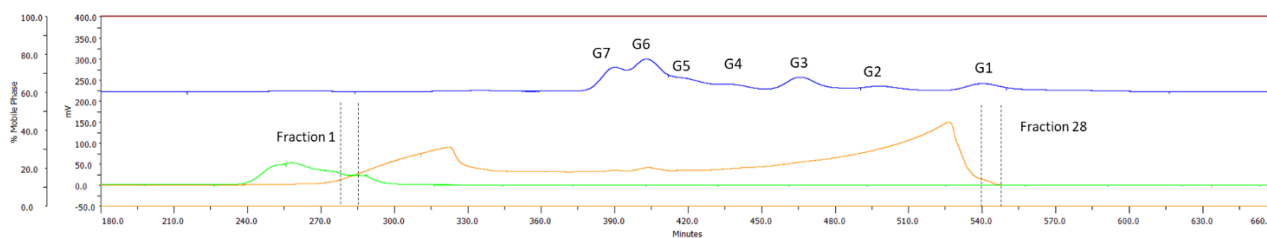


Figure 52 Comparison of the GPC chromatograms of 10 mg of glycogen debranched with 0.15 U of isoamylase in sodium acetate buffer (pH 4.5, 0.1 M; in orange) with the standards (G1 to G7, in blue) and glycogen (in green). The separation was performed with a TSK 40S column (22 mm ID x90 cm) with a flow rate of 0.2 mL/min using MQ water as eluent; the fractions were collected with 7 mL per tube from 150 mins to 650 mins.

The GPC chromatogram of the ISA-hydrolysed products partially overlays the one obtained from glycogen suggesting that a small amount of the starting material was still in solution after 24 h debranching. This hypothesis, however, contradicted the quantitative results reported earlier in **Fig. 49**. Therefore, the fractions corresponding to the overlay and collected between 270 and 300 minutes were analysed by TLC along with the others, and further investigated by HPAEC (**Fig. 53a** and **53b**). In **Fig. 53a**, the products eluted from fraction number 6 onwards have a degree of polymerisation between 1 and 11 glucose residues, and the solutions did not display any precipitate. Differently, fractions 1 to 5 mainly contain material that cannot be separated by TLC and deposit at the bottom line of the TLC with a dark dot at the centre of the spot. In addition, the vials containing those fractions had a white precipitate. Due to the challenges related to the analysis of the precipitate, the supernatants of fractions 1 to 5 were analysed by HPAEC. The results in **Fig. 53b** show that the samples are characterized by a range of oligosaccharides between DP20 and DP37. Considering that long linear oligosaccharides can form aggregates, as double helices, it was hypothesised that the products released by ISA partially precipitated in water due to the formation of complexes, and only some of the chains remained in solution. This hypothesis was supported by the findings of Akai *et al.*¹⁴³ The authors reported that when rabbit liver glycogen was incubated with ISA, a precipitate was observed after 24 h hydrolysis because of the aggregation of long glucan chains released.

The GPC analysis aimed at providing more insights into the intermediate peaks observed by HPAEC in **Fig. 51**. Nevertheless, the separation of the chains achieved by GPC was not efficient enough to have a small number of products per fraction to selectively analyse the unidentified peaks between DP2 and DP11.

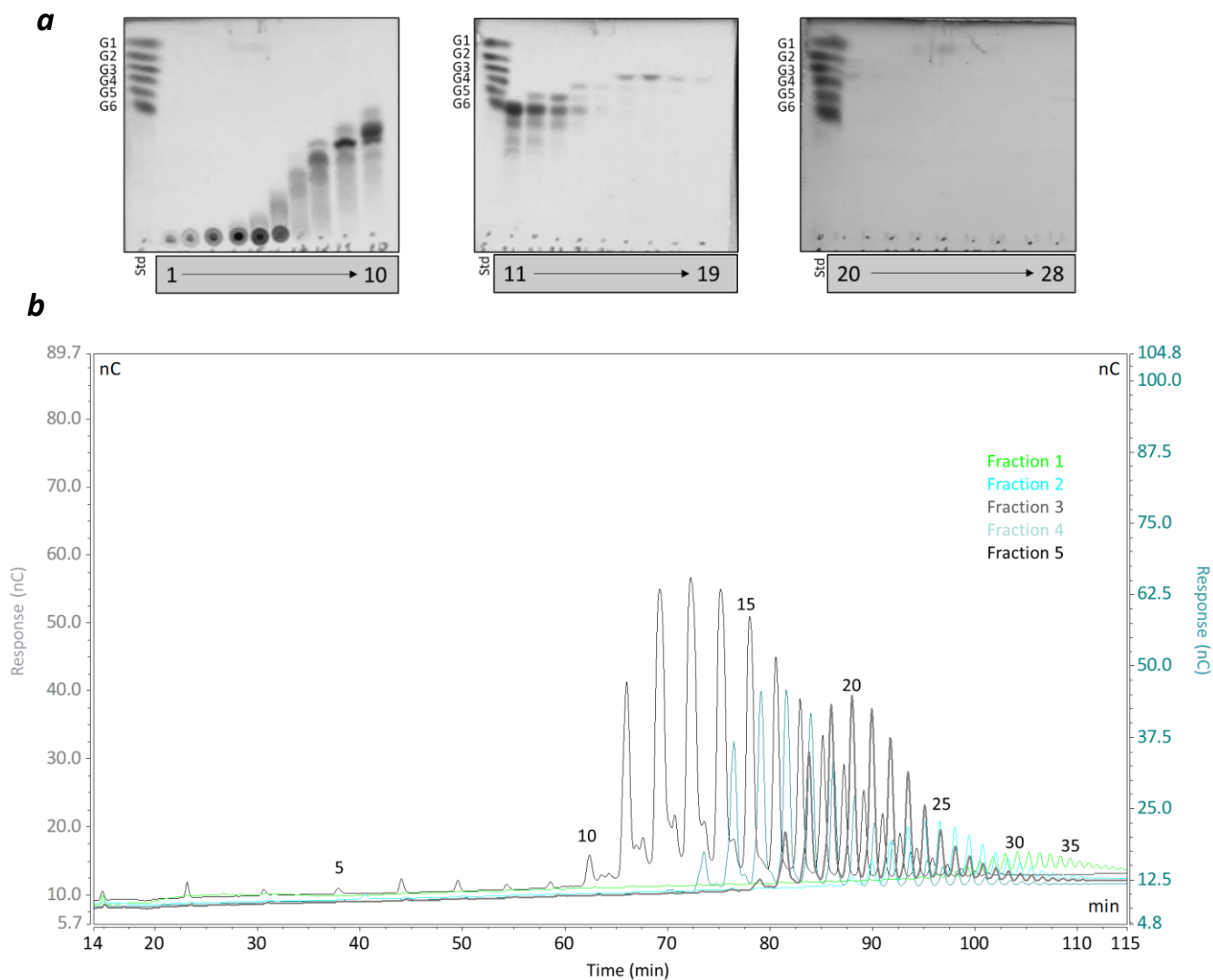


Figure 53 Separation of the products by GPC and analysis of the fractions by TLC and HPAEC. **(a)** At the top, TLCs of all the fractions collected by GPC; the standards are in the first line of each TLC and are named G1 (glucose) to G6 (maltohexaose). **(b)** At the bottom, analysis of the fractions 1-5 by HPAEC. The chromatograms were obtained with a CarboPac PA1 (2x250 mm) column using a flow rate of 0.250 mL/min and the following gradient: 0-2 min of 150 mM NaOH (100%), 2-120 min of 600 mM NaOAc buffer (0-100%), 120-135 min of 150 mM NaOH (100%). Each colour corresponds to the fraction indicated in the insert.

4.1.2. Digestion of glycogen with pullulanase

Pull is more efficient than ISA in digesting short-branched structures such as pullulan, a polysaccharide made of maltotriose units connected by $\alpha(1,6)$ -glycosidic bonds. The digestion of glycogen with Pull can be helpful to target the distribution of short chains rather than long branches, as ISA does, and to characterise the intermediate peaks observed in **Fig. 51**. To carry out the debranching of glycogen with Pull and ISA, the working conditions suitable for both enzymes (sodium acetate buffer pH 4.5, 0.1 M) and the same number of units (0.15 U) were selected, and the reactions were performed simultaneously using 500 μg of glycogen. For this experiment, the end point of the reaction at 24 h was the only one analysed by TLC, HPAEC and BCA assay.

The TLC analysis reported in **Fig. 54a** shows that the products released by ISA or Pull are qualitatively the same, namely chains longer than DP6 with a low abundance of short chains (DP2-DP5). However, it was noticed a difference between the staining intensity of the material released by ISA and that by Pull. Therefore, the BCA assay was performed to quantify the chains released by both enzymes (**Fig. 54b**). Considering the amount of glycogen employed (500 μg equal to 2.8 μmol of glucose), *ca.* 0.3 μmol of chains were expected to be digested by ISA, and a lower value than *ca.* 0.3 μmol by Pull as glycogen is not its preferential substrate. Indeed, the results collected by BCA assay showed that Pull cleaved only *ca.* 0.1 μmol of chains compared to the expected 0.3 μmol that were released by ISA (**Fig. 54b**).

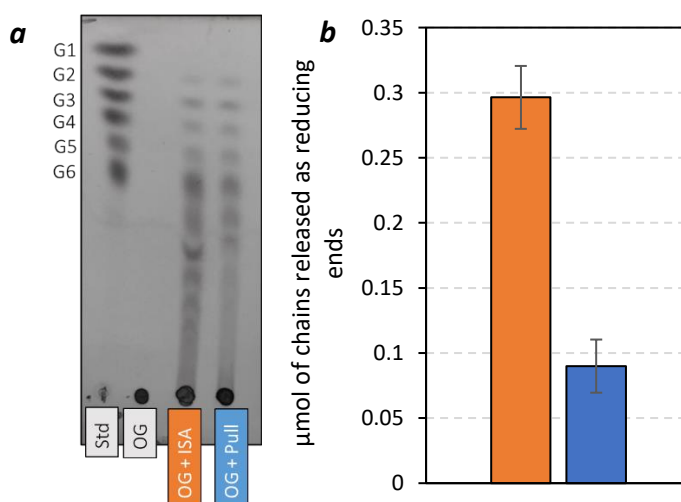


Figure 54 (a) TLC separation of the branches released from oyster glycogen (10 mg/mL) by ISA (0.15 U) and Pull (0.15 U) in sodium acetate buffer (0.1 M, pH 4.5) in 24 h at 40 °C. Each sample was applied 3x0.5 μL ; std = standards, OG = oyster glycogen, and standards are from glucose (G1) to maltohexaose (G6). Mobile phase CH_3CN : EtOAc: iPrOH: H_2O (85:20:50:50). The TLC plate was eluted three times before its development with a solution of 5% H_2SO_4 in EtOH and heating with a heat gun. (b) BCA quantification of the branches released from oyster glycogen (10 mg/mL) by ISA (0.15 U) and Pull (0.15 U); error bars indicate standard deviation from three individual experiments.

The chain length distribution of glycogen obtained with Pull was then analysed and compared to that obtained by ISA digestion (**Fig. 55a** and **55b**). The analysis of the samples by HPAEC confirmed the chain length distribution estimated by TLC for short chains (DP2-DP11) and provided a more detailed profile for long chains between DP12 and DP37. The minor peaks detected between the identified DPs overlay those observed in the sample digested with ISA, and yet, they remained unidentified. When glycogen is incubated with either ISA or Pull, the peak of the distribution curve is at DP6, the abundance of longer chains (>DP6) decreases by increasing DP, and DP3 and DP5 are more abundant than DP2 and DP4. The HPAEC analysis also showed two different profiles of the debranching activity for Pull and ISA. Whilst the former enzyme cleaved preferentially short chains between DP2 and DP5, the latter enzyme mainly digested chains longer than DP6 in the same incubation time (24h). The results reported in **Fig. 55** are consistent with those observed by Rani *et al.*¹⁰ and Matsui *et al.*¹¹

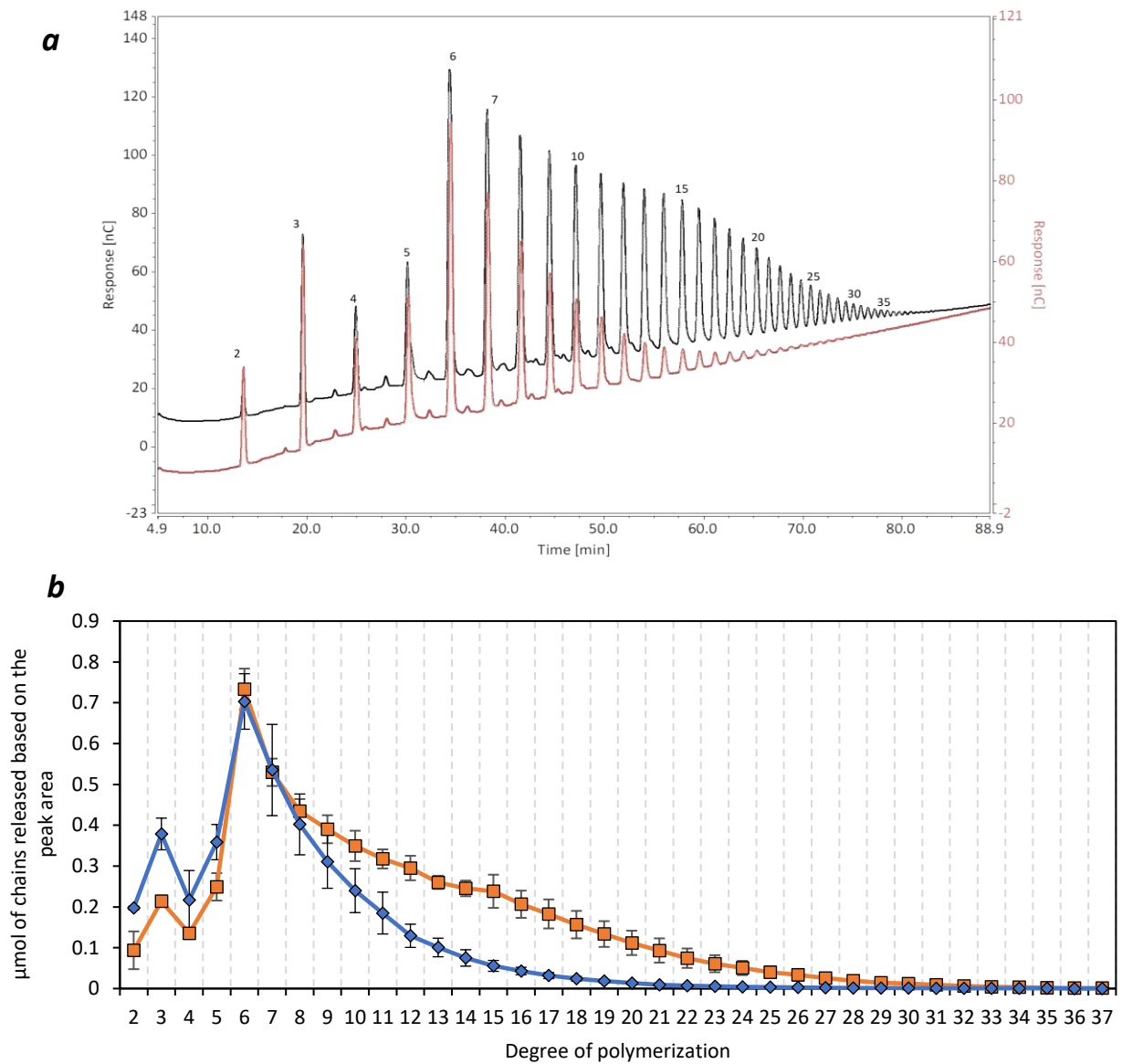


Figure 55 Chain length distribution of oyster glycogen digested with ISA (0.15 U) and Pull (0.15 U) in sodium acetate buffer (0.1 M, pH 4.5) in 24 h at 40 °C. At the top (a), the raw data of both chain length distribution for ISA in black, and Pull in dark red; the chromatograms were obtained with a CarboPac PA1 (2x250 mm) column using a flow rate of 0.250 mL/min and the following gradient: 0-2 min of 150 mM NaOH (100%), 2-120 min of 600 mM NaOAc buffer (0-100%), 120-135 min of 150 mM NaOH (100%). At the bottom (b), the quantitative data per degree of polymerization; the μmol of chains per each degree of polymerisation was calculated using the area (nC x min) of 0.5 μmol glucose standard in 5 μL sample. Chains from 2 to 7 glucose residues were confirmed with the standards. Error bars are from triplicates of three different experiments.

4.1.2.1. GPC analysis of products debranched by pullulanase from glycogen

The results obtained from the BCA assay (**Fig. 54b**) suggested that the sample collected after 24 h debranching with Pull still contain branched material. To further investigate the material left from the digestion of glycogen with Pull, the sample collected at the end of the reaction was analysed by GPC separation (**Fig. 56**) and by TLC analysis (**Fig. 57**).

The GPC chromatogram (**Fig. 56**) shows two major peaks between 240 and 360 minutes, and only the largest partially overlaps that of glycogen; small peaks between 390 and 540 minutes correspond to short oligosaccharides as indicated by the comparison with the standards. In the analysis of the ISA-digest by GPC, a partial overlay of the chromatogram with that of glycogen was also observed and attributed to aggregates of long chains that precipitated in water. In contrast, the material collected between 240 and 300 minutes, and corresponding to the largest peak, did not contain a precipitate. Therefore, the largest peak in **Fig. 56** is more likely to represent glycogen not digested by Pull. To validate this hypothesis, the fractions collected from the GPC analysis were analysed by TLC and, only those containing large material, by HPAEC.

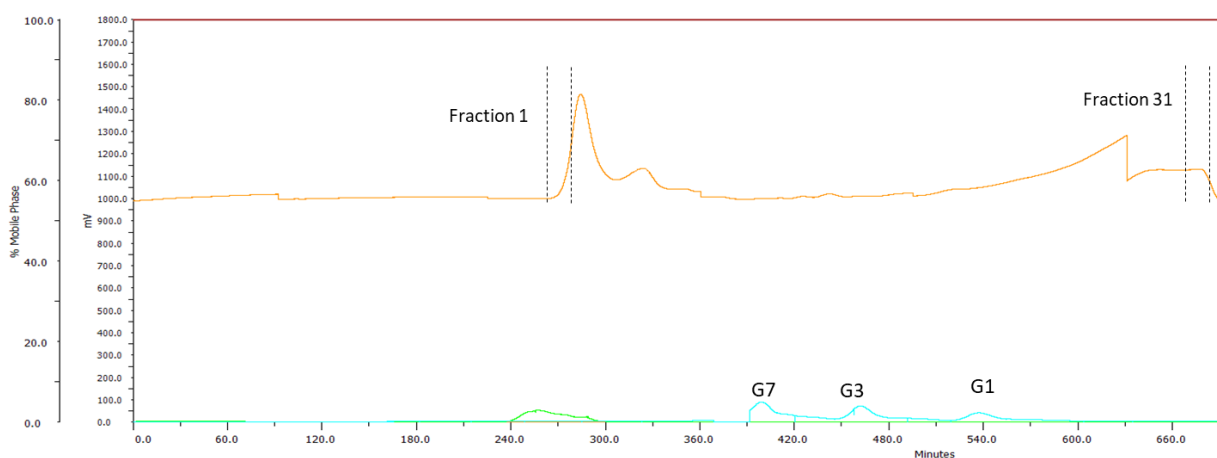


Figure 56 Comparison of the GPC chromatograms of 10 mg of glycogen debranched with 0.15 U of Pull in sodium acetate buffer (pH 4.5, 0.1 M; in orange) with the standards (G1 to G7, in blue) and glycogen (in green). The separation was performed with a TSK40S column with a flow rate of 0.2 mL/min using MQ water as eluent; the fractions were collected with 7 mL per tube from 150 mins to 650 mins.

The TLC analysis of each fraction (**Fig. 57a**) showed material deposited at the baseline of the plate in the fractions 1 to 5, as also observed in the TLC analysis of the ISA digest reported in **Fig. 53a**. The HPAEC analysis (**Fig. 57b**) revealed only a small percentage of long chains (>DP10) for fractions 1 to 4 confirming that the material deposited at the baseline of the TLC was more likely to be glycogen not digested by Pull. Differently, the fraction 5 corresponding to the smallest peak of the GPC chromatogram contained chains mainly longer than DP15. However, the precipitation of material

was not observed for this sample probably because the concentration of chains was not high enough to form a visual precipitate.

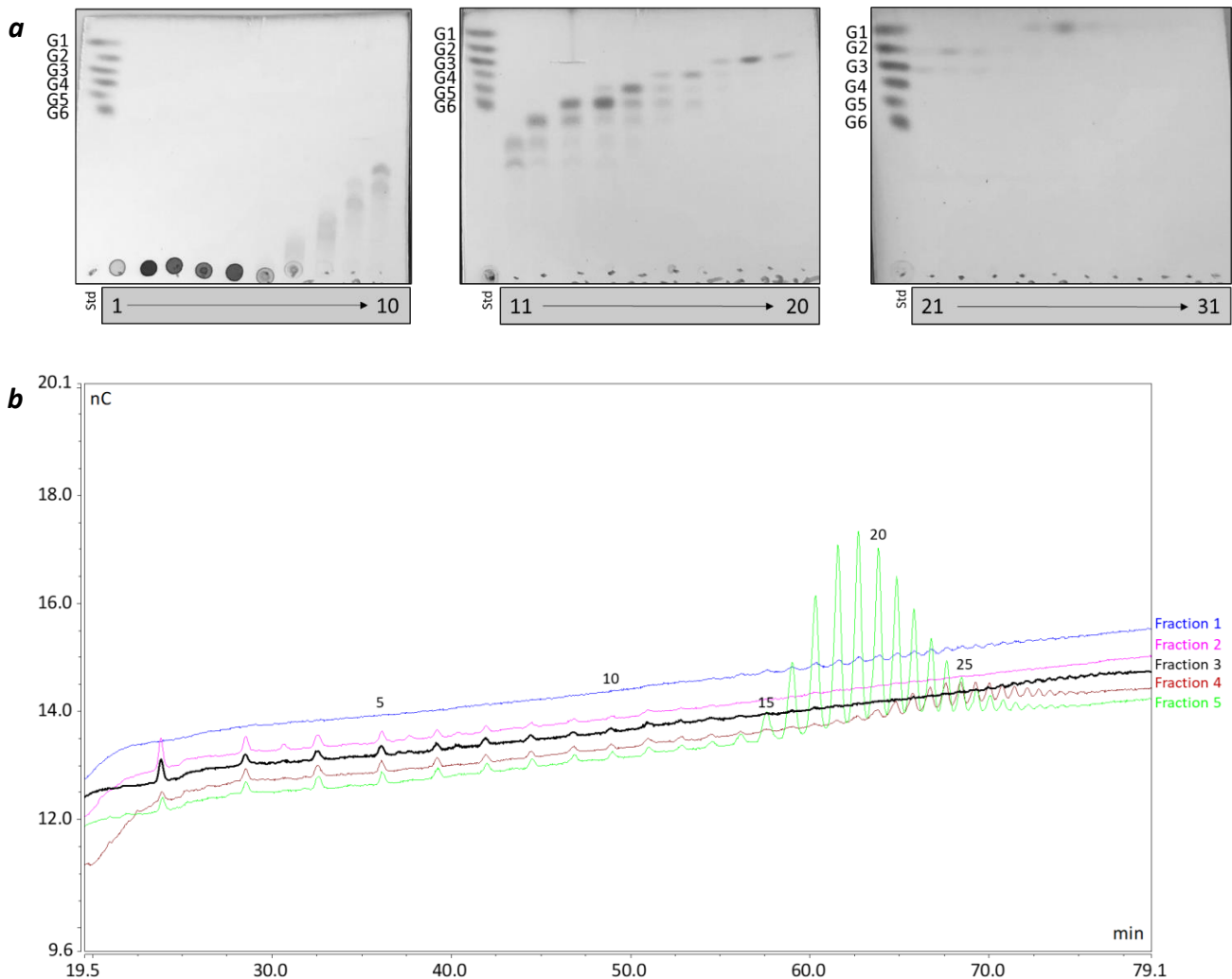


Figure 57 (a) At the top, the TLC analysis of the fractions collected by GPC after digestion of 10 mg of glycogen with 0.15 U of pullulanase. The standards are in the first line of each TLC and are named G1 (glucose) to G6 (maltohexaose). Mobile phase $\text{CH}_3\text{CN}:\text{EtOAc}:\text{IPA}:\text{H}_2\text{O}$ (85:20:50:50). The TLC plate was eluted three times before its development with a solution of 5% H_2SO_4 in EtOH and heating with a heat gun. **(b)** At the bottom, the raw HPAEC data of the fractions 1 to 5. The chromatograms were obtained with a CarboPac PA1 (2x250 mm) column using a flow rate of 0.250 mL/min and the following gradient: 0-2 min of 150 mM NaOH (100%), 2-120 min of 600 mM NaOAc buffer (0-100%), 120-135 min of 150 mM NaOH (100%).

4.2. Digestion of the external chains with β -amylase

4.2.1. Exhaustive digestion of glycogen with β -amylase

Oyster glycogen was incubated with BMY to generate β -limit dextrins (BLD) and maltose using the working conditions suggested by the enzyme supplier, as described in Chapter 2.1.2.2. The progress of the β -amylolysis was monitored by TLC (**Fig. 58a**) and, at completion of the reaction, the limit dextrins were separated from maltose by EtOH precipitation. To establish the concentration of EtOH required to achieve an efficient separation of the β -amylolysis products, four different percentages (25%, 45%, 50%, and 75%) of organic solvent in water were assessed (**Fig. 58b**) using glycogen and maltose as standard mixture. It was observed that 50% EtOH efficiently separated the standards, whereas the others only led to a partial precipitation of glycogen or to the contamination of the precipitate with maltose. Thus, BLD were separated from maltose by using 50% of cold EtOH (**Fig. 58c**), and then incubated with the debranching enzymes as described in the following sections.

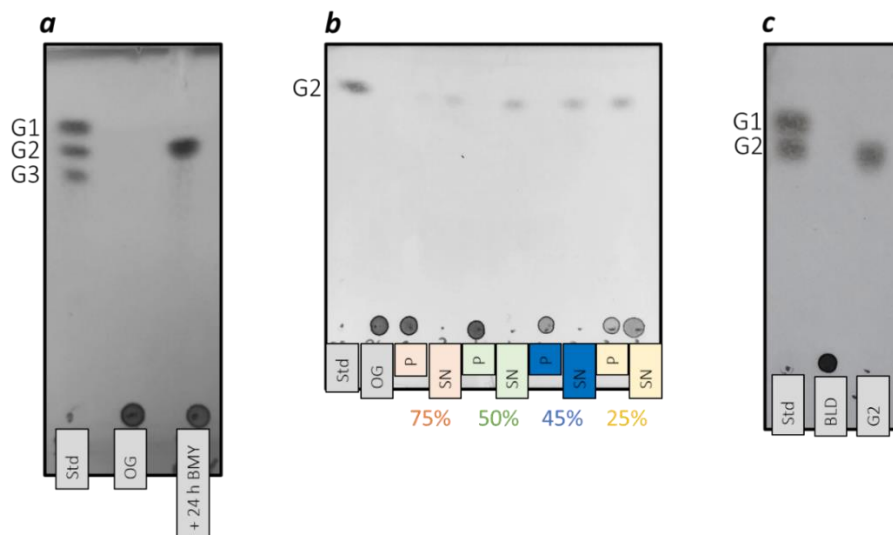


Figure 58 Digestion of glycogen (OG, 10 mg/mL) with BMY (60 U) in phosphate buffer (pH 6.0, 0.2 M) at 37 °C for 24 h and EtOH separation of the products. (a) The β -amylolysis was monitored by TLC every 24 h until no more maltose was observed; (b) four concentrations of EtOH were assessed to selectively precipitate glycogen from maltose: 600, 200, 165, and 68 μ L of 100% cold EtOH were added to 200 μ L of the mixture of glycogen (10 mg/mL) and maltose (2 mg/mL) in phosphate buffer (pH 6.0, 0.2 M) to achieve 75, 50, 45, and 25% of EtOH concentration, respectively; P = precipitate, SN = supernatant. (c) TLC of BLD and maltose after precipitation of the former with 50% cold EtOH. Mobile phase $\text{CH}_3\text{CN}:\text{EtOAc}:\text{iPrOH}:\text{H}_2\text{O}$ (85:20:50:50). The TLC plates were eluted three times before their development with a solution of 5% H_2SO_4 in EtOH and heating with a heat gun.

4.2.2. Quantification of maltose and β -limit dextrins

In the literature, it is reported that the β -amylolysis rate, namely the percentage of maltose released, is between 38% and 42%, and it is commonly measured by reducing end assays using maltose as standard for the calibration curve.^{17,28} Here, the quantification of the maltose was performed by BCA assay (**Fig. 59**). The results show that *ca.* 40% (4 mg/mL) of glycogen was converted into the disaccharide, a value in agreement with the expected range.

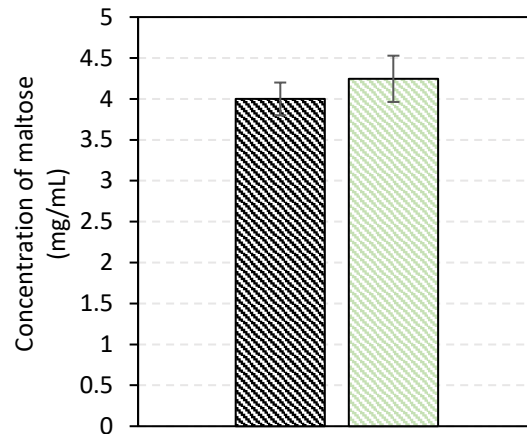


Figure 59 Quantification of maltose released from glycogen by BMV. The column on the left indicates the expected concentration of maltose, whereas the column on the right represents the data collected by BCA assay.

BLDs were digested by the enzyme cocktail described in Chapter 2.3.1.1, and the quantity of glucose formed was quantified by BCA assay (**Fig. 60**). The results show that *ca.* 60% (6 mg/mL) of BLD remained after digestion of glycogen with BMV, and the comparison of this value with that obtained from the β -amylolysis rate confirmed that glycogen was completely converted into the products.

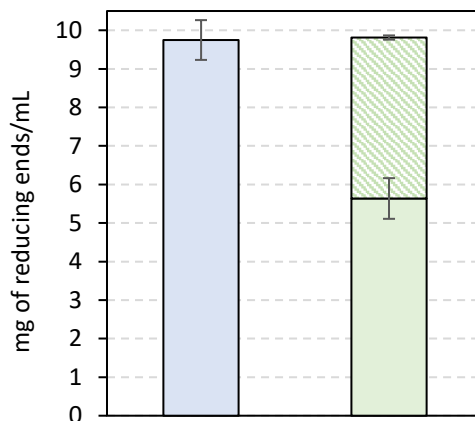


Figure 60 Quantification of BLD by BCA assay and comparison of the results with the quantity of maltose released. The quantity of glycogen is represented by the blue column, whereas that of BLD (■) and maltose are illustrated with a plain green and dotted green column (▨), respectively.

4.2.3. Investigation of the chain length distribution of the β -limit dextrin

BLD were incubated with ISA or Pull, and the CLD was investigated by TLC and HPAEC. The TLC analysis (**Fig. 61a**, insert) shows that DP2 and DP3 were in greater abundance than longer chains (>DP4). The HPAEC analysis confirmed that DP2 and DP3 were the most predominant chain lengths regardless of the debranching enzyme used (**Fig. 61a** and **61b**). In **Fig. 61a**, the raw data show the presence of small unidentified (intermediate) peaks between those assigned to specific DPs. Moreover, the mixture of oligosaccharides resulting from ISA digestion shows more intermediate peaks detected between DP3 and DP15 than those observed in the sample collected after Pull digestion of BLD. Nevertheless, these peaks were not identified. The amount of DP2 calculated by integrating the peak area of the raw data was *ca.* 1.6 μmol for Pull and *ca.* 1.2 μmol for ISA, a difference caused by the higher efficiency of the former enzyme towards maltosyl residues than the latter one. In addition, a small peak shoulder between DP13 and DP20 in the CLD obtained was observed for ISA and not for Pull that might be caused by the selectivity of the former enzyme towards long chains compared to the latter.

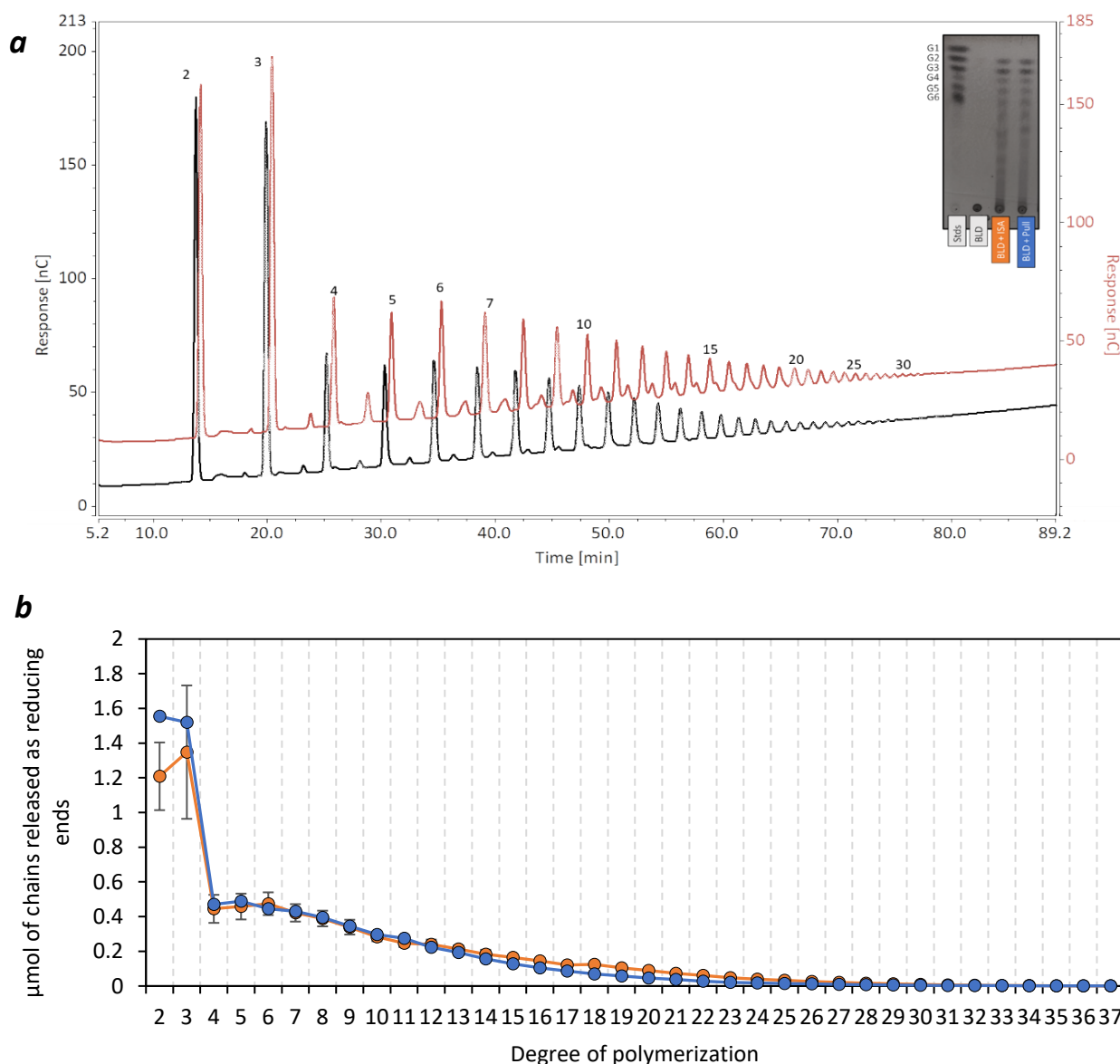


Figure 61 Chain length distribution of BLD digested with *ISA* (0.15 U) and *Pull* (0.15 U) in sodium acetate buffer (0.1 M, pH 4.5) in 24 h at 40 °C. At the top (**a**), the raw data of both chain length distribution for *ISA* in **black** and *Pull* in **dark red**; the chromatograms were obtained with a CarboPac PA1 (2x250 mm) column using a flow rate of 0.250 mL/min and the following gradient: 0-2 min of 150 mM NaOH (100%), 2-120 min of 600 mM NaOAc buffer (0-100%), 120-135 min of 150 mM NaOH (100%). The insert illustrates the TLC analysis of the chain length distribution; mobile phase CH₃CN: EtOAc: *i*PrOH: H₂O (85:20:50:50), and the TLC plate was eluted three times before its development with a solution of 5% H₂SO₄ in EtOH and heating with a heat gun. At the bottom (**b**), the quantitative data per degree of polymerization; the μmol of chains per each degree of polymerisation was calculated using the area (nC x min) of 0.5 μmol glucose standard in 5 μL sample. Chains from 2 to 7 glucose residues were confirmed with the standards. Error bars are from triplicates of three different experiments.

In Chapter 2.1.2.2, it was demonstrated that odd linear chains are converted into glucose and maltose by *BMY*, and glucosyl stubs cannot be digested by *ISA* or *Pull*. If this is the case, the presence of glucose could be detected in BLD, and the amount expected would be possibly equal to the concentration of odd unbranched chains in the structure, namely DP5, DP7, DP9, etc. For instance, if it is assumed that *ca.* 5.3 μmol (in 50 μL) of DP7 in oyster glycogen is unbranched, β -amylolysis

would generate 5.3 μmol of glucose, a quantity that can be easily detected by TLC as showed in previous analysis. Thus, the presence of glucosyl branches is assessed by digestion of BLD with OGL; glycogen was also subjected to hydrolysis with OGL as negative control. The results in **Fig. 62** show only a dark spot at the baseline of the plate related to BLD, and no traces of glucose in neither glycogen nor BLD.

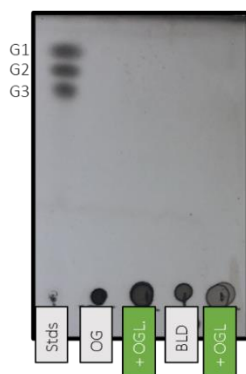


Figure 62 TLC analysis of the digestion of oyster glycogen (OG) and BLD with oligo $\alpha(1,6)$ -glucosidase (OGL) for 24 h (sodium acetate buffer pH 4.5, 0.1 M). Mobile phase CH_3CN : EtOAc: *i*PrOH: H_2O (85:20:50:50); the TLC plate was eluted three times before its development with a solution of 5% H_2SO_4 in EtOH and heating with a heat gun; stds = standards, G1 = glucose, G2 = maltose, G3 = maltotriose.

4.2.4. Quantification of the branches released from β -limit dextrin

The debranching of oyster glycogen by Pull resulted in a partial hydrolysis of the branches in the polysaccharide. To evaluate that the same activity occurred for BLD, the quantity of chains released was quantified by BCA assay (**Fig. 63**). Pull digested *ca.* 0.9 mg/mL of chains from BLD compared to the 0.1 μmol of chains released from glycogen suggesting that this enzyme was more effective in the cleavage of branches in BLD than it was in glycogen. In contrast, no significant differences were noticed between the debranching of glycogen and BLD by ISA.

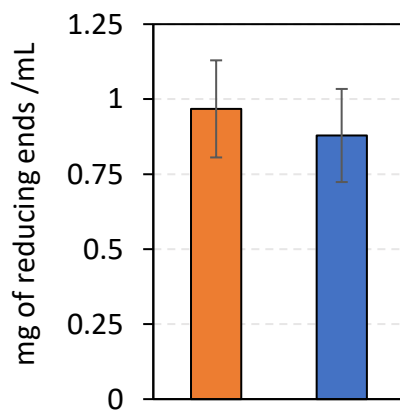


Figure 63 Quantification of the reducing ends released from BLD by ISA and Pull. The measurement was performed by BCA assay, and the standard deviations are from three different triplicates.

4.3. Digestion of glycogen with glycogen phosphorylase

4.3.1. Exhaustive digestion of glycogen with glycogen phosphorylase

Phosphorylase-limit dextrans (PLD) were generated following the same procedure used for BLD. Briefly, oyster glycogen was exhaustively digested with glycogen phosphorylase using the working conditions reported in Chapter 2.1.3.1, and the reaction was monitored by TLC (**Fig. 64a**). The same percentages of EtOH tested to separate maltose from BLD (**Fig. 58**) were also used for the precipitation of a standard mixture of glycogen and G1P (**Fig. 64b**), and with 50% cold EtOH providing the most efficient separation (**Fig. 64c**). Then, the CLD of PLD was investigated by debranching treatment with ISA or Pull, while G1P was quantified as described below.

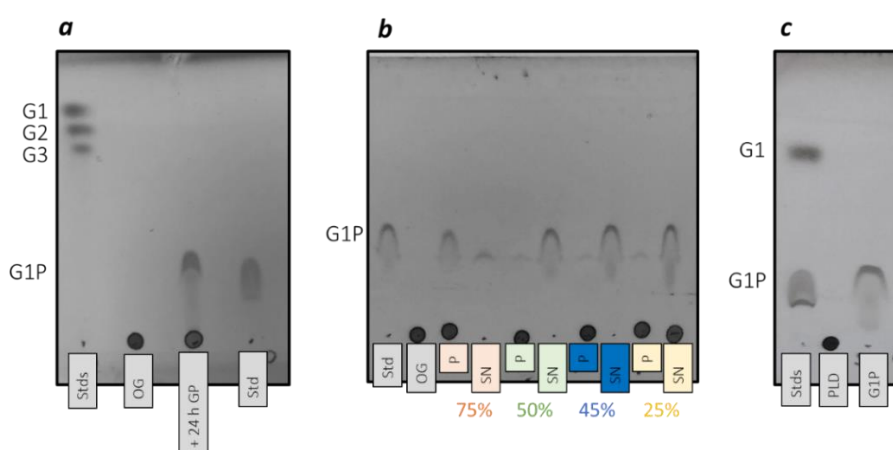


Figure 64 Digestion of glycogen (10 mg/mL) with glycogen phosphorylase (10 U) in phosphate buffer (pH 6.8, 0.2 M) at 37 °C for 24 h. **(a)** The phosphorylation was monitored by TLC every 24 h until no more G1P was observed; **(b-c)** G1P was separated from PLD by EtOH precipitation, and the concentration of organic solvent was established on a mixture glycogen (10 mg/mL) and G1P (2 mg/mL); the four concentrations of EtOH evaluated are 75, 50, 45, and 25% which were obtained by addition of 600, 200, 165, and 68 μ L of 100% cold EtOH to 200 μ L of the mixture of in phosphate buffer (pH 6.8, 0.2 M); P = precipitate, SN = supernatant. Mobile phase $\text{CH}_3\text{CN}:\text{EtOAc}:\text{iPrOH}:\text{H}_2\text{O}$ (85:20:50:50). The TLC plate was eluted three times before its development with a solution of 5% H_2SO_4 in EtOH and heating with a heat gun.

4.3.2. Quantification of glucose 1-phosphate and phosphorylase-limit dextrin

The quantification of G1P is commonly performed with colorimetric assays based on the conversion of G1P into G6P by phosphoglucomutase.^{75,147} Then, G6P participates in a redox reaction that leads to the reduction of a colourless probe into a coloured product that absorbs in the UV-Vis range (**Fig. 65a**). This method is highly selective towards G1P, but the costs of the commercially available kit or the purchase of its single components may not be widely accessible. For this reason, an alternative method was developed to quantify G1P based on the dephosphorylation of the sugar with alkaline phosphatase (ALP) (**Fig. 65b**). The reaction was monitored by TLC, and the BCA assay was used to quantify the glucose released.

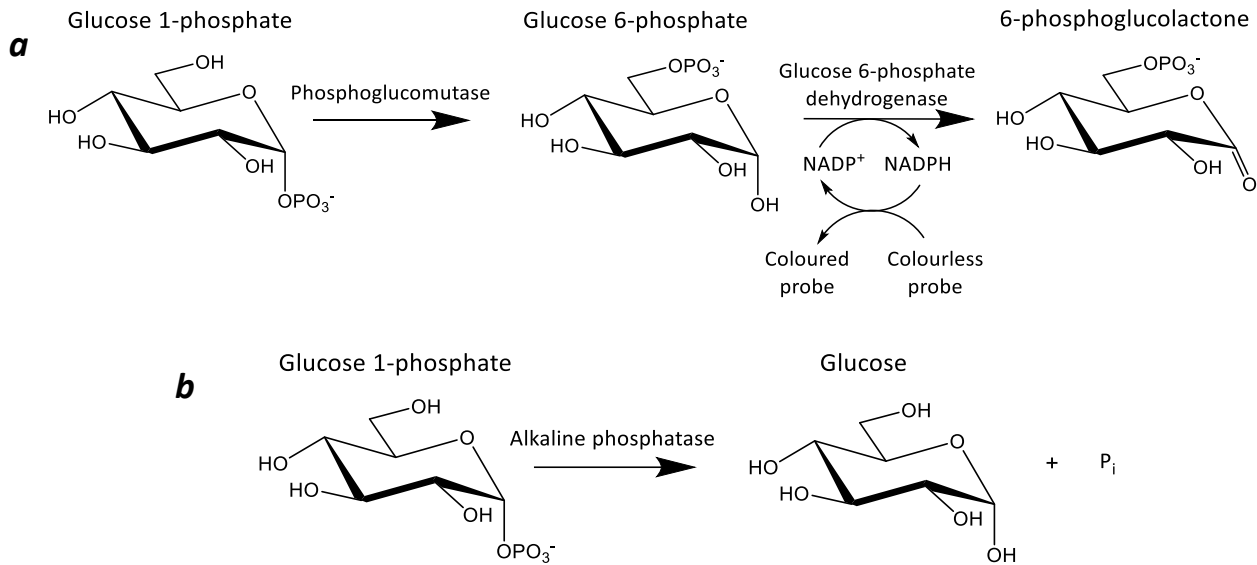


Figure 65 (a) Quantification of G1P reported in literature^{75,147} vs **(b)** dephosphorylation of G1P by alkaline phosphatase.

Literature reports that 30-40%¹² of glycogen is converted into G1P by the phosphorolysis, meaning that 3-4 mg/mL of G1P are expected to be released from 10 mg/mL of glycogen used in these experiments. Here, *ca.* 3.3 mg/mL (33%) of G1P were measured after digestion of glycogen by GP, which value is within the range expected (**Fig. 66a**). The complete conversion of glycogen into PLD and G1P was confirmed by digestion of PLD into glucose using the enzymatic cocktail. The results (**Fig. 66b**) show that *ca.* 6.4 mg/mL is the amount of PLD measured by BCA assay, and the comparison of this value with that of G1P confirms that the starting material was completely converted into the products.

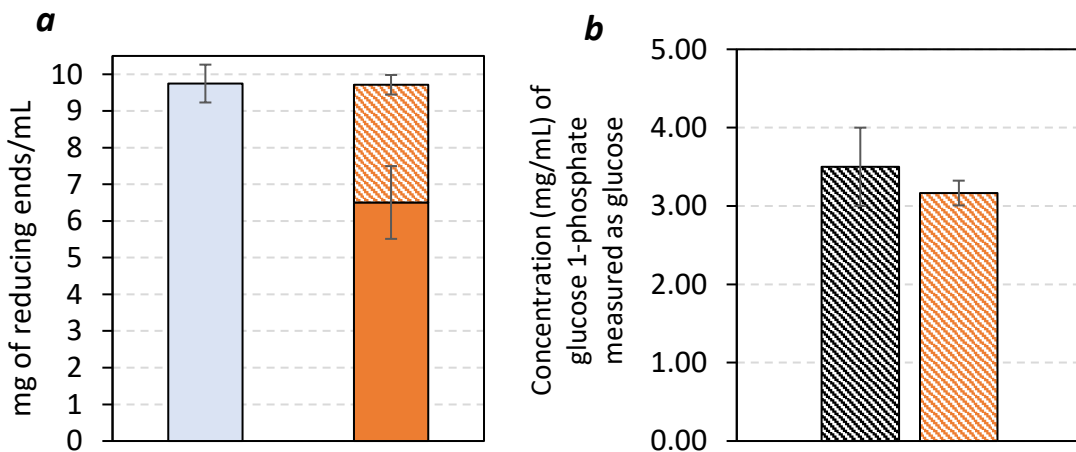


Figure 66 Quantification of the products released from glycogen by phosphorolysis. In the graph at the top **(a)**, the concentrations of G1P expected (--) and experimentally measured (--). In the graph at the bottom **(b)**, the concentration of glycogen (in blue) is compared to the concentration of PLD (in orange) and G1P (--). The experimental data were collected from three individual experiments and quantified by BCA assay.

4.3.3. Investigation of the chain-length distribution in phosphorylase-limit dextrin

The estimation of the CLD by TLC (**Fig. 67**, insert) shows that the structure of PLD is predominantly made of chains longer than DP4 with a low abundance of DP2 and DP3. The raw data of the HPAE analysis support these results and show intermediate unidentified peaks between those assigned to each DP, regardless of the debranching enzyme used (**Fig. 67**).

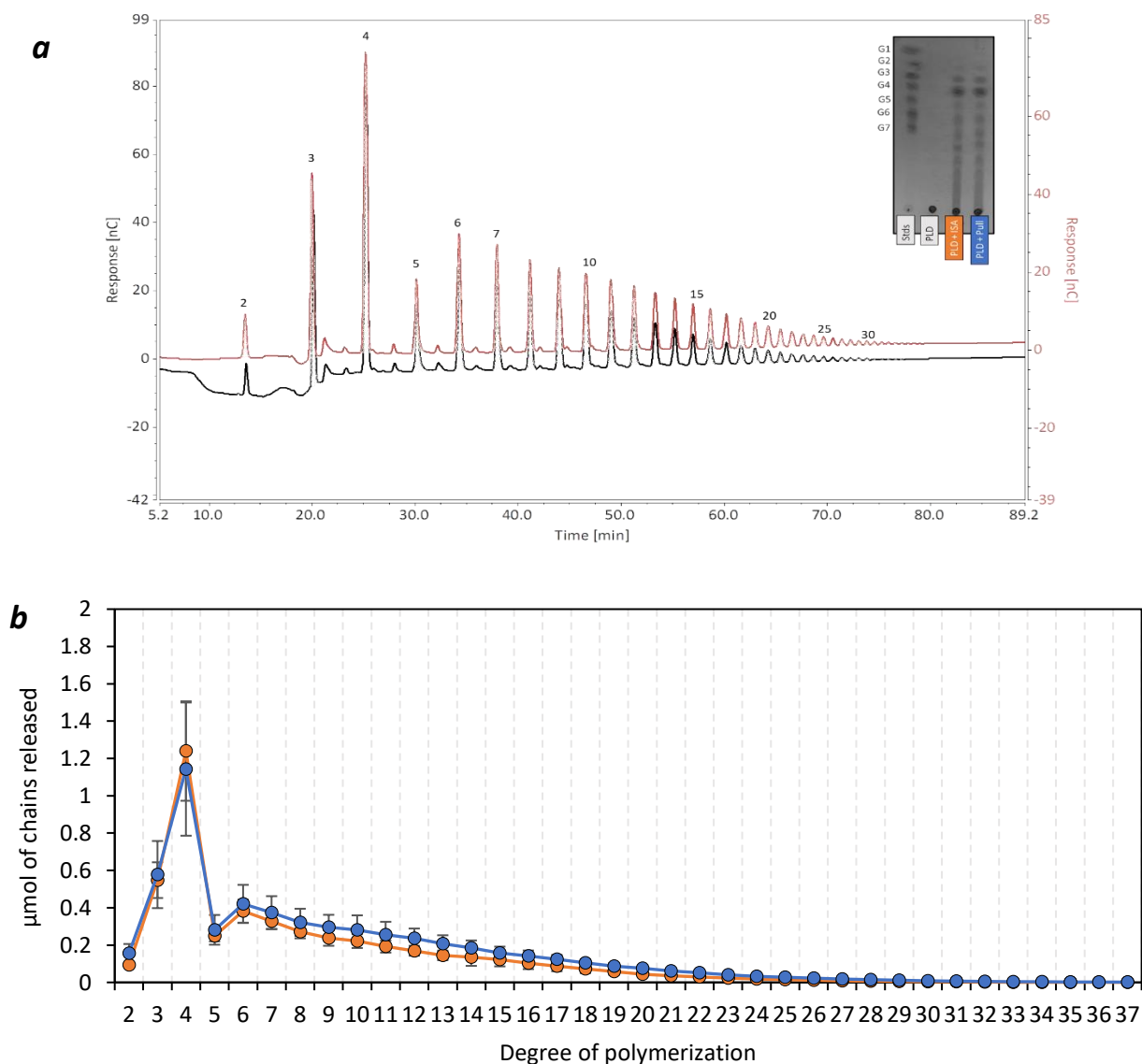


Figure 67 Chain length distribution of PLD digested with *ISA* (0.15 U) and *Pull* (0.15 U) in sodium acetate buffer (0.1 M, pH 4.5) in 24 h at 40 °C. At the top (**a**) the raw data of both chain length distribution for *ISA* in **black**, and *Pull* in **dark red**; the chromatograms were obtained with a CarboPac PA1 (2x250 mm) column using a flow rate of 0.250 mL/min and the following gradient: 0-2 min of 150 mM NaOH (100%), 2-120 min of 600 mM NaOAc buffer (0-100%), 120-135 min of 150 mM NaOH (100%). The insert illustrates the TLC analysis of the chain length distribution; mobile phase CH₃CN: EtOAc: *i*PrOH: H₂O (85:20:50:50), and the TLC plate was eluted three times before its development with a solution of 5% H₂SO₄ in EtOH and heating with a heat gun. At the bottom (**b**), the quantitative data per degree of polymerization; the μmol of chains per each degree of polymerisation was calculated using the area (nC x min) of 0.5 μmol glucose standard in 5 μL sample. Chains from 2 to 7 glucose residues were confirmed with the standards. Error bars are from triplicates of three different experiments.

The peak of the CLD at DP4 is the result of the activity of GP on branches bearing an even number of glucose residues as explained in Chapter 2.1.3.1. Differently, DP2 and DP3 are not products of the phosphorolysis but rather chain lengths part of the glycogen structure. If this is the case, the amount of DP2 and DP3 of PLD must be the same of that measured in oyster glycogen. The comparison of the quantitative data collected by HPAE analysis in glycogen and PLD does not show an increase in the amount of DP2 and DP3 after phosphorolysis (**Fig. 68**).

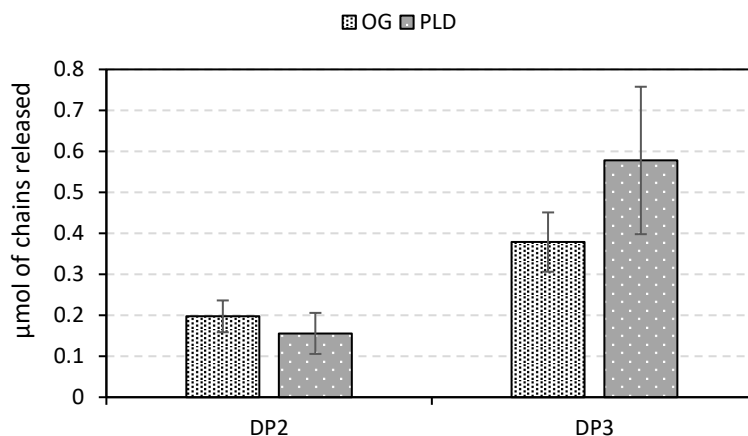


Figure 68 Comparison of the amount of DP2 and DP3 released from OG and PLD by ISA. The quantitative data of OG are those measured by HPAEC analysis and reported in **Fig. 50**.

In Chapter 2.1.3.1, it was demonstrated that GP can easily convert DP5 into DP4 during prolonged incubation time (24 h), meaning that DP5 must not be detected in PLD after completion of phosphorolysis. However, the results (**Fig. 67**) show that DP5 is one of the peaks in the CLD, and that its amount (*ca.* 0.2 μmol) corresponds to the one measured in glycogen. These findings suggest that DP5 may contain a branching point that prevents its digestion into DP4, and the potential location of the $\alpha(1,6)$ -glycosidic bond will be investigated in the next section.

The CLD collected for PLD showed that Pull and ISA followed the same debranching trend with no significant difference in the amount of branches released per DP. To assess the debranching rate of both enzymes towards PLD, the amount of chains released was quantified by BCA assay and the collected data are reported in **Fig. 69**. The results show that PLD were largely debranched by ISA but to a slightly lesser extent by Pull. It is possible that the length of the external chains, mainly with DP4, were not as suitable for Pull activity as they were for ISA.

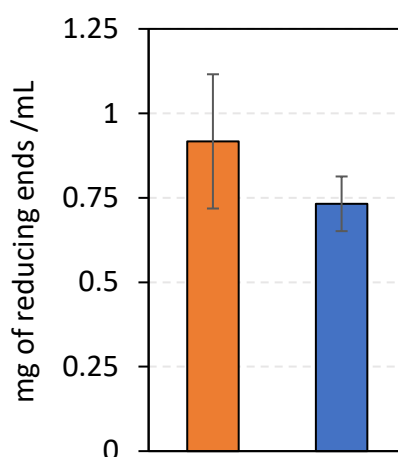


Figure 69 Quantification of the reducing ends released from PLD by ISA and Pull. The measurement was performed by BCA assay, and the standard deviations are from three different triplicates.

4.4. Discussion

4.4.1. The digestion of glycogen with pullulanase and isoamylase provides insights into the distribution of short and long chains

4.4.1.1. Pullulanase is more efficient towards limit dextrin than on glycogen

In our results, glycogen was debranched more efficiently by ISA than by Pull, and the activity of Pull increased in BLD and PLD. We hypothesised that either the distance between branching points or the length of the chains limit the activity of Pull on glycogen. If the distance between branching points was the problem, the number of reducing ends released by Pull from BLD and PLD would be the same of that measured for glycogen, but the results show a different situation. Thus, we thought that the efficiency of Pull on BLD and PLD is higher than on glycogen for the large number of short-branched oligosaccharides in their structures. When the chains in the external layers are exposed to the activity of BMY and GP, they become more accessible to Pull: the shorter the branches are in branched polysaccharides, the more efficient Pull is in debranching the structure. Indeed, the reducing ends cleaved from BLD by Pull are more than those digested from PLD because the external layer of the former dextrin has a high number of DP2-DP3, a length shorter than that found in the latter dextrin. These results also provide an explanation for the scarce debranching activity of Pull towards glycogen.

4.4.1.2. The outer layers of glycogen are populated by branched structures more accessible to pullulanase than to isoamylase

In studies published in the early 1970s,^{108,143} the incomplete degradation of glycogen by Pull was attributed to its activity as *exo*-acting enzyme resulting in the inability to penetrate the interior layers of the polysaccharide. In contrast, ISA was classified as an *endo*-acting enzyme, and thus

capable of digesting complex branched structures such as glycogen and amylopectin. In 1978, the substrate specificity of Pull and ISA was elucidated by Kainuma *et al.*¹¹⁰ reporting that this enzyme was highly efficient towards short-branched structures. Considering these studies and the experimental data reported in earlier sections of this chapter, we hypothesise that Pull is more efficient towards the external layers of glycogen for the presence of a large number of short-branched structures. When the enzyme reaches the internal layers bearing longer branches than those found in the outer tiers, the activity is reduced. When glycogen is subjected to β -amylolysis and phosphorolysis, the amount of short-branched structures increases and also the debranching efficiency of Pull. For these reasons, the debranching of glycogen or its limit dextrins by Pull must be performed when information on short chains and branching points situated in the external layers are needed, whereas ISA is more suitable to investigate the overall structural features of glycogen or its limit dextrins. Further information on the arrangements of the branches digested by Pull in the outer most layers of glycogen will be speculated in the following sections.

4.4.2. Potential branching arrangements in the outer layers of glycogen

Literature focuses more on the applications and structural analysis of amylopectin BLD due to their wide industrial applications than on glycogen BLD. Similarly, PLDs are more used as substrates to assess the activity of BMY¹¹⁹ and GDE,^{75,148} rather than for structural studies. For this reason, we found particularly challenging to search information on the structural analysis of glycogen BLD and PLD to validate our data, and, to the best of our knowledge, we found one paper published about BLD and PLD that is discussed below.

In the proceedings from a starch congress published by Bertoft and Mäkelä in 2007 (**Fig. 70**),⁵ the CLD of BLD and PLD of glycogen from oyster were examined. Following an overnight digestion of glycogen with BMY or GP (the exact incubation time of the treatment was not specified), both limit dextrins were debranched with ISA and/or Pull, and the CLD analysed by HPAEC. The debranching of BLD from oyster glycogen resulted in a large amount of DP2 and DP3, and longer chains than DP3 had a decreasing concentration per DP. For PLD, the authors reported a major peak at DP4 and a minor one at DP6. Lastly, the authors showed that the β -amylolysis and phosphorolysis rate was 48% and 32%, respectively.

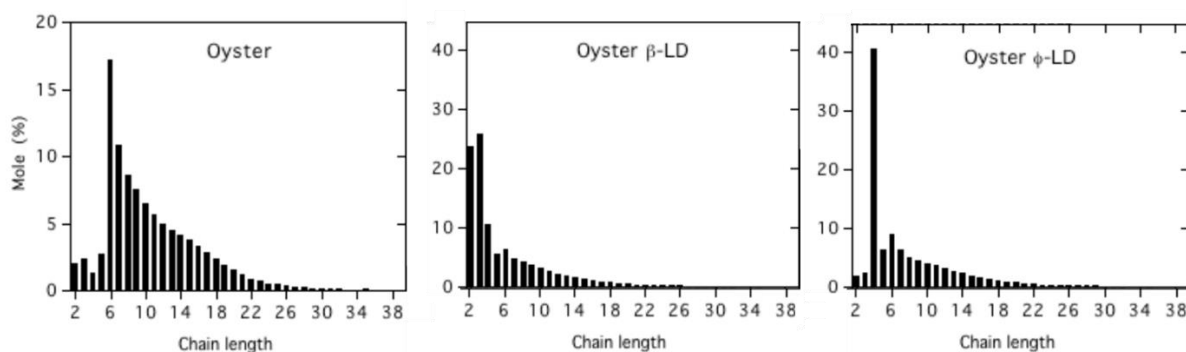


Figure 70 Chain length distribution of oyster glycogen, and the related β - and phosphorylase (ϕ)-limit dextrins. Image taken from Bertoft and Mäkelä.⁵

Here, our findings are consistent with those reported by the authors except for a small discrepancy in the percentage of maltose and G1P released. However, we have already mentioned that small discrepancies may occur among glycogen of the same species due to variations in the time of extraction and feeding state.

In the discussion section of the results reported by Bertoft and Makela,⁵ DP2 and DP3 were identified as the products of the activity of BMV towards even and odd unbranched chains, respectively. In contrast, in the present studies, we demonstrated that odd-length branches are converted into DP1 by β -amylolysis, but glucose residues were not detected in BLD. Therefore, we hypothesise that DP3 is the product of branches with an odd number of glucose residues bearing a branching point.

4.4.2.1. *DP3 is generated by odd-length branches bearing a branching point on the second or third glucose residue*

In section 4.2.3, we observed that BLD do not have glucose stubs and we suggested earlier that DP3 is the product of the β -amylolysis conversion of only branched chains. To investigate the potential structures that could generate DP3 after BMV digestion, we used the DP15 models. The theoretical branched structures were digested following the substrate specificity of BMV resulting from experimental data and reported in Chapter 2.1.2.2. By screening the **Appendix 2** containing the whole set of DP15 models, the structures bearing a branching point on the third glucose residue from the non-reducing end are the only ones that could generate DP3 after BMV digestion. **Fig. 71** shows an example of one of these structures.



Figure 71 Illustration of a branched structure with DP6 and DP9 that can generate DP3 after digestion with BMV.

4.4.2.2. *The minimum distance between two branching points is of two or three glucose residues*

To support the hypothesis that DP3 in the CLD of BLD comes from the arrangement proposed in the previous paragraph, we must demonstrate that:

- (I) glycogen has not odd unbranched chains, or if so, they are in a negligible amount
- (II) the distance of two glucose residues between branching points is the only possible branching arrangement that β -amylolysis can convert into DP3

Firstly, in Chapter 2.1.2.2, we discussed the activity of BMV, and DP2 is the β -amylolysis product of branches with an even number of glucose residues. Therefore, the amount of DP2 measured in BLD is equal to the quantity of even unbranched chains exposed to the surface of glycogen. The phosphorolysis shortens odd and even unbranched chains to DP4, and the position of the branching point on the reducing end represents the unique possibility to form DP4 by the activity of GP on a branched chain. However, structures containing a branching point on the reducing end were discarded from the DP15 model because they are not substrates of the activity of ISA and Pull. Therefore, the amount of DP4 that we measured in PLD is the sum of even and odd unbranched chains that populated glycogen before its phosphorolysis. If we consider that the CLD of BLD and PLD were obtained from the same glycogen source and in the same working conditions, we can estimate the amount of odd linear chains by subtracting the amount of DP2 from that of DP4 as follows:

$$DP2 = \text{even unbranched chains} = 1.5 \mu\text{mol} \pm 0.008$$

$$DP3 = \text{odd unbranched chains} + \text{odd branched chains} = 1.5 \mu\text{mol} \pm 0.0004$$

$$DP4 = \text{even unbranched chains} + \text{odd unbranched chains} = 1.14 \mu\text{mol} \pm 0.40$$

$$DP4 = DP2 + \text{odd unbranched chains}$$

$$\begin{aligned} \text{odd branched chains} &= (DP4_{PLD} - DP4_{Glycogen}) - (DP2_{BLD} - DP2_{Glycogen}) \\ &= (1.14 \mu\text{mol} \pm 0.40 - 0.2 \mu\text{mol} \pm 0.04) - (1.5 \mu\text{mol} \pm 0.008 - 0.2 \mu\text{mol} \pm 0.04) = \\ &= (1.14 \mu\text{mol} \pm 0.40 - 1.5 \mu\text{mol} \pm 0.008) = -0.36 \pm 0.408 = \sim 0 \end{aligned}$$

This result suggests that glycogen is not populated by odd linear chains, and the DP3 generated by β -amylolysis is in fact the product of branched chains, explaining the lack of glucose stubs in BLD.

Secondly, we modelled the possible branched structures that can be generated by GBE using a substrate of 15 glucose residues (DP15). Among the designed combinations, we noticed that only odd-length B-chains bearing a branching point on the third or second glucose unit from the reducing end of a chain can be converted into DP3 by the activity of BMY. **Fig. 72** shows two examples of branching arrangements modelled with odd (DP9) and even (DP10) B-chains. When B-chains have an odd number of glucose residues as those illustrated in **Fig. 72a** and **72b**, the β -amylolysis products are always chains with DP3 regardless of the position of the branching point on the third or second glucose unit. In contrast, even B-chains (**Fig. 72c** and **72d**) are digested into DP4 or DP2 depending on whether the $\alpha(1,6)$ -glycosidic bond is located on the third or second glucose residue, respectively. Therefore, the presence of DP3 in BLD is more likely to be the result of BMY on structures represented in **Fig. 72a** and **72b**.

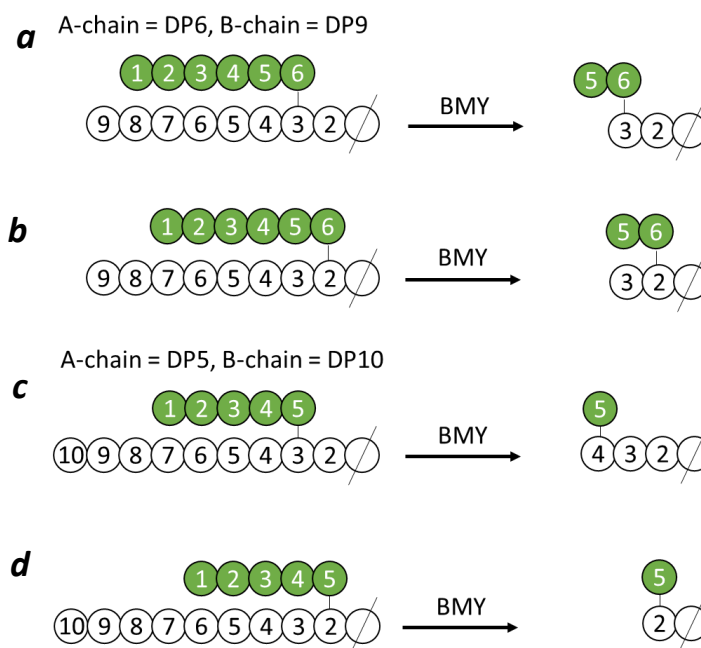


Figure 72 Branched structures designed by combination of odd and even B-chains bearing a branching point on the third or second glucose residue from the reducing end followed by their digestion with BMY. The length of the chain used was 15 glucose residues that was in turn split into DP9 and DP6 (**a** and **b**), and DP10 and DP5 (**c** and **d**).

To further support that glycogen contains branches on the third glucose residue from the reducing end, we modelled the products that are more likely to be generated by phosphorolysis of the branched structures in **Fig. 73**. When GP acts upon substrates as those depicted in **Fig. 73**, DP5 and DP6 are the products regardless of the length of the B-chain. If we assume that glycogen was largely branched on the third or second glucose residue from the reducing end, PLD would be populated

by DP4, the product from A-chains, and DP5 and DP6, the products from branched chains. In the CLD of PLD (**Fig. 67**), we observed that DP6 was the second most abundant chain length after DP4, whereas DP5 was in much lower amount than DP4 and DP6. Furthermore, we noticed that the only substrates converted into DP6 by phosphorolysis are those in **Fig. 73**. Indeed, a branching point on the fourth glucose residue from the reducing end results in a chain of DP7. This data suggested that the DP6 in PLD was generated by the conversion of odd and even B-chains branched on the third glucose residue.

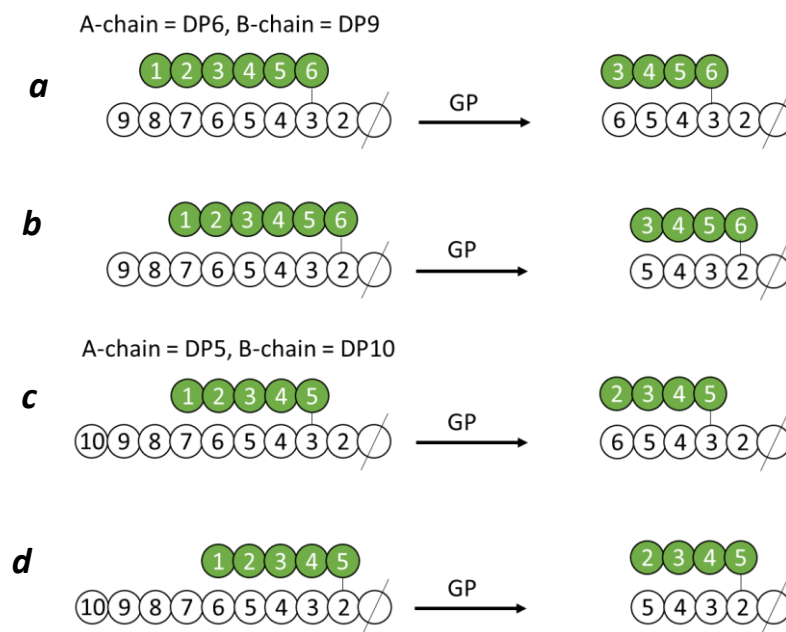


Figure 73 Branched structures designed by combination of odd and even B-chains bearing a branching point on the third or second glucose residue from the reducing end followed by their digestion with GP. The length of the chain used was 15 glucose residues that was in turn split into DP9 and DP6 (**a** and **b**), and DP10 and DP5 (**c** and **d**).

4.4.2.3. *Chains longer than DP5 in both β - and phosphorylase-limit dextrans are generated from branches bearing branching points on the non-reducing end*

In the previous section, we discussed that DP5 and DP6 are the products of the GP activity on B-chain with a branching point on the third or second glucose residue (**Fig. 72**), and we also reported that BMY would convert these branched structures into DP2, DP3, and DP4 (**Fig. 73**). If we assumed that branches on the third or second glucose residue of a B-chain largely characterised glycogen, we would not expect to see chains longer than DP5 and DP6 in the structure of BLD and PLD. Nevertheless, the CLDs of BLD (**Fig. 61**) and PLD (**Fig. 67**) report chains equal or longer than DP5. Therefore, glycogen is also branched in other positions than those suggested so far. Among the models designed in Chapter 3 and **Appendix 2**, chains longer than DP5 are only generated from B-

chains bearing a branching point on the non-reducing end or on the penultimate glucose residue. In **Fig. 74**, we report some hypothetical substrates with odd B-chains and modelled the products after BMY and GP digestion. As result, none of the B-chains represented can be digested by BMY and GP suggesting that they can be potential structures in glycogen that generated chains longer than DP5 in both BLD and PLD.

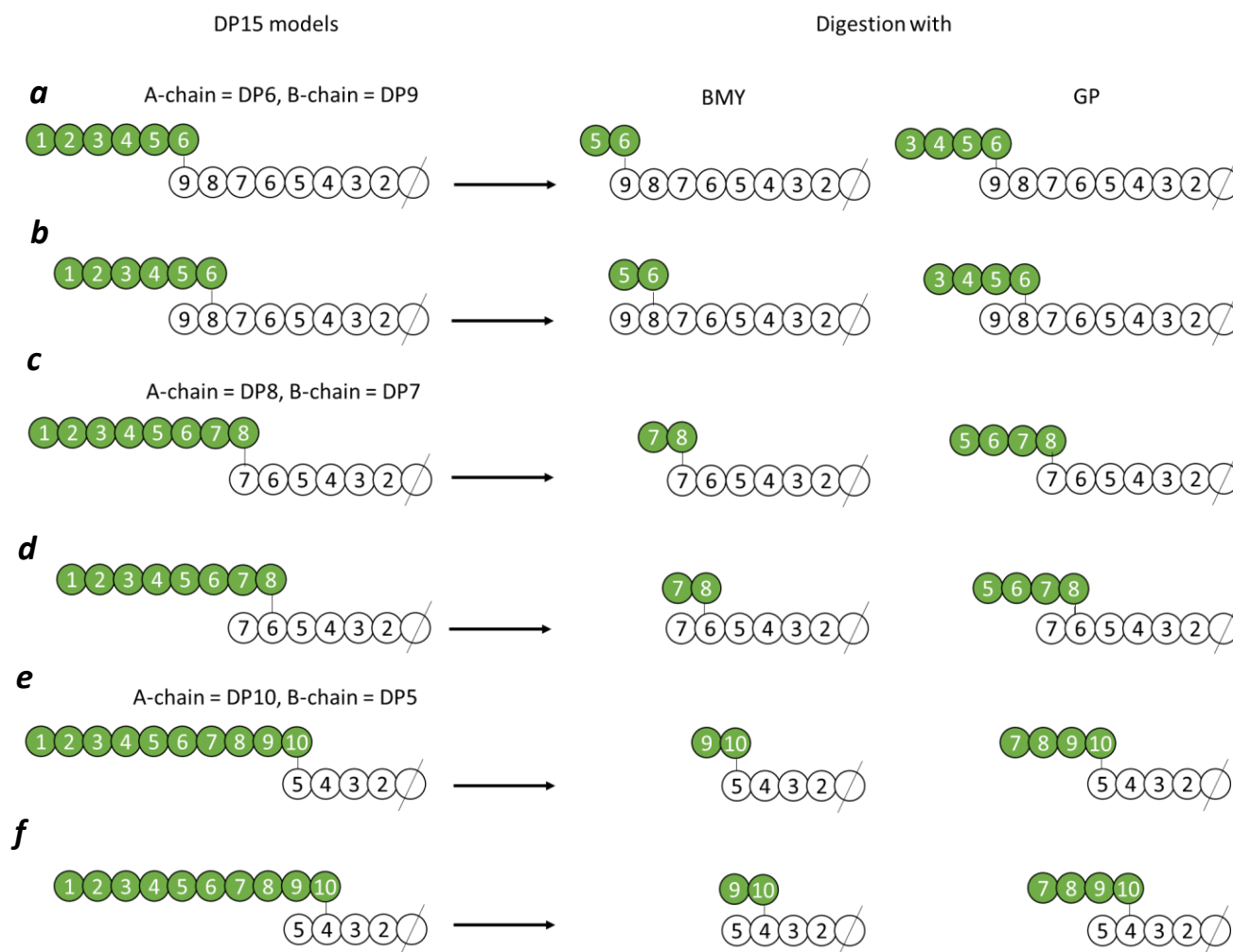


Figure 74 Branched structures designed by combination of odd and even B-chains bearing a branching point on the third or second glucose residue from the reducing end followed by their digestion with BMY and GP. The length of the chain used was 15 glucose residues that was in turn split into DP9 and DP6 (**a** and **b**), DP7 and DP8 (**c** and **d**), and DP5 and DP10 (**e** and **f**).

4.4.3. The substrate specificity of GBE can be hypothesised by investigating the CLD of glycogen

In the most recent mathematical model proposed by Deng *et al.*,¹⁵ the glycogen surface is mostly populated by short chains due to the limitations imposed to the activity of GBE by the dense surface. As we explained in Chapter 1, GBE enzyme removes a fragment (X_1) from the non-reducing end of a chain, and it is transferred onto another chain to form a new branch (X_2). The length of X_1 is of a

DP equal or greater than the minimum chain length that GBE can cleave, while X_2 is long enough to be elongated by GYS. With increasing number of new branches, glycogen structure becomes more crowded reducing the space available for the activity of GBE and GYS (crowding effect); for these reasons, it has been reported that glycogen can only have 12 tiers which outer most layers contain the highest percentage of branches (see Chapter 1).^{2,149,150} When GBE is exposed to the crowding effect, the chain length of X_1 might be reduced to the minimum substrate required for its activity; the cleavage and transfer of longer chains than that might create additional steric hindrances compromising the overall structure.

Based on the model proposed by Deng *et al.*,¹⁵ the predominant chain length observed in a certain species might be indicative of the minimum substrate required for the GBE activity (X_1). In our studies, the peak at DP6 in the CLD of oyster glycogen could represent X_1 , and in Chapter 3, we investigated the potential chain length distribution that a glycogen structure would have when DP6 is the preferential chain length for GBE. Nevertheless, the results from the DP15 models were not consistent with the experimental data or those reported in literature due to the limited combinations available with a chain of DP15.

The discrepancies between the experimental data presented in these studies and the theoretical models proposed might be the results of a GBE substrate specificity different from the one proposed for the DP15 model. In this model, we assumed that GBE always uses a substrate of 15 glucose residues to create new branches of different length. However, we believe that the chain length of the substrate selected and branched by GBE varies broadly rather than being constant as projected in the DP15 model, while the length of X_1 is more likely to remain the same (**Fig. 75**).

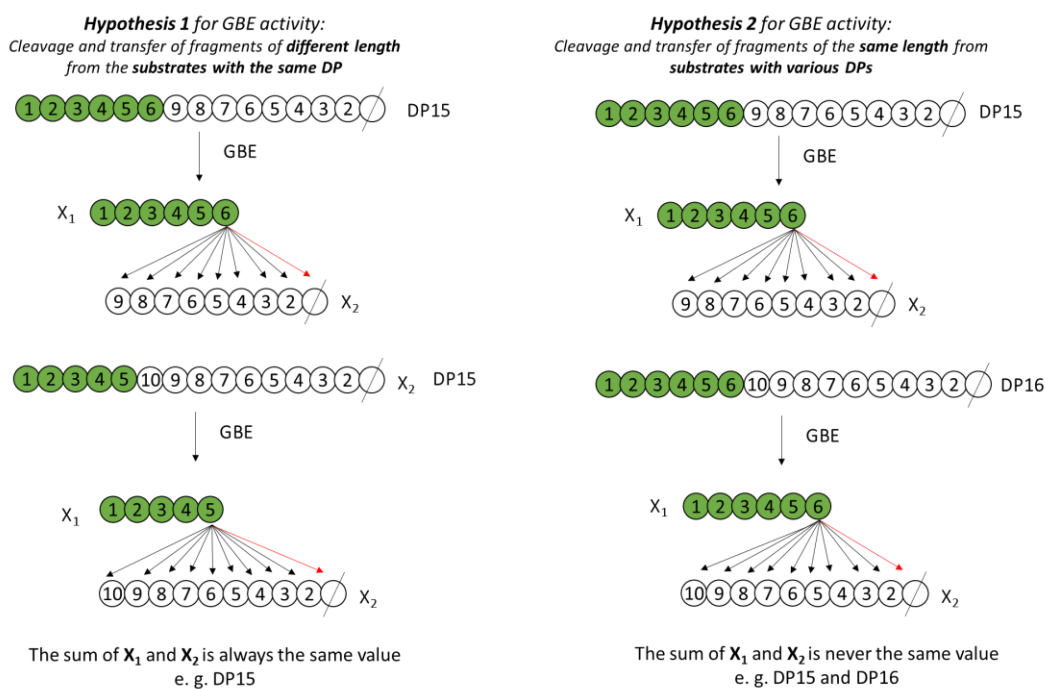


Figure 75 Possible mechanism of action suggested for GBE. In the first hypothesis, GBE is more likely to branch glycogen using substrate with a constant number of glucose residues; the total amount of branching arrangements is generated by the positions that X₁ occupies on X₂. In the second hypothesis, GBE cleaves fragments of the same length, e. g. DP6, from substrates bearing different number of glucose residues from each other, e. g. DP15 and DP16. The red arrow indicates the position discarded from the current models. The reducing end of the chain is illustrated with ∅.

To validate the second hypothesis proposed for the activity of GBE, we investigated the theoretical CLD by using chain lengths between DP8 and DP17, and by maintaining DP6 or DP7 as the length of the X₁.

4.4.3.1. Chain length distribution obtained from short-branched structures designed with chains between DP8 and DP17

Linear chains between DP8 and DP17 were branched by transferring X₁ equal to DP6 or DP7 onto X₂ (**Fig. 76**). The library of models (**Appendix 3**) created with this method were theoretically debranched, and the chain length distribution was investigated as explained in **Fig. 38**. For consistency with the models in the **Appendix 1**, the chains bearing glucose stubs or on the reducing end were not counted for the chain length distribution.

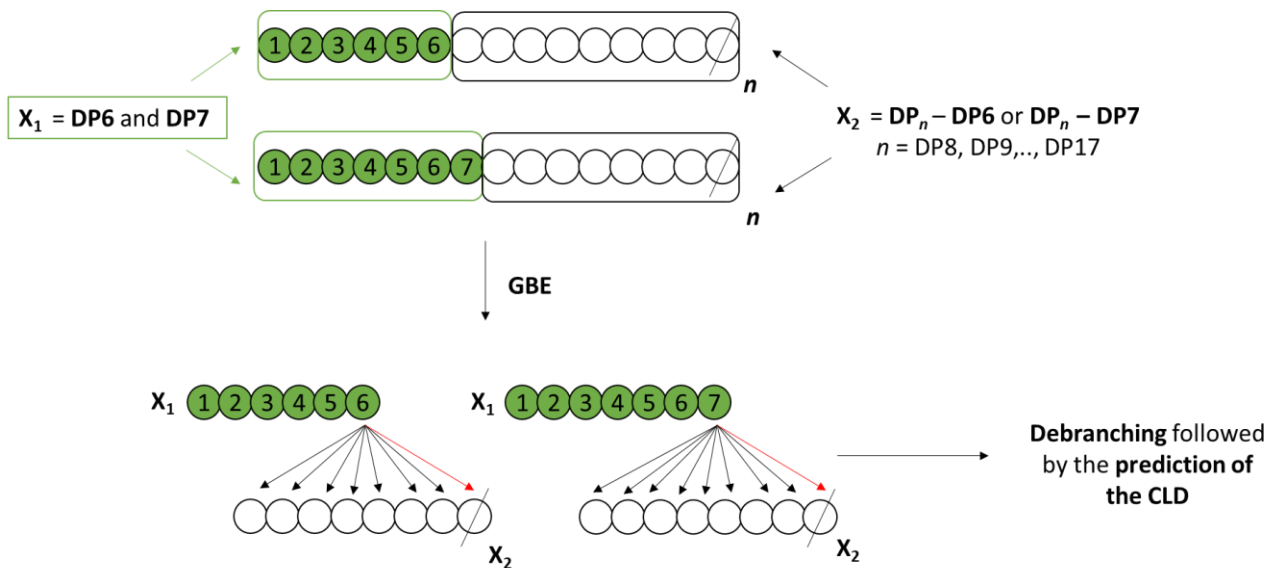


Figure 76 Methodology followed to create the library of models reported in **Fig. 57**. Chains between DP8 and DP17 were split into X_1 and X_2 ; the length of X_1 is maintained constant at DP6 or DP7, whereas the length of X_2 depends on the amount of glucose residues (DP) in the initial substrate (n). For each substrate (DP8 to DP17), DP6 and DP7 were placed on every glucose residue of X_2 excluding the reducing end (illustrated with crossed circle and indicate by the red arrow). Once the library was completed, the structures were debranched following the method described in **Fig. 38**.

The CLD illustrated in **Fig. 77** follows a trend that resembles the one measured for oyster glycogen for chains between DP2 and DP11. Two major peaks are observed at DP6 and DP7, and chains longer than DP7 are less abundant than these DPs. The CLD did not include glucosyl residues because they cannot be debranched by ISA or Pull.

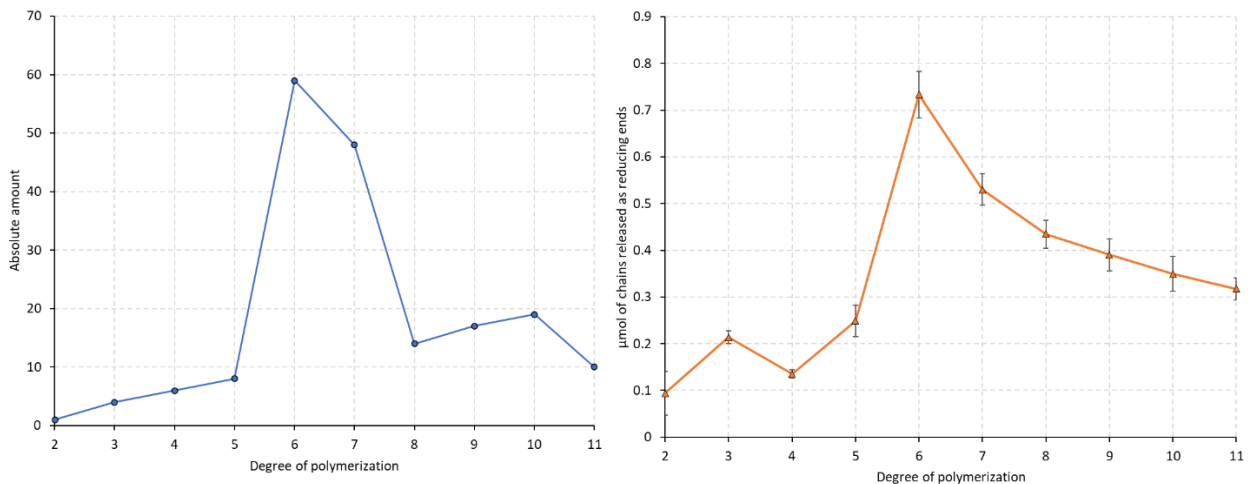


Figure 77 Comparison of the chain length distribution calculated by debranching the models in the **Appendix 2** with chains between DP8 and DP17 (on the left, in blue) with the one obtained experimentally (on the right, in orange) by debranching oyster glycogen with ISA.

4.4.3.2. Chain length distribution of β - and phosphorylase-limit dextrin generated from short-branched structures designed with chains between DP8 and DP17

To further support the proposed GBE activity, we investigated the CLD of β - and phosphorylase-limit dextrin generated by the structures reported in **Appendix 3**. The substrate specificity of BMY

and GP found experimentally was applied to the models, and the theoretical CLD was investigated as described in **Fig. 38**. The resulting CLD were compared with those measured experimentally for glycogen, BLD, and PLD after treatment with the debranching enzymes.

In **Fig. 78**, the theoretical model of glycogen has a peak at DP6 that was shifted to DP2 after β -amylolysis. However, we noticed that the amount of DP2 in the theoretical model of BLD is larger than that of DP3, whereas the proportion of DP2 and DP3 were the same in glycogen BLD. We think that the results from the theoretical model suggest that BLD from oyster glycogen may contain structures with DP2 that were not debranched neither by ISA nor by Pull. In the chromatogram reported for BLD (**Fig. 61**), we indeed noticed intermediate peaks that may represent structures bearing maltosyl stubs. Interestingly, in the models resulting from BMY digestion, we noticed that any of the branched structures generated glucose residues, as also was observed experimentally in oyster glycogen. The CLD calculated for phosphorylase limit dextrin resembles the one obtained experimentally. DP4 and DP6 are the two major peaks, with the former length in greater abundance than the latter, while DP5 is in a lower abundance than DP4 and DP6. Among the branched models reported in Appendix 3, DP5 was one of the products of the phosphorolysis only in presence of a branching point at least on the third glucose residues.

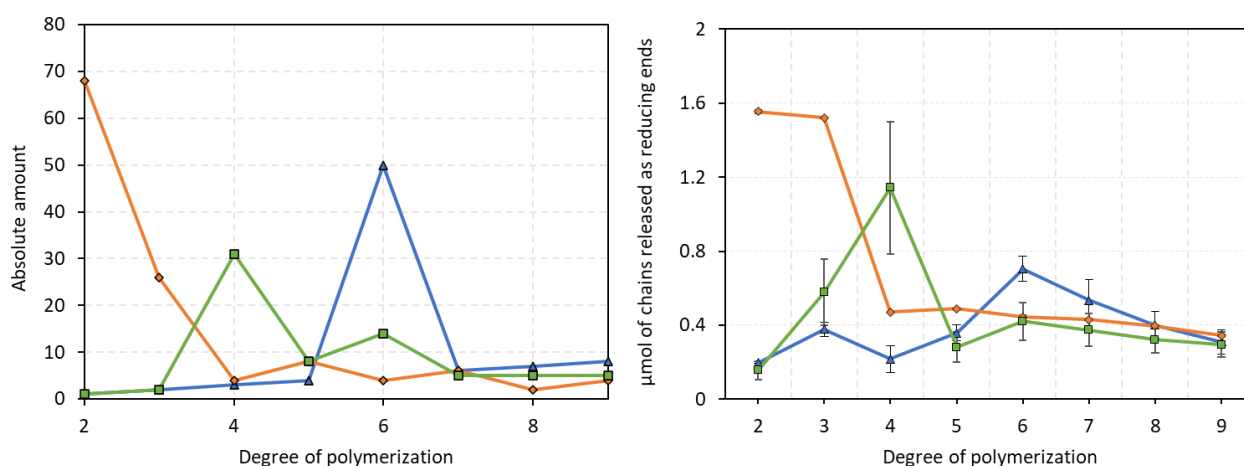


Figure 78 Comparison of the theoretical (left) and experimental (right) CLDs of glycogen, BLD, and PLD debranched enzymatically. The CLDs were calculated as described in **Fig. 38**, and they are illustrated with a blue line for glycogen, in orange for BLD, and in green for PLD.

The comparison of the theoretical models with the experimental data supported the hypothesis that GBE is more likely to transfer and cleave the same X_1 from a variety of chain lengths. Furthermore, the application of this hypothesis also supported that the lack of DP1 in the experimental data is more likely to be attributed to structures bearing branching points on the third glucose residues as mentioned earlier in this section. Finally, to prove that the models created with chains between DP8

and DP17 provides a better representation of the CLD of glycogen or its limit dextrin, we investigated the CLD generated by the structures reported for the DP15 model.

The predicted CLD of the phosphorylase limit dextrin resembles the one reported in literature for oyster glycogen. In contrast, the CLD of β -limit dextrin never shows a peak at DP1 but rather at DP2 and DP3. Considering the models reported in **Appendix 2**, the large number of DP1 was counted from the conversion of odd chains into glucose stubs, while the DP2 was the product of even chains. Furthermore, it was noticed that the chains longer than DP2 were the products of the activity of BMY on chains bearing a branching point on the non-reducing end or the penultimate glucose residue. For example, DP3 was generated by a chain containing a branch on the third or second glucose residue from the reducing end, DP5 from a chain on the fourth or on the fifth glucose residue, and so on for all other DPs (**Fig. 79**).

Despite the shared similarities, the DP15 model is not a good fit to interpret the experimental data as instead is the model created with chains between DP8 and DP17.

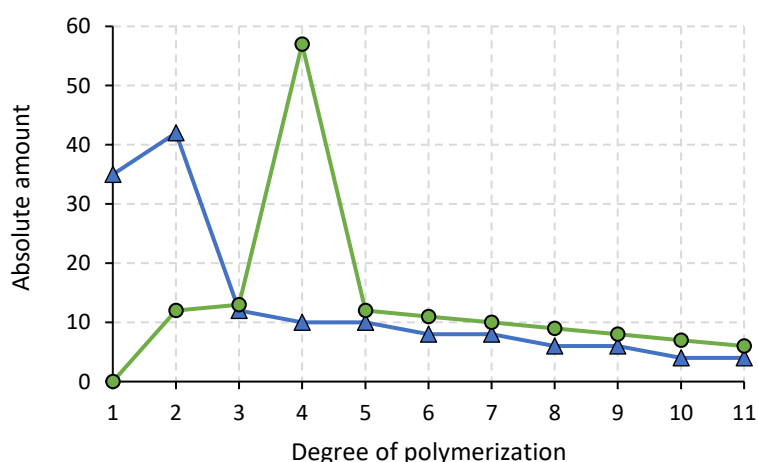


Figure 79 Chain length distribution predicted from the DP15 models reported in **Appendix 2**. Only those resulted from the BMY and GP digestion are selected for the calculations of the CLD. The CLD of BLD is in *blue*, and that of PLD is in *green*.

Chapter 5 - Investigation of the structure of glycogen from mammalian sources

5.1. Review of the current methodologies to extract glycogen from mammalian sources

Claude Bernard,¹ the discoverer of glycogen, was the first to develop an extraction protocol for the polysaccharide from liver. Very few steps were involved, and they consisted of boiling samples for 3 hours in a solution of 30% NaOH (1.5 or 2 volumes per weight of tissue), followed by addition of EtOH in the concentration of 33% to 50% at 20-25 °C to precipitate glycogen. This methodology was applied by other scientists, such as Illingworth *et al.*,¹⁴⁵ to study the structure of glycogen in GSD patients. Carroll *et al.*¹⁵¹ explored other procedures, based upon the homogenization of tissues in 5% trichloroacetic acid (TCA), followed by the precipitation of glycogen in 5 volumes of 95% EtOH. While both protocols were effective in isolating glycogen from the other components of the tissues, the use of such harsh conditions were later proved to be deleterious for the structure of glycogen.¹⁵² Indeed, in the 1960s, hot alkali or acid extraction methods were shown to influence the molecular weight and the chemical structure of glycogen. These findings were recently supported by Wang *et al.*,¹⁵³ proving that the extraction of glycogen with KOH or TCA influenced the size of the particles and the yield of the material extracted.

In 1990, Vardanis¹⁵⁴ proposed an alternative extraction technique that did not include hot alkali or acid conditions instead using a Tris buffer with mechanical homogenization. The Tris buffer proved to be an inhibitor of glucosidase activity, limiting the hydrolysis of glycogen particles.^{27,153} A tissue sample was homogenized in ice with Tris HCl (pH 7.5), EDTA, and NaF. The homogenate was then centrifuged at low speed (10,000 *g*) to remove the insoluble material, and the supernatant underwent ultracentrifugation (350,000 *g*) to precipitate glycogen. The pellet was then fractionated by SEC to study the size of glycogen particles. In the following years, this procedure was combined to a sucrose density gradient ultracentrifugation.^{27,124,155} This type of centrifugation consists of using various concentrations of sucrose between 25% and 75% that are placed in a column density gradient, and the homogenate is layered on top of it. During centrifugation at high speeds, the components of the samples separate from each other for their size and shape with the largest molecule trapped at the bottom in the highest concentration of sucrose. In this way, macromolecules, such as glycogen, sediments while the contaminants remain in the

supernatant.^{27,156} Although this method limits the use of harsh conditions and damages to glycogen, one disadvantage of the sucrose density gradient is that glycogen yield is low because small and less dense particles remain in the supernatant. Furthermore, there are a high number of time-consuming steps involved. The use of a 30% sucrose gradient was suggested by Wang *et al.*¹⁵³ to solve the yield issue, but the number of steps required did not decrease. An example of the protocol based on sucrose gradient centrifugation is reported below in **Fig. 80**.

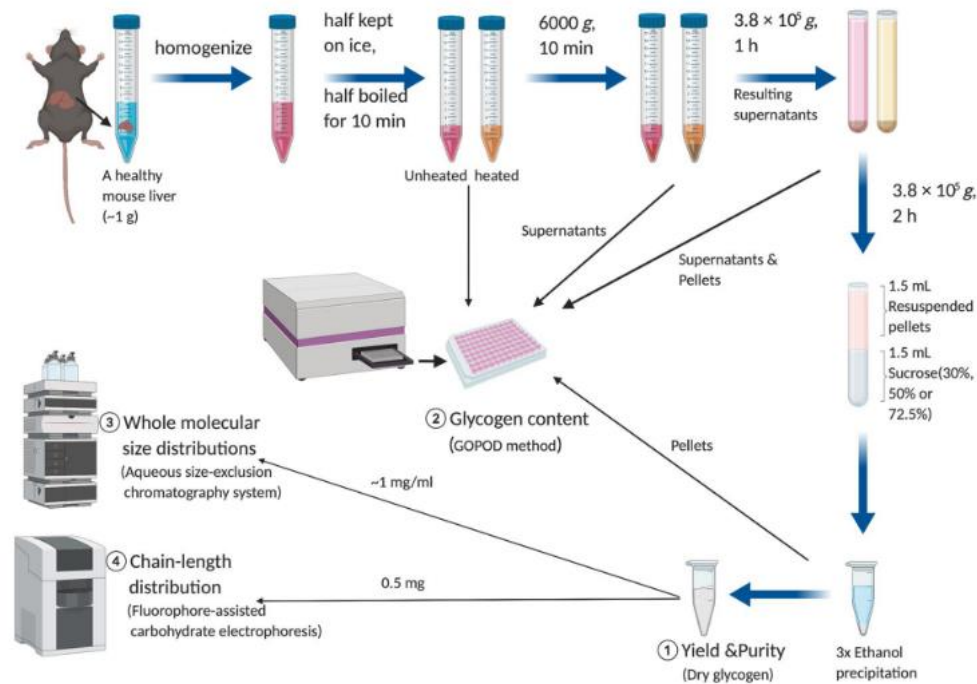


Figure 80 Protocol to extract glycogen from mouse liver samples proposed and described by Wang *et al.*¹⁵³

In the present study, a rapid and mild extraction technique is proposed as alternative option to the sucrose gradient centrifugation. To limit the use of harsh conditions and minimise the structural damages, glycogen was extracted using heat and mild acidic buffer combined with ethanol precipitation. The protocol was initially developed using HepG2 cells and later adapted to mouse liver samples. The developed protocol aimed at providing a simple procedure to be applied on both tissues and cell lines from healthy and GSDs sources. At this time, the yield, and the effects of each step on the particle size were not evaluated as the purpose was to investigate the chain length distributions of glycogen in healthy and GSDs sources.

5.1.1. Development of the protocol to extract glycogen from tissues and cells

When tissues or cells are removed from animals or media, glycogen is rapidly degraded by the action of the degradative enzymes at room temperature.¹⁵⁷ For this reason, samples must be either immediately processed or freeze in liquid nitrogen (*snap freezing*) to prevent glycogen degradation. In these studies, both approaches were applied. The material obtained from cells was freshly prepared and rapidly processed, whereas mouse liver samples were snap frozen for a later use.

5.1.1.1. Extraction from HepG2 cells

The cell line selected for the development of the protocol was the immortalised mammalian HepG2. This cell line is an adherent one meaning that the proteins on the membrane (integrins) interact with the culture plate. Commercial polystyrene plates are pre-treated with a plasma gas to add oxygen-containing functional groups providing a negative net charge.¹⁵⁸ In this way, integrins bind to the plastic surface, and the growth and proliferation of the cells is promoted. As consequence, a detachment step is required to collect the cells from the plate, and trypsin, a serine protease, is commonly selected for this purpose (**Fig. 81**, steps 1-8).

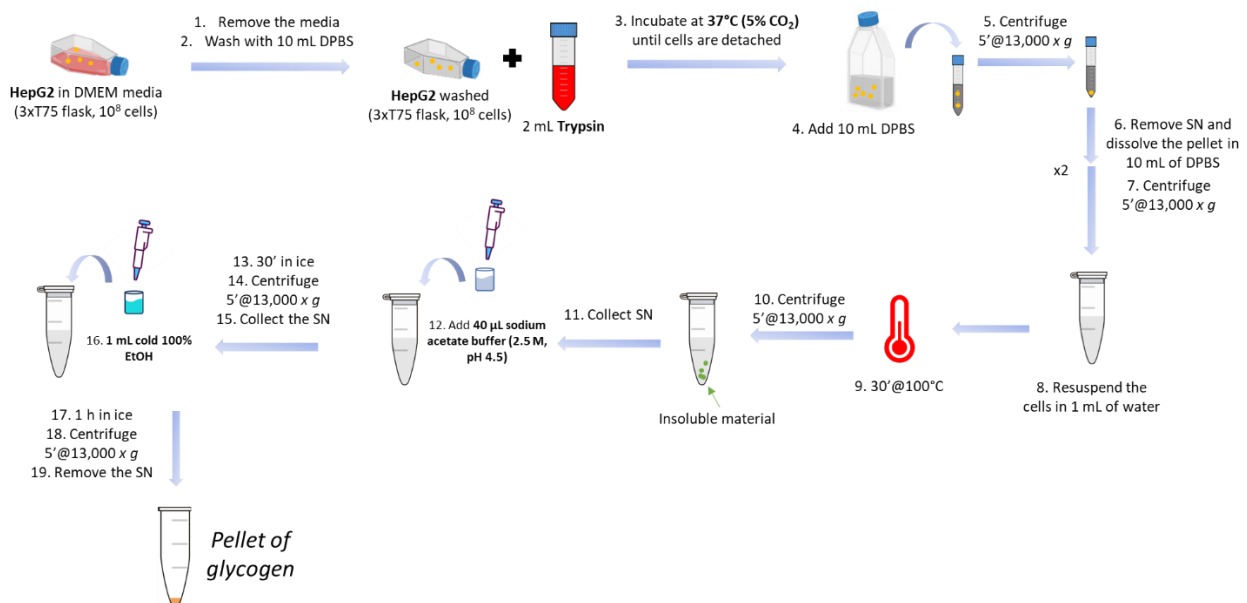


Figure 81 Summary of the extraction protocol of glycogen from HepG2 cells.

After the cells are entirely detached from the plate, they are rapidly collected and pelleted by centrifugation. Then, they are resuspended in water, and immediately boiled for 30 minutes at 100 °C to inactivate the degradative enzymes (**Fig. 81**, step 9-10). During these first steps, the high temperature damages the phospholipid layer of the cell membrane, releasing material stored in the cytosol, such as glycogen. Heating for prolonged period was a concerning step of the protocol due to the potential impact on the chemical structure of glycogen. Nevertheless, the recent studies

published by Wang *et al.*¹⁵³ showed that boiling the sample for either 1 min or 120 min does not influence the chain length distribution of the polysaccharide.

The boiled sample was centrifuged to pellet the insoluble material, and the supernatant containing glycogen was treated with acidic acetate buffer (pH 4.5, 0.1 M). The low pH created a hostile environment for the nucleic acids causing their denaturation and subsequent precipitation. As a matter of fact, a white precipitate was observed after addition of the acetate buffer which is separated from the solution by centrifugation. Finally, the supernatant containing glycogen is treated with 50% cold EtOH (**Fig. 81**, steps 11-19) to collect the polysaccharide.

5.1.1.2. Extraction of glycogen from mouse liver

The protocol developed on HepG2 cells was transferred and optimised on samples from mouse liver. Due to the unfeasibility to process fresh liver immediately, the liver samples were frozen to preserve the integrity of glycogen.

The procedure followed the same principles used for HepG2 cells, except the heating step was increased from 30 minutes to 1 hour to complete the disruption of the tissue (**Fig. 82**).

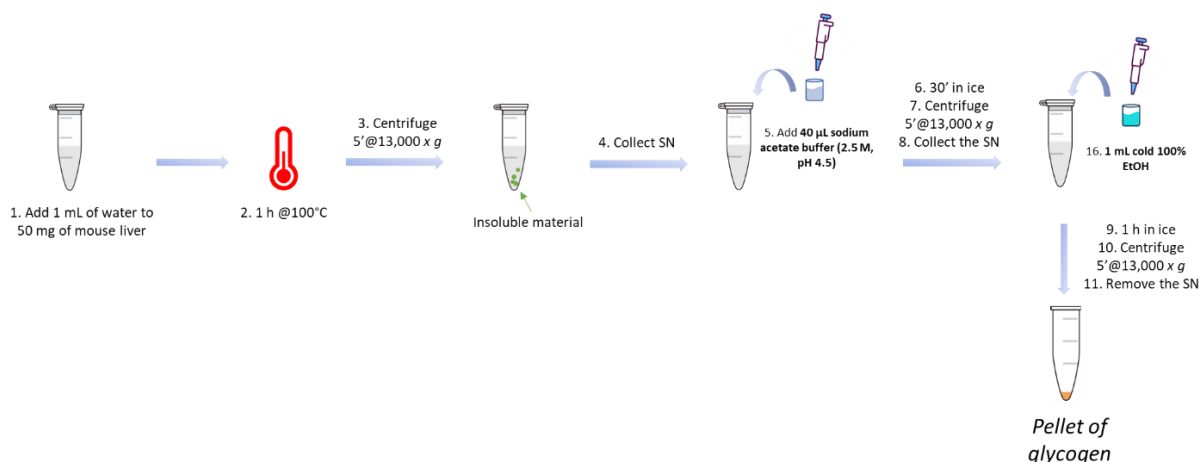


Figure 82 Summary of the extraction protocol of glycogen from mouse liver samples.

5.2.Chain length distribution of glycogen from HepG2 cells and mouse liver

To investigate the CLD of glycogen extracted from HepG2 cells and mouse liver, the same debranching procedure reported in Chapter 4.1 for oyster glycogen was applied. Briefly, the pellet of glycogen was dissolved in acetate buffer, treated with *Ps.* isoamylase for 24 h, and the products were analysed by HPAEC (**Fig. 83a** and **83b**); TLC analysis was not possible at this stage due to the small quantity of glycogen extracted. In addition, due to the low number of chains released from glycogen extracted from HepG2 cells, the values of the relative areas were used to facilitate the comparisons of the CLD between the three different sources.

In **Fig. 83a**, the raw data of the chromatogram collected for mouse liver are characterised by a group of predominant chains between DP3 and DP8 and the peak detected before DP3 does not correspond to DP1 or DP2 which was therefore considered unidentified. It is important to bear in mind that mouse liver was not processed immediately, and degradative enzymes might have caused the partial digestion of the chains altering the real CLD.

The peaks detected between those confirmed with the standards, namely the intermediate peaks between DP3 and DP7, may be the results of branched structures not digested with ISA. The raw data of oyster glycogen shows the same intermediate peaks, and further enzymatic treatments were performed for their analysis without a successful outcome as reported in Chapter 3. Differently, the raw data collected for HepG2 glycogen do not show intermediate peaks, and DP7 is the most abundant chain length.

The integration of the raw data of the three sources to calculate the relative areas revealed a peak shoulder between DP12 and DP15 for HepG2 and mouse liver glycogen, but not for oyster glycogen. Considering that HepG2 and mouse are from the mammalian class, glycogen is expected to share more structural similarities than with a source from a different class such as oyster (from Bivalvia). Nevertheless, the data reported in **Fig. 83a** show that oyster glycogen contains structural features more closely related to both HepG2 cells and mouse liver than those shared by glycogen from the mammalian sources. In the discussion section, further interpretation of these data is presented.

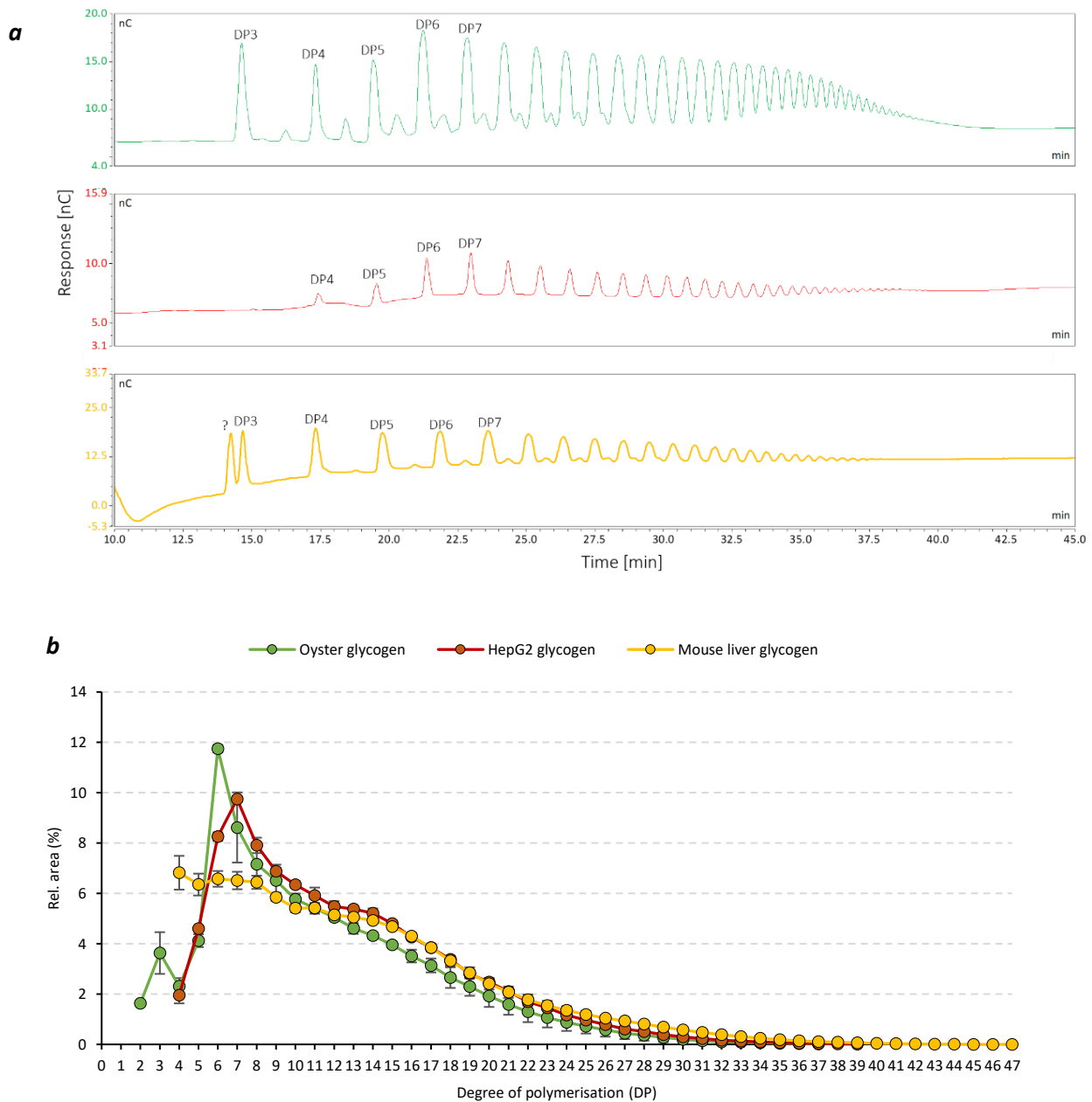


Figure 83 Chain length distribution of oyster glycogen (green), glycogen extracted from HepG2 cells (red), and mouse liver (yellow) digested with ISA (0.15 U) in sodium acetate buffer (0.1 M, pH 4.5) in 24 h at 40 °C. At the top (a), the raw HPAE data; the number at the top of the peaks indicate the degree of polymerisation. The chromatogram was obtained with a CarboPac PA1 (2x250 mm) column using a flow rate of 0.250 mL/min and the following gradient: 0-2 min of 150 mM NaOH (100%), 2-55 min of 600 mM NaOAc buffer (0-100%), 55-60 min of 150 mM NaOH (100%). At the bottom (b), the relative areas (%) were calculated by dividing the area of each peak per the total value.

5.2.1. Preliminary measurements of the degree of branching in glycogen from HepG2 cells

The samples analysed by HPAEC were assessed by BCA assay to measure the number of reducing ends before their digestion into glucose to quantify the total glycogen. **Table 3** contains the concentration of branches released by ISA and the total glycogen in 10^8 HepG2 cells. Preliminary studies on the degree of branching in HepG2 glycogen revealed a striking difference with oyster glycogen. The percentage of branches in HepG2 cells is 20%, a value that is two times higher than

that observed in the commercial oyster glycogen (10%). To the best of our knowledge, literature does not report information on the structure of glycogen in HepG2 cells. However, it is important to bear in mind that these measurements are preliminaries. The growth of more HepG2 cells to evaluate the reducing end value in the sample of glycogen was not possible due to continuous contamination of the cells with fungi. Therefore, the value reported in **Table 3** may be an overestimation of the actual number of reducing ends in HepG2 glycogen.

Table 3 Quantity of glycogen and reducing ends released from HepG2 cells.

Quantity of glycogen in 10 ⁸ cells	Quantity of reducing ends released from HepG2 glycogen by ISA
5.42 µg ± 1.4	1.1 µg ± 2.2
Degree of branching: 20.2%	
Degree of branching of oyster glycogen: 10%	

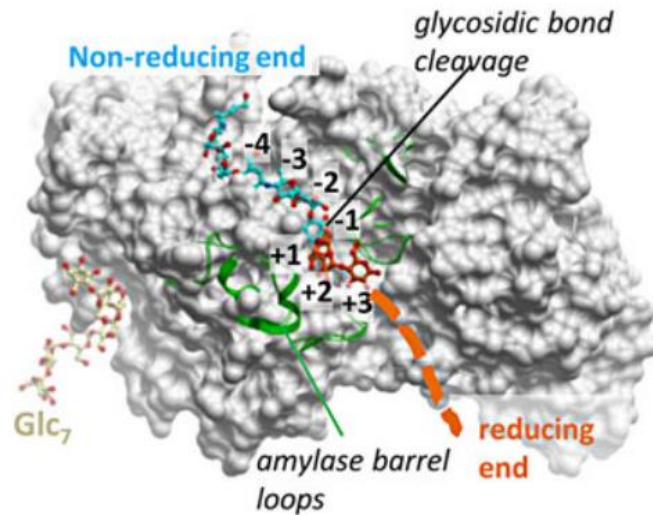
5.3. Discussion

5.3.1. The peak in the CLD of HepG2 glycogen is a possible anchoring point for the branching activity of GBE

According to the DP15 model explained in Chapter 2, the chain length distribution of glycogen from HepG2 cells provides insights into the substrate specificity of GBE expressed in mammalian cell line. The major peak at DP7 observed in **Fig. 83b** identifies the preferential chain length cleaved and transferred by GBE, while chains in a minor abundance as those included in the peak shoulder (DP10-DP16) are selected less frequently than DP7. These findings suggest that the catalytic site of GBE in HepG2 cells can accommodate substrates equal or longer than DP7, a length one unit larger than that observed for oyster glycogen.

To date, the substrate specificity of human GBE or from HepG2 cells is not clear. In 2015, the crystallisation of the human GBE by Froese *et al.*⁶² with maltoheptaose revealed a non-catalytic binding cleft that it could be used by the enzyme as anchor point to start the branching reaction (**Fig. 84**). If this is the case, the major peak observed in every glycogen chain length distribution might represent the preferred substrate cleaved and transferred by GBE and the chain length used by the enzyme to anchor the structure during the synthesis. However, more studies are needed to validate this hypothesis.

Yet, Froese *et al.*⁶² modelled a deca-saccharide into the active site showing that the cleavage occurred between the third and fourth glucose residue from the reducing end, named +1 and -1 in **Fig. 84**, respectively. As result, DP7 was the substrate cleaved and transferred onto an acceptor chain while DP3 was the remaining stub. These results collected by molecular docking can provide an explanation to the presence of short chains observed in every glycogen CLD. For instance, short chains between DP2 and DP5 for oyster glycogen or between DP4 and DP6 for HepG2 cells represent the chain length left after that GBE has cleaved an $\alpha(1,4)$ -glycosidic bond. In the outer most layers of glycogen, the resulting stubs may not be suitable substrates for glycogen synthase, thus remaining in the structure to be further digested by the GDE. This hypothesis converges with the one suggested by Sullivan *et al.*,¹⁵ which proposed that GBE on glycogen external layers maintains its substrate specificity towards the chains to be transferred while the remaining chain is gradually shortened from the inner to the outer shell. However, these assumptions are based on mathematical models and further experimental studies are required in their support.



Modelling step 1: hydrolysis

Active site donor chain prior to glycosidic bond cleavage

Figure 84 Surface representation of the complex of human GBE with maltoheptaose (Glc₇) and the deca-saccharide to identify non-catalytic binding cleft and to model the hydrolysis of the chain by GBE. The cleavage site is located between the third and the fourth from the reducing end of the deca-saccharide. The cleavage site of the deca-saccharide is located between the positions -1 and +1. Image adapted from Froese *et al.*⁶²

5.3.2. Possible degradation of mouse liver glycogen by degradative enzymes

A different scenario from HepG2 cells was observed for the distribution of chains in mouse liver glycogen. The polysaccharide did not show any predominant chain length but rather a range of DPs between DP3 and DP8 more abundant than others. To compare our data, only one paper published by Sullivan *et al.*¹⁵⁹ in 2012 was found about the chain length distribution of glycogen. Other papers published by Nitschke *et al.*⁹² (2017) and Sullivan *et al.* (2019)³¹ report the CLD of the mice skeletal muscle rather than liver, and for this reason, those studies were not compared with our data.

Sullivan *et al.*¹⁵⁹ used mice constantly fed and sacrificed at different time of the day; a method also followed for the animals used in these studies. The distribution of the chains collected by the authors using FACE technique shows a major peak at DP3 and a peak shoulder between DP12 and DP20 (**Fig. 85**). The differences observed between our data and those collected by Sullivan *et al.*¹⁵⁹ suggested that the structure of glycogen may have been altered by the enzymatic degradation. The high proportion of short chains (DP3-DP8) could be generated by the activity of glucosidases on the external layers of glycogen before they are inactivated by heat.

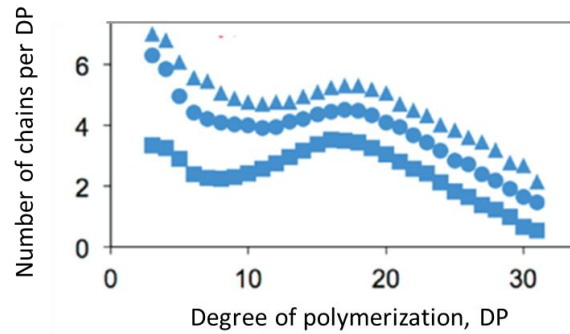


Figure 85 Chain length distribution of glycogen measured by FACE technique from mouse liver samples. The x-axis indicates the degree of polymerisation, while the y-axis represents the number of chains per degree of polymerisation. Each distribution was collected from a single mouse. Image adapted from Sullivan *et al.*¹⁵⁹

In the extraction procedure used by Sullivan *et al.*,¹⁵⁹ a mechanical homogenisation of the mouse liver sample was performed with a glycogen isolation buffer containing Tris which buffer is known to inactivate glucosidases. The use of this component may explain the difference with our results. However, both mouse liver and HepG2 cells express glucosidases. If the glucosidases were not inactivated following the protocol developed, the CLD of HepG2 glycogen would have been populated by short chains as seen for mouse liver, and this was not observed in **Fig. 83**. To conclude, more studies aiming at comparing the extraction of glycogen from mouse liver with and without Tris buffer using the developed methodology are required to confirm or not the reported CLD.

5.4. Preliminary studies on the structure of glycogen from GSDIa HepG2 cells

GSD type I indirectly affects glycogen metabolism. This genetic mutation of the G6PC gene impairs the activity of glucose 6-phosphatase, the transmembrane protein that converts glucose 6-phosphate into glucose in the endoplasmic reticulum (ER) (**Fig. 86**).¹⁶⁰ As consequence, glycogen metabolism is altered.^{21,82} However, it is not clear yet how GSDIa might affect glycogen metabolism and structure.

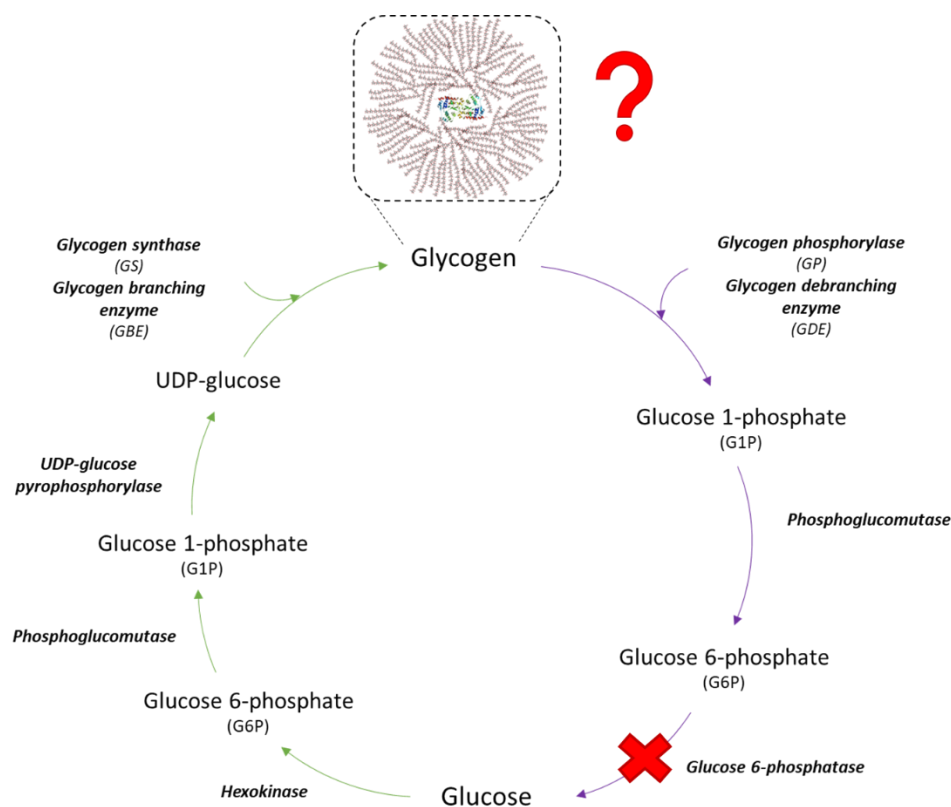


Figure 86 Image reported from Chapter 1.

Here, in collaboration with PhD student María Rodríguez Peiris and Prof Kathrin Thedieck, HepG2 cells were genetically modified to express the GSDIa type. The wild-type cell line does not express G6PC gene. Therefore, the cells were induced to express the G6PC gene before the expression of the GSDIa mutations. Three cells line were generated with the following genetic mutations located in the catalytic site: R83C (Arg → Cys), A124T (Ala → Thr), and T255I (Thr → Ile).⁹⁴ The extraction protocol used for the wild type HepG2 cells was transferred onto the GSDIa models, and the glycogen debranched following the same methodology reported for the wild type cells line.

5.4.1. Results and Discussions

The results in **Fig. 87** shows the CLD of glycogen from controls and the three GSDIa mutant cell lines. The analysis of the CLD of glycogen from HepG2 cells bearing the GSDIa shows a peak at DP7, and chains between DP4 and DP6 were less abundant than DP7, as also observed in the controls; intermediate peaks between DP1 and DP3 were detected but not identified.

Our findings suggest that mutations affecting the catalytic site of glucose 6-phosphatase do not have an impact on the CLD of glycogen. Based on the theoretical models proposed in Chapter 3 and 4, the peak at DP7 represents the minimum chain length selected by GBE to create new branches. Since the peak of the distribution does not change in GSDIa samples, it was hypothesised that the

substrate specificity of GBE is not influenced by GSDIa. However, further studies on the degree of branching are needed to evaluate the impact of GSDIa on the branching frequency of GBE, and treatments with BMY and GP will be useful to evaluate the distance between branching points in HepG2 cells and HepG2 GSDIa cells. To the best of our knowledge, these are the first studies on the chain length distribution of glycogen from HepG2 cells with GSDIa mutations.

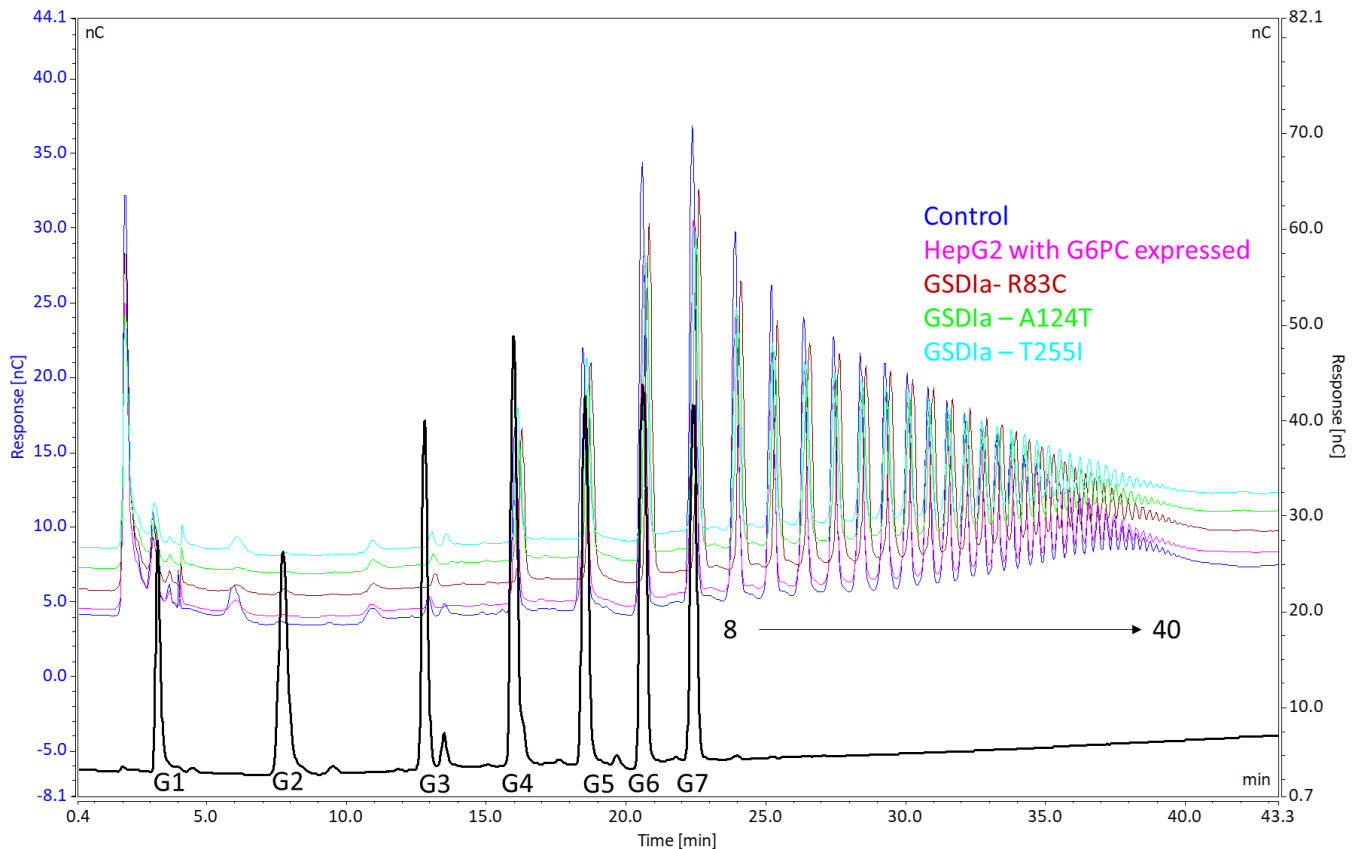


Figure 87 Chain length distribution of glycogen extracted from HepG2 cells bearing GSDIa mutations. Each glycogen sample was digested with ISA (0.15 U) in sodium acetate buffer (0.1 M, pH 4.5) in 24 h at 40 °C. The raw HPAE data; the number at the top of the peaks indicate the degree of polymerisation. The chromatogram was obtained with a CarboPac PA1 (2x250 mm) column using a flow rate of 0.250 mL/min and the following gradient: 0-2 min of 150 mM NaOH (100%), 2-55 min of 600 mM NaOAc buffer (0-100%), 55-60 min of 150 mM NaOH (100%). The raw data are from an individual experiment.

Chapter 6 - Conclusions

Glycogen has a complex structure, and its structural features depend on the species or on the physiological state of the organism at the time of glycogen extraction. Here, we demonstrated that glycogen from mammalian sources can be extracted and analysed using mild conditions and user-friendly techniques. The proposed approach also provides the standard procedure that can be applied on glycogen from GSDs sources to evaluate the impact of this metabolic disorders on glycogen structure.

The experimental procedure was successfully developed following a *top-down* approach. The use of enzymes prevented time-consuming and tedious method developments required for an analytical chemistry-based approach. In the present studies, three commercial debranching enzymes were selected to target specific information on the structure of glycogen. The broad substrate specificity of *Ps.* isoamylase towards complex branched structure was exploited to provide an overview on the structural features of glycogen. In contrast, the efficiency of pullulanase towards short-branched oligosaccharides was preferred when it was required a focus on the short chains of part of the outer most layers of glycogen as in BLD and PLD. Then, the selectivity of oligo $\alpha(1,6)$ -glucosidase for glucosyl stubs was used to assess the presence of glucose residues in glycogen, which enzyme was proved to be crucial to study the branching arrangement of BLD and PLD.

The combination of the experimental data with theoretical models represented another strength of the presented methodology. Thanks to this approach it was possible to elucidate the structures generating DP3 from β -amylolysis. We indeed proposed that DP3 was the product of BMY from structures branched on the third glucose residue from the reducing end instead of unbranched odd chains as often suggested in literature. Furthermore, the theoretical models were demonstrated to be an efficient tool to elucidate the activity of GBE showing that the peaks in the chain length distribution were indicative of the preferential chain length selected by GBE to create new branches. Finally, the design of branched models using substrates between DP8 and DP17 suggested that the GBE was more likely to select the same chain length cleaved and transferred onto the same chain.

The application of the debranching treatments to glycogen from HepG2 cells, HepG2 GSDIa type cells, and wild-type mouse liver validated the developed methodology. The samples of glycogen collected with a new extraction protocol from HepG2 cells showed a peak at DP7. These results suggested that GBE in this species has a selectivity towards the cleavage and transfer of chains with seven glucose residues. The same chain length distribution was measured in HepG2 GSDIa mutant

lines. These results suggested that this type of GSD has little as no impact on the length of the chains, and, consequently, on the substrate specificity of GBE. The same methodology was also applied to mouse liver samples, but the results were not consistent with those reported in literature, due to possible degradation of the sample.

Finally, the presented methodology has a potential for the investigation of the activity of GSDs defected enzymes. The commercial enzymes could be substituted with enzymes extracted from wild-type or GSDs sources using standards oligosaccharides as substrates for their activity. Then, the products obtained from defected enzymes would be compared with those from wild type to get more insights into how the substrate specificity is influenced by GSDs mutations.

Chapter 7 - Materials and Methods

The following products were purchased from Sigma-Aldrich. Standard oligo- and poly- saccharides: glycogen from oyster (dry powder), glucose (G1), maltose (G2), maltohexaose (G6) and maltoheptaose (G7). Enzymes: *phosphorylase a* from rabbit muscle (lyophilised powder 20-30 U/mg); alkaline phosphatase from calf intestine (2 U/ μ g of protein, 1000 U, 20 U/ μ L); α -amylase from barley (1000 U/mg, 10,000 U/mL in 5 mL of 3.2 M ammonium sulphate); amyloglucosidase from *Aspergillus niger* (lyophilized powder 70 U/mg). Mobile phase for TLC and TLC plates: acetonitrile (CH₃CN), ethyl acetate (EtOAC), and isopropanol (iPrOH); supelco TLC silica gel 60 F254 (20x20 cm), 25 units. Eluents for HPAEC: sodium acetate anhydrous (NaOAc); sodium hydroxide 18.4 M (NaOH). BCA reagents: sodium carbonate (Na₂CO₃), sodium bicarbonate (NaHCO₃), bicinchoninic acid (BCA), copper sulphate pentahydrate (CuSO₄ x 5H₂O), and L-serine. Others: Amicon® Ultra-4 centrifugal filters (10 kDa cutoff) for glycogen purification; amberLite MB mix bead anion exchange resin.

The following products were purchased from Carbosynth. Standard oligosaccharides: maltotriose (G3), maltotetraose (G4), maltopentaose (G5), isomaltose, and isomaltotriose.

The following products were purchased from Megazyme. Standard oligosaccharides: 6³- α -glucosyl-maltotriose (G1-G3), and 6³- α -maltotriosyl-maltotriose (G3-G3). Enzymes: *Pseudomonas* isoamylase (600 U, 180 U/mg, 200 U/mL in 3.2 M ammonium sulphate), *Klebsiella pneumonia* pullulanase (2000 U, 78 U/mg, 1000 U/mL in 3.2 M ammonium sulphate), β -amylase from barley (10,000 U/mL, 435 U/mg, 20,000 U in 3.2 M ammonium sulphate) and oligo α (1,6)-glucosidase (6000 U, 145 U/mg, 1000 U/mL in 3.2 M ammonium sulfate). Milli-Q H₂O was used in all experiments in which the use of water is mentioned.

The following instruments were employed for the analysis of the samples. BMG Labtech - POLARstar Omega Plate Reader was employed to record the absorption intensity at 560 nm using Costar 96-well plates clear bottom flat from Sigma-Aldrich. Centrifugation of the samples were performed with Sorvall™ ST 16 Centrifuge Series (Thermo Fisher) and bench centrifuge Mini centrifuge IKA. Heat-inactivation of the enzyme was performed with the heating block Dri-Blocks® Techne. Evaporation of the solvents in the samples were performed with the rotavapor Büchi. Separation of glycogen chains was performed with Dionex 6000 with the column used CarboPac PA-1 analytical column (2x250 mm) with a guard column (2x50 mm), and with the GPC Gilson with RI detector using the column TSK40S 22x90 cm.

7.1. Purification of commercially available oyster glycogen

A stock solution of commercially available oyster glycogen was purified from glucose impurities as follows. 100 mg of oyster glycogen were dissolved in 5 mL of water, and 1 mL of this solution was transferred to a centrifugal tube (4 mL) with an insert of 10 kDa cut-off. The tube was centrifuged for 20 minutes at 4,000 rpm at 4 °C using a Sorvall™ ST 16 Centrifuge Series (Thermo Fisher). The filtered solution with glucose impurities was removed from the tube, while the insert containing purified glycogen was refilled with 1 mL of the stock solution and centrifuged again as indicated above. This process was repeated until the whole stock solution (5 mL) was filtered. Once the centrifugation step was completed, purified glycogen in the insert was transferred into a glass vial, and 500 µL of water were added to the insert to collect residues of glycogen. Purified oyster glycogen was frozen at -80 °C for 3 h and dried under vacuum overnight. The dried oyster glycogen had a pale-yellow colour, and it was stored at 4 °C.

7.2. Enzymatic treatments

7.2.1. Debranching of oyster glycogen with ISA and Pull

The debranching of oyster glycogen, PLD or BLD with ISA or Pull was performed using aliquots taken from the stock solution of the sample in water (10 mg/mL). Before addition of the enzymes to glycogen, stock solution of each enzyme was prepared as follows. For ISA, 50 µL of 200 U/mL of enzyme were added to 150 µL of reaction buffer (acetate buffer pH 4.5, 0.1 M) to reach 50 U/mL; the units and concentrations used for the assay are 0.15 U (0.83 µg) and 2.6 U/mL. For Pull, 50 µL of 1000 U/mL of enzyme were added to 450 µL of reaction buffer (acetate buffer pH 4.5, 0.1 M); the units and concentrations used for the assay are 0.15 U (1.9 µg) and 2.6 U/mL. Then, the stock solutions were used to prepare the reaction mixture. 50 µL of sample was mixed with 3 µL of sodium acetate buffer (pH 4.5, 2.5 M) to reach 0.1 M. Pre-mixed in separate Eppendorf: (a) 12 µL of *ps.* isoamylase (50 U/mL) with 6 µL of AB (0.1 M, pH 4.5), and (b) 12 µL of AB (0.1 M, pH 4.5) with 6 µL of pullulanase (100 U/mL). Then, 4.5 µL of mix (a) or (b) were added to 53 µL of glycogen, BLD or PLD in acetate buffer. The samples were incubated at 40 °C for 24 h, and the reaction was stopped by heat-inactivation of the enzyme in the heating block at 100 °C for 5 minutes. The inactivated enzyme was centrifuged 2 minutes at 13,000 $\times g$ and separated from the sample. Each sample was desalted with the mix bed anion exchange resins before TLC analysis.

7.2.2. Digestion of oyster glycogen with BMY or GP

The stock solutions of β -amylase or glycogen phosphorylase were prepared prior to their addition to glycogen. For the stock solution of 1500 U/mL β -amylase, 150 μ L of 10000 U/mL of the enzyme were added to 200 μ L of PB (pH 6.0, 1 M) and 650 μ L of H₂O; the units and concentrations used for the reaction are 60 U (0.13 mg) and 120 U/mL. For the stock solution of *phosphorylase a*, 10 mg of enzyme were dissolved in 2 mL of reaction buffer (potassium phosphate buffer pH 6.8, 0.2 M) and freeze at -20 °C in 100 μ L aliquots (10 U each, 100 U/mL).

The addition of β -amylase or glycogen phosphorylase to glycogen was performed as follows in a total volume of 500 μ L. 20 mg of glycogen were dissolved in 1 mL of water and vortex until complete dissolution of the polysaccharide. For the digestion with β -amylase, 250 μ L of glycogen (20 mg/mL) were added to 100 μ L of PB (pH 6.0, 1 M), 110 μ L of water and 40 μ L of β -amylase (1500 U/mL). For the digestion with glycogen phosphorylase, 250 μ L of glycogen (20 mg/mL) were added to 100 μ L of PB (pH 6.8, 1 M), 50 μ L of water and 100 μ L of phosphorylase a (100 U/mL). Both reactions were incubated for 24 h at 37 °C and the enzymes were inactivated by heating the sample at 100 °C for 5 minutes. The enzyme was precipitated with 2 minutes at 13,000 $\times g$ and the supernatant was separated from the precipitate. 500 μ L of cold EtOH was added to the mixture of limit dextrin and glucose 1-phosphate or maltose to reach 50% (v/v), and the samples were left in ice for 1 h. After 1 h, the samples were centrifuged for 2 minutes at 13,000 $\times g$, and the limit dextrin precipitated was separated from the supernatant containing glucose 1-phosphate or maltose. Both limit dextrans were dissolved in 300 μ L of water to which 300 μ L of cold EtOH was added and left in ice again for 1 h. After completion of the EtOH precipitation, the precipitated limit dextrin was dissolved in 300 μ L of water. For the successive incubation of limit dextrin with BMY or GP, 100 μ L PB (1 M), 160 μ L of water, and 40 μ L of β -amylase or 100 μ L of phosphorylase a to the samples. Repeat the digestion and the following steps until no more glucose 1-phosphate or maltose is released.

Standard oligosaccharides (2 mg/mL) were digested under the same conditions of the reaction with glycogen. The digestion of standards oligosaccharides with 24 h GP were prepared in 4 mg/mL to enhance the possibility to determine the presence of G3 by TLC.

For the precipitation of the standards in EtOH, a solution of 200 μ L of 10 mg/mL of OG with 2 mg/mL of glucose 1-phosphate or maltose was treated with 600, 200, 165 and 68 μ L of cold EtOH, and placed in ice for 1 h. The samples were centrifuged for 2 minutes at 13,000 $\times g$. The supernatant was separated from the precipitate, and the EtOH was evaporated by rotavapor before freeze-drying.

The precipitate and the freeze-dried supernatant were both re-dissolved in 100 μ L of water and analysed by TLC.

7.2.3. Dephosphorylation of G1P

The samples collected from each incubation with phosphorylase a were merged and the mixture of the water/EtOH solution was evaporated with the rotavapor. The sample was freeze-dried and dissolved in 1 mL of water. 1 mL of Tris-HCl (pH 9.0, 1 M) and 2 μ L of ALP (5 U/ μ L) were added to 1 mL of sample and incubated at 40 °C for 24 h. The progress of the reaction was monitored by TLC. After completion, the enzyme was inactivated by heating the sample for 5 minutes at 100 °C, and the buffer removed with the anion exchange resin before quantification with the BCA assay.

7.2.4. Digestion of glycogen, BLD and PLD by enzymatic cocktail

The stock solutions of AMY, AMG, and ISA were prepared prior their addition to the samples. For AMY, 200 μ L of 2000 U/mL were added to 800 μ L of reaction buffer (pH 4.5, 0.1 M); the units and concentrations used for the reaction are 10 U (10 μ g) and 160 U/mL. For AMG, 6.2 mg of enzyme were dissolved in 1 mL of reaction buffer (pH 4.5, 0.5M); the units and concentrations used for the reaction are 0.5 U (7 μ g) and 8.1 U/mL. For ISA, the stock solution was the same reported in the section 6.2. The mixture of the three enzymes was prepared by addition of 5.1 μ L of AMY to 1.15 μ L of AMG and 3 μ L of ISA, which solution was transferred to 52.3 μ L of sample in acetate buffer. The sample was incubated at 40 °C for 24 h and the enzyme was inactivated by heating at 100 °C for 5 mins. Before TLC analysis, the sample was desalted with a mix bead anion exchange resin.

7.2.5. Digestion of the samples with OGL

The stock solution of OGL was prepared by addition of 20 μ L of 200 U/mL of enzyme to 180 μ L of the reaction buffer (pH 4.5, 0.1 M); the units and concentrations used for the assay are 0.025 U (3.4 μ g) and 0.5 U/mL. The reaction was performed as follows. 50 μ L of the sample were treated with 2.3 μ L of AB (pH 4.5, 2.5 M) and 1.25 μ L of 20 U/mL of OGL, and incubated for 24 h at 40 °C. The enzyme was inactivated by heating the sample at 100 °C for 5 mins. The sample was desalted with the mix bead anion exchange resin prior the TLC analysis.

7.3. Quantitative and qualitative analysis of the samples

7.3.1. Quantification of the samples by BCA assay

The protocol for the BCA assay was reported by Kobayashi *et al.*¹⁰² BCA reagent was freshly prepared by mixing equal volumes of solution A (3.2 g Na₂CO₃, 1.2 g NaHCO₃ and 97.1 mg BCA in 50 mL water) and solution B (62 mg CuSO₄ x 5H₂O and 63 mg L-serine in 50 mL water). Each sample obtained from

the debranching treatment was diluted 1:100 in MQ water, glucose from the dephosphorylation treatment and from the enzymatic cocktail, and maltose were diluted 1:2000 in MQ water. The calibration curve with glucose and maltose were prepared from a solution of 6.25 µg/mL in water and diluted seven times with a DF of 1:2. To control the reliability of the assay, three known concentrations of glucose and maltose (6, 0.8 and 0.1 µg/mL) were always measured with the samples. Then, 100 µL of BCA reagent were added to each sample and standard, heated in a water bath at 80 °C for 40 minutes, and left at room temperature for 10 minutes. 150 µL of the solution was placed in a 96-well plate, and the absorbance was read at 560 nm.

7.3.2. HPAEC analysis of the chain length distribution of glycogen, PLD, and BLD

The protocol reported was adapted by Ryu *et al.*²⁷ The branch-chain length distribution of glycogen obtained before and after treatment with BMY and GP was determined by separation of the hydrolysed branches using an HPAEC system (ICS-5000, Dionex equipped with a pulse amperometric detector). The sample loop was 25 µL and the sample injected was 5 µL. Eluents A and B consisted of 150 mM NaOH and 150 mM NaOH containing 600 mM NaOAc, respectively. Chromatographic separation of the linear malto-oligosaccharides was achieved by a linear gradient mode from 100% of eluent A to 0% in 2 h followed by 15 mins of 100% A to equilibrate the column. The elution of the sample occurred at an operating flow rate at 0.250 mL/min. For the injection, 50 µL of the sample was diluted with 50 µL of water, filtered through a 0.2 µm PTFE filter and transferred into an interlocked vial with fused glass insert for HPLC analysis.

Samples of glycogen collected from HepG2 cells and mouse liver were eluted with the following linear gradient mode: from 0% to 100% of eluent B in 55 mins followed by 5 mins of 100% A to equilibrate the column.

7.3.3. GPC analysis of the samples digested by ISA and Pull

The samples digested by ISA and Pull were separated by GPC as follows. 10 mg of oyster glycogen were dissolved in 948 µL of sodium acetate buffer (pH 4.5, 0.1 M), treated with 52 µL of 50 U/mL of ISA or 26 µL of 100 U/mL of Pull, and incubated for 24 h at 40 °C. The enzyme was inactivated by heating the sample at 100 °C for 5 mins. Then, the solution was filtered through a 0.2 µm PTFE filter and injected in the GPC using a TSK40S column 22 mm ID x90 cm, the void volume was 320 mL. The flow rate was 0.2 mL/min with a collection of each fraction every 14 mins (7 mL per tube) that started at 150 mins and ended at 750 mins. At completion of the run, each fraction was freeze-dried, and dissolved in 50 µL of water.

7.4. Growth of HepG2 cells for the extraction of glycogen

Human HepG2 cells were kindly provided by Prof Julie Gough. The cells were cultured in DMEM medium supplemented with 10% foetal bovine serum (FBS) and 2 mM L-glutamine, and they were maintained at 37 °C in a humidified atmosphere of 5% CO₂. A laminar flow hood was used while working with HepG2 cells.

7.4.1. Thawing cells

A vial of 10⁷ HepG2 cells (1.5 mL) was thawed at room temperature, and the content was transferred into a corning tube containing 10 mL of DMEM. Then, the cells were pelleted by centrifugation (490 g x 5 min), resuspended in 5 mL of medium, and placed in a T25 flask. At 80% confluency evaluated by visual estimation, the cells were passaged.

7.4.2. Passaging cells

The growth medium (DMEM) was removed, and the cells washed twice with 10 mL of DPBS to remove any residue left from the medium. Then, the cells were incubated with 10 mL of trypsin at 37 °C with 5% CO₂ until they were completely detached from the flask. The trypsinisation was inactivated by addition of 20 mL of DMEM followed by centrifugation of the solution (300 g x 3 min). The pellet containing cells was resuspended into 5 mL of medium and transferred into a T75 flask.

When the cells reached the 80% confluency, the pellet obtained after trypsinisation was resuspended in 15 mL and divided into three T75 to generate 10⁸ cells.

7.4.3. Extraction of glycogen

The content of three T75 flasks was used to extract glycogen. Initially, each flask underwent trypsinisation, and the content of the three flasks was merged into a corning tube to collect the cells by centrifugation (300 g x 3 min). The pellet was immediately dissolved in 1 mL of cold water, rapidly transferred into a 2 mL eppendorf, and heated at 100 °C x 30 min to lyse the cells. The vial containing the cell lysate was centrifuge at 13000 g x 5 min, and the supernatant containing glycogen and nucleic acids was transferred into another vial to which 1 mL of cold acetate buffer (pH 4.5, 0.1 M) was added. The sample was placed in ice for 30 min followed by centrifugation at 13000 g x 5 min. The pellet was discarded while the supernatant was treated with 1 mL of cold 100% EtOH and placed in ice for 1 h. The vial was centrifuged at 13000 g x 5 min to collect glycogen and processed immediately as described in the next section.

7.5. Extraction of glycogen from mouse liver samples

1 g of frozen liver from three healthy mice was kindly provided by Prof Barbara Bakker and prepared by PhD candidate Ligia Akemi Kiyuna. For the extraction of glycogen, 50 mg of mouse liver were rapidly weight, dissolved in 1 mL of water, and heated at 100 °C for 1 h. The vial containing the tissue lysate was centrifuge at 13000 *g* x 5 min, and the supernatant containing glycogen and nucleic acids was transferred into another vial to which 1 mL of cold acetate buffer (pH 4.5, 0.1 M) was added. The sample was placed in ice for 30 min followed by centrifugation at 13000 *g* x 5 min. The pellet was discarded while the supernatant was treated with 1 mL of cold 100% EtOH and placed in ice for 1 h. The vial was centrifuged at 13000 *g* x 5 min to collect glycogen and processed immediately as described in section 7.6.

7.6. Debranching of glycogen extracted from HepG2 cells, GSDIa HepG2 cells, and mouse liver

Glycogen from GSDIa cells was kindly provided by Prof Kathrin Thedieck and PhD candidate Maria Rodriguez Peiris following the extraction protocol developed and described in section 6.2.1. The pellet of glycogen freshly extracted from HepG2 cells, GSDIa HepG2 cells, or mouse liver was dissolved in 50 µL of acetate buffer (pH 4.5, 0.1 M), and incubated with 3 µL of 50 U/mL of *ps.* isoamylase at 40 °C for 24 h. The reaction was stopped by heating at 100 °C x 5 min, and the inactivated enzyme pelleted by centrifugation at 13000 *g* x 5 min. The HPAE analysis was performed as described in section 7.3.2.

Chapter 8 – References

1. Young, F. G. Claude Bernard and the discovery of glycogen: A century of retrospect. *British Medical Journal* **1**, 1431–1437 (1957).
2. Meléndez, R., Meléndez-Hevia, E. & Cascante, M. How did glycogen structure evolve to satisfy the requirement for rapid mobilization of glucose? A problem of physical constraints in structure building. *Journal of Molecular Evolution* **45**, 446–455 (1997).
3. Kanungo, S., Wells, K., Tribett, T. & El-Gharbawy, A. Glycogen metabolism and glycogen storage disorders. *Annals of Translational Medicine* **6**, 474–474 (2018).
4. Roach, P. J., Depaoli-roach, A. A., Hurley, T. D. & Tagliabracci, V. S. Glycogen and its metabolism: some new developments and old themes. *Biochemical Journal* **441**, 763–787 (2012).
5. Bertoft, E. & Mäkelä, J. (2007). *Starch: Achievements in understanding of structure and functionality*. New York, USA: Nova Science.
6. Adeva-Andany, M. M., González-Lucán, M., Donapetry-García, C., Fernández-Fernández, C. & Ameneiros-Rodríguez, E. Glycogen metabolism in humans. *BBA Clinical* **5**, 85–100 (2016).
7. Ellingwood, S.S., & Cheng, A. Biochemical and clinical aspects of Glycogen Storage Diseases. *Journal of Endocrinology* **233**, 131–141 (2018).
8. Prats, C., Graham, T. E. & Shearer, J. The dynamic life of the glycogen granule. *Journal of Biological Chemistry* **293**, 7089–7098 (2018).
9. Melendez-Hevia, E., Waddell, T. G. & Shelton, E. D. Optimization of molecular design in the evolution of metabolism: The glycogen molecule. *Biochemical Journal* **295**, 477–483 (1993).
10. Meléndez, R., Meléndez-Hevia, E. & Canela, E. I. The fractal structure of glycogen: A clever solution to optimize cell metabolism. *Biophysical Journal* **77**, 1327–1332 (1999).
11. Zeeman, S. C., Kossmann, J. & Smith, A. M. Starch: Its metabolism, evolution, and biotechnological modification in plants. *Annual Review Plant Biology* **61**, 209–234 (2010).
12. Illingworth, B., Larner, J. & Cori, G. Structure of glycogens and amylopectins. *Journal of Biological Chemistry* **199**, 631–640 (1952).
13. Preiss, J. & Walsh, D. A. (1981). *The comparative biochemistry of glycogen and starch*. New York, USA: John Wiley & Sons.
14. McArdle, W. D., Katch, F. I. & Katch, V. L. (2006). *Exercise physiology: Energy, nutrition, and human performance*. Philadelphia, USA: Lippincott Williams & Wilkins.

15. Deng, B., Sullivan, M., Wu, A. C., Li, J., Cheng, C. & Gilbert, G. The mechanism for stopping chain and total-molecule growth in complex branched polymers, exemplified by glycogen. *Biomacromolecules* **16**, 1870–1872 (2015).
16. Illingworth, B. & Cori, G. T. Structure of glycogens and amylopectins. *Journal of Biological Chemistry* **199**, 653–660 (1952).
17. Matsui, M., Kakuta, M. & Misaki, A. Comparison of the unit-chain distributions of glycogens from different biological sources. *Bioscience, Biotechnology, and Biochemistry* **57**, 623–627 (1993).
18. Matsui, M., Kakut, M. & Misaki, A. Fine structural features of oyster glycogen: Mode of multiple branching. *Carbohydrate Polymers* **31**, 227–235 (1996).
19. Bezborodkina, N. N., Chestnova, A. Y., Vorobev, M. L. & Kudryavtsev, B. N. Spatial Structure of Glycogen Molecules in Cells. *Biochemistry (Moscow)* **83**, 467–482 (2018).
20. Archibald, A. R., Fleming I. D., Liddle, M. A., Manners, D. J., Mercer, G. A. & Wright, A. α -1,4-Glucosans (part XI): The Absorption spectra of glycogen- and amylopectin-iodine complexes. *Journal of the Chemical Society* **0**, 1183-1190 (1961).
21. Levin, B., Burgess, A. & Mortimer P. E. Glycogen storage disease type IV, Amylopectinosis. *Archives of Disease in Childhood* **43**, 548-555 (1968).
22. Özen, H. Glycogen storage diseases: New perspectives. *World Journal of Gastroenterology* **13**, 2541–2553 (2007).
23. Li, S. C., Chen, C. M., Goldstein, J. L., Wu, J. Y., Lemyre, E., Burrow, T. A., Kang, P. B., Chen, Y. T. & Bali, D. S. Glycogen storage disease type IV: Novel mutations and molecular characterization of a heterogeneous disorder. *Journal of Inherited Metabolic Disorders* **33**, 83–90 (2010).
24. McBride, A., Ghilagaber, S., Nikolaev, A. & Hardie, D. G. The glycogen-binding domain on the AMPK β subunit allows the kinase to act as a glycogen sensor. *Cell Metabolism* **9**, 23–34 (2009).
25. Illingworth, B. & Brown, D. H. Action of amylo-1,6-glucosidase on low molecular weight substrates and the assay of this enzyme in glycogen storage disease. *PNAS* **48**, 1619–1623 (1962).
26. Larner, J., Illingworth, B., Cori, F. & Cori, T. Analysis by stepwise enzymatic degradation. *Journal of Biological Chemistry* **199**, 641–651 (1952).
27. Ryu, J. H., Drain, J., Kim, J. H., McGee, S., Gray-Weale, A., Waddington, L., Parker, G. J., Hargreaves, M., Yoo, S. H. & Stapleton, D. Comparative structural analyses of purified glycogen particles from rat liver, human skeletal muscle, and commercial preparations. *International Journal of Biological Macromolecules* **45**, 478–482 (2009).

28. Rani, M. R. S., Shibanuma, K. & Hizukuri, S. Studies on the fine structure of oyster glycogen. *Carbohydrates Research* **65**, 397–402 (1991).
29. Sullivan, M., Harcourt, B., Xu, P., Forbes, J. & Gilbert, R. Impairment of liver glycogen storage in the db/db animal model of type 2 diabetes: A potential target for future therapeutics? *Current Drug Targets* **16**, 1088–1093 (2015).
30. Sullivan, M. A., Li, J., Li, C., Vilaplana, F., Stapleton, D., Gray-Weale, A., Bowen, S., Zheng, L. & Gilbert, R. G. Molecular structural differences between type-2-diabetic and healthy glycogen. *Biomacromolecules* **12**, 1983–1986 (2011).
31. Sullivan, M. A., Nitschke, S., Skwara, E. P., Wang, P., Zhao, X., Pan, X. S., Chaown, E. E., Wang, T., Perri, A. M., Lee, J. P. Y., Vilaplana, F., Minassian, B. A. & Nitschke, F. Skeletal muscle glycogen chain length correlates with insolubility in mouse models of polyglucosan-associated neurodegenerative diseases. *Cell Reports* **27**, 1334–1344 (2019).
32. Deng, B., Sullivan, M. A., Li, J., Tan, X., Zhu, C., Schulz, B. L. & Gilbert, R. G. Molecular structure of glycogen in diabetic liver. *Glycoconjugate Journal* **32**, 113–118 (2015).
33. Powell, P. O., Sullivan, M. A., Sheehy, J. J., Schulz, B. J., Warren, F. J. & Gilbert, R. G. Acid hydrolysis and molecular density of phytoglycogen and liver glycogen helps understand the bonding in glycogen α (composite) particles. *PLoS One* **10**, 1–20 (2015).
34. Gilbert, R. G. & Sullivan, M. A. The molecular size distribution of glycogen and its relevance to diabetes. *Australian Journal of Chemistry* **67**, 538–543 (2014).
35. Sullivan, M., Harcourt, B., Xu, P., Forbes, J. & Gilbert, R. Impairment of Liver Glycogen Storage in the db/db Animal Model of Type 2 Diabetes: A Potential Target for Future Therapeutics? *Current Drug Targets* **16**, 1088–1093 (2015).
36. Philp, A., Hargreaves, M. & Baar, K. More than a store: regulatory roles for glycogen in skeletal muscle adaptation to exercise. *American Journal of Physiology, Endocrinology, and Metabolism* **302**, 1343–1351 (2012).
37. Han, H. S., Kang, G., Kim, J. S., Choi, B. H. & Koo, S. H. Regulation of glucose metabolism from a liver-centric perspective. *Experimental and Molecular Medicine* **48**, 1–10 (2016).
38. Skurat, A. v., Dietrich, A. D., Zhai, L. & Roach, P. J. GNIP, a novel protein that binds and activates glycogenin, the self-glucosylating initiator of glycogen biosynthesis. *Journal of Biological Chemistry* **277**, 19331–19338 (2002).
39. Ward, P. S. & Thompson, C. B. Signalling in control of cell growth and metabolism. *Cold Spring Harb Perspectives in Biology* **4**, 1–15 (2012).

40. Smythe, C. & Cohen, P. The discovery of glycogenin and the priming mechanism for glycogen biogenesis. *European Journal of Biochemistry* **200**, 625–631 (1991).
41. Krisman, C. R. & Barengo, R. A precursor of glycogen biosynthesis: α -1,4-glucan-protein. *European Journal of Biochemistry* **52**, 117–123 (1975).
42. Rodriguez, I. R. & Whelan, W. J. A novel glycosyl-amino acid linkage: Rabbit-muscle glycogen is covalently linked to a protein via tyrosine. *Biochemistry and Biophysical Research Communications* **132**, 829-836 (1985).
43. Lin, A., Mu, J., Yang, J. & Roach, P. J. Self-glucosylation of glycogenin, the initiator of glycogen biosynthesis, involves an inter-subunit. *Archives of Biochemistry and Biophysics* **363**, 163-170 (1999).
44. Gibbons, B. J., Roach, P. J. & Hurley, T. D. Crystal structure of the autocatalytic initiator of glycogen biosynthesis, glycogenin. *Journal of Molecular Biology* **319**, 463–477 (2002).
45. Issoglio, F. M., Carrizo, M. E., Romero, J. M. & Curtino, J. A. Mechanisms of monomeric and dimeric glycogenin autoglucosylation. *Journal of Biological Chemistry* **287**, 1955–1961 (2012).
46. Visuttijai, K., Hedberg-Oldfors, C., Thomsen, C., Glamuzina, E., Kornblum, C., Tasca, G., Hernandez-Lain, A., Sandstedt, J., Dellgren, G. & Roach, P. Glycogenin is dispensable for glycogen synthesis in human muscle, and glycogenin deficiency causes polyglucosan storage. *Journal of Clinical Endocrinology and Metabolism* **105**, 557–566 (2020).
47. Hurley, T. D., Walls, C., Bennett, J. R., Roach, P. J. & Wang, M. Direct detection of glycogenin reaction products during glycogen initiation. *Biochemistry and Biophysical Research Communications* **348**, 374-378 (2006).
48. Bazán, S., Issoglio, F. M., Carrizo, M. E. & Curtino, J. A. The intramolecular autoglucosylation of monomeric glycogenin. *Biochemistry and Biophysical Research Communications* **371**, 328–332 (2008).
49. Roach, P. J. & Skurat, A. V. Self-glucosylating initiator proteins and their role in glycogen biosynthesis. *Progress in Nucleic Acid Research and Molecular Biology* **57**, 289-316 (1997).
50. Chaikuad, A., Froese, D. S., Berridge, G., von Delft, F., Opperman, U. & Yue, W. W. Conformational plasticity of glycogenin and its maltosaccharide substrate during glycogen biogenesis. *PNAS* **108**, 21028-21033 (2011).
51. Romero, J. M., Issoglio, F. M., Carrizo, M. E. & Curtino, J. A. Evidence for glycogenin autoglucosylation cessation by inaccessibility of the acquired maltosaccharide. *Biochemistry and Biophysical Research Communications* **374**, 704–708 (2008).

52. Hurley, T. D., Walls, C., Bennett, J. R., Roach, P. J. & Wang, M. Direct detection of glycogenin reaction products during glycogen initiation. *Biochemistry and Biophysical Research Communications* **348**, 374–378 (2006).
53. Smythe, C. & Cohen, P. The discovery of glycogenin and the priming mechanism for glycogen biogenesis. *European Journal of Biochemistry* **200**, 625-631 (1991).
54. Buschiazzo, A., Ugalde, J. E., Guerin, M. E., Shepard, W., Ugalde, R. A., Alzari, P. M. Crystal structure of glycogen synthase: Homologous enzymes catalyze glycogen synthesis and degradation. *EMBO Journal* **23**, 3196–3205 (2004).
55. Baskaran, S., Roach, P. J., Depaoli-Roach, A. A. & Hurley, T. D. Structural basis for glucose-6-phosphate activation of glycogen synthase. *PNAS* **107**, 17563-17568 (2010).
56. Picton, C., Woodgett, J., Hemmings, B. & Cohen, P. Multisite phosphorylation of glycogen synthase from rabbit skeletal muscle. Phosphorylation of site 5 by glycogen synthase kinase-5 (casein kinase-II) is a prerequisite for phosphorylation of sites 3 by glycogen synthase kinase-3. *FEBS Letters* **150**, 191–196 (1982).
57. Roach, P. J. Multisite and hierarchal protein phosphorylation. *Journal of Biological Chemistry* **266**, 14139–14142 (1991).
58. Marr, L., Biswas, D., Daly, L., Browning, C., Vial, S. C. M., Maskell, D. P., Hudson, C., Bertrand, J. A., Pollard, J., Ranson, N. A., Khatter, H., Evers, C. E., Sakamoto, K. & Zeqiraj, E. Mechanism of glycogen synthase inactivation and interaction with glycogenin. *Nature Communications* **13**, 1-14 (2022).
59. Baskaran, S., Chickwana, V. M., Contreras, C. J., Davis, K. D., Wilson, W. A., DePaoli-Roach, A. A., Roach, P. J. & Hurley, T. Multiple glycogen-binding sites in eukaryotic glycogen synthase are required for high catalytic efficiency toward glycogen. *Journal of Biological Chemistry* **286**, 33999–34006 (2011).
60. Drula, E., Garron, M. L., Dogan, S., Lombard, V., Henrissat, B. & Terrapon, N. The carbohydrate-active enzyme database: Functions and literature. *Nucleic Acids Research* **50**, 1-7 (2021).
61. Drueckes, P., Palm, D. & Schinzel, R. Carbohydrate binding at the active site of *Escherichia coli* maltodextrin phosphorylase. *Progress in Biotechnology* **10**, 59-69 (1995).
62. Froese, S. D., Michaeli, A., McCorvie, T. J., Krojer, T., Sasi, M., Melaev, M., Goldblum, A., Zatsepin, M., Lossos, A., Álvarez, R., Escribá, P. V., Minassian, B. A., von Delft, F., Kakhlon, O., & Yue, W. W. Structural basis of glycogen branching enzyme deficiency and pharmacologic rescue by rational peptide design. *Human Molecular Genetics* **24**, 5667–5676 (2015).

63. BeMiller, J. N. & Whistler., R. L. (2009). *Starch: Chemistry and Technology*. USA: Elsevier academic Press.
64. Kuriki, T., Stewart, D. C. & Preiss, J. Construction of chimeric enzymes out of maize endosperm branching enzymes I and II: Activity and properties. *Journal of Biological Chemistry* **272**, 28999–29004 (1997).
65. Ciric, J. & Loos, K. Synthesis of branched polysaccharides with tunable degree of branching. *Carbohydrate Polymers* **93**, 31–37 (2013).
66. Cuan, H. P. & Preiss, J. Differentiation of the properties of the branching isozymes from maize (*Zea mays*). *Plant Physiology* **102**, 1269-1273 (1993).
67. Leonidas, D. D., Zographos, S. E., Tsitsanou, K. E., Skamnaki, V. T., Stravodimosand, G. & Kyriakis, E. Glycogen phosphorylase revisited: Extending the resolution of the R- And T-state structures of the free enzyme and in complex with allosteric activators. *Acta Crystallography Structural Biology Communications* **77**, 303–311 (2021).
68. Oikonomakos, N. G. Glycogen phosphorylase as a molecular target for type 2 diabetes therapy. *Current Protein Peptides Science* **3**, 561–586 (2002).
69. Oikonomakos, N. G., Schnier, J. B., Zographos, S. E., Skamnaki, V. T., Tsitsanou, E. K., & Johnson, L. N. Flavopiridol inhibits glycogen phosphorylase by binding at the inhibitor site. *Journal of Biological Chemistry* **275**, 34566–34573 (2000).
70. Henke B.R. & Sparks S.M. Glycogen phosphorylase inhibitors. *Mini Reviews in Medicinal Chemistry* **6**, 845–857 (2006).
71. Zmasek, C. M. & Godzik, A. Phylogenomic analysis of glycogen branching and debranching enzymatic duo. *BMC Evolutionary Biology* **14**, 1–13 (2014).
72. Tomasik, P. & Horton, D. (2012). *Enzymatic conversions of starch*. *Advances in Carbohydrate Chemistry and Biochemistry*. USA: Elsevier Inc, Academic Press.
73. Cuesta-Seijo, J. A., Ruzanski, C., Krucewicz, K., Meier, S., Hägglund, P., Svensson, B. & Palcic, M. M. Functional and structural characterization of plastidic starch phosphorylase during barley endosperm development. *PLoS One* **12**, 1–25 (2017).
74. Zois, C. E. & Harris, A. L. Glycogen metabolism has a key role in the cancer microenvironment and provides new targets for cancer therapy. *Journal of Molecular Medicine* **94**, 137–154 (2016).
75. Zhai, L., Feng, L., Xia, L., Yin, H. & Xiang, S. Crystal structure of glycogen debranching enzyme and insights into its catalysis and disease-causing mutations. *Nature Communication* **7**, 1–11 (2016).

76. Watanabe, Y., Makino, Y. & Omichi, K. Donor substrate specificity of 4- α -glucanotransferase of porcine liver glycogen debranching enzyme and complementary action to glycogen phosphorylase on debranching. *Journal of Biochemistry* **143**, 435–440 (2008).
77. Ikeda, A., Makino, Y. & Matsubara, H. Glycogen debranching pathway deduced from substrate specificity of glycogen debranching enzyme. *Glycoconjugate Journal* **39**, 345–355 (2022).
78. Akman, H. O., Raghavan, A. & Craigen, W. J. Animal models of glycogen storage disorders. in *Progress in Molecular Biology and Translational Science* **100**, 369–388 (2011).
79. Zirin, J., Nieuwenhuis, J. & Perrimon, N. Role of Autophagy in Glycogen Breakdown and Its Relevance to Chloroquine Myopathy. *PLoS Biology* **11**, 1–16 (2013).
80. Kelsall, I. R., McCrory, E. H., Xu, Y. Q., Scudamore, C. L., Nanda, S. K., Mancebo-Gamella, P., Wood, N. T., Knebel, A., Matthews, S. J. & Cohen, P. HOIL-1 ubiquitin ligase activity targets unbranched glucosaccharides and is required to prevent polyglucosan accumulation. *EMBO Journal* **41**, (2022).
81. Roach, P. J. Glycogen phosphorylation and lafora disease. *Molecular Aspects Medicine* **46**, 78–84 (2016).
82. Turnbull, J., Wang, P., Girard, J. M., Ruggieri, A., Wang, T. J., Draginov, A. G., Kameka, A. P., Pencea, N., Zhao, X., Ackerley, C. A. & Minassian, B. A. Glycogen hyperphosphorylation underlies Lafora body formation. *Annals of Neurology* **68**, 925–933 (2010).
83. Sun, T., Yi, H., Yang, C., Kishnani, P. S. & Sun, B. Starch binding domain-containing protein 1 plays a dominant role in glycogen transport to lysosomes in liver. *Journal of Biological Chemistry* **291**, 16479–16484 (2016).
84. Moslemi, A. R., Lindberg, C., Nilsson, J., Tajsharghi, H., Andersson, B. & Oldfords, A. Glycogenin-1 deficiency and inactivated priming of glycogen synthesis. *New England Journal of Medicine* **362**, 1203–1210 (2010).
85. Cifuentes, J. O., Comino, N., Trastoy, B., D'Angelo, C. & Guerin, M. E. Structural basis of glycogen metabolism in bacteria. *Biochemical Journal* **476**, 2059–2092 (2019).
86. Cho, Y. G. & Kang, K. K. Functional analysis of starch metabolism in plants. *Plants* **9**, 1–6 (2020).
87. Kasapkara, Ç. S., Aycan, Z., Açoğlu, E., Senel, S., Oguz, M. M., & Ceylancı, S. The variable clinical phenotype of three patients with hepatic glycogen synthase deficiency. *Journal of Pediatric Endocrinology and Metabolism* **30**, 459–462 (2017).

88. Weinstein, D. A., Correia, C. E., Saunders, A. C. & Wolfsdorf, J. I. Hepatic glycogen synthase deficiency: An infrequently recognized cause of ketotic hypoglycaemia. *Molecular Genetics Metabolism* **87**, 284–288 (2006).
89. Arko, J. J., Debeljak, M., Tansek, M. Z., Battelino, T. & Groselj, U. A patient with glycogen storage disease type 0 and a novel sequence variant in GYS2: a case report and literature review. *Journal of International Medical Research* **48**, 1-8 (2020).
90. Illingworth, B. & Brown, D. Lack of an α -1,4-glucan: α -1,4-glucan 6-glycosyl transferase in a case of type IV glycogenosis. *PNAS* **56**, 725–729 (2020).
91. Lossos, A., Meiner, M., Barash, V., Soffer, D., Schlesinger, I., Abramsky, O., Argov, Z., Shpitzen, S. & Meiner, V. Adult polyglucosan body disease in Ashkenazi Jewish patients carrying the Tyr329Ser mutation in the glycogen-branching enzyme gene. *Annals Neurology* **44**, 867–872 (1998).
92. Nitschke, F., Sullivan, M., Wang, P., Zhao, X., Chown, E. E., Perri, A. M., Israelian, L., Juana-López, L., Bovolenta, P., Rodríguez de Córdoba, S., Steup, M. & Minassian, B. E. Abnormal glycogen chain length pattern, not hyperphosphorylation, is critical in Lafora disease. *EMBO Molecular Medicine* **9**, 906–917 (2017).
93. Wilson, L. H., Cho, J. H., Estrella, A., Smyth, J. A., Wu, R., Chengsupanimit, T., Brown, L. M., Weinstein, D. A. & Lee, Y. M. Liver glycogen phosphorylase deficiency leads to profibrogenic phenotype in a murine model of glycogen storage disease type vi. *Hepatology Communications* **3**, 1544-1555 (2019).
94. Melis, D., Rossi, A., Pivonello, R., Salerno, M., Balivo, F., Spadarella, S., Muscogiuri, G., Dalla Casa, R., Formisano, P., Andria, G., Colao, A. & Parenti, G. Glycogen storage disease type Ia (GSDIa) but not Glycogen storage disease type Ib (GSDIb) is associated to an increased risk of metabolic syndrome: Possible role of microsomal glucose 6-phosphate accumulation. *Orphanet Journal of Rare Disorders* **10**, 1-8 (2015).
95. Cheetham, N. W. H., Hansawek, N. & Saecou, P. An HPLC method for determining chain-length distribution in some glycogens. *Carbohydrate Research* **215**, 59–65 (1991).
96. Morrison, M., Kuyper, A. C. & Orten, J. M. A study of the periodate method for determining end-group values. *Journal of Biological Chemistry* **75**, 1502–1504 (1953).
97. Kristiansen, K. A., Potthast, A. & Christensen, B. E. Periodate oxidation of polysaccharides for modification of chemical and physical properties. *Carbohydrate Research* **345**, 1264–1271 (2010).

98. Pandeirada, C. O., Achterweust, M., Janssen, H. G., Westphal, Y. & Schols, H. A. Periodate oxidation of plant polysaccharides provides polysaccharide-specific oligosaccharides. *Carbohydrate Polymers* **291**, 1-12 (2022).
99. Cui, S. W. (2005). *Food Carbohydrates: Chemistry, Physical Properties, and Applications*. UK: Taylor&Francis.
100. Gunja-smith, Z., Marshall, J. J. & Smith, E. E. Enzymatic determination of the unit chain length of glycogen and related polysaccharides. *FEBS Letters* **13**, 309–311 (1971).
101. Gunja-smith, Z., Marshall, J. J., Mercier, C., Smith, E. E. & Whelan, W. J. A revision of the Meyer-Bernfeld Model of Glycogen and Amylopectin. *FEBS Lett* **12**, 101-104 (1970).
102. Kobayashi, T., Sasaki, S., Utsumi, Y., Fujita, N., Umeda, K., Sawada, T., Kubo, A., Abe, J. C., Colleoni, C., Ball, S. & Nakamura, Y. Comparison of chain-length preferences and glucan specificities of isoamylase-type α -glucan debranching enzymes from rice, cyanobacteria, and bacteria. *PLoS One* **11**, 1–21 (2016).
103. Robyt, J. F. & Whelan, W. J. Reducing value methods for maltodextrins: Chain-length dependence of alkaline 3,5-dinitrosalicylate and chain-length independence of alkaline copper. *Analytical Biochemistry* **45**, 510–516 (1972).
104. Goncalves, C., Rodriguez-Jasso, R. M., Gomes, N., Teixeira, J. A. & Belo, I. Adaptation of dinitrosalicylic acid method to microtiter plates. *Analytical Methods* **2**, 2046–2048 (2010).
105. Hatanaka, C. & Kobara, Y. Determination of glucose by a modification of Somogyi-Nelson method. *Agricultural and Biological Chemistry* **44**, 2943-2949 (1980).
106. Harada, T., Yokobayashi, K. & Misaki, A. Formation of isoamylase by *Pseudomonas*. *Applied Microbiology* **16**, 1439–1444 (1968).
107. Katsuya, Y., Mezaki, Y., Kubota, M. & Matsuura, Y. Three-dimensional structure of *Pseudomonas* isoamylase at 2.2 Å resolution. *Journal of Molecular Biology* **281**, 885–897 (1998).
108. Harada, T., Misaki, A., Akai, H., Yokobayashi, K. & Sugimoto, K. Characterization of *Pseudomonas* isoamylase by its actions on amylopectin and glycogen: Comparison with *Aerobacter pullulanase*. *BBA - Enzymology* **268**, 497–505 (1972).
109. Hii, S. L., Tan, J. S., Ling, T. C. & Ariff, A. Pullulanase: Role in starch hydrolysis and potential industrial applications. *Enzyme Research* **2012**, 1-14 (2012).
110. Kainuma, K., Kobayashi, S. & Tokuya, H. Action of *Pseudomonas* isoamylase on various branched oligo- and poly- saccharides. *Carbohydrate Research* **61**, 345–357 (1978).

111. Abdullah, M. & French, D. Substrate specificity of pullulanase. *Archives of Biochemistry and Biophysics* **137**, 483-493 (1970).
112. Yokobayashi, K., Akai, H., Sugimoto, T., Hirao, M., Sugimoto, K. & Harada, T. Comparison of the kinetic parameters of *Pseudomonas* isoamylase and *Aerobacter* pullulanase. *BBA - Enzymology* **293**, 197–202 (1973).
113. Taniguchi, H. & Honnda, Y. (2009). *Encyclopedia of Microbiology (3rd Edition)*. USA: Elsevier Inc, Academic Press
114. Zhou, X., Wang, C., Yue, S., Zheng, Y., Li, C. & Yu, W. Mutual interactions between α -amylase and amyloglucosidase in the digestion of starch with distinct chain-length distributions at a fully gelatinized state. *Food & Function* **13**, 3453–3464 (2022).
115. Youngquist, R. W. (1962) Beta-amylase action on high molecular weight maltosaccharides. *Iowa State University*.
116. de Sales, P. M., de Souza, P. M., Simeoni, L. A., Magalhães, P. de O. & Silveira, D. α -amylase inhibitors: A review of raw material and isolated compounds from plant source. *Journal of Pharmacy and Pharmaceutical Sciences* **15**, 141–183 (2012).
117. Lee, E. Y. C. & Whelan, W. J. (1971). *The Enzymes (3rd Edition)*. USA: Elsevier Inc., Academic Press.
118. Kainuma, K. (1984). *Starch: Chemistry and Technology (2nd Edition)*. USA: Academic Press Inc.
119. Lee, E. Y. C. The action of sweet potato β -amylase on glycogen and amylopectin: Formation of a novel limit dextrin. *Archives of Biochemistry and Biophysics* **146**, 488–492 (1971).
120. Szabó, K., Kandra, L. & Gyémánt, G. Studies on the reversible enzyme reaction of rabbit muscle glycogen phosphorylase b using isothermal titration calorimetry. *Carbohydrate Research* **477**, 58–65 (2019).
121. Schinzel, R. & Palm, D. *Escherichia coli* maltodextrin phosphorylase: contribution of active site residues Glutamate-637 and Tyrosine-538 to the phosphorolytic cleavage of α -glucans. *Biochemistry* **29**, 9956–9962 (1990).
122. Brown, D. H., Illingworth, B. & Cori, C. F. The mechanism of the de novo synthesis of polysaccharide by phosphorylase. *PNAS* **47**, 479-485 (1961).
123. Meyer, F., Heilmeyer, L. M. G., Haschke, R. H. & Fischer, E. H. Control of phosphorylase activity in a muscle glycogen particle. *Journal of Biological Chemistry* **245**, 6642–6648 (1970).

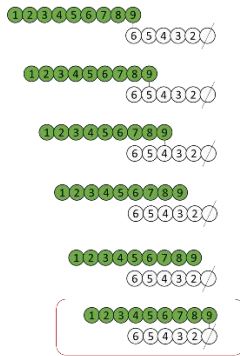
124. Sullivan, M. A., Aroney, S. T. N., Li, S., Warren, F. J., Joo, J. S., Mak, K. S., Stapleton, D. I., Bell-Anderson, K. S. & Gilbert, R. G. Changes in glycogen structure over feeding cycle sheds new light on blood-glucose control. *Biomacromolecules* **15**, 660–665 (2014).
125. Fermont, L., Szydłowski, N. & Colleoni, C. Determination of glucan chain length distribution of glycogen using the Fluorophore-Assisted Carbohydrate Electrophoresis (FACE) method. *Journal of Visualized Experiments* **2022**, 1–15 (2022).
126. Morell, M. K., Samuel, M. S. & O'Shea, M. G. Analysis of starch structure using fluorophore-assisted carbohydrate electrophoresis. *Electrophoresis* **19**, 2603–2611 (1998).
127. Wu, A. C., Witt, T. & Gilbert, R. G. Characterization methods for starch-based materials: State of the art and perspectives. *Australian Journal of Chemistry* **66**, 1550–1563 (2013).
128. O'Shea, M. G. O., Samuel, M. S., Konik, C. M. & Morell, M. K. Fluorophore-assisted carbohydrate electrophoresis (FACE) of oligosaccharides: efficiency of labelling and high-resolution separation.
129. Corradini, C., Cavazza, A. & Bignardi, C. High-Performance Anion-Exchange Chromatography Coupled with Pulsed Electrochemical Detection as a powerful tool to evaluate carbohydrates of food interest: principles and applications. *International Journal of Carbohydrate Chemistry* **2012**, 1–13 (2012).
130. J.S. Rohrer, L. Basumallick & D. Hurum, High-performance anion-exchange chromatography with pulsed amperometric detection for carbohydrate analysis of glycoproteins. *Biochemistry (Moscow)* **78**, 697–709 (2013).
131. Shi, Y.-C. & Seib, P. A. The structure of four waxy starches related to gelatinization and retrogradation. *Carbohydrate Research* **227**, 131-145 (1992).
132. Koizumi, K., Fukuda, M. & Hizukuri, S. Estimation of the distributions of chain length of amylopectins by high-performance liquid chromatography with pulsed amperometric detection. *Journal of Chromatography* **585**, 233-238 (1991).
133. Barth, H. G., Boyes, B. E. & Jackson, C. Size Exclusion Chromatography. *Analytical Chemistry* **66**, 595–620 (1994).
134. Hussain, H., Ngaini, Z. & Chong, N. F. M. Modified bichinonic acid assay for accurate determination of variable length reducing sugars in carbohydrates. *International Food Research Journal* **25**, 2614–2619 (2018).

135. Utsumi, Y., Yoshida, M., Perigio, F., Sawada, T., Kitamura, S. & Nakamura, Y. Quantitative assay method for starch branching enzyme with bicinchoninic acid by measuring the reducing terminals of glucans. *Journal of Applied Glycoscience* **56**, 215–222 (2009).
136. Walker, J. M. The bicinchoninic acid (BCA) assay for protein quantitation. *Methods in Molecular Biology* **32**, 5–8 (1994).
137. Braissant, O., Astasov-Frauenhoffer, M., Waltimo, T. & Bonkat, G. A Review of methods to determine viability, vitality, and metabolic rates in microbiology. *Frontiers in Microbiology* **11**, 1–25 (2020).
138. Zhang, Y., Yuan, Z., Mahmood, N., Huang, S. & Xu, C. C. Sustainable bio-phenol-hydroxymethylfurfural resins using phenolated de-polymerized hydrolysis lignin and their application in bio-composites. *Industrial Crops Production* **79**, 84–90 (2016).
139. Masuko, T. *et al.* Carbohydrate analysis by a phenol-sulfuric acid method in microplate format. *Analytical Biochemistry* **339**, 69–72 (2005).
140. Fox, J. D. & Robyt, J. F. Miniaturization of three carbohydrate analyses using a microsample plate reader. *Analytical Biochemistry* **195**, 93–96 (1991).
141. Miller, G. L. Use of dinitrosalicylic acid reagent for determination of reducing sugar. *Analytical Chemistry* **31**, 426–428 (1959).
142. Matsui, M., Kakuta, M. & Misaki, A. Comparison of the unit-chain distributions of glycogens from different biological sources, revealed by anion exchange chromatography. *Bioscience, Biotechnology, and Biochemistry* **57**, 623–627 (1993).
143. Akai, H., Yokobayashi, K., Misaki, A. & Harada, T. Complete hydrolysis of branching linkages in glycogen by pseudomonas isoamylase: Distribution of linear chains. *BBA - General Subjects* **237**, 422–429 (1971).
144. Manners, D. J. Recent developments in our understanding of glycogen structure. *Carbohydrate Polymers* **16**, 37–82 (1991).
145. Illingworth, B., Larner, J. & Cori, T. G. Enzymatic determination of chain length. *Journal of Biological Chemistry* **199**, 631–640 (1952).
146. Gaborieau, M. & Castignolles, P. Size-exclusion chromatography (SEC) of branched polymers and polysaccharides. *Analytical and Bioanalytical Chemistry* **399**, 1413–1423 (2011).
147. Zhu, A., Romero, R. & Petty, H. R. An enzymatic colorimetric assay for glucose-6-phosphate. *Analytical Biochemistry* **419**, 266–270 (2011).

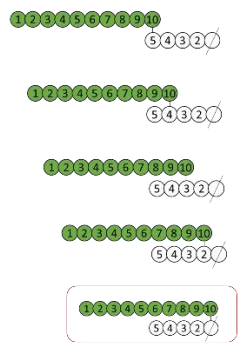
148. Jeanningros, R., Creuzet-Sigal, N., Frixon, C. & Cattaneo, J. Purification and properties of a debranching enzyme from *Escherichia coli*. *BBA - Enzymology* **438**, 186–199 (1976).
149. Prats, C., Graham, T. E. & Shearer, J. The dynamic life of the glycogen granule. *Journal of Biological Chemistry* **293**, 7089–7098 (2018).
150. Meléndez, R., Meléndez-Hevia, E., Mas, F., Mach, J. & Cascante, M. Physical constraints in the synthesis of glycogen that influence its structural homogeneity: A two-dimensional approach. *Biophysical Journal* **75**, 106–114 (1998).
151. Carroll, N. V., Longley, R. W. & Roe, J. H. The determination of glycogen in liver and muscle by use of anthrone reagent. *Journal of Biological Chemistry* **220**, 583-593 (1956).
152. Bueding, E. & Orrell, S. A. A Mild Procedure for the isolation of polydisperse glycogen from animal tissues. *Journal of Biological Chemistry* **239**, 4018–4020 (1964).
153. Wang, Z., Liu, Q., Wang, L., Gilbert, R. G. & Sullivan, M. A. Optimization of liver glycogen extraction when considering the fine molecular structure. *Carbohydrate Polymers* **261**, 1-11 (2021).
154. Vardanis, A. Fractionation of particulate glycogen and bound enzymes using high-performance liquid chromatography. *Analytical Biochemistry* **187**, 115-119 (1990).
155. Stapleton, D., Nelson, C., Parsawar, K., McClain, D., Gilbert-Wilson, R., Barker, E., Rudd, B., Brown, K., Hendrix, W., O'Donnell, P., & Parker, G. Analysis of hepatic glycogen-associated proteins. *Proteomics* **10**, 2320–2329 (2010).
156. Raschke, S., Guan, J. & Iliakis, G. (2009). *Methods in Molecular Biology*. UK: Humana Press.
157. Geddes, R. & Rapson, K. B. Post-mortem degradation of glycogen. *FEBS Letters* **31**, 324-326 (1973).
158. Lerman, M. J., Lembong, J., Muramoto, S., Gillen, G. & Fisher, J. P. The evolution of polystyrene as a cell culture material. *Tissue Engineering Part B Reviews* **24**, 359–372 (2018).
159. Sullivan, M. A., O'Connor, M. J., Umana, F., Roura, E., Jack, K., Stapleton, D. I. & Gilbert, R. G. Molecular insights into glycogen α -particle formation. *Biomacromolecules* **13**, 3805–3813 (2012)
160. Chou, J. Y., Jun, H. S. & Mansfield, B. C. Type I glycogen storage diseases: disorders of the glucose-6-phosphatase/glucose-6-phosphate transporter complexes. *Journal of Inherited Metabolic Disorders* **38**, 511–519 (2015).

Appendix 1 – Combinations of X_1 with X_2
Substrates for the enzymatic treatment with ISA and Pull

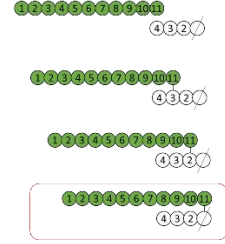
DP9 + DP6



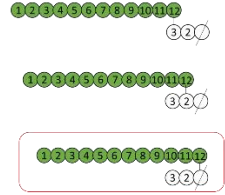
DP10 + DP5



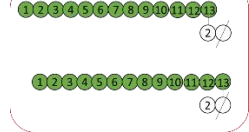
DP11 + DP4



DP12 + DP3



DP13 + DP2



DP14 + DP1



Appendix 2

Appendix 2 - DP15 models

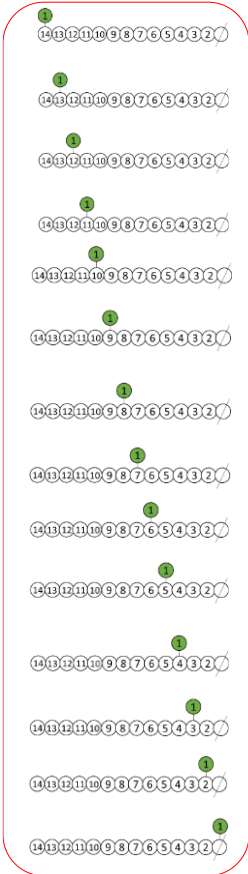
Substrates for the enzymatic treatment with ISA and Pull combined with BMY and GP digestion. The structures circled in red are not digested by these enzymes

DP1 + DP14

Pull and ISA

β-amylase +
Pull/ISA or OGL

Glycogen Phosphorylase
Pull/ISA or OGL



DP2 + DP13



1 x DP2
1 x DP13

1 x DP2
1 x DP13

1 x DP2
1 x DP13

1 x DP2
1 x DP13

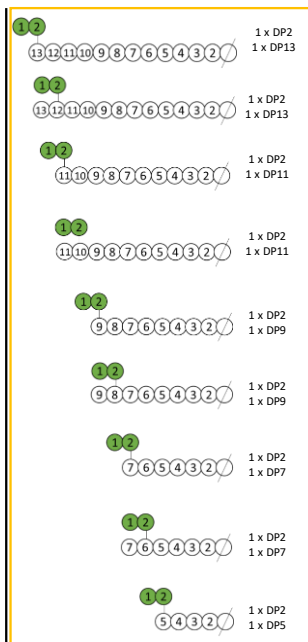
1 x DP2
1 x DP13

1 x DP2
1 x DP13

1 x DP2
1 x DP13

1 x DP2
1 x DP13

1 x DP2
1 x DP13



1 x DP2
1 x DP13

1 x DP2
1 x DP13

1 x DP2
1 x DP11

1 x DP2
1 x DP11

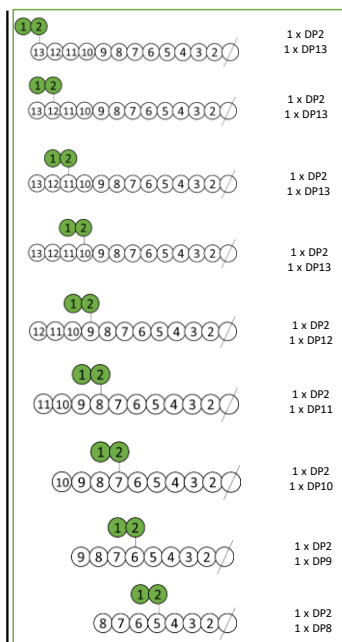
1 x DP2
1 x DP9

1 x DP2
1 x DP9

1 x DP2
1 x DP7

1 x DP2
1 x DP7

1 x DP2
1 x DP5



1 x DP2
1 x DP13

1 x DP2
1 x DP13

1 x DP2
1 x DP13

1 x DP2
1 x DP13

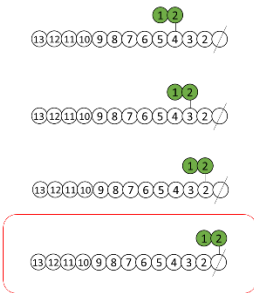
1 x DP2
1 x DP12

1 x DP2
1 x DP11

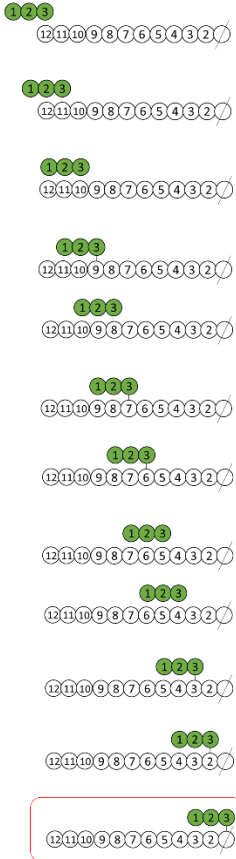
1 x DP2
1 x DP10

1 x DP2
1 x DP9

1 x DP2
1 x DP8



DP3 + DP12



DP4 + DP11



1 x DP2
1 x DP13

1 x DP2
1 x DP13

1 x DP2
1 x DP13

1 x DP3
1 x DP12

1 x DP3
1 x DP12

1 x DP3
1 x DP12

1 x DP3
1 x DP12

1 x DP3
1 x DP12

1 x DP3
1 x DP12

1 x DP3
1 x DP12

1 x DP3
1 x DP12

1 x DP3
1 x DP12

1 x DP3
1 x DP12

1 x DP3
1 x DP12

1 x DP3
1 x DP12

1 x DP4
1 x DP11

1 x DP4
1 x DP11

1 x DP4
1 x DP11

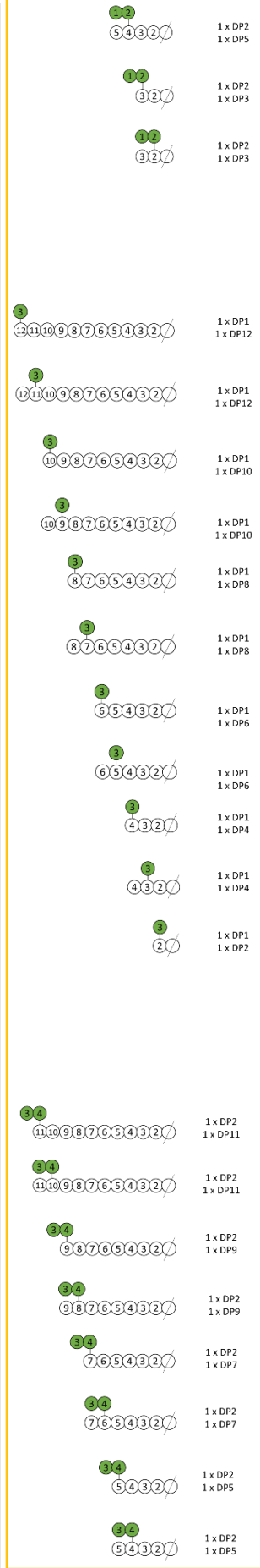
1 x DP4
1 x DP11

1 x DP4
1 x DP11

1 x DP4
1 x DP11

1 x DP4
1 x DP11

1 x DP4
1 x DP11



1 x DP2
1 x DP5

1 x DP2
1 x DP3

1 x DP2
1 x DP3

1 x DP1
1 x DP12

1 x DP1
1 x DP12

1 x DP1
1 x DP10

1 x DP1
1 x DP10

1 x DP1
1 x DP8

1 x DP1
1 x DP8

1 x DP1
1 x DP6

1 x DP1
1 x DP6

1 x DP1
1 x DP4

1 x DP1
1 x DP4

1 x DP1
1 x DP2

1 x DP2
1 x DP11

1 x DP2
1 x DP11

1 x DP2
1 x DP9

1 x DP2
1 x DP9

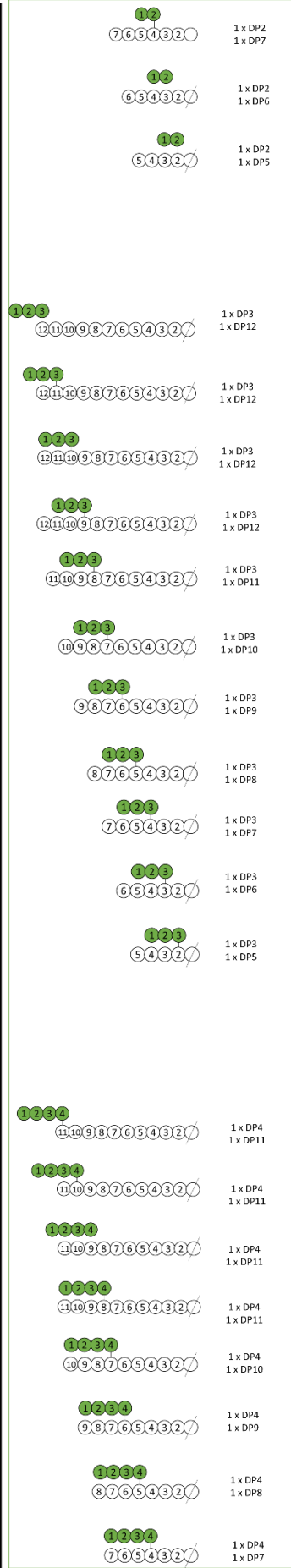
1 x DP2
1 x DP7

1 x DP2
1 x DP7

1 x DP2
1 x DP5

1 x DP2
1 x DP5

1 x DP2
1 x DP5



1 x DP2
1 x DP7

1 x DP2
1 x DP6

1 x DP2
1 x DP5

1 x DP3
1 x DP12

1 x DP3
1 x DP12

1 x DP3
1 x DP12

1 x DP3
1 x DP12

1 x DP3
1 x DP11

1 x DP3
1 x DP10

1 x DP3
1 x DP9

1 x DP3
1 x DP8

1 x DP3
1 x DP7

1 x DP3
1 x DP6

1 x DP3
1 x DP5

1 x DP4
1 x DP11

1 x DP4
1 x DP11

1 x DP4
1 x DP11

1 x DP4
1 x DP11

1 x DP4
1 x DP10

1 x DP4
1 x DP9

1 x DP4
1 x DP8

1 x DP4
1 x DP7

1 x DP4
1 x DP7

1 2 3 4
11 10 9 8 7 6 5 4 3 2 1

1 2 3 4
11 10 9 8 7 6 5 4 3 2 1

1 2 3 4
11 10 9 8 7 6 5 4 3 2 1

DP5 + DP10

1 2 3 4 5
10 9 8 7 6 5 4 3 2 1

1 2 3 4 5
10 9 8 7 6 5 4 3 2 1

1 2 3 4 5
10 9 8 7 6 5 4 3 2 1

1 2 3 4 5
10 9 8 7 6 5 4 3 2 1

1 2 3 4 5
10 9 8 7 6 5 4 3 2 1

1 2 3 4 5
10 9 8 7 6 5 4 3 2 1

1 2 3 4 5
10 9 8 7 6 5 4 3 2 1

1 2 3 4 5
10 9 8 7 6 5 4 3 2 1

1 2 3 4 5
10 9 8 7 6 5 4 3 2 1

1 2 3 4 5
10 9 8 7 6 5 4 3 2 1

DP6 + DP9

1 2 3 4 5 6
9 8 7 6 5 4 3 2 1

1 2 3 4 5 6
9 8 7 6 5 4 3 2 1

1 2 3 4 5 6
9 8 7 6 5 4 3 2 1

1 2 3 4 5 6
9 8 7 6 5 4 3 2 1

1 2 3 4 5 6
9 8 7 6 5 4 3 2 1

1 2 3 4 5 6
9 8 7 6 5 4 3 2 1

1 2 3 4 5 6
9 8 7 6 5 4 3 2 1

1 2 3 4 5 6
9 8 7 6 5 4 3 2 1

1 2 3 4 5 6
9 8 7 6 5 4 3 2 1

1 x DP4
1 x DP11

1 x DP4
1 x DP11

1 x DP5
1 x DP10

1 x DP5
1 x DP10

1 x DP5
1 x DP10

1 x DP5
1 x DP10

1 x DP5
1 x DP10

1 x DP5
1 x DP10

1 x DP5
1 x DP10

1 x DP5
1 x DP10

1 x DP5
1 x DP10

1 x DP6
1 x DP9

1 x DP6
1 x DP9

1 x DP6
1 x DP9

1 x DP6
1 x DP9

1 x DP6
1 x DP9

1 x DP6
1 x DP9

1 x DP6
1 x DP9

1 x DP6
1 x DP9

1 x DP6
1 x DP9

3 4
3 2 1

1 x DP2
1 x DP3

3 4
3 2 1

1 x DP2
1 x DP3

5
10 9 8 7 6 5 4 3 2 1

1 x DP1
1 x DP10

5
10 9 8 7 6 5 4 3 2 1

1 x DP1
1 x DP10

5
8 7 6 5 4 3 2 1

1 x DP1
1 x DP8

5
8 7 6 5 4 3 2 1

1 x DP1
1 x DP8

5
6 5 4 3 2 1

1 x DP1
1 x DP6

5
6 5 4 3 2 1

1 x DP1
1 x DP6

5
4 3 2 1

1 x DP1
1 x DP4

5
4 3 2 1

1 x DP1
1 x DP4

5
2 1

1 x DP1
1 x DP2

5 6
9 8 7 6 5 4 3 2 1

1 x DP2
1 x DP9

5 6
9 8 7 6 5 4 3 2 1

1 x DP2
1 x DP9

5 6
7 6 5 4 3 2 1

1 x DP2
1 x DP7

5 6
7 6 5 4 3 2 1

1 x DP2
1 x DP7

5 6
5 4 3 2 1

1 x DP2
1 x DP5

5 6
5 4 3 2 1

1 x DP2
1 x DP5

5 6
3 2 1

1 x DP2
1 x DP3

5 6
3 2 1

1 x DP2
1 x DP3

1 2 3 4
6 5 4 3 2 1

1 x DP4
1 x DP6

1 2 3 4
5 4 3 2 1

1 x DP4
1 x DP5

2 3 4 5
10 9 8 7 6 5 4 3 2 1

1 x DP4
1 x DP10

2 3 4 5
10 9 8 7 6 5 4 3 2 1

1 x DP4
1 x DP10

2 3 4 5
10 9 8 7 6 5 4 3 2 1

1 x DP4
1 x DP10

2 3 4 5
10 9 8 7 6 5 4 3 2 1

1 x DP4
1 x DP10

2 3 4 5
9 8 7 6 5 4 3 2 1

1 x DP4
1 x DP9

2 3 4 5
8 7 6 5 4 3 2 1

1 x DP4
1 x DP8

2 3 4 5
7 6 5 4 3 2 1

1 x DP4
1 x DP7

2 3 4 5
6 5 4 3 2 1

1 x DP4
1 x DP6

2 3 4 5
2 1

1 x DP4
1 x DP2

3 4 5 6
9 8 7 6 5 4 3 2 1

1 x DP4
1 x DP9

3 4 5 6
9 8 7 6 5 4 3 2 1

1 x DP4
1 x DP9

3 4 5 6
9 8 7 6 5 4 3 2 1

1 x DP4
1 x DP9

3 4 5 6
9 8 7 6 5 4 3 2 1

1 x DP4
1 x DP9

3 4 5 6
8 7 6 5 4 3 2 1

1 x DP4
1 x DP8

3 4 5 6
7 6 5 4 3 2 1

1 x DP4
1 x DP7

3 4 5 6
6 5 4 3 2 1

1 x DP4
1 x DP6

3 4 5 6
5 4 3 2 1

1 x DP4
1 x DP5

DP7+ DP8

1234567
8765432

1 x DP7
1 x DP8

1234567
8765432

1 x DP7
1 x DP8

1234567
8765432

1 x DP7
1 x DP8

1234567
8765432

1 x DP7
1 x DP8

1234567
8765432

1 x DP7
1 x DP8

1234567
8765432

1 x DP7
1 x DP8

1234567
8765432

1 x DP7
1 x DP8

1234567
8765432

DP8+ DP7

12345678
7654321

1 x DP8
1 x DP7

12345678
7654321

1 x DP8
1 x DP7

12345678
7654321

1 x DP8
1 x DP7

12345678
7654321

1 x DP8
1 x DP7

12345678
7654321

1 x DP8
1 x DP7

12345678
7654321

1 x DP8
1 x DP7

12345678
7654321

DP9+ DP6

123456789
654321

1 x DP9
1 x DP6

123456789
654321

1 x DP9
1 x DP6

123456789
654321

1 x DP9
1 x DP6

123456789
654321

1 x DP9
1 x DP6

123456789
654321

1 x DP9
1 x DP6

123456789
654321

DP10+ DP5

12345678910
54321

1 x DP10
1 x DP5

12345678910
54321

1 x DP10
1 x DP5

12345678910
54321

1 x DP10
1 x DP5

12345678910
54321

1 x DP10
1 x DP5

12345678910
54321

7
8765432

1 x DP1
1 x DP8

7
8765432

1 x DP1
1 x DP8

7
654321

1 x DP1
1 x DP6

7
654321

1 x DP1
1 x DP6

7
4321

1 x DP1
1 x DP4

7
4321

1 x DP1
1 x DP4

7
21

1 x DP1
1 x DP2

78
7654321

1 x DP2
1 x DP7

78
7654321

1 x DP2
1 x DP7

78
54321

1 x DP2
1 x DP5

78
54321

1 x DP2
1 x DP5

78
321

1 x DP2
1 x DP3

78
321

1 x DP2
1 x DP3

4567
8765432

1 x DP4
1 x DP8

4567
8765432

1 x DP4
1 x DP8

4567
8765432

1 x DP4
1 x DP8

4567
8765432

1 x DP4
1 x DP8

4567
7654321

1 x DP4
1 x DP7

4567
654321

1 x DP4
1 x DP6

4567
54321

1 x DP4
1 x DP5

6789
7654321

1 x DP4
1 x DP7

6789
7654321

1 x DP4
1 x DP7

6789
7654321

1 x DP4
1 x DP7

6789
7654321

1 x DP4
1 x DP7

6789
654321

1 x DP4
1 x DP6

6789
54321

1 x DP4
1 x DP5

6789
654321

1 x DP4
1 x DP6

6789
654321

1 x DP4
1 x DP6

6789
654321

1 x DP4
1 x DP6

6789
654321

1 x DP4
1 x DP6

6789
654321

1 x DP4
1 x DP6

78910
54321

1 x DP4
1 x DP5

78910
54321

1 x DP4
1 x DP5

78910
54321

1 x DP4
1 x DP5

78910
54321

1 x DP4
1 x DP5

78910
54321

1 x DP4
1 x DP5

DP11+ DP4



1 x DP11
1 x DP4



1 x DP11
1 x DP4



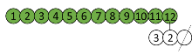
1 x DP11
1 x DP4



DP12+ DP3



1 x DP12
1 x DP3



1 x DP12
1 x DP3



DP13+ DP2



DP14+ DP1



1 x DP1
1 x DP4



1 x DP1
1 x DP4



1 x DP1
1 x DP2



1 x DP2
1 x DP3



1 x DP2
1 x DP3



1 x DP4
1 x DP4



1 x DP4
1 x DP4



1 x DP4
1 x DP4



1 x DP4
1 x DP3



1 x DP4
1 x DP3

Appendix 3

Appendix 3

Models designed by using X_1 equal to DP6 or DP7

	Pull and ISA	β -amylase + Pull/ISA or OGL	Glycogen Phosphorylase Pull/ISA or OGL	
DP6 + DP11		1 x DP6 1 x DP11		1 x DP2 1 x DP11
		1 x DP6 1 x DP11		1 x DP2 1 x DP11
		1 x DP6 1 x DP11		1 x DP2 1 x DP9
		1 x DP6 1 x DP11		1 x DP2 1 x DP9
		1 x DP6 1 x DP11		1 x DP2 1 x DP7
		1 x DP6 1 x DP11		1 x DP2 1 x DP7
		1 x DP6 1 x DP11		1 x DP2 1 x DP7
		1 x DP6 1 x DP11		1 x DP2 1 x DP7
		1 x DP6 1 x DP11		1 x DP2 1 x DP3
		1 x DP6 1 x DP11		1 x DP2 1 x DP3
		1 x DP6 1 x DP11		1 x DP2 1 x DP3
	DP6 + DP10		1 x DP6 1 x DP10	
		1 x DP6 1 x DP10		1 x DP2 1 x DP10
		1 x DP6 1 x DP10		1 x DP2 1 x DP8
		1 x DP6 1 x DP10		1 x DP2 1 x DP8
		1 x DP6 1 x DP10		1 x DP2 1 x DP8
		1 x DP6 1 x DP10		1 x DP2 1 x DP6
		1 x DP6 1 x DP10		1 x DP2 1 x DP4
		1 x DP6 1 x DP10		1 x DP2 1 x DP4
		1 x DP6 1 x DP10		1 x DP2 1 x DP2
		1 x DP6 1 x DP10		1 x DP2 1 x DP2
		1 x DP6 1 x DP10		1 x DP2 1 x DP2
DP6 + DP9			1 x DP6 1 x DP9	
		1 x DP6 1 x DP9		1 x DP2 1 x DP9
		1 x DP6 1 x DP9		1 x DP2 1 x DP7
		1 x DP6 1 x DP9		1 x DP2 1 x DP7
		1 x DP6 1 x DP9		1 x DP2 1 x DP5
		1 x DP6 1 x DP9		1 x DP2 1 x DP4
		1 x DP6 1 x DP9		1 x DP2 1 x DP3
		1 x DP6 1 x DP9		1 x DP2 1 x DP3
		1 x DP6 1 x DP9		1 x DP2 1 x DP3
		1 x DP6 1 x DP9		1 x DP2 1 x DP3
		1 x DP6 1 x DP9		1 x DP2 1 x DP3

Appendix 3

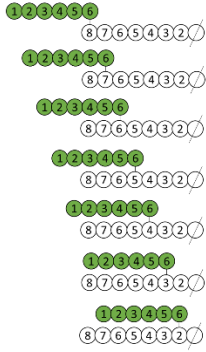
Models designed by using X_1 equal to DP6 or DP7

Pull and ISA

β -amylase +
Pull/ISA or OGL

Glycogen Phosphorylase
Pull/ISA or OGL

DP6 + DP8



1 x DP6
1 x DP8

1 x DP6
1 x DP8

1 x DP6
1 x DP8

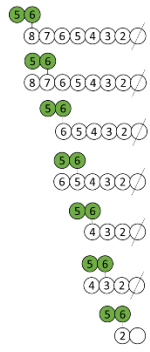
1 x DP6
1 x DP8

1 x DP6
1 x DP8

1 x DP6
1 x DP8

1 x DP6
1 x DP8

1 x DP6
1 x DP8



1 x DP2
1 x DP8

1 x DP2
1 x DP8

1 x DP2
1 x DP6

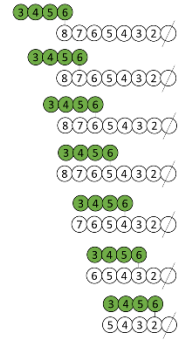
1 x DP2
1 x DP6

1 x DP2
1 x DP4

1 x DP2
1 x DP4

1 x DP2
1 x DP2

1 x DP2
1 x DP2



1 x DP4
1 x DP8

1 x DP4
1 x DP8

1 x DP4
1 x DP8

1 x DP4
1 x DP8

1 x DP4
1 x DP7

1 x DP4
1 x DP6

1 x DP4
1 x DP5

DP6 + DP7



1 x DP6
1 x DP7

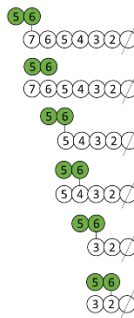
1 x DP6
1 x DP7

1 x DP6
1 x DP7

1 x DP6
1 x DP7

1 x DP6
1 x DP7

1 x DP6
1 x DP7



1 x DP2
1 x DP7

1 x DP2
1 x DP7

1 x DP6
1 x DP5

1 x DP6
1 x DP5

1 x DP6
1 x DP3

1 x DP6
1 x DP3

1 x DP6
1 x DP6
1 x DP3



1 x DP4
1 x DP7

1 x DP4
1 x DP7

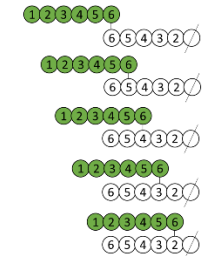
1 x DP4
1 x DP7

1 x DP4
1 x DP7

1 x DP4
1 x DP6

1 x DP4
1 x DP5

DP6 + DP6



1 x DP6
1 x DP6

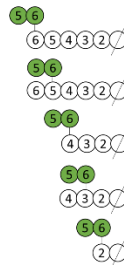
1 x DP6
1 x DP6

1 x DP6
1 x DP6

1 x DP6
1 x DP6

1 x DP6
1 x DP6

1 x DP6
1 x DP6



1 x DP2
1 x DP6

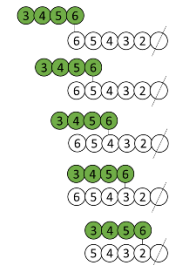
1 x DP2
1 x DP6

1 x DP2
1 x DP4

1 x DP2
1 x DP4

1 x DP2
1 x DP4

1 x DP2
1 x DP2



1 x DP4
1 x DP6

1 x DP4
1 x DP6

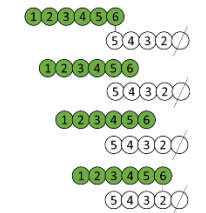
1 x DP4
1 x DP6

1 x DP4
1 x DP6

1 x DP4
1 x DP5

1 x DP4
1 x DP5

DP6 + DP5

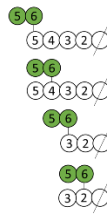


1 x DP6
1 x DP5

1 x DP6
1 x DP5

1 x DP6
1 x DP5

1 x DP6
1 x DP5



1 x DP2
1 x DP5

1 x DP2
1 x DP5

1 x DP2
1 x DP3

1 x DP2
1 x DP3



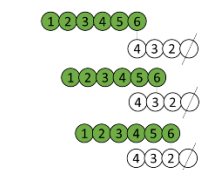
1 x DP4
1 x DP5

1 x DP4
1 x DP5

1 x DP4
1 x DP5

1 x DP4
1 x DP5

DP6 + DP4



1 x DP6
1 x DP4

1 x DP6
1 x DP4

1 x DP6
1 x DP4



1 x DP2
1 x DP4

1 x DP2
1 x DP4

1 x DP2
1 x DP2



1 x DP4
1 x DP4

1 x DP4
1 x DP4

1 x DP4
1 x DP4

Appendix 3

Models designed by using X_1 equal to DP6 or DP7

	Pull and ISA	β -amylase + Pull/ISA or OGL	Glycogen Phosphorylase Pull/ISA or OGL
DP6 + DP3			
	<p>1 x DP6 1 x DP3</p> <p>1 x DP6 1 x DP3</p>	<p>1 x DP2 1 x DP3</p> <p>1 x DP2 1 x DP3</p> <p>1 x DP2 1 x DP2</p>	<p>1 x DP6 1 x DP3</p> <p>1 x DP6 1 x DP3</p> <p>1 x DP4 1 x DP2</p>
DP6 + DP2			
	<p>1 x DP6 1 x DP2</p>	<p>1 x DP2 1 x DP2</p>	<p>1 x DP4 1 x DP2</p>
DP7 + DP10			
	<p>1 x DP7 1 x DP10</p> <p>1 x DP7 1 x DP10</p> <p>1 x DP7 1 x DP10</p> <p>1 x DP7 1 x DP10</p> <p>1 x DP7 1 x DP10</p> <p>1 x DP7 1 x DP10</p> <p>1 x DP7 1 x DP10</p> <p>1 x DP7 1 x DP10</p> <p>1 x DP7 1 x DP10</p> <p>1 x DP7 1 x DP10</p> <p>1 x DP7 1 x DP10</p> <p>1 x DP7 1 x DP10</p>	<p>1 x DP1 1 x DP10</p> <p>1 x DP1 1 x DP10</p> <p>1 x DP1 1 x DP8</p> <p>1 x DP1 1 x DP8</p> <p>1 x DP1 1 x DP6</p> <p>1 x DP1 1 x DP6</p> <p>1 x DP1 1 x DP5</p> <p>1 x DP1 1 x DP3</p> <p>1 x DP1 1 x DP3</p>	<p>1 x DP4 1 x DP10</p> <p>1 x DP4 1 x DP10</p> <p>1 x DP4 1 x DP9</p> <p>1 x DP4 1 x DP9</p> <p>1 x DP4 1 x DP8</p> <p>1 x DP4 1 x DP8</p> <p>1 x DP4 1 x DP7</p> <p>1 x DP4 1 x DP6</p> <p>1 x DP4 1 x DP5</p>
DP7 + DP9			
	<p>1 x DP7 1 x DP9</p> <p>1 x DP7 1 x DP9</p> <p>1 x DP7 1 x DP9</p> <p>1 x DP7 1 x DP9</p> <p>1 x DP7 1 x DP9</p> <p>1 x DP7 1 x DP9</p> <p>1 x DP7 1 x DP9</p> <p>1 x DP7 1 x DP9</p>	<p>1 x DP1 1 x DP9</p> <p>1 x DP1 1 x DP9</p> <p>1 x DP1 1 x DP7</p> <p>1 x DP1 1 x DP7</p> <p>1 x DP1 1 x DP5</p> <p>1 x DP1 1 x DP5</p> <p>1 x DP1 1 x DP3</p> <p>1 x DP1 1 x DP3</p>	<p>1 x DP4 1 x DP9</p> <p>1 x DP4 1 x DP9</p> <p>1 x DP4 1 x DP9</p> <p>1 x DP4 1 x DP9</p> <p>1 x DP4 1 x DP8</p> <p>1 x DP4 1 x DP7</p> <p>1 x DP4 1 x DP6</p> <p>1 x DP4 1 x DP5</p>
DP7 + DP8			
	<p>1 x DP7 1 x DP8</p> <p>1 x DP7 1 x DP8</p> <p>1 x DP7 1 x DP8</p> <p>1 x DP7 1 x DP8</p> <p>1 x DP7 1 x DP8</p>	<p>1 x DP1 1 x DP8</p> <p>1 x DP1 1 x DP8</p> <p>1 x DP1 1 x DP6</p> <p>1 x DP1 1 x DP6</p> <p>1 x DP1 1 x DP4</p>	<p>1 x DP4 1 x DP8</p> <p>1 x DP4 1 x DP8</p> <p>1 x DP4 1 x DP8</p> <p>1 x DP4 1 x DP8</p> <p>1 x DP4 1 x DP7</p>

Appendix 3

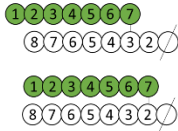
Models designed by using X_1 equal to DP6 or DP7

Pull and ISA

β-amylose +
Pull/ISA or OGL

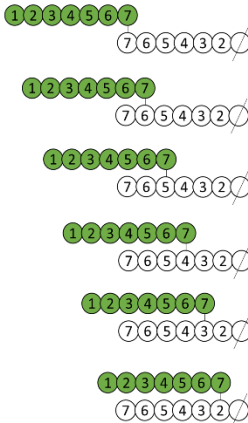
Glycogen Phosphorylase +
Pull/ISA or OGL

DP7 + DP8



1 x DP7
1 x DP8

DP7 + DP7



1 x DP7
1 x DP7

1 x DP7
1 x DP7

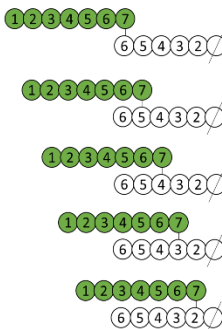
1 x DP7
1 x DP7

1 x DP7
1 x DP7

1 x DP7
1 x DP7

1 x DP7
1 x DP7

DP7 + DP6



1 x DP7
1 x DP6

1 x DP7
1 x DP6

1 x DP7
1 x DP6

1 x DP7
1 x DP6

1 x DP7
1 x DP6

DP7 + DP5



1 x DP7
1 x DP5

1 x DP7
1 x DP5

1 x DP7
1 x DP5

1 x DP7
1 x DP5

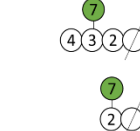
DP7 + DP4



1 x DP7
1 x DP4

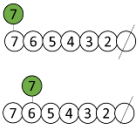
1 x DP7
1 x DP4

1 x DP7
1 x DP4



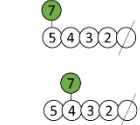
1 x DP1
1 x DP4

1 x DP1
1 x DP2



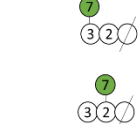
1 x DP1
1 x DP7

1 x DP1
1 x DP7



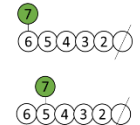
1 x DP1
1 x DP5

1 x DP1
1 x DP5



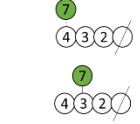
1 x DP1
1 x DP3

1 x DP1
1 x DP3



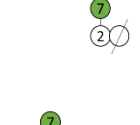
1 x DP1
1 x DP6

1 x DP1
1 x DP6



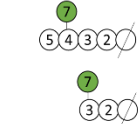
1 x DP1
1 x DP4

1 x DP1
1 x DP4



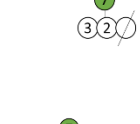
1 x DP1
1 x DP2

1 x DP1
1 x DP5



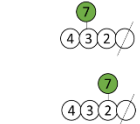
1 x DP1
1 x DP5

1 x DP1
1 x DP3



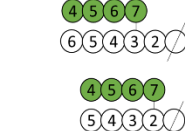
1 x DP1
1 x DP3

1 x DP1
1 x DP4



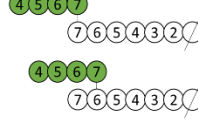
1 x DP1
1 x DP4

1 x DP1
1 x DP4



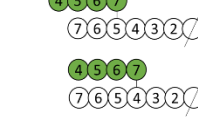
1 x DP4
1 x DP6

1 x DP4
1 x DP5



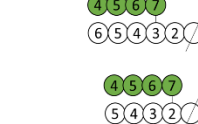
1 x DP4
1 x DP7

1 x DP4
1 x DP7



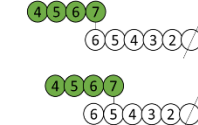
1 x DP4
1 x DP7

1 x DP4
1 x DP7



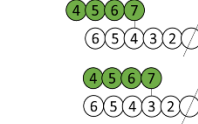
1 x DP4
1 x DP6

1 x DP4
1 x DP5



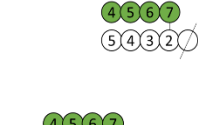
1 x DP4
1 x DP6

1 x DP4
1 x DP6



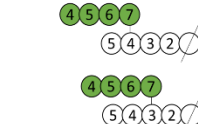
1 x DP4
1 x DP6

1 x DP4
1 x DP6



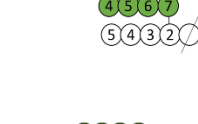
1 x DP4
1 x DP5

1 x DP4
1 x DP5



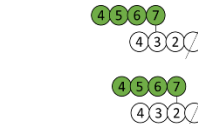
1 x DP4
1 x DP5

1 x DP4
1 x DP5



1 x DP4
1 x DP5

1 x DP4
1 x DP5



1 x DP4
1 x DP4

1 x DP4
1 x DP4

Appendix 3

Models designed by using X_1 equal to DP6 or DP7

